IDAHO TRANSPORTATION DEPARTMENT

RESEARCH REPORT

RP 212

Lithologic Characterization of Active ITD Aggregate Sources and Implications for Aggregate Quality

By

Virginia S. Gillerman and Kerrie N. Weppner

Idaho Geological Survey

Prepared for

Idaho Transportation Department

Research Program

Division of Highways, Resource Center

http://itd.idaho.gov/highways/research/

March 2014

Standard Disclaimer

This document is disseminated under the sponsorship of the Idaho Transportation Department and the United States Department of Transportation in the interest of information exchange. The State of Idaho and the United States Government assume no liability of its contents or use thereof.

The contents of this report reflect the view of the authors, who are responsible for the facts and accuracy of the data presented herein. The contents do not necessarily reflect the official policies of the Idaho Transportation Department or the United States Department of Transportation.

The State of Idaho and the United States Government do not endorse products or manufacturers. Trademarks or manufacturers' names appear herein only because they are considered essential to the object of this document.

This report does not constitute a standard, specification or regulation.

1. Report No. FHWA-ID-14-212	2. Government Accession No.	3. Recipient's Catalog No.
4. Title and Subtitle Lithologic Characterization of Active ITD Aggregate Sources and Implications for Aggregate Quality		5. Report Date March 2014 6. Performing Organization Code
7. Author(s) Virginia S. Gillerman, and Kerrie N. Weppner		8. Performing Organization Report No.
9. Performing Organization Name and Address Idaho Geological Survey 322 E. Front St., #242 Boise, ID 83702		10. Work Unit No. (TRAIS) 11. Contract or Grant No. RP212
12. Sponsoring Agency Name and Address Idaho Transportation Department Division of Highways, Resource Center, Research Program PO Box 7129 Boise, ID 83707-7129		13. Type of Report and Period Covered Final Report 03/01/2011 - 01/15/2014 14. Sponsoring Agency Code
15. Supplementary Notes e.g. Project performed in cooperation with the Idaho Transportation Department and FHWA.		
16. Abstract Aggregate from 40 material sources across Idaho were sampled and the lithologies identified quantitatively. Aggregate compositions are compared with commercial AASHTO T 303 and ASTM C1293 results and the geologic map of Idaho to identify those rock types and geographic areas most susceptible to alkali-silica reactivity (ASR). Petrography on I-84 concrete and the commercial and experimental mortar bars confirmed the conclusion that rhyolites from young Snake River Plain (SRP) volcanism as well as certain "siliceous quartzites" in the mid-SRP region have very high ASR potential. However, much of Idaho has ASR reactive aggregate. The geographic regions with the most consistent, lowest ASR values in aggregate are in the Boise and Payette River drainages.		
17. Key Words Aggregate, ASR, alkali-silica reactivity, Idaho, geology	18. Distribution Statement Copies available online at http://itd.idaho.gov/highways/research/	
19. Security Classification (of this report) Unclassified	20. Security Classification (of this page) Unclassified	21. No. of Pages 242 / 22. Price None

FHWA Form F 1700.7

METRIC (SI*) CONVERSION FACTORS

APPROXIMATE CONVERSIONS TO SI UNITS

Symbol	When You Know	Multiply By	To Find	Symbol
		LENGTH		
in	inches	25.4		mm
ft	feet	0.3048		m
yd	yards	0.914		m
mi	Miles (statute)	1.61		km
		AREA		
in^2	square inches	645.2	millimeters squared	cm^2
ft^2	square feet	0.0929	meters squared	m^2
yd^2	square yards	0.836	meters squared	m^2
mi^2	square miles	2.59	kilometers squared	km^2
ac	acres	0.4046	hectares	ha
		MASS (weight)		
oz	Ounces (avdp)	28.35	grams	g
lb	Pounds (avdp)	0.454	kilograms	kg
T	Short tons (2000 lb)	0.907	megagrams	mg
		VOLUME		
fl oz	fluid ounces (US)	29.57	milliliters	mL
gal	Gallons (liq)	3.785	liters	liters
ft^3	cubic feet	0.0283	meters cubed	m^3
yd^3	cubic yards	0.765	meters cubed	m^3

Note: Volumes greater than 1000 L shall be shown in m^3

		TEMPERATURE (exact)		
^oF	Fahrenheit temperature	5/9 (^oF-32)	Celsius temperature	^oC
		ILLUMINATION		
fc	Foot-candles	10.76	lux	lx
fl	foot-lamberts	3.426	candela/m^2	cd/cm^2
		FORCE and PRESSURE or STRESS		
lbf	pound-force	4.45	newtons	N
psi	pound-force per square inch	6.89	kilopascals	kPa

APPROXIMATE CONVERSIONS FROM SI UNITS

Symbol	When You Know	Multiply By	To Find	Symbol
		LENGTH		
mm	millimeters	0.039	inches	in
m	meters	3.28	feet	ft
m	meters	1.09	yards	yd
km	kilometers	0.621	Miles (statute)	mi
		AREA		
mm^2	millimeters squared	0.0016	square inches	in^2
m^2	meters squared	10.764	square feet	ft^2
km^2	kilometers squared	0.39	square miles	mi^2
ha	hectares (10,000 m^2)	2.471	acres	ac
		MASS (weight)		
g	grams	0.0353	Ounces (avdp)	oz
kg	kilograms	2.205	Pounds (avdp)	lb
mg	megagrams (1000 kg)	1.103	short tons	T
		VOLUME		
mL	milliliters	0.034	fluid ounces (US)	fl oz
liters	liters	0.264	Gallons (liq)	gal
m^3	meters cubed	35.315	cubic feet	ft^3
m^3	meters cubed	1.308	cubic yards	yd^3

		TEMPERATURE (exact)		
^oC	Celsius temperature	9/5 ^oC+32	Fahrenheit temperature	^oF
		ILLUMINATION		
lx	lux	0.0929	foot-candles	fc
cd/cm^2	candela/m^2	0.2919	foot-lamberts	fl
		FORCE and PRESSURE or STRESS		
N	newtons	0.225	pound-force	lbf
kPa	kilopascals	0.145	pound-force per square inch	psi

Acknowledgements

The project concept was initially proposed by Keith Nottingham, Idaho Transportation Department (ITD) District 3 Geologist, and Bill Capaul, ITD District 1 Geologist. The new Idaho Geological Survey (IGS) state geologic map at 1:750,000 scale was a key source of information for the GIS maps and was crucial to the geological correlations.[1] Bill Phillips in the Idaho Geological Survey office in Moscow also assisted with the project.

Kelly Byrne and David Ferrera (ITD District 3) facilitated source sampling and sample processing in the District 3 lab. John Arambarri and Clint Hoops of ITD provided thoughtful feedback on the project. The statewide ITD district geologists and engineers provided useful information about source operators and source locations. Editorial help from Inez Hopkins of ITD improved the format and appearance of the final report. Rich Reed, a registered professional geologist and engineer in Idaho with Idaho Engineering and Geology, Inc., assisted with an introduction to field procedures and prior methodology. He also reviewed and provided licensed professional approval of the final report. The Department of Geosciences at Boise State University, and Dr. Jen Pierce especially, provided laboratory and office space. Dr. George Murgel and Dr. Robert Hamilton of the Department of Civil Engineering at Boise State University helped us acquire background information and allowed use of laboratory facilities. Numerous private industry aggregate operators allowed access to their sand and gravel pits and provided useful discussions as we toured the facilities and deposits. The Boise office of Strata Geotech, and especially Kristi Barnett, who worked with us to conduct the AASHTO T 303 testing on the custom mortar bars, provided terrific assistance for the laboratory analysis portion of the project. We thank all of the above persons and organizations.

Table of Contents

List of Tables

List of Figures

List of Acronyms and Abbreviations

ASR - Alkali Silica Reactivity

CA - Coarse Aggregate

Chalc. – Chalcedony

FA - Fine Aggregate

60% CA/40% FA - 60 Percent Coarse Aggregate and 40 Percent Fine Aggregate

GIS - Geographic Information Systems

IGS - Idaho Geological Survey

ITD - Idaho Department of Transportation

Ma - million years

SCM - Supplementary Cementitious Materials

Glossary of Geology Terms

Aggregate – Crushed rocks derived from bedrock, or sand and gravel-sized pieces of rocks.

Alluvium – A general term for unconsolidated detrital (fragments of other rocks) deposits made by rivers, streams, floodplains, and alluvial fans. The term applies to recent deposition that occurred during the Quaternary period (2.6 Ma to present).

Amorphous – A textural term that literally means "without form" and applies to rocks and minerals that have no internal crystalline structure (but typically do have a glassy texture).

Aphyric – A textural term applied to igneous rocks that are very fine – grained.

Argillaceous – Refers to rocks that have a significant clay content.

Argillite – A fine-grained low-grade metamorphic rock derived from mudstone or shale.

Basin Delineation – The determination of watershed (basin) boundaries. Watersheds are separated by topographic highs, where any precipitation falling within a specific watershed will flow to a specific water body (stream, river, lake, reservoir, or ocean).

Caliche – A hardened layer of calcium carbonate.

Carbonate – A mineral compound characterized by a fundamental anionic structure of CO_3^{-2}. Limestone, aragonite, calcite are examples of carbonate rocks.

Chalcedony – A cryptocrystalline variety of quartz (SiO_2) that commonly occurs as a banded lining in cavities in rocks, or in vugs (i.e., cavities) in volcanic rocks. Agate is a type of chalcedony.

Chert/Cherty – A hard, dense microcrystalline or cryptocrystalline sedimentary rocks composed of quartz (SiO_2) and amorphous silica (opal).

Clasts – Fragment of other rocks found in sedimentary rocks produced from the physical disintegration of another rock.

Cryptocrystalline – A textural term referring to rocks made up of crystals that are not visible or distinguishable under a regular microscope.

Crystalline – A material composed of crystals (megascopic or microscopic) which require an orderly internal array of molecules or atoms; minerals are natural, inorganic, crystalline substances.

Detrital – Pertaining to or formed from the detritus of other rocks, or formed from minerals of pre – existing rocks.

Devitrification – The process of crystallization of a formerly amorphous (see amorphous) glass.

Dolostone – A term for the sedimentary rock dolomite with a chemical composition of $CaMg(CO_3)^2$.

Duripan – Refers to the hardened soil horizon formed by the precipitation of calcium carbonate (see caliche).

Felsic – Antonym of mafic (see mafic). A compositional term used to describe igneous rocks (rocks that cooled from a molten state) that contain >65 percent SiO_2 by weight, and are relatively rich in feldspars. Felsic rocks are characteristically lighter in color than mafic rocks.

Feldspars – Are a group of rock-forming tectosilicate minerals that make up as much as 60 percent of the Earth's crust. Examples of feldspars are as follows; Potassium feldspar ($KAlSi_3O_8$), Albite ($NaAlSi_3O_8$), Anorthite ($CaAl_2Si_2O_8$).

Fines – The portion of aggregate used in concrete with a grain-size <0.187" (<4.75 mm) that passes through a No. 4 sieve.

Gel Pat Test – To accelerate ASR on concrete cores, we used a modified gel pat test. Four pieces of concrete core were cut, polished and immersed in 1M NaOH solution and placed in sealed plastic containers in 100°F oven for 200 days (Fournier and Berube, 1993).

Granophyric – From "granophyre" which is a subvolcanic rock that contains quartz and alkali feldspar in characteristic angular intergrowths."Granophyric" refers to the texture of a granophyre.

Gneiss – A foliated rock (layers of dark-colored minerals and light-colored minerals) formed by high – grade regional metamorphic processes of pre-existing igneous or sedimentary rocks.

Lithified – Refers to unconsolidated sediment that has been changed to stone or petrified.

Lithology – Rock type.

Mafic – Antonym of felsic (see felsic). A compositional term used to describe igneous rocks (rocks that cooled from a molten state) that contain 45 - 52 percent SiO_2 by weight, are rich in magnesium and iron, and are characteristically darker in color than felsic rocks.

Metamorphic Rock – Develops from the chemical and textural transformation of a pre – existing rock during a process called metamorphism. Metamorphism means "to change in form" and occurs due to heat, pressure and chemically active fluids.

Metasedimentary – (Metasediment) is sediment or sedimentary rock that appears to have been altered by metamorphism.

Micropegmatite – Quartz and alkali feldspar intergrowth so fine that it can be resolved only under a microscope.

Mortar Bar – A small piece of concrete, typically made in the laboratory to specific size and composition for testing the properties of the concrete.

Opal – An amorphous form of hydrated silica, typically identified by an "opaline" iridescent shine and containing 6 – 10 percent of water. Opal precipitates from low temperature groundwater or hydrothermal fluids and can form coatings on cobbles in aggregate or veins in altered soil and volcanic rocks.

Palagonite – An alteration product from the interaction of water with volcanic glass of chemical composition similar to basalt.

Pedogenic – A soil-forming process pertaining to the addition, transfer, transformation, or remove soil constituents.

Pit Face/Pitting – Having a hollow or an indentation on the surface.

Plutonic – A plutonic rock comes from a pluton which is a body of intrusive igneous rock (rock that cooled from a magma or molten state) that cooled slowly below the surface of the Earth. Slow cooling allows the growth of individual crystals to occur, giving the rock a coarse texture. Granite is a common plutonic rock.

Pop-outs – Individual pieces of aggregate that physically "pop out" of solidified concrete. In this document, popping out likely occurs due to swelling of fine – grained aggregate.

Porphyritic – A textural term referring to igneous rocks (rocks that cooled from a magma) that contain coarse crystals (phenocrysts) in a fine-grained matrix. Rocks with porphyritic textures (porphyry) are indicative of two rates of cooling; 1. slow cooling below the surface in a rising magma and 2. rapid cooling as the magma gets closer to the surface.

Porphyry – A variety of igneous rock with large-grained crystals (feldspar and quartz) in a fine-grained feldspathic matrix. These rocks have a porphyritic texture (see porphyritic).

Quartz – A common mineral composed of silica. Quartz is an abundant mineral in most sands.

Rhyolite – Igneous, volcanic rock of felsic (silica-rich) composition. Commonly fine-grained and may exhibit a porphyritic texture.

Silica – Silicon dioxide (SiO_2), of which the most common, naturally occurring form is the mineral quartz. Chalcedony, chert, agate, jasper, and opal are other natural forms of silica.

Siliceous – A rock with a high silica-content (SiO_2).

Siltite – A low-grade metamorphosed siltstone.

Source Code – Each aggregate source that supplies ITD with aggregate has a source code (i.e., Ad-136c). The first two letters refer to the county where the sources is located (i.e., Ad = Ada county), followed by a number (source identifier) and either the letter c (contractor owned) or the letter s (state owned).

Spherulite – Small, spheroidal body consisting of radiating crystals found in obsidian and other glassy volcanic rocks.

Tuff – Consolidated volcanic ash ejected from vents during a volcanic eruption. See also welded tuff.

Vitrophyre – A volcanic rock with larger crystals (phenocrysts) embedded in a glassy groundmass.

Vug – Small to medium-sized cavities in rocks that may be formed through a variety of processes.

Welded Tuff – A pyroclastic rock (a rock formed of rock fragments that were ejected from a volcano during a volcanic eruption) that was sufficiently hot at the time of deposition so that it is welded together.

Table 1. Geologic Time Scale

Division	Period	Epoch	Age (Millions of years)
	Quaternary	Holocene	0.01
		Pliestocene	2.6
	Neogene	Pliocene	5.3
Cenozoic		Miocene	23.0
		Oligocene	33.9
	Paleogene	Eocene	56.0
		Paleocene	66.0
	Cretaceous	Cretaceous	100.0
Mesozoic	Jurassic	Jurrasic	201.0
	Triassic	Triassic	252.0
	Permian	Permian	299.0
	Carboniferous	Pennsylvanian	323.0
		Mississippan	359.0
Paleozoic	Devonian	Devonian	419.0
	Silurian	Silurian	445.0
	Ordivician	Ordivician	485.0
	Cambrian	Cambrian	541.0
		Neoproterozoic	1000.0
	Proterozoic	Mesoproterozoic	1600.0
Precambrian		Paleproterozoic	2500.0
	Archean	Archean	4000.0
	Hadean	Hadean	

Executive Summary

This project studied relationships between lithology (rock type) and alkali-silica reactivity (ASR) of 40 aggregate sources certified for concrete production by the Idaho Transportation Department (ITD) with the intention of identifying geologic units that are more (or less) susceptible to ASR. ASR refers to a chemical reaction between aggregate and alkalis in the cement. The reaction produces an expansive gel that causes damaging cracking in concrete and subsequent failure of the concrete before its projected lifespan. The research was a response to known issues of high ASR potential in many Idaho sources, particularly in southern Idaho where ASR-related deterioration required treatment and partial replacement of Interstate 84 (I-84) concrete near Mountain Home, Idaho.

Methodology

Aggregate source lithologies were sampled and quantitatively inventoried from 40 concrete-certified material sources across Idaho (Figure 1). Source locations and upstream drainage basins were delineated in ArcGIS 10.1 for the sources, which were predominantly fluvial gravels. The source lithologies were compared to the mapped geologic units that outcrop in each drainage basin in order to confirm the accuracy of the inventories and also to see the rock type variation and correlative units. For each of the sampled sources, the commercial AASHTO T 303 and ASTM C 1293 results were used as a guide or proxy for the general ASR potential of the source. The AASHTO T 303 test is a 16-day test that measures expansion of concrete mortar bars, where passing is ≤0.10 percent expansion. The ASTM C 1293 test is a 1 year test that measures expansion of concrete mortar bars, where passing is ≤0.04 percent expansion. The ASR expansion potential (from AASHTO T 303 and ASTM C 1293 tests) was correlated to the lithologies present in each particular source. More specific determination of ASR susceptible lithologies was made by petrographic analysis performed on the AASHTO T 303 mortar bars and on ASR-affected concrete cores from I-84 concrete.

In addition, the AASHTO T 303 test was conducted on mortar bars made from specifically selected lithologies present in the sources. Petrographic analysis of thin sections of I-84 concrete and the AASHTO T 303 mortar bars helped identify specific rock types that experienced ASR within concrete. Thin sections were also examined from samples of cracked I-84 pavement subjected to a gel pat test (i.e., warm soaking in 1 M sodium hydroxide (NaOH)) for over 300 days.

Observations and Results

The vast majority of AASHTO T 303 expansion values on unmitigated Idaho aggregate exceed the 0.1 percent threshold. Only a few sources pass either the AASHTO T 303 or ASTM C 1293 test, however there are clear patterns in terms of both rock types and geography.

A more complete explanation of the geologic units and ASR potential is provided in this report. But in general, the following Idaho aggregate lithologies and locations are:

Very Highly Reactive for ASR:

- *Rhyolites of Miocene to Holocene age (i.e. < 23 Ma)*
    - Including obsidian, welded tuffs and volcanic glass.
    - Snake River Plain river canyons and adjoining volcanic highlands.
- *Siliceous quartzites and impure Sandstone*
    - Secondary quartz overgrowths and fine-grained, cherty matrix.
    - Central Snake River Plain (Wood River Valley?)
- *Pedogenic material*, such as opal and low-temperature silica.
- *Tuffaceous and volcanic-derived soil.*

Moderately Reactive for ASR:

- *Older Tertiary Rhyolites, Dacites* (Eocene age)
    - Challis Volcanics and subvolcanic porphyritic intrusives.
- *Precambrian quartzites and siltstones from the Belt Supergroup*
    - Exposed in northern Idaho and Lemhi and Custer County areas.
- *Other miscellaneous volcanics, metavolcanics and metamorphic rocks*
    - Seven Devils area, western Idaho and some in eastern Idaho.

Non-Reactive or Minimally Reactive for ASR:

- *Granitic rocks* of the Idaho Batholith or other unaltered intrusives.
- *Basalt*, including those basalts of the Columbia River Group and the younger Snake River Plain.
- *Sedimentary rocks* of southeastern Idaho (including limestones).

The Boise and Payette River watersheds have consistently lower AASHTO T 303 values (<0.20 percent) and many pass the ASTM C 1293 expansion limit of ≤0.04 percent. These two basins are dominated by granitic plutonic rocks, basalt and Eocene porphyries. In general, the highest quality aggregate is typically located within the modern flood plain or a younger, unweathered alluvial terrace unit. Fluvial aggregate deposits from the large drainage of the Snake River Plain have AASHTO T 303 values exceeding 0.4 percent expansion and contain significant amounts of young, reactive rhyolites as well as siliceous quartzites. Any material from these sources requires mitigation.

Petrographic analysis supported results of the lithologic inventories and spatial analysis. Basalt, granite, carbonates, and some higher grade metamorphic rocks exhibited minimal ASR-related cracking and expansion. Rhyolites of the Snake River Plain volcanic province in southern Idaho (<20 million years old) experienced the greatest cracking and expansion (AASHTO T 303 = 0.69 percent). Many of these units contain obsidian, volcanic glass, and cryptocrystalline silica. In comparison, older (Eocene) porphyritic rocks of rhyolite to intermediate composition experienced relatively less cracking and expansion, although AASHTO T 303 values were still high (0.45 percent). Pedogenic opal coatings formed on older gravel clasts can be chipped away from less reactive clasts during aggregate processing and end up in fine aggregate (FA). Certain cherty or silica-cemented quartzites, especially in the central Snake River Plain sources, also experienced ASR-related expansion and cracking. Petrographic examination and gel

pat solution chemistry suggest that silica leaching or partial dissolution may be a contributing problem, even without substantial ASR gel formation.

The only characteristic which this study examined was ASR. No attempt was made to tabulate or review other important properties such as hardness, durability, etc., which might render some of the units of low ASR potential less favorable for aggregate production and use.

Recommendations and Additional Research

This study highlights the importance of the development of a simple database that tabulates source material, ASR test results, mitigation used and other properties, including pavement and structure performance on each ITD project. Development and review of such a database would facilitate quality assurance and cost savings in the future.

This study identifies areas where quality aggregate is located. However, implementation of land use planning and discussions with counties and private land owners to ensure future access to high quality, low ASR potential aggregate in Boise and Payette River watersheds is important to safeguard these valuable resources.

Due to the variability and common occurrence of quartzite in aggregate sources, additional research is recommended on the differences in lithology, unit correlations, and ASR development of the various "quartzites" around Idaho. Additional petrography on Idaho quartzites and AASHTO T 303 testing would enhance understanding of the specific quartzites that are potentially reactive or non-reactive.

Lastly, implementation of special training for operators on recognition of duripans, pedogenic material, and other potentially deleterious material in their pits, and onways to remove it during processing could be a useful program.

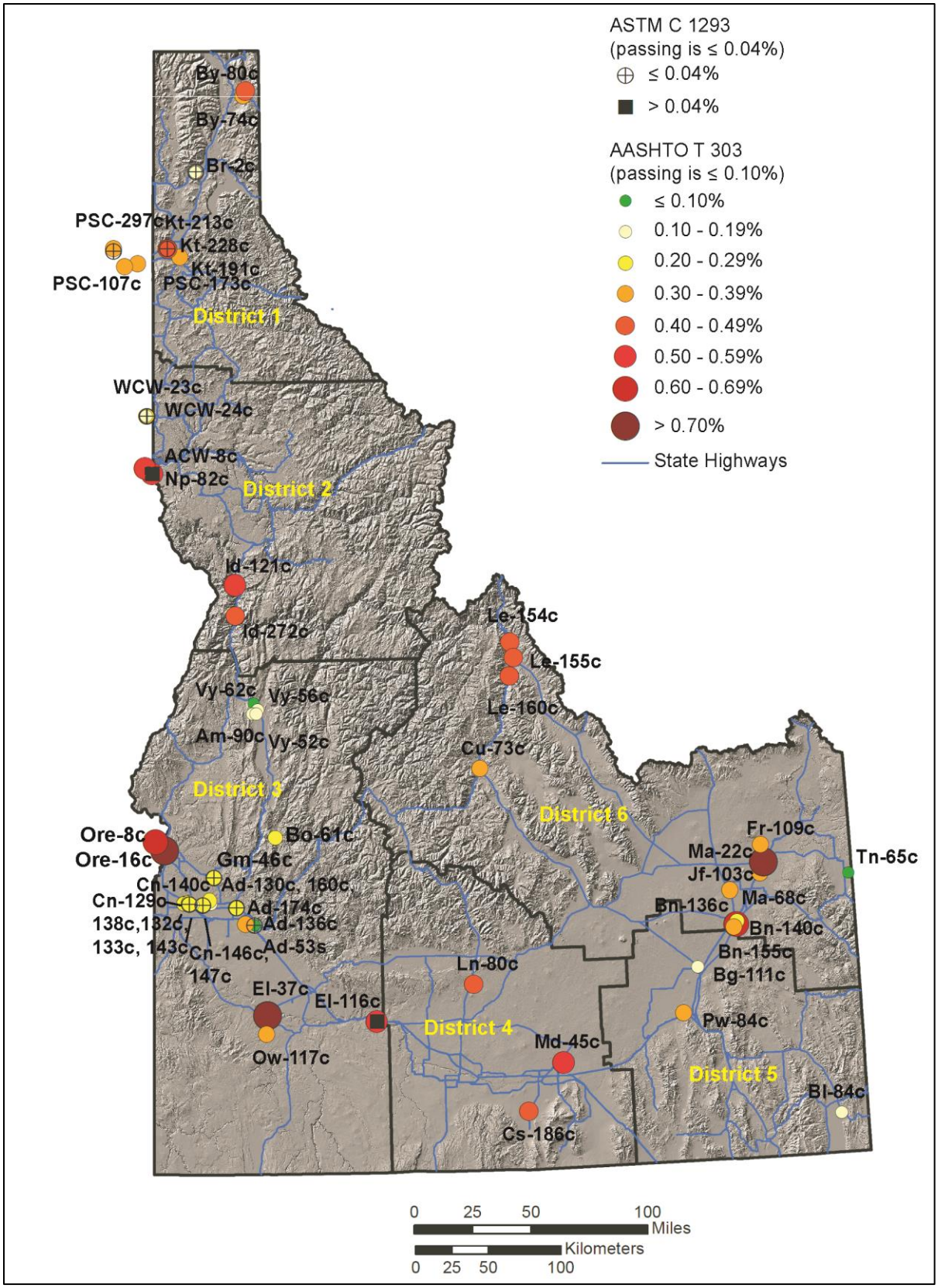

Figure 1. Map of Aggregate Sources, AASHTO T 303 and ASTM C 1293 Results

Chapter 1
Introduction

Many factors affect the durability and quality of concrete used for road and bridge construction by the Idaho Transportation Department (ITD) and local highway districts.[2] Poor quality concrete can lead to excessive wear, cracking, pitting, and other damaging/harmful circumstances.[3] While problems may sometimes be the result of improper methods of roadway construction and concrete manufacturing, the quality of the aggregate used in the concrete is a major influence on the durability and chemical stability of the concrete and road surface. Aggregates constitute 60 to 75 percent of the concrete volume (and more by mass), so they greatly affect the fresh and hardened properties of concrete, the mix design proportions, and economic factors.[3] Multiple national and international engineering specifications, such as American Association of State Highway and Transportation Officials (AASHTO) and American Society for Testing and Materials (ASTM) standards, have been developed to provide engineering guidelines for cement, aggregate, and concrete construction standards. Like other state and federal transportation entities, ITD has an extensive list of specifications and standards required for source certification to of concrete used in ITD projects. Still, lapses in wear and durability caused by premature cracking can require unforeseen and expensive road and bridge repairs. In Idaho, portions of I-84 developed premature cracking that required the treatment and partial replacement of large pavement slabs near the city of Mountain Home, Idaho (Figure 2). Aggregate for that section of the highway pavement was obtained from several pits in the Snake River Plain. Although mitigation was done, the fly ash used turned out to be unusually high in alkalis (Nottingham, personal communication) and cracks developed. A cause of this cracking was determined to be alkali-silica reactivity (ASR), one of the two types of alkali-aggregate reactions (AAR).[4,5]

In conjunction with the FHWA project study, Idaho Engineering and Geology, Inc. (IEG), on behalf of ITD, examined and evaluated various potential mitigation treatment measures, rates of cracking, and subsequent pavement ratings. IEG documented rates of increased cracking in both treated and un-treated I-84 concrete pavement slabs and noted substantial differences in widths and lengths of cracks in the surface of the concrete pavement slabs caused by differences in moisture and temperature (i.e. the overall differences were related to seasonal climate). In other words the physical degree of cracking of concrete surfaces can vary dramatically between summer and winter. Reed concluded that it was important to compare and evaluate rates of cracking of concrete surfaces during identical times of the year, and that some cracking is likely related to other properties of the aggregate and pavement conditions, such as weak, relatively porous aggregate (typically sedimentary) in freeze-thaw situations.[4,5] Subsequently, this section of I-84 was selected as a field site for a project sponsored by the Federal Highway Administration to look at mitigation and treatments for ASR-affected concrete.[5] As part of that multistate FHWA project, Thomas et al. and Giannini documented mitigation treatments on hardened concrete, and Tremblay described additional mitigation experiments and provided initial petrography on the pavement slabs.[6,7,8]

ASR is a chemical reaction between amorphous and cryptocrystalline silica (SiO_2) minerals or natural glass found in the aggregate and the alkali components [i.e., sodium (Na) and potassium (K)] present in

cement or other sources, such as weathering feldspars or alkali-rich fly ash used in secondary cementitious materials(SCMs).[9,3] Stanton first correlated expansive cracking with certain aggregates and alkalis in California during the 1930s and 1940s.[10] The reaction produces an alkali-silica gel which expands and cracks the concrete, reducing the service life of the structure.[10] The degree of ASR development varies widely, according to the type of aggregate, moisture and climate, exposure, cement type, mitigation (i.e. additives, sealers, etc.), and time. However the simplest and cheapest solution is to avoid using ASR-prone aggregate. A recent Federal Highway Administration (FHWA) report discusses ASR in transportation structures and its diagnosis and mitigation.[11]

Figure 2. I-84 Concrete Exhibiting Cracking Caused by ASR

Several standard tests, specifications and mitigation procedures have been developed to identify the potential for ASR in aggregate prior to construction.[11] These tests and mitigation protocols have been extensively documented in the technical literature and with the FHWA's Alkali-Silica Reactivity Development and Deployment Program established in 2006.[3,5,6,9,11,12,13,14,15] The AASHTO T 303, the most commonly used test, is an accelerated method designed to evaluate potential long-term expansion within only a few days by increasing the severity of the chemical attack in the testing lab above what could be expected in a natural environment. It measures expansion of a specially prepared concrete mortar bar that is soaked for 14 days in 1 M NaOH solution over a 16-day period. Another test is the ASTM C 1293 test. This test measures expansion of a concrete mortar bar that is prepared with NaOH added to the concrete mix and stored in a humid environment over a one-year period. Current regulations and specifications of ITD require sources to pass the AASHTO T 303 test (expansion

≤ 0.10 percent is passing). If a source fails the AASHTO T 303 test, the source may undergo the longer ASTM C 1293 test (expansion ≤ 0.04 percent is passing) or have a comparative geologic evaluation conducted by a registered professional engineer/geologist. If native aggregate does not meet the test limits or pass the geologic evaluation, it must be mitigated with additives, such as fly ash or lithium, prior to its use in concrete.[2] Other additives, or secondary cementitious materials (SCMs), are also being evaluated and developed nationally. The exact process of how SCMs reduce expansion is complex and poorly known and was not included in this study. The current study examined the geographic distribution and petrologic and mineralogic characteristics of natural aggregate in order to understand how it might behave in concrete and unmitigated mortar bars.

Aggregate quality, including properties of durability and chemical composition, is related to mineral composition, rock type, and geologic history. However, the relationship is not always obvious. For example, testing for ASR in concrete has shown conflicting results depending on the length and type of test, even on the same source. In Idaho, few sources pass the AASHTO T 303 test,and expansion values of Idaho aggregate vary widely from 0.02 up to 0.8 percent. However, several of the sources that fail the AASHTO T 303 test actually pass the year-long ASTM C 1293 test (e.g., Br-2c, Kt-213c, PSC-297c, Cn-146c, Gm-46c, Ad-130c and Ad-174c). Consequently, a better understanding of those sources which pass the ASTM C 1293 test but fail the AASHTO T 303 test, might improve future aggregate selection and source planning for Idaho's roadways. ITD sources are designated by a two-letter abbreviation of the county followed by a sequentially determined number and sometimes a lower case letter indicating ownership. For example, Kt-213c refers to Material Source No. 213 in Kootenai County, and it is commercially owned. Source Ad-136c is another commercially owned pit, located in Ada County.

Idaho's diverse geology provides significant lithologic differences and heterogeneity in aggregate used for road construction and related concrete structures by ITD and local highway districts. However a statewide geologic study with regards to ASR had not been done previously. It was proposed that a better correlation of ASR test results that are available in ITD source files with geologic characteristics, such as aggregate composition and clast lithology, in material sources around the state could help ITD determine the need and utility of 16-day versus 1-year testing procedures for specific sources or geologic regions. Identifying geologically-similar sources can also facilitate finding potentially better (i.e. lower ASR risk) material sources and perhaps save testing costs and time, as well as identifying aggregate most at risk for serious ASR-related problems. This study primarily uses a geological approach to identify potentially reactive (or nonreactive) aggregate across Idaho with the goal of assisting ITD to obtain higher quality aggregate and providing a cheaper and faster means of approving sources for use in concrete production.

Chapter 2
Methods

Lithologic Analysis Methods

Field Sampling Methods

Native, pit face and dredged aggregate, and ¾ in. minus stock material from 36 sources in Idaho, 2 sources in Oregon and 2 sources in Washington were sampled. Sampling procedures followed standards defined in Idaho IR-142. Three 40-60 pound sample bags were collected from each source; 2 samples were analyzed and 1 was archived. Only aggregate sources qualified for concrete production by ITD were selected for sampling; this was to compare each source's lithologic composition with its unmitigated AASHTO T 303 test, which is required for source baseline concrete certification and usage on ITD projects. During the field visit, the geologic setting of the source was noted and photographs taken of the pit walls.

Sample Processing Methods

Samples were manually screened through a 4 in. metal screen to separate + 4 in.-sized cobbles, and subsequently through a 1½ in. screen to separate +1½ in. cobbles. The remainder of the sample was mechanically sieved into size fractions shown in Table 2, according to AASHTO T 27/T 11. Samples were weighed before sieving to determine the total mass of the bulk sample. Each size fraction was weighed after sieving and the percent of the total mass per size fraction was recorded. Size fractions were washed, dried and stored in gallon-size storage bags. Size fractions too large to fit into gallon-sized bags were split using a mechanical splitter according to AASHTO T 248. However, +4 in. sized cobbles and 4 - 1.5 in. sized clast fractions were not split because the clasts were too large to pass through the mechanical splitter.

Lithologic Inventory Methods

A quadrat method was used to inventory coarse aggregate (>0.187 in. and <1.5 in. clasts) lithologies using a 10 in. x 10 in. wooden tray and a 10 in. x 10 in. quadrat (screen with 1 in. squares x 100). Standard rock and mineral identification methods were used to identify rock types, and clasts were organized in the tray according to rock-type. With the screen overlying the full tray, the number of squares covering a specific lithology were counted and recorded as a percentage of rock-type present in the size fraction (Figure 3; Table 2, Appendix A). For example, when 20 squares covered ½ in. quartzite in the tray, then 20 percent of the ½ in. size fraction was recorded as quartzite. Larger size fractions (>4 in. and >1.5 in. gravels) were inventoried simply by counting the number of lithologies and dividing by the total number of cobbles because of their large size.

Figure 3. Example of Quadrat Grid (left) and Inventoried Lithologies in Tray (right)

Samples of FA (<0.187 in.) were mechanically sieved for 10 minutes in a 12 in. diameter sieve into size fractions shown in Table 2. Fine aggregate samples were weighed before sieving and the percent of the total mass of each size fraction was documented. The FA was then split according to AASHTO T 248. After splitting, each size fraction was placed in a round 3 in. diameter tray and lithologies were identified and quantified under a microscope using percent abundance estimation charts.

Table 2. Aggregate Splitter Size Fractions

Sieve Number/ Designation	Sieve Size Opening (inches)	Sieve Size Opening (mm)
4 in.	4.0	100.0
1 ½ in.	1.5	37.5
1 in.	1.0	25.0
.75 in.	0.75	19.0
.5 in.	0.5	12.5
.375 in.	0.375	9.5
No. 4	0.187	4.75
No. 10	0.078	1.98
No. 16	0.0464	1.4
No. 20	0.0334	0.885
No. 35	0.0196	0.5
No. 60	0.0098	0.25
pan	<0.0098	<0.25

All size fractions were viewed under a long wave UV light (365 nm) and a shortwave UV light (254 nm) to identify pedogenic carbonate coats and amorphous silica, such as chert, opal and chalcedony. These minerals are known to fluoresce under UV light.[16] Under long wave UV light, pedogenic carbonate coatings are typically bright white. Under shortwave UV light, chalcedony, opal and pedogenic opaline

coatings produce greenish fluorescence; chert produces orange-colored fluorescence. The percent of fluorescent minerals per size fraction was estimated visually using percent abundance charts, and repeated for three times per size fraction. Percent abundance of the three estimates were averaged and the result recorded.

Results of the lithologic inventories and percentages of fluorescent minerals were organized by size fraction and input into a spreadsheet for fine and coarse aggregate (CA) at each source. The percent mass for each size fraction was applied in calculating a weighted average. For example, if 4 in. cobbles comprised 25 percent of the total mass of the sample and 25 percent of 4 in. cobbles were inventoried as quartzite then total 4 in. quartzite represents 6.25 percent of the total sample inventory (i.e., 0.25 x 0.25 = 0.0625). This information was used to produce bar graphs which illustrate the total lithologic composition of each aggregate source. Coarse aggregate inventories were graphed for multiple sources on a single graph in order to better compare them. A bar graph for each individual source was also created to compare variations between FA and CA lithologic inventories. These bar graphs also show a weighted 60% CA/40% FA blend for each source for comparison; a 60% CA/40% FA blend is typical of most concrete mixes. Figure 4 is an example of a bar graph showing lithologies of the CA, the FA, and the 60% CA/40% FA blend for an individual source. The AASHTO T 303 test result (in % expansion) is located after the source identifier code in the graph title.

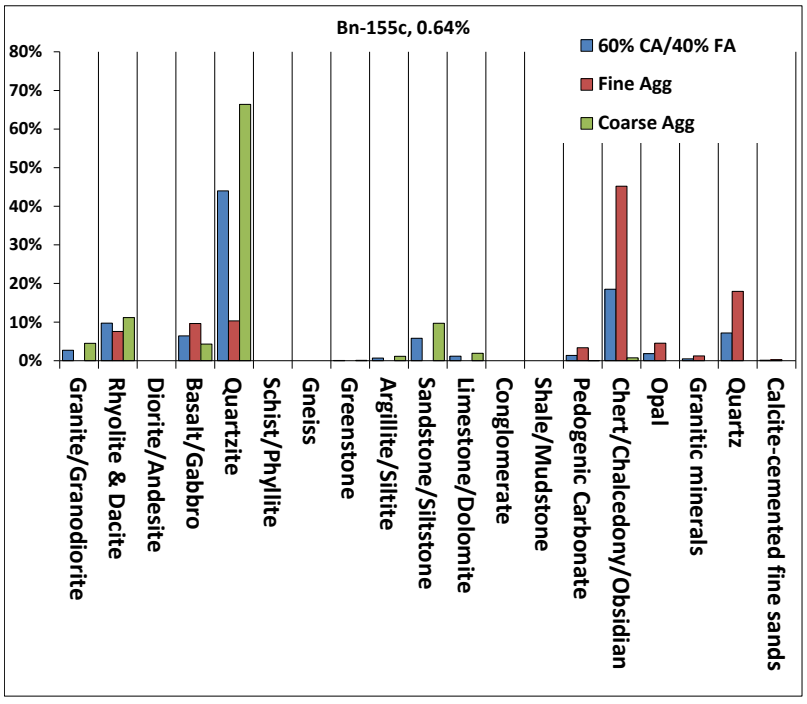

Figure 4. Example of Bar Graph Presentation of Source Lithologic Inventories

Petrographic and Laboratory Analysis Methods

Thin sections were made from 3 different concrete materials:

1. Field-cracked, ASR-affected I-84 concrete.
2. Slabs of identical I-84 concrete after soaking for 100-days in 1 M NaOH solution.
3. Mortar bars made from “suspect” lithologies.

Anhydrous thin section preparation was used to avoid possible washing away of ASR gel.[17] Sawed pieces of concrete and mortar bars were sent to Spectrum Petrographics, Inc., of Vancouver, WA, for commercial thin section preparation work, which included anhydrous grinding and polishing. Thin sections were mostly prepared with blue dye to help identify voids and cracking in the sections, such as that caused by ASR. Petrographic work and microphotography were conducted on these thin sections.

The I-84 thin sections were prepared from 4-inch diameter cores drilled from slabs of mildly cracked pavement removed from I-84, near Mountain Home. Cracking along this section of I-84 was reported to be caused by ASR deterioration.[4,5, 7 , 8] To accelerate ASR on the I-84 concrete cores, a modified gel pat test was used.[18] For the gel pat test four pieces of I-84 cores were cut, polished and immersed in 1M NaOH solution and placed in sealed plastic containers in 100°F oven for 200 days.[18] Thin sections for petrographic examination were then prepared from the gel pat tested concrete cores. Any indication of alteration was also recorded, such as the presence of white, powdery reaction product on clasts which waspresumed to be ASR gel.

To further evaluate potentially problematic source lithologies, those specific lithologies (i.e. rock types) were selected to be the aggregate for AASHTO T 303 mortar bar testing. These “designer” mortar bars were made from single or mixed lithologies that were suspected of being reactive. The desired rock types were crushed, sieved and weighed according to test specifications. This coarse aggregate sample was provided to Strata, a certified commercial testing lab in Boise, Idaho. Strata used the test aggregate to prepare a standard mortar bar and test its expansion during the AASHTO T 303 test. The lab was only provided with the sample number, and the lab had no knowledge of the aggregate composition. The ASR expansion results were reported to IGS in the usual graphical format. In addition, a control (cn) sample of the manufactured mortar was collected prior to its 16-day immersion in the NaOH solution. Thin sections were made from these mortar bars after completion of the AASHTO T 303 test and also from the same concrete (control sample) that did not undergo AASHTO T 303 test. The mortar bar thin sections were prepared by Spectrum using anhydrous procedures and a blue epoxy to make the cracking more visible. A few sections were also made from unmitigated mortar bars of specific source aggregate that were provided by Strata with permission of the source operator.

Geomorphic and Geographic Information System Analysis Methods

Thirty meter resolution digital elevation models and ArcGIS Spatial Analyst and Hydrology software tools were used to delineate drainage basins upslope of each sampling location.[19] Delineated upstream watershed basins provide topographic and geographic boundaries for gravels found in each aggregate source, i.e., alluvial gravels cannot travel beyond a drainage divide. The delineated drainage basin was used as a "cookie cutter" to clip mapped geologic units in Idaho within the basin area. Selection and clipping out only those geologic units exposed within a known drainage basin, enabled correlation of the individual lithologic inventories with the geologic units from where the aggregate may have come from in each source.[1] The ArcGIS steps used to delineate watersheds are described in Appendix B.

Chapter 3
Petrography and Laboratory Results

Introduction

Petrography is the study and formulation of detailed descriptions of rocks or, in this case, concrete. A number of methods can be used but in each case, the principal objectives are to determine the mineral content, textures, and chemistry of the components of rocks or concrete. The descriptions and methods can be at the macroscopic or microscopic scale, and petrographic observations are frequently the best way to truly identify the processes ongoing in a rock or slab of concrete. ASTM C 856 outlines standard procedures for petrographic examinations of hard concrete, and Fournier and others discuss petrographic examination as part of the diagnosis of ASR in transportation structures.[(11)] Petrography is somewhat qualitative, rather than strictly numerical, and requires considerable expertise and experience on the part of the practitioner.

A petrographic microscope is typically the starting point; it allows observations at 20 to 500 times magnification of a thin (typically 0.03 mm thick) slice of rock or concrete in order to view individual grains or particles. A unique system of dual polarizing lens which can be rotated into “uncrossed or plain light” and “crossed polarizing light” allows different minerals to be identified by the different ways in which each mineral’s internal structure alters the light being transmitted through the specimen on the microscope. For example, in Figure 5, there are 2 actual photos of the same image under the microscope. Figure 5a is photographed under plain or uncrossed polars and Figure 5b is photographed under crossed polars. With uncrossed polars, both quartz (SiO_2) and calcite ($CaCO_3$) are colorless, but under crossed polars, the quartz is a dull gray colar, but the calcite shows twinkly pastels. Other properties also help distinguish minerals. In addition to mineral identification, the in-situ petrographic examination is particularly useful to see textures and cross-cutting relationships, such as the presence of ASR gel or fractures, which may not be visible in hand specimen or field exposures. Advanced techniques such as a scanning electron microscope (SEM) or electron microprobe or x-ray diffraction can also be used for finer scale observations and chemical determinations.

Concrete Petrography Introduction

As a baseline for viewing thin sections of the ASR-affected concrete pavement and mortar bars, a thin section of a sample of freshly cured, “good” strong, laboratory-made concrete is shown in Figure 5. The matrix is dark and solid with no cracks and only minor air voids (about 2 percent). The aggregate from an unknown source included granitics, impure sandstone and minor limestone.

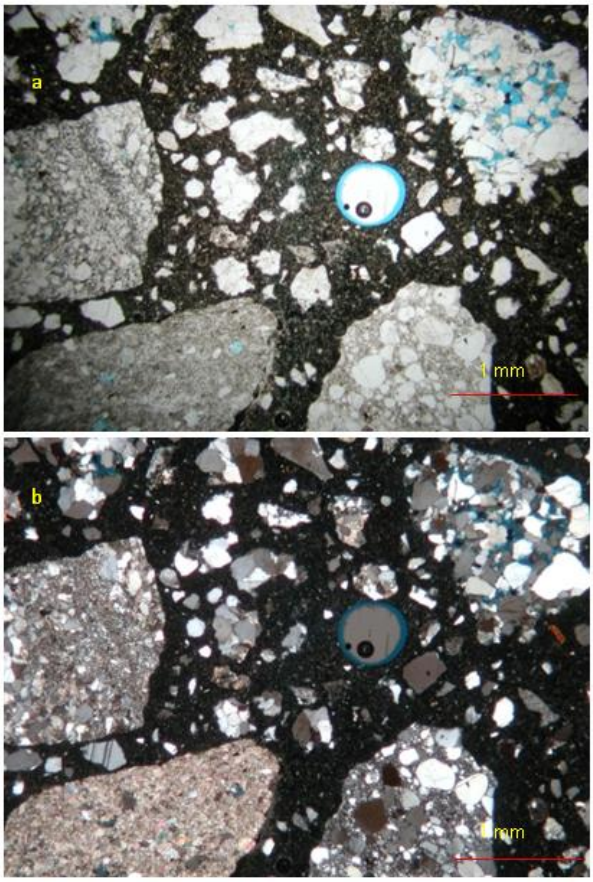

Figure 5a. DSCN9895_4GE006, Untreated Laboratory Test Concrete, CE341 to Specification, x20 Mag., Plain Light, Blue Epoxy

Figure 5b. DSCN9896_4GE006, Laboratory Test Concrete x20 Mag., Crossed Polars

Petrography of I-84 Concrete

In order to examine the aggregate used in the cracked portions of I-84 near Mountain Home, Idaho, a number of thin sections were prepared to study the different lithologies used in the concrete pavement. Samples of the cracked concrete were sawed from 4-inch diameter cores drilled by ITD from pavement slabs removed from I-84 and left in the Mountain Home maintenance yard. Figures 6 and 7 show only a few select representative examples from those sections. Rock types observed included obsidian (O), fine-grained chert (Ch), cherty quartzite (ChQ), and some puzzling round “spherules” of unknown material in the matrix.

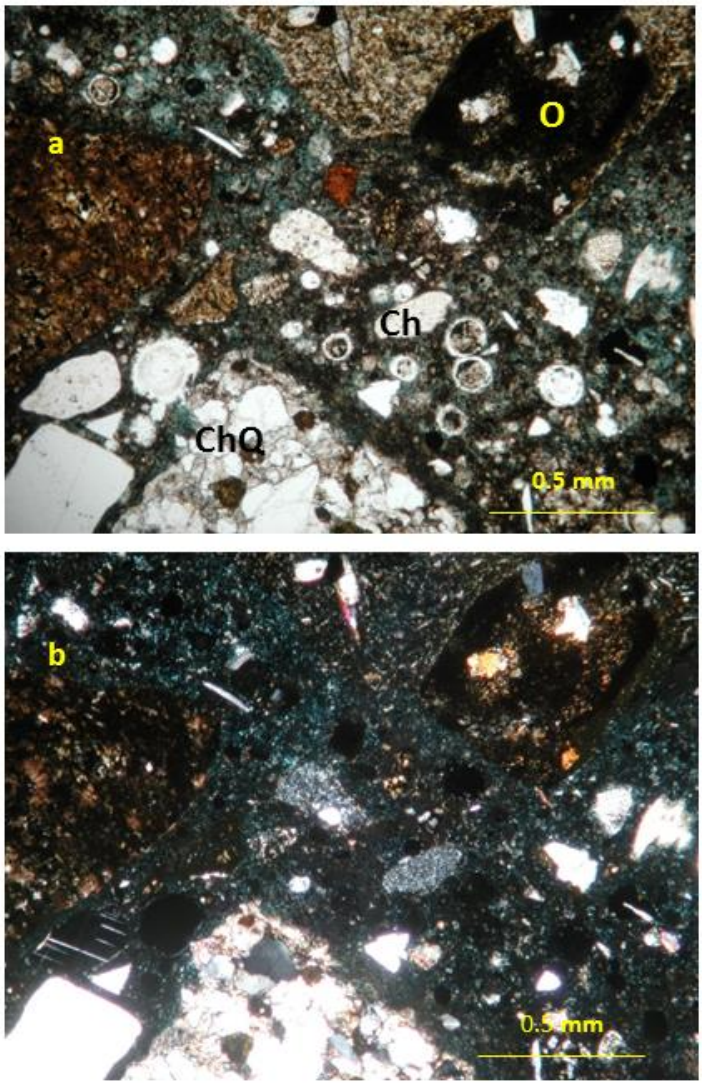

Figure 6a. DSCN9636_3ME010, Mountain Home Concrete Core MH3BTv2, x40 Mag., Plain Light

Figure 6b. DSCN9637_3ME010, Mountain Home Concrete, x40 Mag. Crossed Polarizing Light

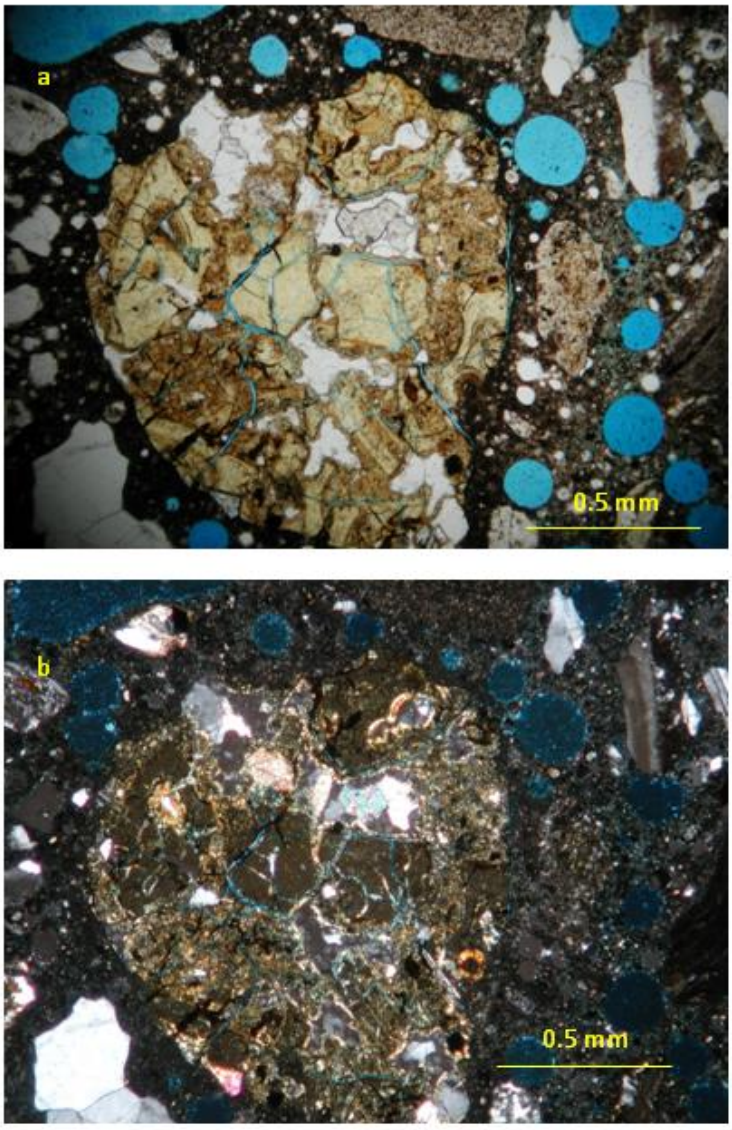

Figure 7a. DSCN9645_3ME012, Mountain Home Concrete Core, MH2aT1v, x40 Mag., Under Plain Light

Figure 7b. DSCN9646_3ME012, Mountain Home Concrete Core, MH2aT1v, x40 Mag., Crossed Polars

Notable features present in the several thin sections examined of the Mountain Home concrete included: an abundance of large, rounded (i.e. uncrushed) clasts, abundant voids and spherules in the paste, a few clasts of soil (i.e. pedogenic) material such as shown in Figure 7, and highly diverse lithologies composing the CA. These included welded tuffs, rhyolites, chert, cherty sandstone/quartzite, mudstone, mafic volcanics, tuffs and pedogenic material.

Gel Pat Test Results

Thin sections were prepared from the presumed ASR-affected Mountain Home 4-inch diameter concrete cores after 200 days in the 1M NaOH solution, and 3 pieces of the concrete were left in solution for another 100 days to further reaction progress and enhance the results. After removing the concrete cores that remained in solution for 300 days, the samples were allowed to air dry. Visual inspection of the concrete cores showed accumulation of white powdery material on specific clasts. This white powder is interpreted as ASR gel or a related reaction product. Figure 8 shows how the powder was specifically concentrated on phenocrysts of rhyolite porphyry clasts (marked with arrow). Only clasts of intermediate and felsic volcanics exhibited these powdery films. Figure 9 shows the darkened reaction rinds or coatings around intermediate and felsic volcanic rocks enlarged under the microscope (Figures 8, 9). Figure 10 shows a white rhyolite clast, approximately 1 mm in diameter, which actually cracked during the 300-day immersion in the NaOH solution. Many of the volcanic clasts were cracked and possibly altered to clay (Figures 8, 10). Quartzite and argillite clasts appeared to be visually unaffected after 300 days in solution. The matrix of the originally polished concrete cores was etched and pockmarked.

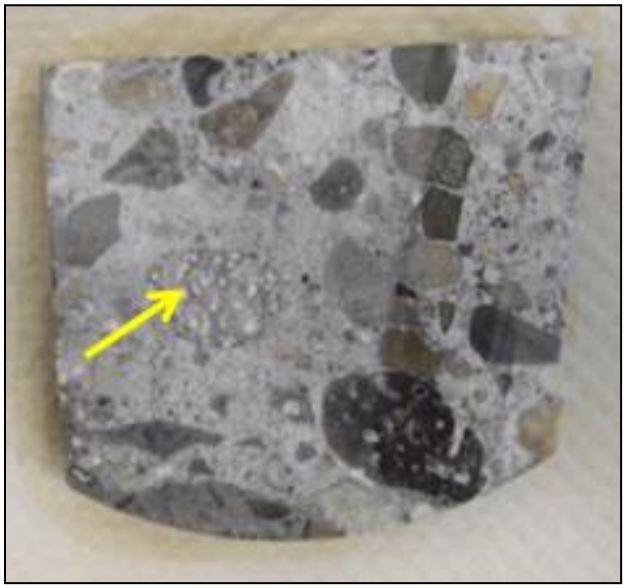

Figure 8. Core Sample After 300 Days in 1 M NaOH Solution

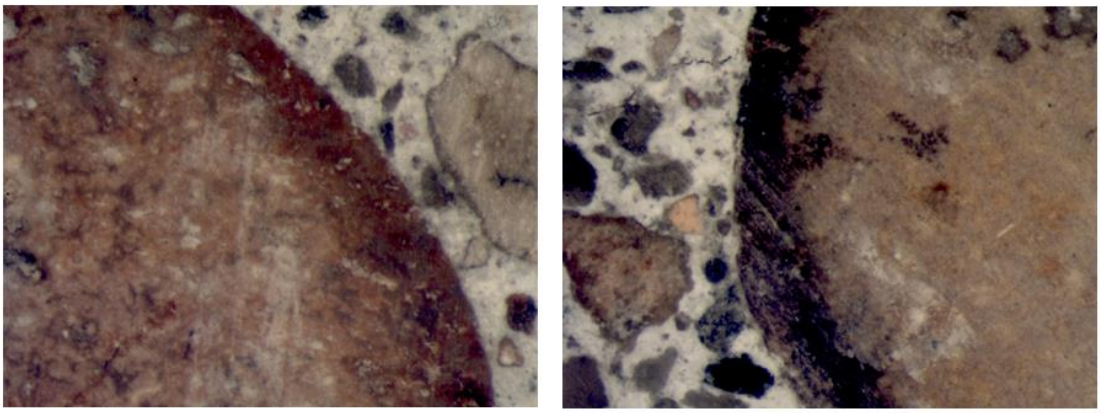

Figure 9. Magnified Images of Darkened Reaction Rims on Volcanic Clasts After 300 Days in Gel Pat Test Solution (1M NaOH)

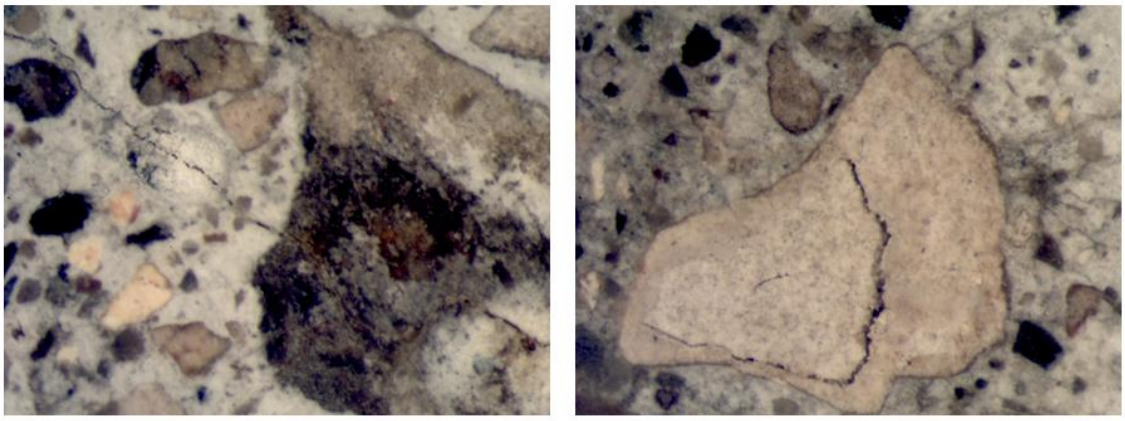

Figure 10. Magnified Images of Cracked Rhyolite Clasts After 300 Days in Gel Pat Test Solution (1M NaOH)

In thin sections prepared from samples immersed for 140 days in solution, dark rinds were seen on rhyolitic welded tuffs, as shown in Figure 11. The bluish color in the tuff clast is from the blue embedding epoxy and is interpreted as indicating thinning and possible dissolution of the rhyolitic matrix. However, adjacent basalt clasts in the lower right part of the photo are fresh with only a very thin crack separating the clast from the matrix (Figure 11).

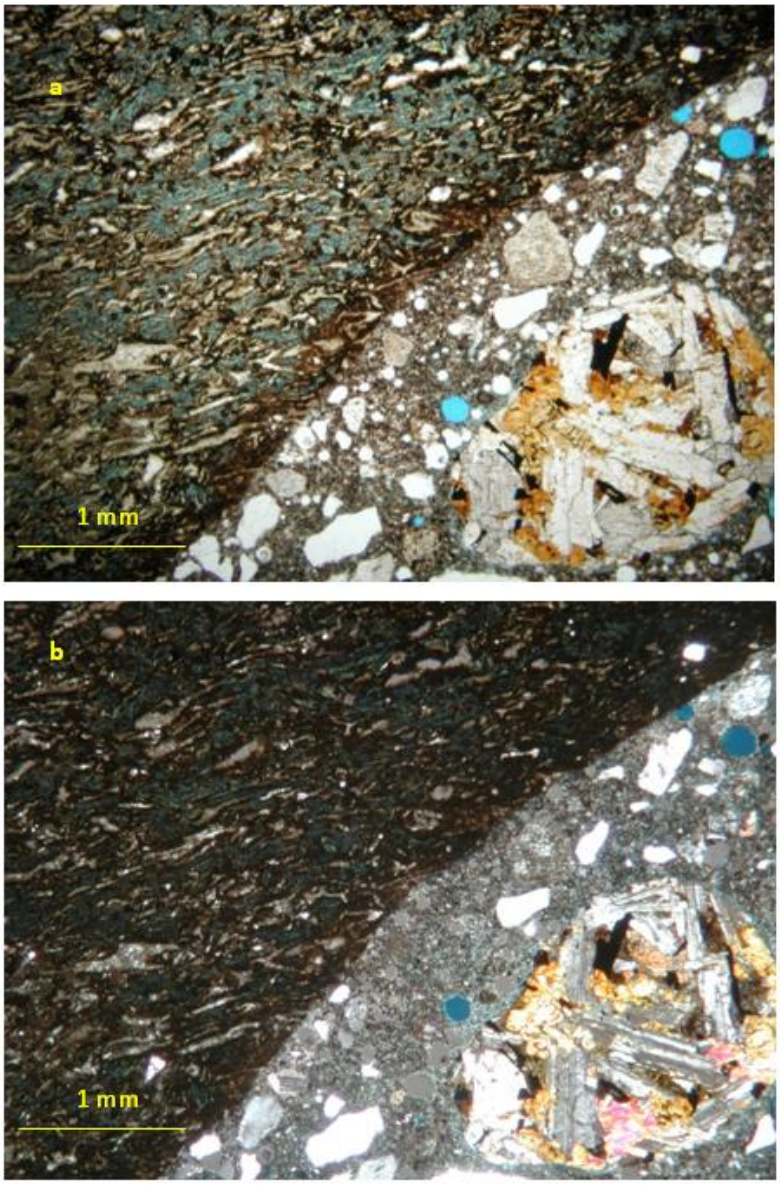

Figure 11a. DSCN9876_4GE003, Gel Pat Sample GP4a at x20 Mag., in Plain Light, After 140 Days in Solution

Figure 11b. DSCN9861_4GE003, Gel Pat Sample GP4a, Under x20 Mag., Crossed Polars

In 1 gel pat sample, shown in Figure 12, a very fine-grained siliceous matrix sandstone clast (lower right portion of Figure 12a) had an open crack, allowing the bright blue epoxy to show. Hemispherical (botryoidal-textured bits of gel) line the crack under high magnification. Multiple cracks were seen in the clasts and matrix of the sample. Quartz grains visible on the right side of the photo in Figure 13 show overgrowths of secondary quartz (Q) around the original detrital grains.

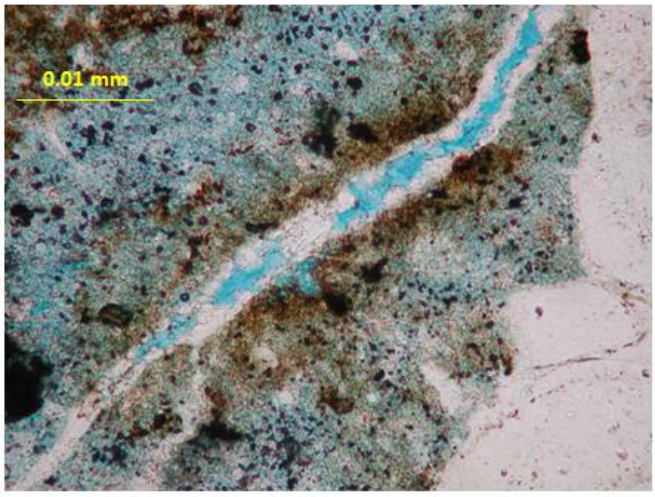

Figure 12. DSCN9870_4GE001, Gel Pat Sample GP1a After 140 Days in Solution

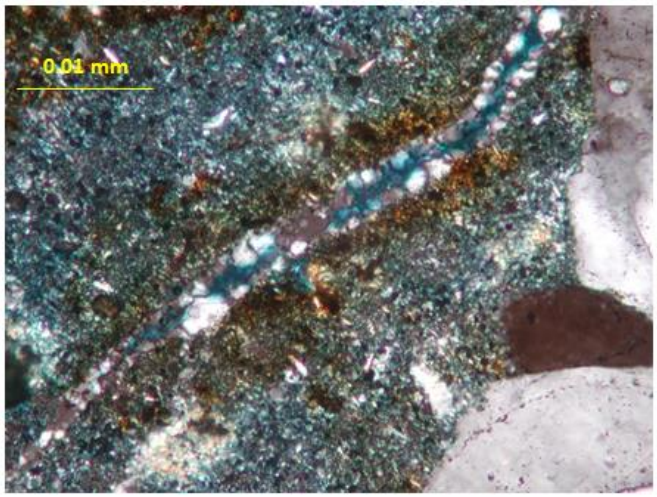

Figure 13. DSCN9871_4GE001, Gel Pat Sample GP1a After Soaking, Cross Polarized

Gel Pat Solution Chemistry

Samples of the immersion solution for the Mountain Home concrete cores were extracted at several times during the gel pat test. Observations of the 4 samples soaking in the 1 M NaOH solution showed a gelatinous white material floating in the solution by Day 30. The first solution sample was taken on Day 34 (October 24, 2012). Additional solution samples were extracted at 112 days, 141 days and 309 days (July 26, 2013) when the experiment ended. The slabs for thin sections were removed on Day 140 after the initial immersion. Solution compositions were chemically analysed by ICP-MS (Inductively Coupled Plasma Mass Spectrometer) at the Geosciences Department at Boise State University. Figure 14 shows those results. The most notable change in the solution composition is a huge increase in dissolved silica. Other elements show only very minor shifts from the initial 1 M NaOH composition. The solution pH

measured approximately 13 at day 400 in the remainder solution (90 days after all slabs had been removed).

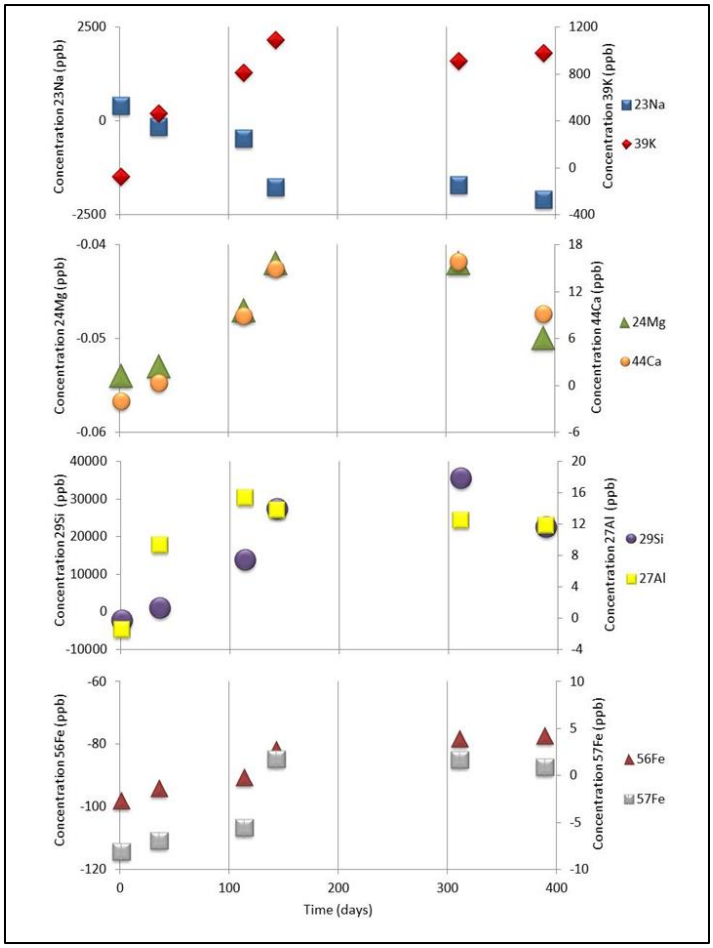

Figure 14. Chemistry of Aqueous Solution During Gel Pat Test

AASHTO T 303 Tests and Petrography of Mortar Bars

The experimental mortar bars are an excellent and convenient way to examine specific rock types under the microscope because they offer a “before-and-after” look at the artificially accelerated ASR process that occurs during the AASHTO T 303 test, which is required for concrete certification of new sources and for maintenance of concrete certification for older sources. These commercial mortar bars, if saved and analyzed petrographically, offer an inexpensive archive and documentation of the lithologies that are reacting and expanding during the testing period. Table 3 lists the project-designed mortar bars and their results from the commercial AASHTO T 303 tests.

The first mortar bar test was designed to compare volcanic versus sedimentary lithologies present in southwestern Idaho at material source pits with known ASR problems. Coarse and fine aggregate for Mortar Bar IGS-1 was made from crushed rhyolite from the Boise River terraces (Ad-53s and Ad-136c),

and crushed basalt and obsidian from Boise and Snake River Plain sources (Table 3; Figure 15). This mixture of volcanic lithologies had a high AASHTO T 303 expansion of 0.66 percent.

Coarse and fine aggregate for Mortar Bar IGS-2 was made from crushed conglomerate and argillite (El-116c) and crushed quartzite from Snake River Plain sources (El-116c, El-37c, Ore-8c and Ore-16c). This mixture of sedimentary and metasedimentary lithologies had a moderately high AASHTO T 303 expansion of 0.37 percent (Figure 15). The difference in the degree of visual cracking between the IGS 1 and IGS 2 mortar bars was readily apparent and correlated well with the expansion results. Figure 16 shows the more intense cracking on the IGS 1 bar which was extremely noticeable when the 2 bars were placed side-by-side. These first 2 bars were soaked for the standard 16-day trial.

Table 3. Summary of Mortar Bar Test Results

Mortar Bars			
IGS ID	**Lab ID**	**AASHTO T 303 % Expansion**	**Duration of AASHTO T 303 Test (Days)**
IGS-1	285	0.66	16
IGS-2	286	0.37	16
IGS-3	177	0.13	28
IGS-4	178	0.60	28
IGS-5	185	0.45	28
IGS-6	186	0.70	28

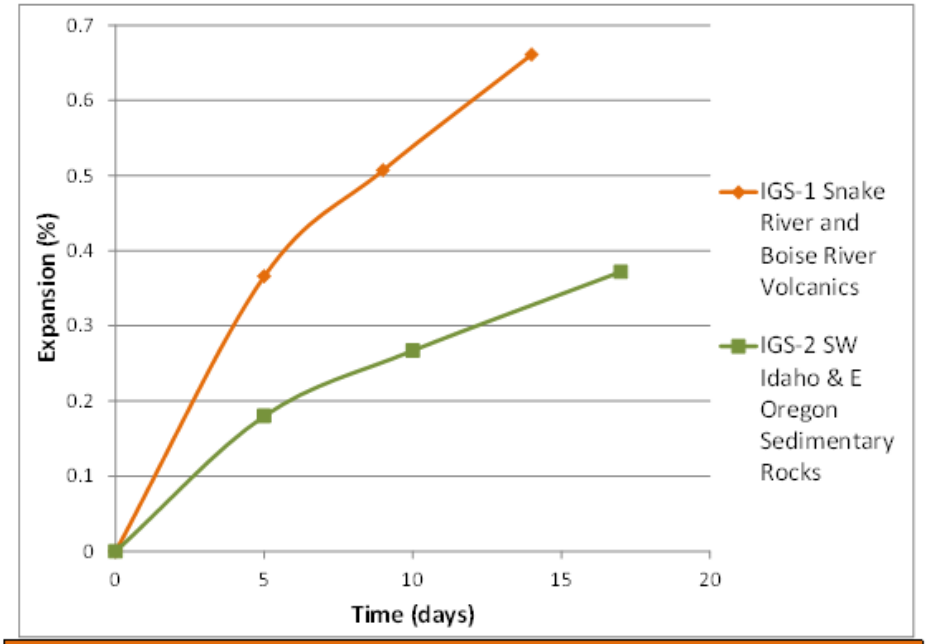

SAMPLE: IGS-1							
Sieve size	#8	#16	#30	#50	#100		
Size fraction weight (g)	99.00	247.50	247.50	247.50	148.50	990.00	
SAMPLE: IGS-1							% of mortar bar
Obsidian	33.00	57.39	28.45	17.55	12.35	148.74	15%
Rhyolite	33.00	98.68	113.15	130.80	79.00	454.63	46%
Basalt	33.00	91.43	105.90	99.15	61.08	390.56	39%
Total weight (g)	99.00	247.50	247.50	247.50	152.43	993.93	100%

SAMPLE: IGS-2							
Sieve size	#8	#16	#30	#50	#100		
Size fraction weight (g)	99.00	247.50	247.50	247.50	148.50	990.00	
SAMPLE: IGS-2						Sum	% of mortar bar
Quartzite	33.00	82.50	82.50	83.36	53.55	334.91	34%
Conglomerate	33.00	82.50	82.50	83.36	53.55	334.91	34%
Argillite	33.00	82.50	82.50	80.78	41.40	320.18	32%
Total weight (g)	99.00	247.50	247.50	247.50	148.50	990.00	100%

Figure 15. AASHTO T 303 Expansion of Mortar Bars (Upper Graph) and Composition of Mortar Bars (Lower 2 Tables)

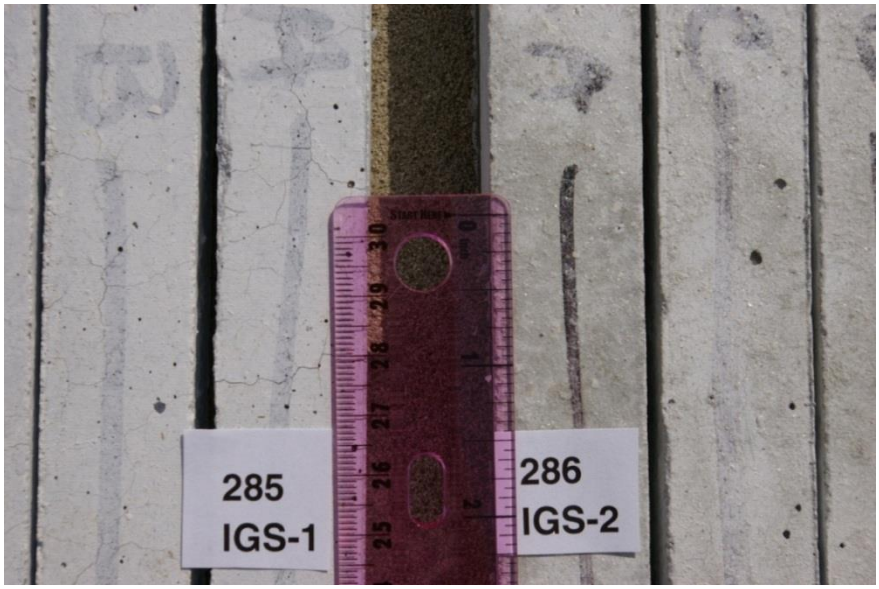

Figure 16. Mortar Bars IGS-1 and IGS-2 After AASHTO T 303 16-Day Expansion Test
IGS-1 Illustrates a More Intense Pattern of Cracking than IGS-2

For each AASHTO T 303 test, some concrete was reserved as a control sample to compare the same concrete before-and-after the AASHTO T 303 test. Petrographic comparison of the control sample (Figure 17) allowed for identification of alteration in specific lithologic clasts within the mortar bars. For IGS-1, the AASHTO T 303 tested bar showed notably more cracks in thin section with some clasts. In particular, aphyric (i.e. very,very fine-grained) volcanics appear to have partially dissolved so that the clast appeared bluish in color due to the blue epoxy behind the thin slice of concrete. Rhyolite and obsidian displayed the greatest amount of visual cracking and alteration in the post-AASHTO T 303 bar shown in Figures 18. While welded tuff and palagonite experienced cracking during the AASHTO T 303 tests, basalt showed only rare cracking. The single grains of coarse quartz in the FA were typically unaffected by the mortar bar test (i.e., no expansion, cracking, or dissolution were visibly observed).

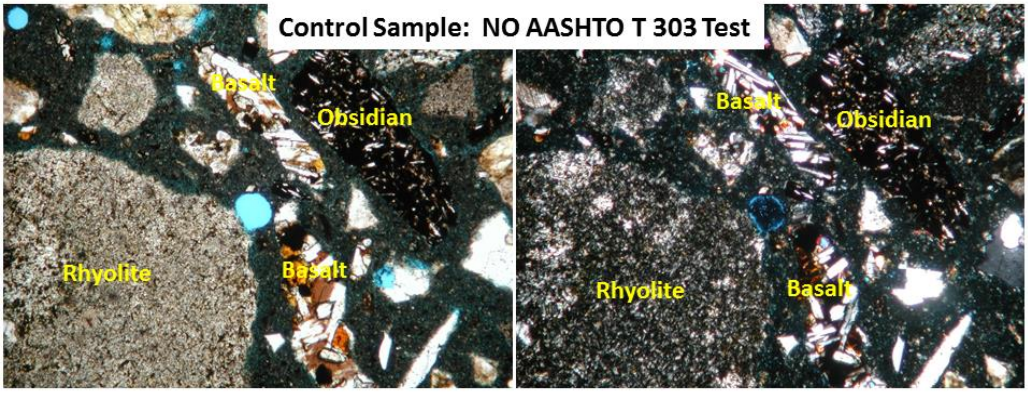

Figure 17. IGS-1 Control Sample (3ME001), at x40 Mag. in Plain
(DSCN9619 on Right) and Polarized Light (DSCN9620 on Left)

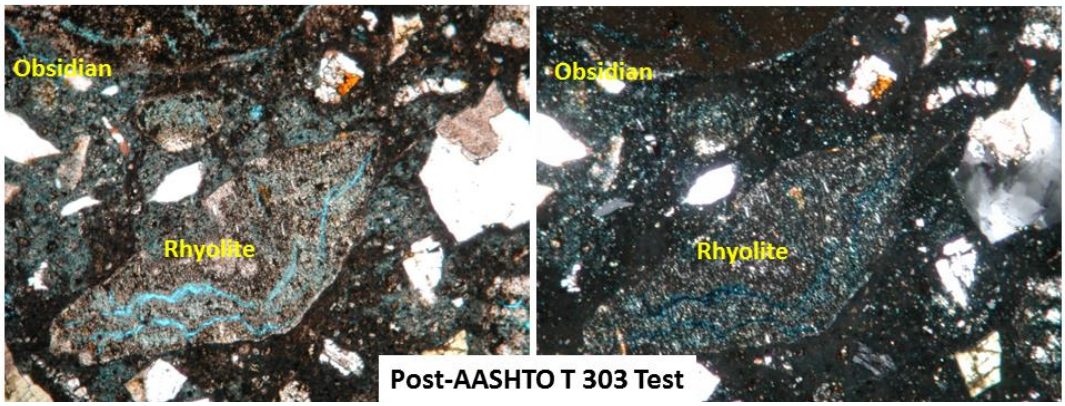

Figure 18. IGS-1 Mortar Bar CN285 (3ME005) After AASHTO T 303 Test (DSCN9621) Plain Light and DSCN9622 Polarized Light at x40 Mag.)

When compared to the same lithology in the control sample (Figure 17), rhyolite and obsidian clasts in the samples of the mortar bar subjected to the AASHTO T 303 are extensively cracked with the blue epoxy highlighting the cracks (Figure 18). Under higher magnification, as shown in Figure 19, the extensive cracking in the volcanic clasts is more apparent and some rhyolite clasts show dark reaction rims while the clasts have a bluish color interpreted to indicate potential dissolution and thinning of the clast matrix. However, a small clast of coarser-grained granite in the upper right corner of the photo is not affected by the test procedures.

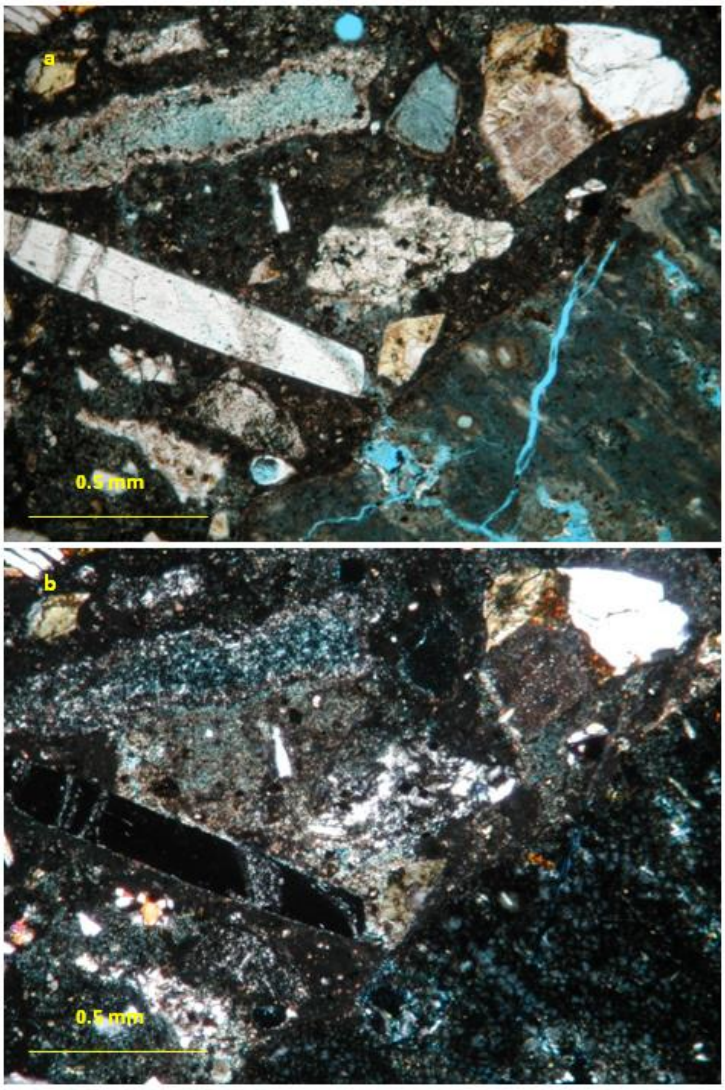

Figure 19a. DSCN9623_3ME005, Mortar Bar CN285 (IGS-1) After AASHTO T 303 Test, x40 Mag., Plain Light

Figure 19b. DSCN9624_3ME005, Mortar Bar CN285 (IGS-1) After AASHTO T 303 Test, x40 Mag., Crossed Polars

Post-AASHTO T 303 mortar bars made up of sedimentary and metasedimentary rocks (IGS-2) were not as fractured as their volcanic counterparts, however they still revealed significant impacts from the accelerated expansion testing. In comparison to the untested control sample of metasedimentary clasts, shown in Figure 20, the "quartzite" experienced the most cracking, plucking, and void formation during the NaOH soaking test, as indicated by the blue-colored epoxy zones shown in Figure 21. In particular, it was noted that many quartzites or well-lithified sandstones were actually composed of a fine-grained silica cement or matrix in between the larger detrital quartz grains. These cherty quartzites and impure silica-cemented sandstone clasts were the most affected with cracking or dissolution along the grain boundaries and disappearance of the rock matrix, such that part of the aggregate appeared blue. More

argillaceous or shale-like clasts were less affected. Strongly metamorphosed, pure quartzite with sutured boundaries was generally sparse and not as affected as the cherty quartzite. However, some quartz-rich fragments showed brittle fracturing which was possibly accentuated by ASR. The concrete matrix typically contains round air holes or "vugs" and in the post-testing sample these are partially filled with crescents of gray material which has the optical properties and appearance of ASR gel (Figure 21).

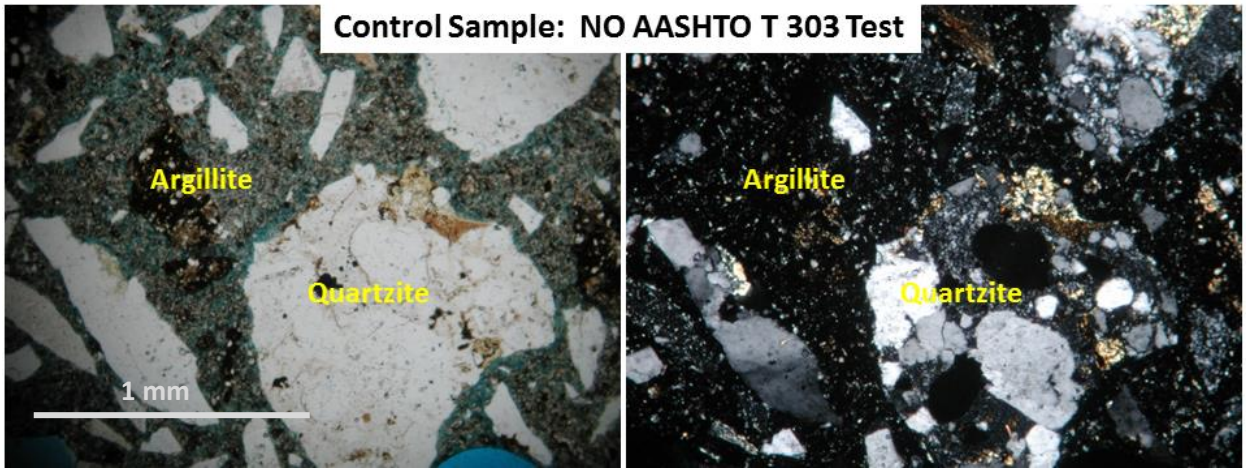

Figure 20. IGS-2 Concrete Control Sample (CN286, 3ME002). Photo DSCN9630 on Left in Plain Light and DSCN9631 on the Right in Polarized Light at x40 Mag.

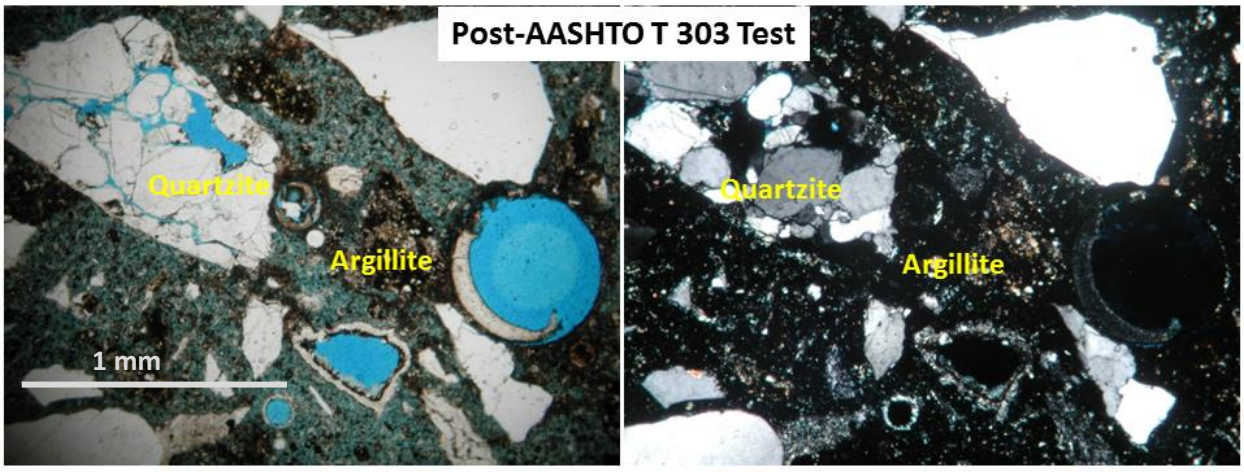

Figure 21. IGS-2 Mortar Bar CN286 After AASHTO T 303 Test (Section 3ME007) DSCN9634 in Plain Light On the Left and DSCN9635 in Polarized Light, x40 Mag. On the Right

A second set of the designed mortar bars (IGS-3 and IGS-4) was made to attempt to evaluate the potential effect of the "caliche" or pedogenic carbonate coatings observed on gravels in several material pits in Ada County where the overall material is similar. In general, most pedogenic carbonates are composed of calcite which precipitates, sometimes along with opal or chalcedony, on the bottoms of clasts and in layers, locally forming a hardpan (duripan) surface. It is a common secondary deposit in the

Snake River Plain geographic area and can form in basalt, gravels, loess (wind-blown dust deposits), and soil. Figure 22 shows the compositions of the mortar bars and the AASHTO T 303 test results.

IGS-3 was prepared with pedogenic (soil-related) carbonate precipitated on sand grains at Ad-136c. IGS-4 was made from FA at Ad-53s where the geology consists of a well-developed pedogenic carbonate horizon formed in silty units and coarse gravels, representing river gravels interbedded with floodplain deposits. Both IGS-3 and IGS-4 also contained crushed, non-reactive basalt from stockpiles at Ad-53s and underwent a 28-day AASHTO T 303 test (instead of the standard 16-day testing length). Though it is unlikely that concrete would be made solely of this pedogenic material, several field sites (e.g., Ad-136c, Ad-53s, El-116c, Le-154c, Ow-117c) have abundant pedogenic carbonate coatings present on more durable aggregate clasts. This raised the question whether these coatings would increase potential for ASR.

The IGS-4 mortar bar made from pedogenic carbonate formed on silty deposits at Ad-53 experienced a high expansion of nearly 0.60 percent at the end of the 28-day test (Figure 22). However, the IGS-3 mortar bar composed of pedogenic carbonate formed on sand at Ad-136 only experienced 0.13 percent expansion after 28-days and would have passed the 16-day version of the AASHTO T 303 test as it only had expanded 0.08 percent. The great variation in the shape of the two curves for somewhat similar material is notable, but the major difference was the type of sediment composing the clasts with the silt probably being softer.

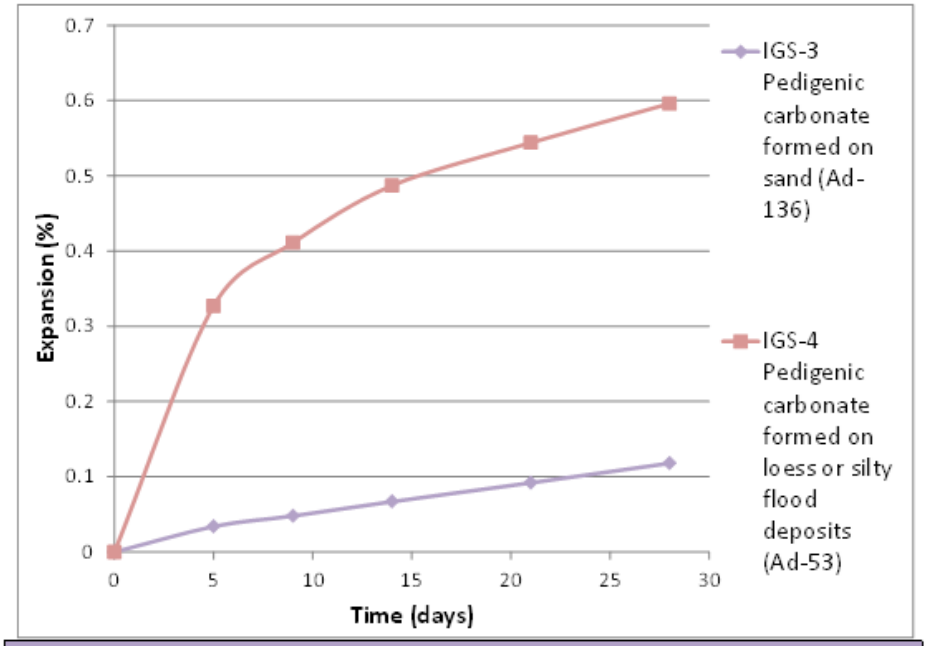

SAMPLE: IGS-3							
Sieve size	#8	#16	#30	#50	#100		
Size fraction weight (g)	99.00	247.50	247.50	247.50	148.50	990.00	
SAMPLE: IGS-3						Sum	% of mortar bar
Ad-136 sandy ped-carbonate	49.50	123.75	123.75	123.75	74.25	495.00	50%
Crushed basalt (Ad-53c)	49.50	123.75	123.75	123.75	74.25	495.00	50%
Total weight (g)	99.00	247.50	247.50	247.50	148.50	990.00	100%

SAMPLE: IGS-4							
Sieve size	#8	#16	#30	#50	#100		
Size fraction weight (g)	99.00	247.50	247.50	247.50	148.50	990.00	
SAMPLE: IGS-4						Sum	% of mortar bar
Ad-53 ped carbonate on loess	49.50	123.75	123.75	123.75	74.25	495.00	50%
Crushed basalt (Ad-53c)	49.50	123.75	123.75	123.75	74.25	495.00	50%
Total weight (g)	99.00	247.50	247.50	247.50	148.50	990.00	100%

Figure 22. AASHTO T 303 Expansion of IGS-3 and IGS-4 Mortar Bars (Upper Graph) and Composition of Mortar Bars (Lower 2 Tables)

As shown in Figure 23, mortar bar IGS-3 was composed largely of 2 rock types for CA, brown muddy sand and inert basalt, plus a few carbonate clasts and fine quartz sand aggregate. The control sample showed an especially air-rich matrix and clasts that were already cracked without any ASR-related processing, possibly due to the mortar bar manufacturing process. Figure 24 shows the post-AASHTO T 303 test sample with greatly enlarged cracks in the sandstone clasts and matrix. Approximately 50 percent of the muddy sandstone was cracked, but basalt clasts were unaffected. This suggests that cracking in IGS-3 mortar bar was due to the softness of the material and poor thin section preparation rather than ASR.

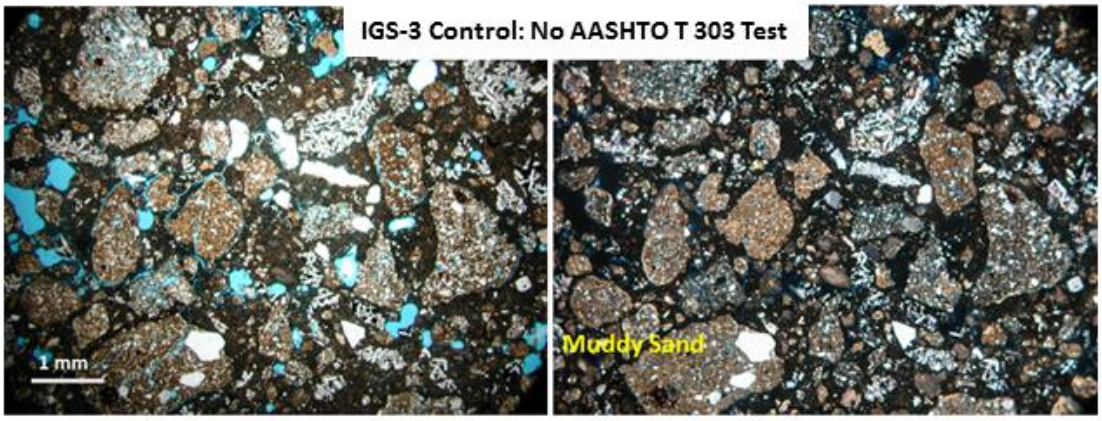

Figure 23. IGS-3 Concrete Control Sample (IGS-3CN, 4PB001) in Plain Light (Left, DSCN9898) and Polarized Light (Right, DSCN9899) in Blue Epoxy at x20 Mag.

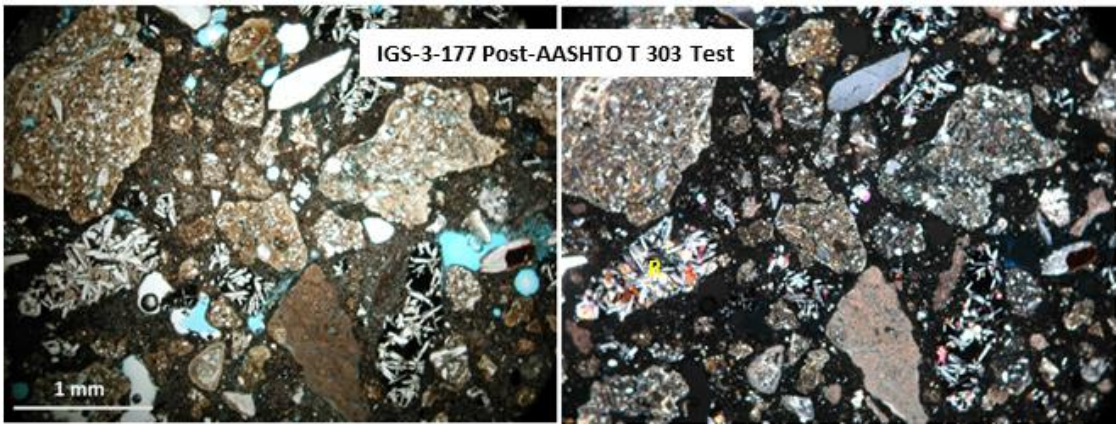

Figure 24. IGS-3-177 Concrete Mortar Bar After 28-Day AASHTO T 303 Test (Section 4PB002), DSCN9903 On the Left and DSCN9904 On the Right, x40 Mag.

IGS-4 contained a more diverse group of clast than IGS-3, and the matrix was characteristically denser with a gray to brownish gray color. IGS-4, as shown in Figure 25, was composed of approximately 50 percent inert basalt (B), some granite (GR, stains yellow for potassium feldspar), FA (quartz grains), 10 percent soft brown sandstone, carbonate (C), rhyolite and rhyolite porphyry (P). Figure 26 shows the IGS-4 (CN178) mortar bar after completion of the AASHTO T 303 test. It exhibited large cracks through the matrix and some clasts. Rhyolite (a fairly small percent of the sample) was most affected by the AASHTO T 303 test, showing a bluish color which is interpreted as partial dissolution of the silica in the rhyolite. Under the higher magnification view of Figure 27, additional cracking is apparent in the IGS-4 post-testing sample. Cracks cut the groundmass mortar (indicated with a blue arrow) and extend across the blue-tinged matrix of the rhyolite porphyry but not into a feldspar phenocryst. Granite (GR) showed only minor cracking, and basalt (B) was unaffected. One slab of pedogenic carbonate (C) was also cracked. In general, the pronounced difference in expansion between IGS-3 and IGS-4 seems most correlative to the difference in amount of the brownish muddy sand clasts which composed almost half of IGS-3. Basalt and granite clasts showed little ASR-related expansion or cracking.

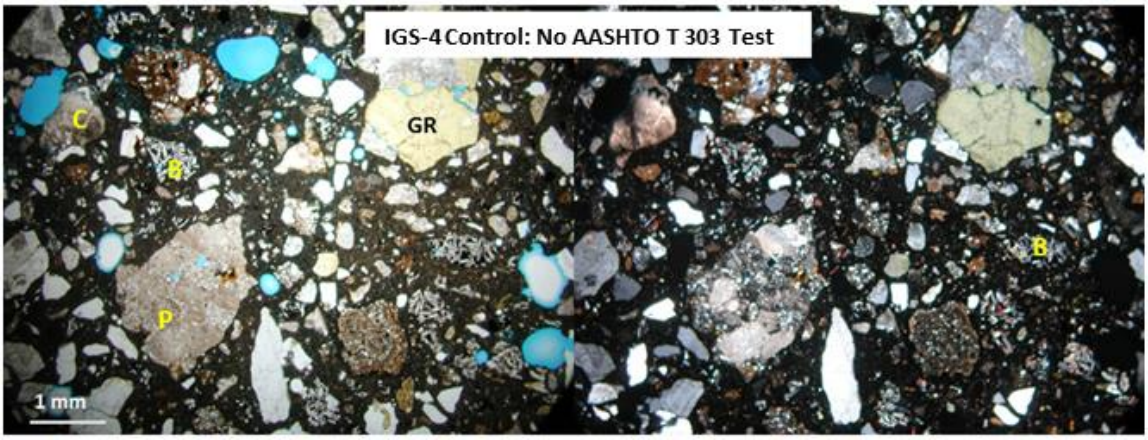

Figure 25. IGS-4 Concrete Control Sample (4PB003) Before AASHTO T 303 Test (DSCN9907 On the Right and DSCN9908 On the Left at x20 Mag.)

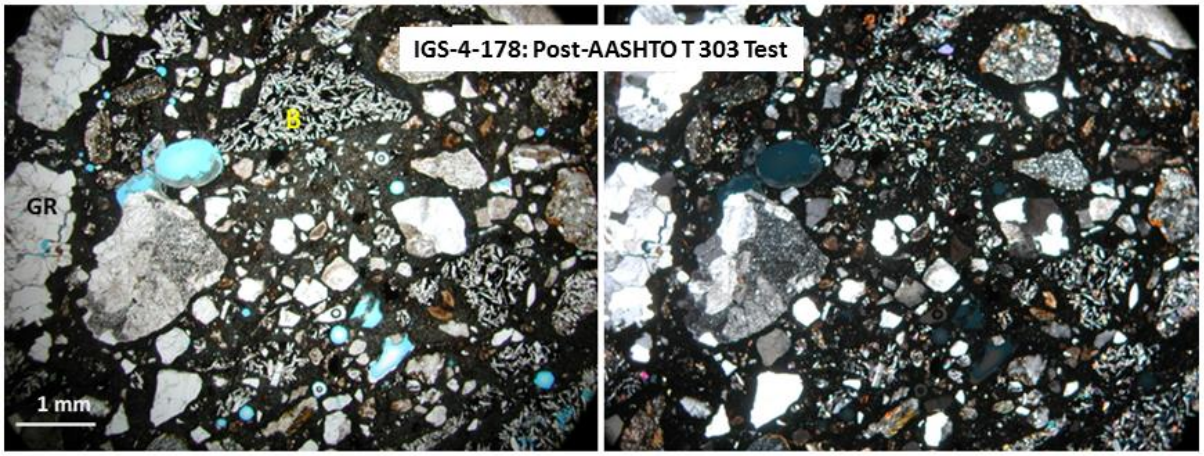

Figure 26. IGS-4-178 Mortar Bar After 28-day AASHTO T 303 Test (Section 4PB004 at x20 Mag.; DSCN9909 On the Right and DSCN9910 On the Left)

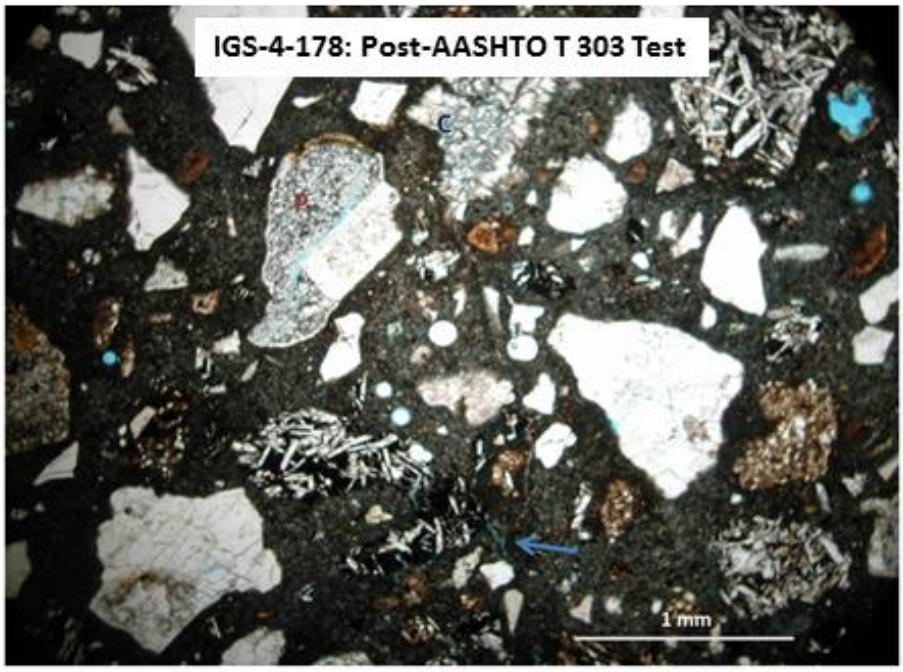

Figure 27. IGS-4-178 Mortar Bar After 28-Day AASHTO T 303 Test with Greater Magnification (Section 4PB004; DSCN9912) x40 Mag.

A third set (IGS-5 and IGS-6) of mortar bars was made to examine different types of rhyolites seen in the source aggregates and of different geologic distribution and type. These two rhyolite-rich mortar bars underwent the 28-day AASHTO T 303 test. Figure 28 lists their composition and illustrates the results of the AASHTO T 303 tests. Coarse and fine aggregate for IGS-5 came from crushed rhyolites found in the active Boise River channel. The geomorphic unit and lithologic character of the Boise River rhyolite cobbles indicate an origin from the Eocene Challis Volcanics Group exposed north and east of Boise. Coarse and fine aggregate for IGS-6 came from crushed rhyolites collected at source Ow-117c in Owyhee County on the south side of the Snake River Plain and is likely of Miocene or Pliocene age (Figure 28). Both mortar bars failed the 16-day test and the 28-day test (Figure 28), but rhyolite from the Snake River Plain (IGS-6) experienced significantly more expansion (0.70 percent) than rhyolite from the Boise River gravels (IGS-5, 0.45 percent). The slope of the IGS-6 expansion curve during the reaction was noticeably steeper and more linear for a longer time than the other samples. In thin section, the rhyolite mortar bar samples were visually more cracked than for the IGS-3 and IGS-4 samples, which contained non-reactive basalt that was not added to IGS-5 or IGS-6.

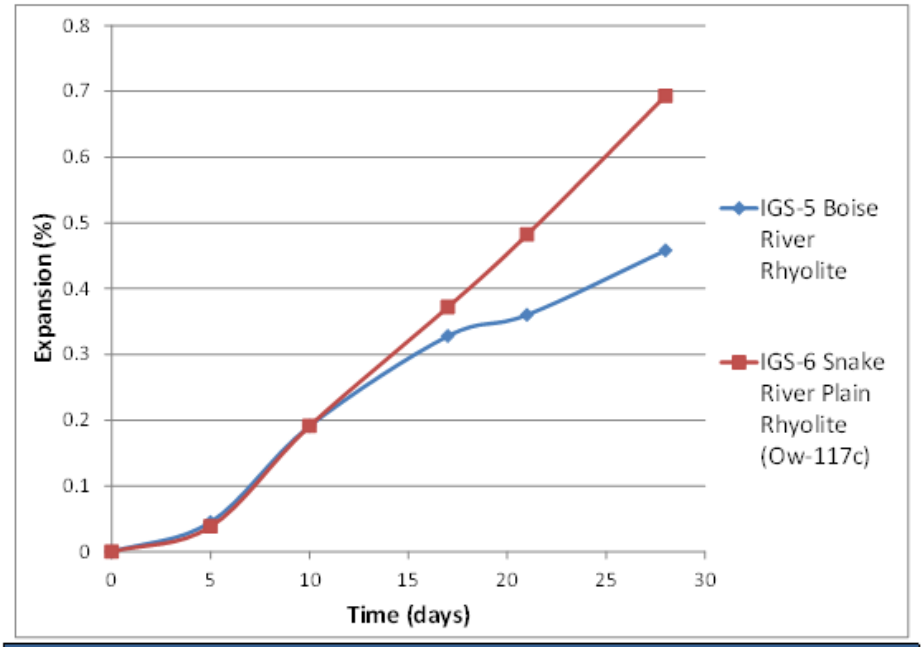

SAMPLE: IGS-5							
Sieve size	#8	#16	#30	#50	#100		
Size fraction weight (g)	99.00	247.50	247.50	247.50	148.50	990.00	
SAMPLE: IGS-5						Sum	% of mortar bar
Boise River Rhyolites	99.00	247.50	247.50	247.50	148.50	990.00	100%
Total weight (g)	99.00	247.50	247.50	247.50	148.50	990.00	100%

SAMPLE: IGS-6							
Sieve size	#8	#16	#30	#50	#100		
Size fraction weight (g)	99.00	247.50	247.50	247.50	148.50	990.00	
SAMPLE: IGS-6						Sum	% of mortar bar
Ow-117c Rhyolites	99.00	247.50	247.50	247.50	148.50	990.00	100%
Total weight (g)	99.00	247.50	247.50	247.50	148.50	990.00	100%

Figure 28. AASHTO T 303 Expansion of Rhyolite-Rich IGS-5 and IGS-6 Mortar Bars (Upper Graph) and Composition of Mortar Bars (Lower 2 Tables)

In a thin section of the IGS-5 control sample, the Boise River rhyolite clasts were fractured in a distinctive elongate shape (Figure 29). The IGS-5 rhyolite was very distinctive petrographically due to its abundant porphyry (P) texture and yellow-stained, potassium feldspar rich composition. In addition, many clasts had abundant granophyric or micropegmatite intergrowths which indicate a subvolcanic environment of emplacement and crystallization as expected for the Eocene volcanic suite (Figure 29). The granophyre has a feathery appearance in the photos. Subsequent to the AASHTO T 303 test, the reacted mortar bar clasts showed moderate to strong cracking, highlighted with blue arrows in the photos, of the clasts, with many cracks extending into and darkening the matrix (Figure 30). Some of the cracks show a dark alteration envelope around them. The porphyritic textures are greatly degraded.

Approximately a quarter of the clasts show cracking and some are semidissolved but only minor gel was observed.

Figure 29. IGS-5 Concrete Control Sample Prior to AASHTO T 303 Test (Section 4PB0005, DSCN9916 and DSCN9917) at x40 Mag.

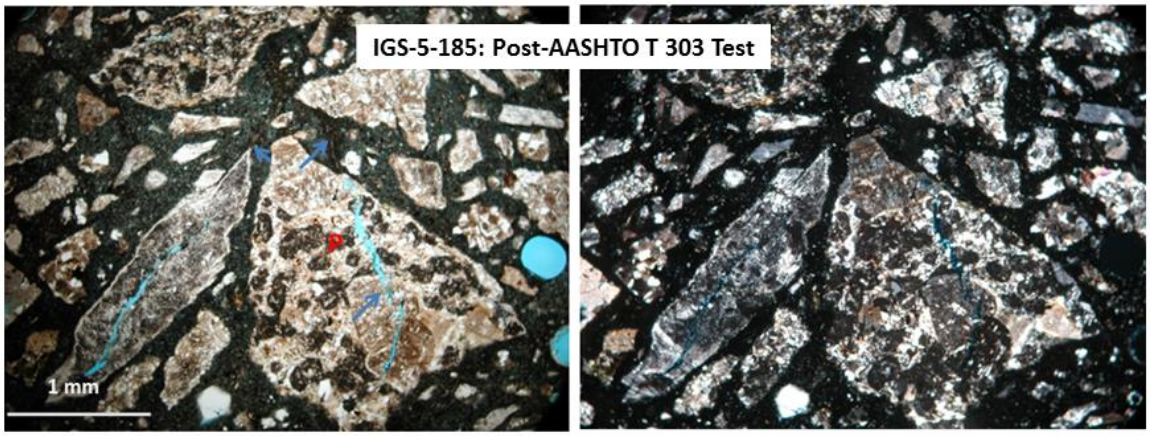

Figure 30. IGS-5-185 Mortar Bar After 28-Day AASHTO T 303 Test Showing Moderate to Strong Cracking (Blue Arrows) which is Highlighted by Blue Epoxy (Section 4PB006, DSCN9924 and DSCN9925) at x40 Mag.

In contrast, IGS-6, which is made up of rhyolites collected from the Snake River Plain, contains very different rhyolite clasts than the rhyolite clasts from the Boise River Basin. These rhyolite (R) clasts are very fine-grained, non-porphyritic and contain spherulites suggestive of devitrified volcanic glass (Figure 31). Very few porphyritic clasts were seen. The post-AASHTO T 303 mortar bar for IGS-6 displayed a wide zone of very intense cracking with wide open cracks extending in elongate directions especially and from clasts into matrix (Figures 32 and 33). Many of the rhyolites showed a very pronounced blue color, interpreted as partial dissolution of the silica-rich rock, such that the blue epoxy shows through the section (Figures 32 and 33). Some of the clasts also showed a light-colored reaction rind. The cracking was most intense on one edge of the section, perhaps because that was the edge in

most contact with the NaOH solution. Rhyolites are typically over 75 percent SiO_2 in composition and any dissolution would release silica.

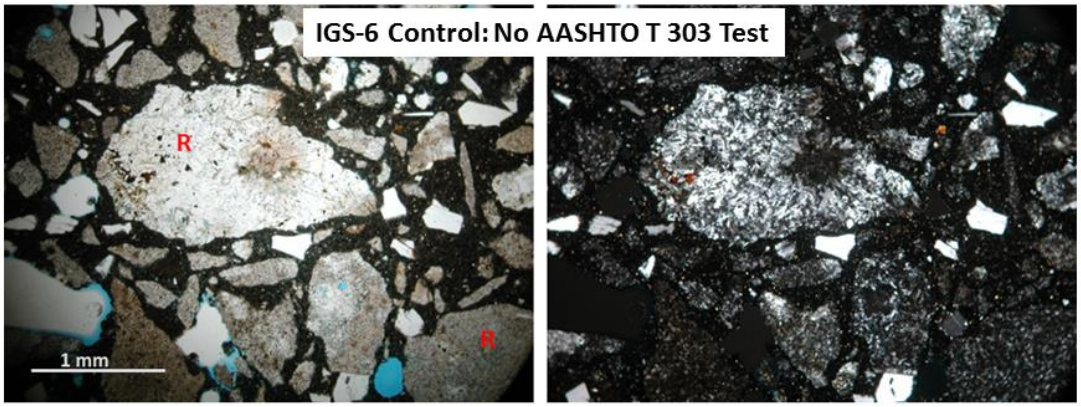

Figure 31. IGS-6 Concrete Control Sample (Section 4PB007; DSCN9928 on the Left and DSCN9929 On the Right), Prior to Testing at x40 Mag.

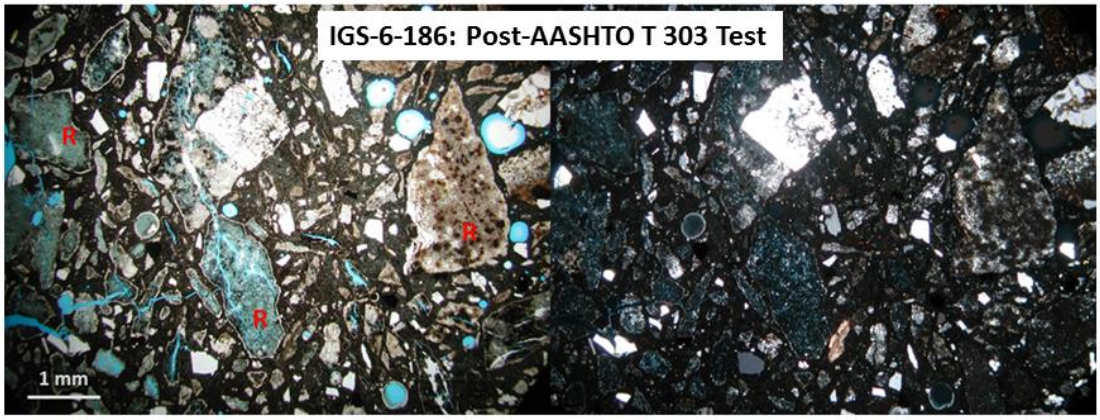

Figure 32. IGS-6-186 Mortar Bar After 28-Day AASHTO T 303 Test (Section 4PB008 at x20 Mag., DSCN9930 On the Left and DSCN9931 On the Right)

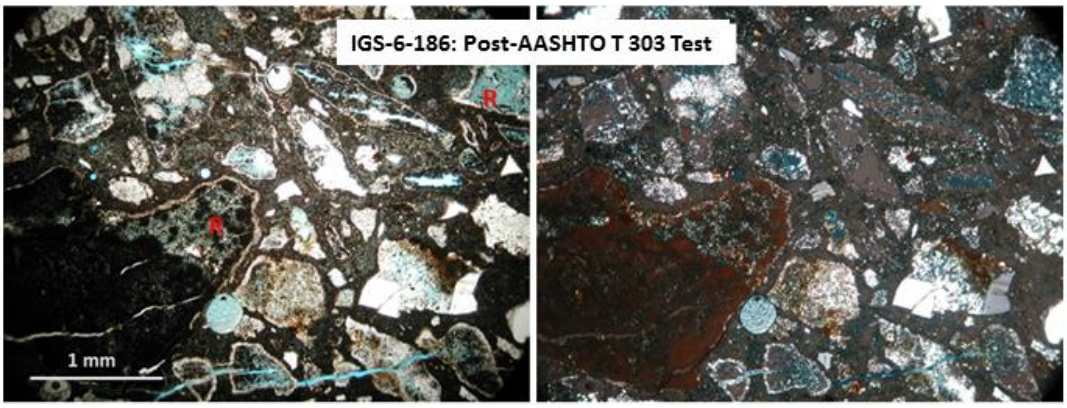

Figure 33. IGS-6-186 Mortar Bar Under Higher Magnification (Section 4PB008 at x40 Mag.; DSCN9934 On the Left and DSCN9935 On the Right)

Additional Mortar Bar Petrography

A commercial mortar bar from source Bo-61c that underwent the required AASHTO T 303 test for concrete certification was also examined under the petrographic microscope. Bo-61c is a Boise County source located in Garden Valley within the Payette River floodplain. The AASHTO T 303 expansion value from this test is 0.22 percent which is lower than most sources in Idaho. The Bo-61c source mortar bar thin sections after the AASHTO T 303 test are shown in Figure 34. Matrix and granitic clasts experienced very little cracking during the16-day test. The lower expansion on the AASHTO T 303 test of the Bo-61c mortar bar substantiates the visual observations under the microscope as to which lithologies are most reactive in the other samples – i.e. not those present in source Bo-61c.

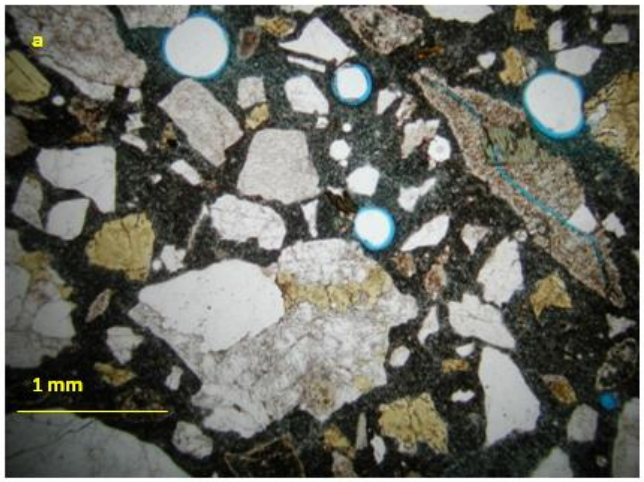

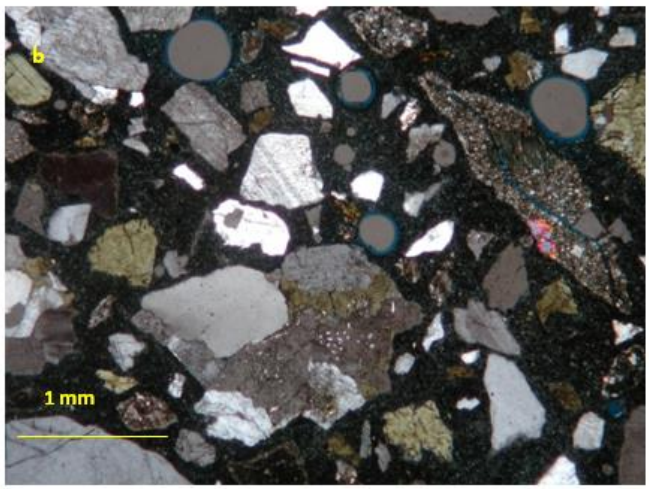

Figure 34a. Mortar Bar with Bo-61c Aggregate After AASHTO T 303 Test (Section 4GE005, DSCN9889) , at x20 Mag., Plain Light, Blue Epoxy

Figure 34b. Mortar Bar with Bo-61c Aggregate After AASHTO T 303 Test (Section 4GE005, DSCN9890) at x20 Mag. Crossed Polars

Chapter 4
Lithologic Analysis Results

Introduction

Comparison of lithology or rock-type with ASR potential (as measured by AASHTO T 303 tests and ASTM C 1293 tests) helps identify lithologies that are more likely to experience ASR. Lithologic inventories of 40 aggregate sources certified to produce concrete for Idaho Transportation Department are presented in this chapter, along with their commercial, unmitigated AASHTO T 303 test results for each aggregate source. The results of the field sampling and quantitative laboratory identifications of the source lithologies are arranged by ITD District, from north to southeast. Discussion of the results is presented in a later section of the report. The general purpose of the quantitative lithologic analysis was to identify those rock types present in each source in order to determine and map the variation in aggregate source compositions. Knowing what rock types are present at each source is a necessary precursor to correlating that source composition with the ASR potential and with the geologic units mapped in Idaho. Only 40 sources were sampled and inventoried, and some areas had greater sampling density than others across the state. Thus, some regions could use additional work but the general patterns did correlate to the geology of the state. Only sources certified for concrete production for ITD were examined as only those had available ASR test results. Sources and questions relevant to asphalt production or other aggregate use were not a part of this study.

Lithologic Characterization Relative to ASR

Figure 35 shows the location of the 40 certified sources for concrete production that were sampled in this study. CA lithologies were inventoried from each source and FA lithologies were also inventoried from the majority of the sources. However, at two sources FA was not available. No fines were available at Ma-22c because it is a dredged source, and at Kt-191c because it is a depleted source and access to pit walls was not permitted. However Kt-191c still contained remnant stock piles that were available for CA sampling.

CA lithologic inventories from multiple sources within the same district are included on single bar graphs. These bar graphs are used to illustrate and compare lithologic inventories and relative ASR within a similar geographic area. The bar graphs show each source in a different color with three sources on most of the graphs. Lithologies are on the bottom with the three different colored bars included in each rock type. The vertical axis is the percent of that rock type for each bar, normalized to 100 percent for each source. The AASHTO T 303 results, in percentage, are shown in the explanation in the upper right by each color-coded source. Lithologic inventory bar graphs for each individual source are also included. These bar graphs compare source CA lithologic inventory, FA lithologic inventory and a 60% CA/40% FA combined lithologic inventory. The 60% CA/40% FA lithologic inventory was included because this ratio of CA to FA is typical of most concrete mixes. The AASHTO T 303 value is in the title portion of the graph, following the source name.

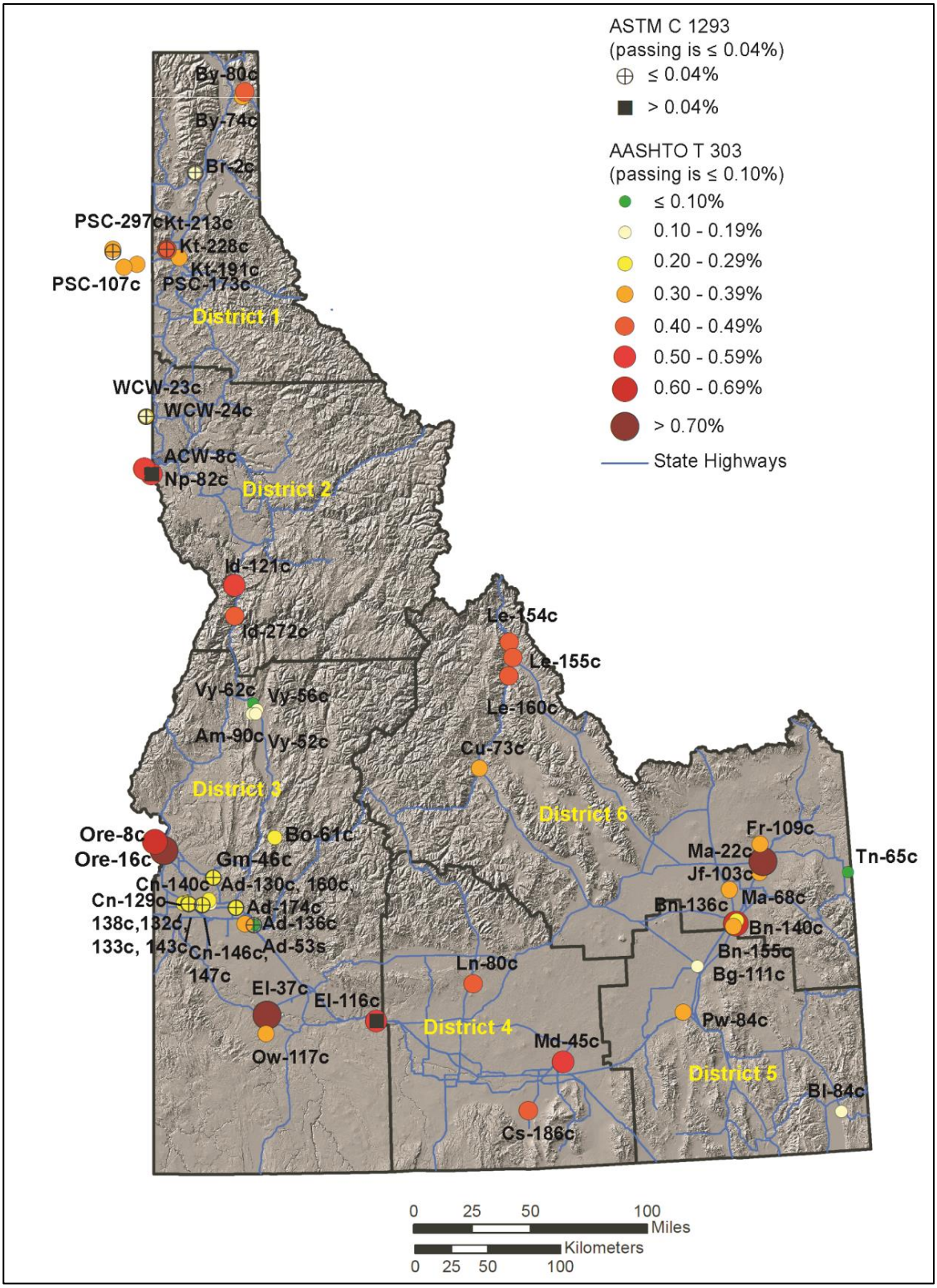

Figure 35. Map of Aggregate Sources, AASHTO T 303 and ASTM C 1293 Test Results

District 1 (Northern Idaho)

Sampled aggregate sources from District 1 include: Br-2c, By-74c, By-80c, Kt-191c, Kt-213c and PSC-173c (Table 4; Figures 36 - 42). AASHTO T 303 tests for District 1 aggregate sources range from 0.20 to 0.43 percent, with Br-2c exhibiting the lowest ASR potential with 0.20 percent expansion (Table 4; Figure 36). Aggregate from source Kt-213c barely passed the ASTM C 1293 test (0.039 percent; with ≤ 0.04 percent is passing) but substantially failed the AASHTO T 303 test (0.41percent; with ≤ 0.1 percent is passing). This example illustrates the ambiguity and discrepancy that exists between the two test methods and the need for additional information and practical approaches for evaluating and approving sources, as suggested by this project.

Table 4. District 1 Source Locations, ASR and Descriptions

ITD Name	Latitude	Longitude	AASHTO T 303 (Percent)	ASTM C 1293 (Percent)	Location Description	Geologic Unit (Cited if Mapped)	Cites
Br-2c	48.252310	-116.645270	0.20		Near Pend Oreille River, west of Sandpoint, ID	Glacial Fluvial Deposits, Missoula Flood Deposits	20
By-74c	48.725544	-116.202419	0.40		Near Kootenai River, North of Bonners Ferry, ID	Glacial Gravels	21
By-80c	48.755190	-116.180990	0.43		500 feet above the Moyie River, North of Bonners Ferry, ID	Glacial Outwash Deposits	21
Kt-191c	47.719454	-116.799343	0.40		Coeur d'Alene, ID (Within the City Limits)	Gravel of the Coeur d'Alene, Glacial Outburst Flood Deposits	22
Kt-213c	47.775012	-116.909632	0.41	0.039	Rathdrum Prairie, Northwest of Coeur d'Alene, ID	Rathdrum Valley Flood Gravels	23
PSC-173c	47.678778	-117.185944	0.38		Near the Spokane River, east of Spokane, WA	Rathdrum Valley Flood Gravels	23

Coarse Aggregate Lithologic Inventories Relative to ASR from District 1

All District 1 sources contain abundant quartzite (40 - 75 percent), with sources from the northernmost part of Idaho (Br-2c, By-74c and By-80c) containing the greatest proportions of quartzite (60 - 75 percent). Sources near Coeur d'Alene (Kt-191c and Kt-213c) and Spokane, WA (PSC-173c) contain approximately 50 percent quartzite with argillite and siltite composing >30 percent of Kt-213c and PSC-173c, while the remaining lithologic components of Kt-191c are 25 percent basalt, 18 percent limestone/dolostone and 15 percent granite/granodiorite. Br-2c is the least reactive source in District 1 and contains >25 percent granite/granodiorite while the remainder of District 1 sources contain ≤15 percent granite/granodiorite (Figure 36 and 37).

Fine Aggregate Lithologic Inventories Relative to ASR from District 1

Fine aggregate from Br-2c is predominantly quartz, quartzite and granite/granodiorite. For the Br-2c CA/FA composite, quartzite is 45 percent of the total with granitic units and minerals also important, but quartz dominates the FA (Figure 38). In Figure 39, FA and CA from PSC-173c show very little difference or variation. Fine aggregate from By-74c and By-80c sources contain higher proportions of quartz and granitic minerals and there is a moderate decrease (<10 percent) in quartzite relative to the CA (Figures 40 and 41). The FA from Kt-213c, shows lower proportions of all lithologic constituents, except that shale/mudstone increases to nearly 40 percent in the CA (Figure 42).

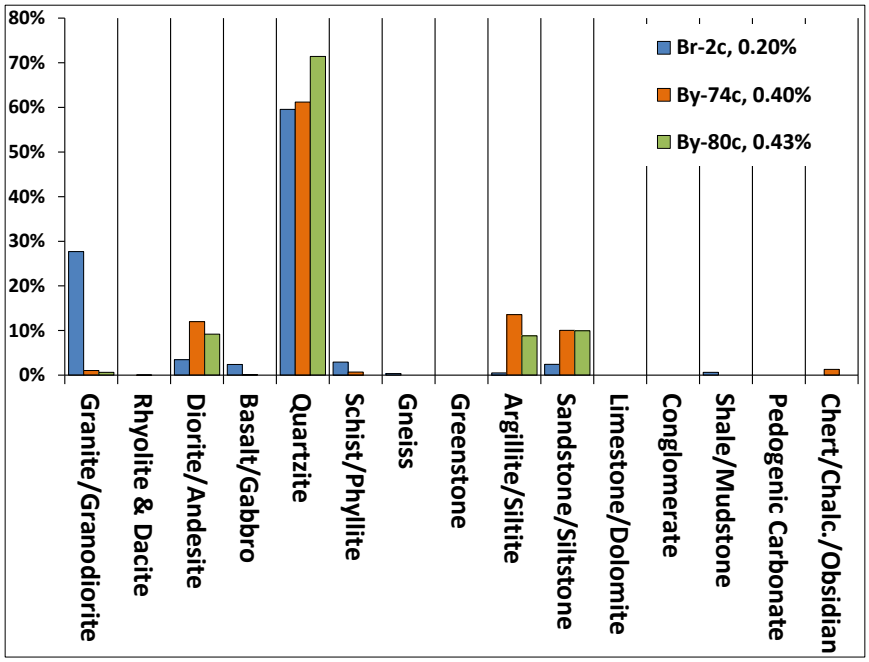

Figure 36. District 1 Source Lithologic Inventories and AASHTO T 303 Test Values (Upper Right) for Br-2c, By-74c and By-80c

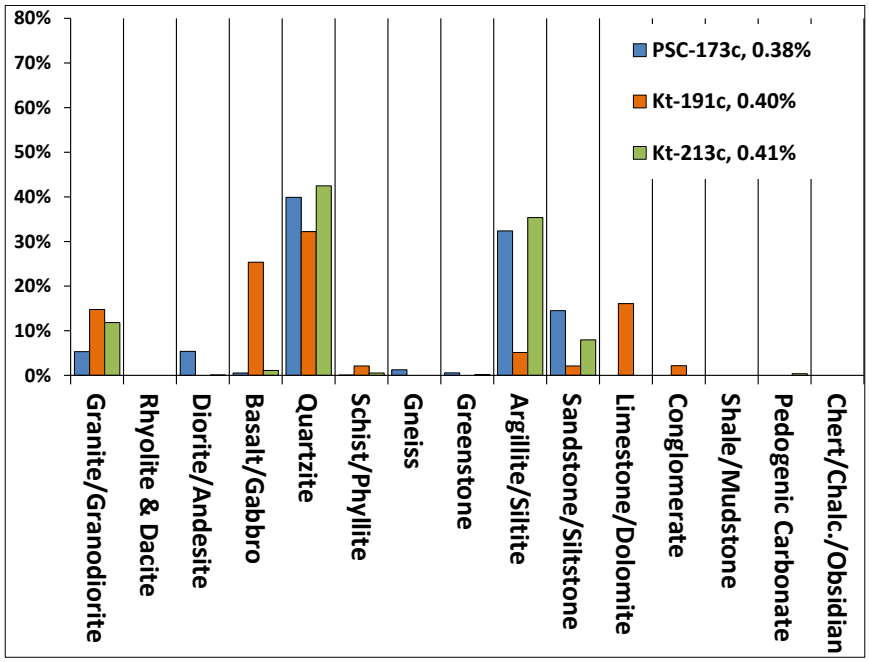

Figure 37. District 1 Source Lithologic Inventories and AASHTO T 303 Test Values (Upper Right) for PSC-173c, Kt-191c and Kt-213c

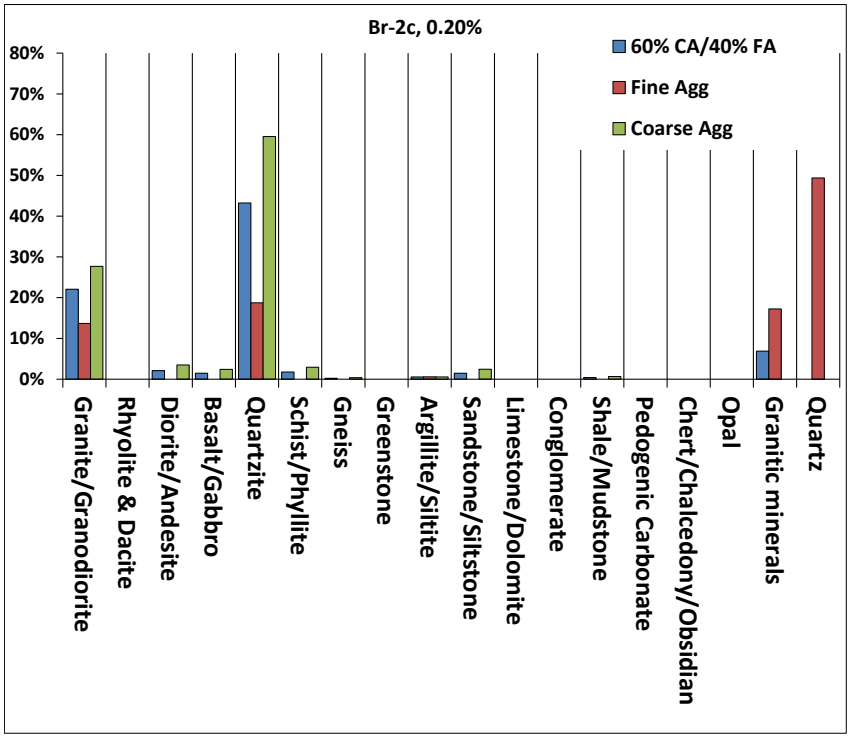

Figure 38. District 1 Br-2c Lithologic Inventory (CA, FA and 60% CA/40% FA) and AASHTO T 303 Test Value (Upper Center)

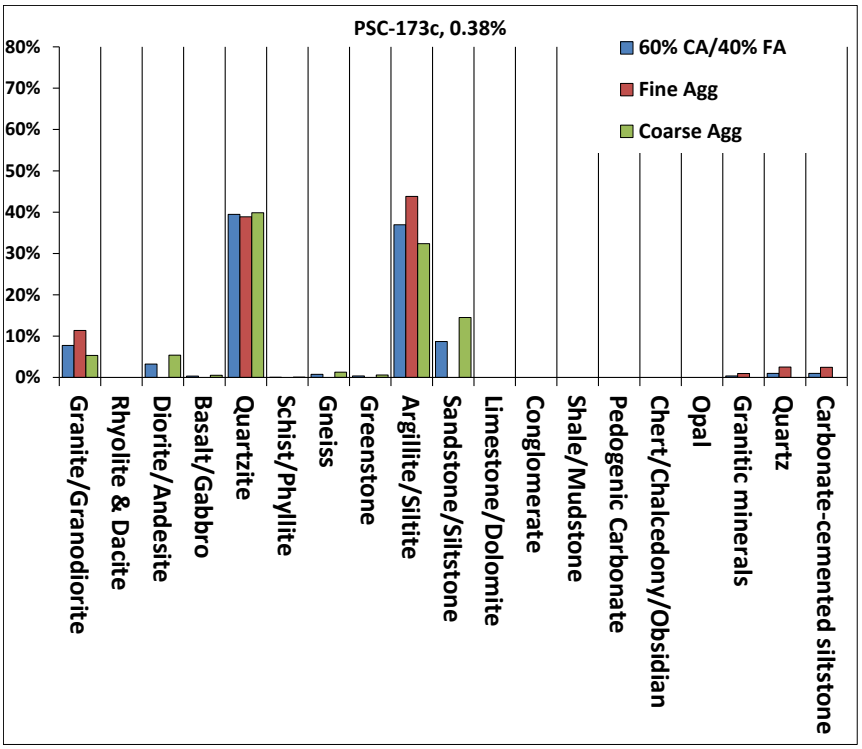

Figure 39. District 1 PSC-173c Lithologic Inventory (CA, FA and 60% CA/40% FA) and AASHTO Test T 303 Value (Upper Center)

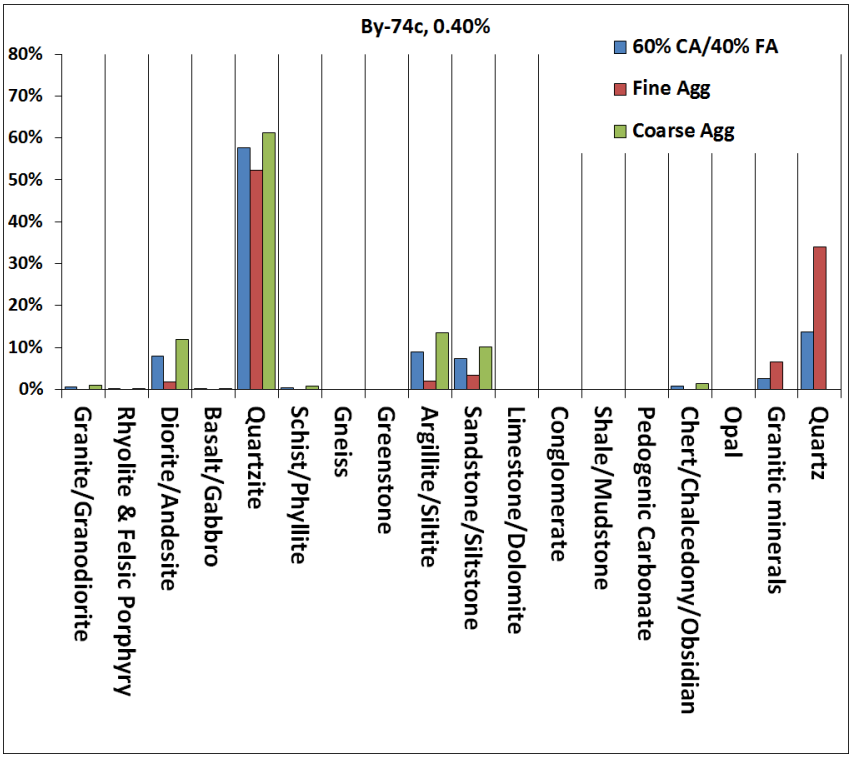

Figure 40. District 1 By-74c Lithologic Inventory (CA, FA and 60% CA/40% FA) and AASHTO T 303 Test Value (Upper Center)

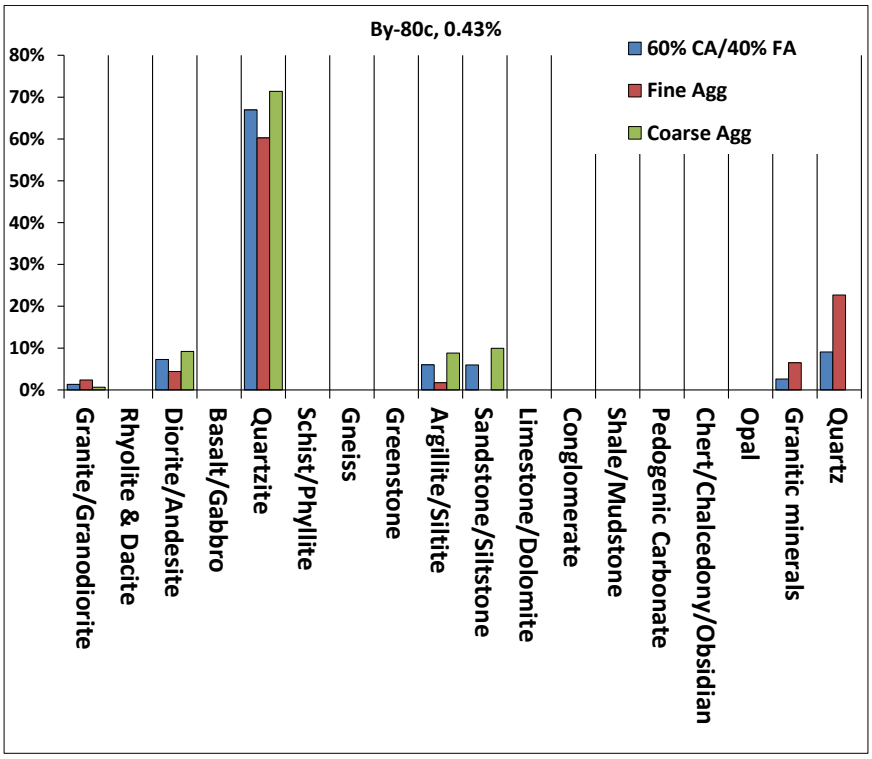

Figure 41. District 1 By-80c Lithologic Inventory (CA, FA and 60% CA/40% FA) and AASHTO T 303 Test Value (Upper Center)

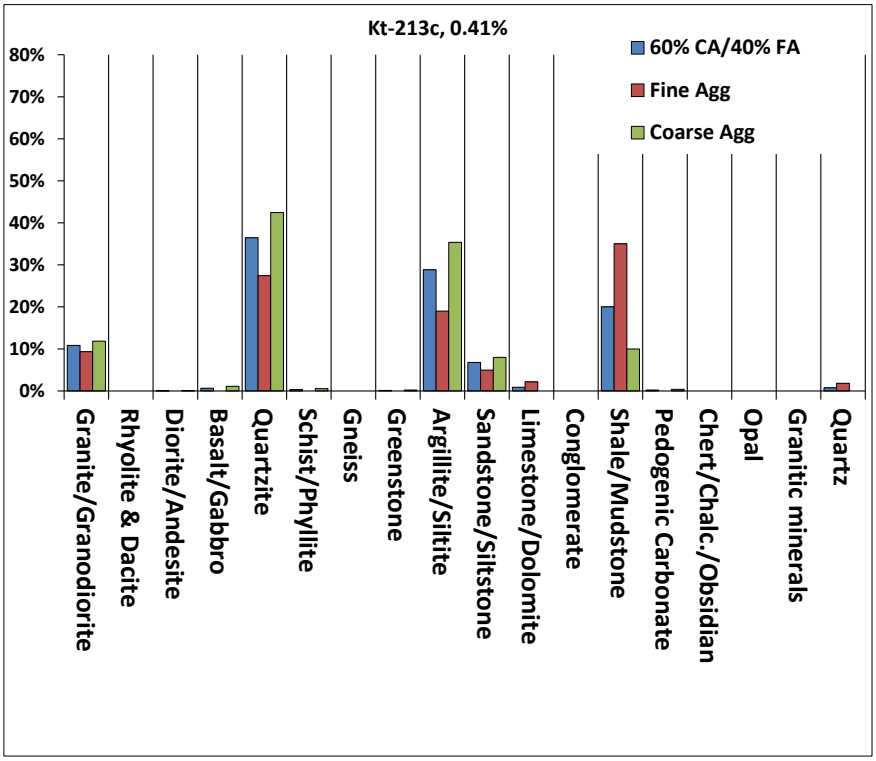

Figure 42. District 1 Kt-213c Lithologic Inventory (CA, FA and 60% CA/40% FA) and AASHTO T 303 Test Value (Upper Center)

District 2 (North-Central Idaho)

Sampled sources from District 2 include ACW-8, Np-82c, Id-121c and Id-272c. AASHTO T 303 tests for District 2 aggregate sources are moderately high, ranging from 0.53 to 0.59 percent, as shown in Table 5. Unmitigated AASHTO T 303 test results for Id-272c were not available, although the source did not pass the test. With fly ash mitigation AASHTO T 303 results for Id-121c meet ITD standards for concrete production.

Table 5. District 2 Source Locations, ASR and Descriptions

ITD Name	Latitude	Longitude	AASHTO T 303 (Percent)	ASTM C 1293 (Percent)	Location Description	Geologic Unit (Cited if Mapped)	Cites
ACW-8c	47.678778	-117.185944	0.38		Near Snake River, Below Confluence with Clearwater River, Clarkston, WA	Alluvium of Snake River	
Id-121c	46.404031	-117.114676	0.359		Near Salmon River, South of Whitebird Pass, ID	Alluvium of Salmon River	24
Id-272c	45.676786	-116.314014	Requires Mitigation		Near Salmon River, North of Riggins, ID	Alluvium of Salmon River	25
Np-82c	45.485639	-116.316111	0.53	0.11	Near Snake River, Below Confluence with Clearwater River, Lewiston, ID	Alluvium of Snake River	26

Coarse Aggregate Lithologic Inventories Relative to ASR from District 2

All sources in District 2 contain volcanic lithologies. Np-82c and ACW-8c contain >20 percent rhyolite and dacite, >35 percent basalt and lesser amounts of intermediate composition volcanic rocks (13 percent and 5 percent, respectively). Id-272c contains nearly equal proportions (between 15 - 22 percent) of granitic rocks, rhyolite and dacite, diorite and andesite, basalt and quartzite. Id-121c contains a majority (55 percent) quartzite, 15 percent basalt and lesser amounts of metamorphic rocks, and felsic and intermediate volcanics (Figure 43).

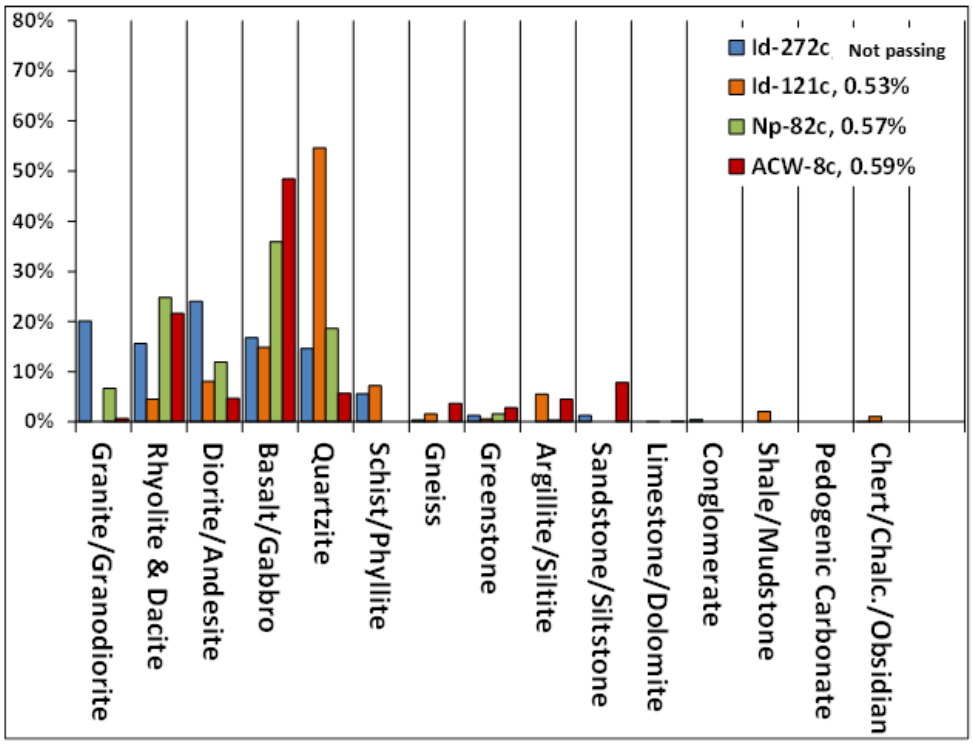

Figure 43. District 2 Source Lithologic Inventories and AASHTO T 303 Test Values (Upper Right) for Id-272c, Id-121c, Np-82c and ACW-8c

Fine Aggregate Lithologic Inventories Relative to ASR from District 2

Fine aggregate from all District 2 sources is comprised of 30 - 50 percent quartz and contains significantly less basalt than the respective CA counterparts. Id-121c and ACW-8c contain 3 - 5 percent opal and ACW-8c contains 5 percent chert, both of which were not found in CA (Figures 44 and 45). In ACW-8c, silica-cemented sands that originated from pedogenic coatings formed on larger clasts make-up 10 percent of fine aggregate (Figure 45). Lithologic inventories for Np-82c and Id-272c are shown in Figures 46 and 47.

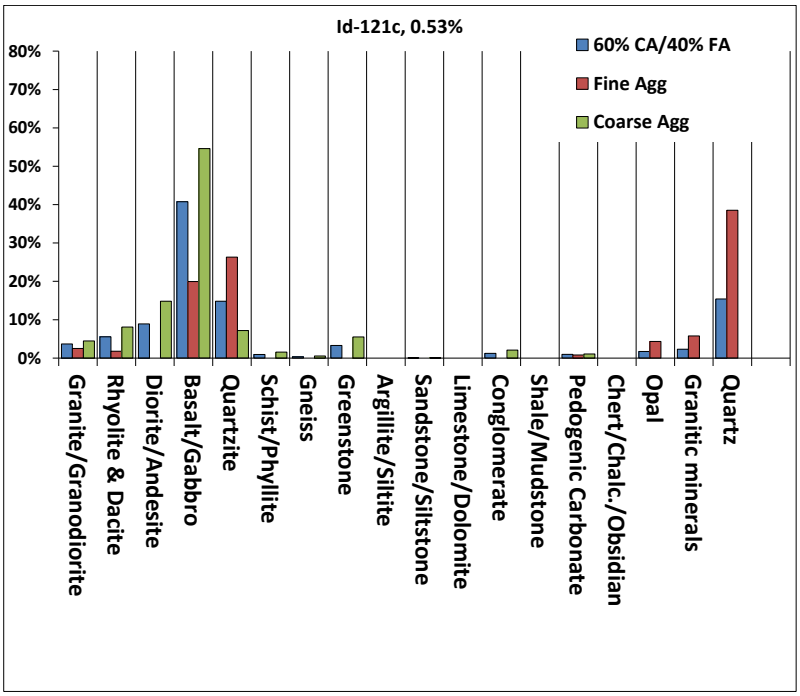

Figure 44. District 2 Id-121c Lithologic Inventory (CA, FA and 60% CA/40% FA) and AASHTO T 303 Test Value (Upper Center)

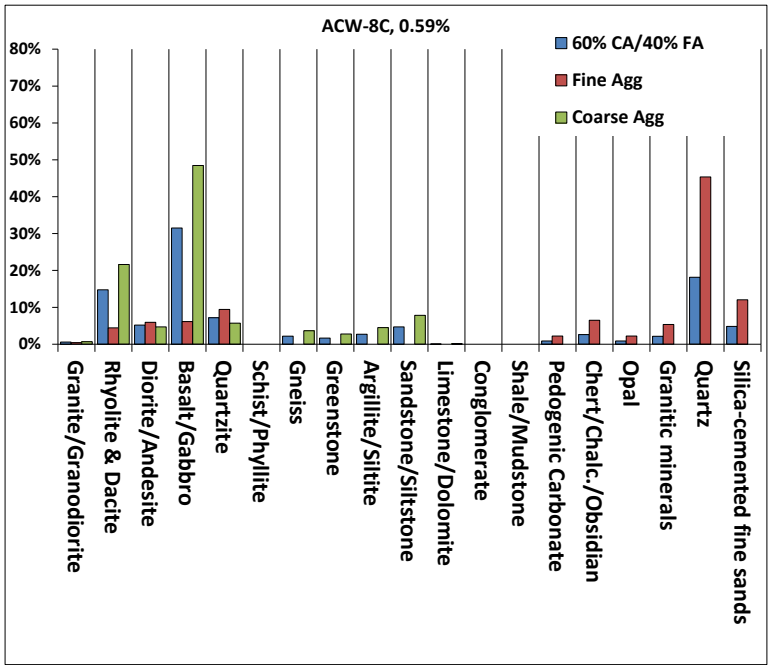

Figure 45. District 2 ACW-8c Lithologic Inventory (CA, FA and 60% CA/40% FA) and AASHTO T 303 Test Value (Upper Center)

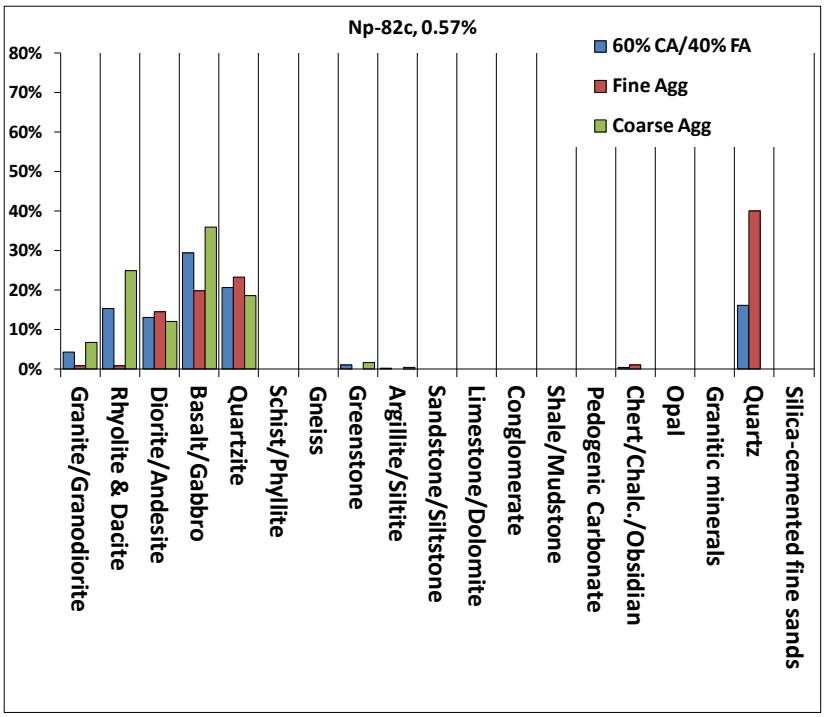

Figure 46. District 2 Np-82c Lithologic Inventory (CA, FA and 60% CA/40% FA) and AASHTO T 303 Test Value (Upper Center)

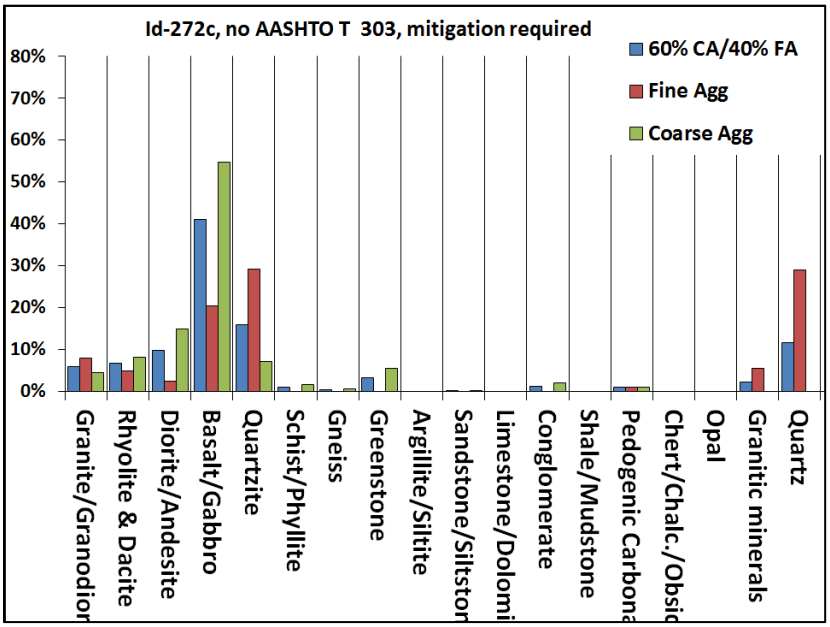

Figure 47. District 2 Id-272c Lithologic Inventory (CA, FA and 60% CA/40% FA) and AASHTO T 303 Test Value (Upper Center)

District 3 (Southwestern Idaho)

Sampled sources from District 3 include; Ad-136c, Ad-53s, Cn-140c, Cn-146c, Bo-61c, Gm-46c, Vy-52c, Vy-56c, El-116c, El-37c and Ow-117c, Ore-16c, Ore-8c, Vy-62c and Am-90c. AASHTO T 303 values for District 3 range from 0.02 to 0.75 percent, displaying the greatest range in the state. Sources with the lowest AASHTO T 303 tests (0.02 - 0.26 percent) are found in modern fluvial deposits and river terrace deposits of the Boise River (Ad-36c, Ad-53s, Cn-140c, and Cn-147c) and of the Payette River (Bo-61c, Gm-46c, Vy-52c and Vy-56c; Table 6), and in basalt outcrops near McCall (Am-90c and Vy-62c; Table 6). Ow-117c with an AASHTO T 303 value of 0.33 percent is located in a tributary of the Snake River that originates from the Owyhee Mountains (Table 6). Sources with highest AASHTO T 303 values (0.57 – 0.75 percent) are located in modern fluvial deposits and river terraces of the Snake River (El-37c, El-116c, Ore-8c and Ore-8c; Table 6). El-116c is located in higher elevation terrace gravels and may have been deposited from an ancestral drainage of unknown extent.

Table 6. District 3 Source Locations, ASR and Descriptions

ITD Name	Latitude	Longitude	AASHTO T 303 (percent)	ASTM C 1293 (Percent)	Location Description	Geologic Unit (Cited if Mapped)	Cites
Ad-53s	43.551915	-116.179732	0.18		Northwest of Exit 57 (I-84), South Side of Interstate, Gowen Terrace	Terrace Gravels	27
Ad-136c	43.552195	-116.171194	0.02	0.020	Pleasant Valley Road, North Side of Interstate 84, Gowen Terraace	Terrace Gravels	27
Am-90c	44.933023	-116.163238	0.15*		North of McCall, ID on SH-55, East of Little Ski Hill.	Columbia River Basalt	30
Bo-61c	44.097553	-115.984613	0.22		Near South Fork of Payette River, South of Garden Valley, ID	Alluvium of South Fork Payette River	
Cn-140c	43.688608	-116.726581	0.26	0.030	Near Boise River, Northwest of Caldwell, ID	Alluvium of Boise River	27
Cn-146c	43.689487	-116.541140	0.16		Near Boise River, West of Star, ID, on SH-44	Alluvium of Boise River	27
El-37c	42.991748	-116.065670	0.75		On Snake River, North of Grandview, ID	Alluvium of Snake River	29
El-116c	42.940041	-115.144143	0.57	0.063	East of Bliss, ID, King Hill	Terrace Gravels of Snake River	
Gm-46c	43.859222	-116.514806	0.22	0.020	Near Payette River, South of Emmett, ID	Alluvium of Payette River	
ORE-8c	44.074199	-117.015502	0.68		Near Snake River, Within City Limits of Ontario, OR	Terrace Gravels of Snake River	
ORE-16c	44.019925	-116.939042	0.74		Northwest of Ontario, OR	Alluvium of Snake River	
Ow-117c	42.872981	-116.079122	0.33		South of Grandview, ID	Alluvium of Shoofly Creek	29
Vy-52c	44.895933	-116.123384	0.14		South Side of McCall, ID (Within the City Limits)	Glacial Outwash Deposits	30
Vy-56c	44.870689	-116.139550	0.19		On North Fork of Payette River, South of McCall, ID	Alluvium of North Fork Payette River	30
Vy-62c	44.869781	-116.169283	0.12		Southwest of McCall, ID	Columbia River Basalts	30

* Aggregate blended with fines from Vy-52c.

Coarse Aggregate Lithologic Inventories Relative to ASR from District 3

All sampled sources in the Boise River Drainage contain rhyolite, dacite, diorite/andesite and basalt. Granite/granodiorite accounts for 25 - 38 percent and rhyolite makes up <25 percent of Ad-136c, Cn-146c and Ad-53s source lithologies (Figure 48). In contrast, no granitic rocks were found in Cn-149c in a source where rhyolite and dacite comprise 50 percent of lithologies. Similar to most of the Boise River sources, granitic rocks comprised 18 – 59 percent in all Payette River sources including Vy-52c, Vy-56c, Bo-61c, and Gm-46c, as shown in Figure 49. Basalt is the other major lithologic component present in all Payette River sources, making up 65 percent of Vy-56c. Rhyolite and dacite are not as widespread in Payette River sources, however these lithologies comprise 10 - 20 percent of Bo-61c and Gm-46c. Snake River Plain sources includes Ow-117c, El-116c, El-37c, Ore-8c and Ore-16c (Figures 50 and 51) and all contain a majority of volcanic lithologies (rhyolite, dacite, diorite/andesite and basalt) with secondary quartzite. All of the western Snake River Plain sources that exhibit high ASR reactivity (El-116c, El-37c, Ore-8c and Ore-16c) contain detectable but minor amounts (<5 percent) of chalcedony and obsidian. Siliceous argillite is present in only 2 sources (10 percent in El-116c and a small amount in El-37c).

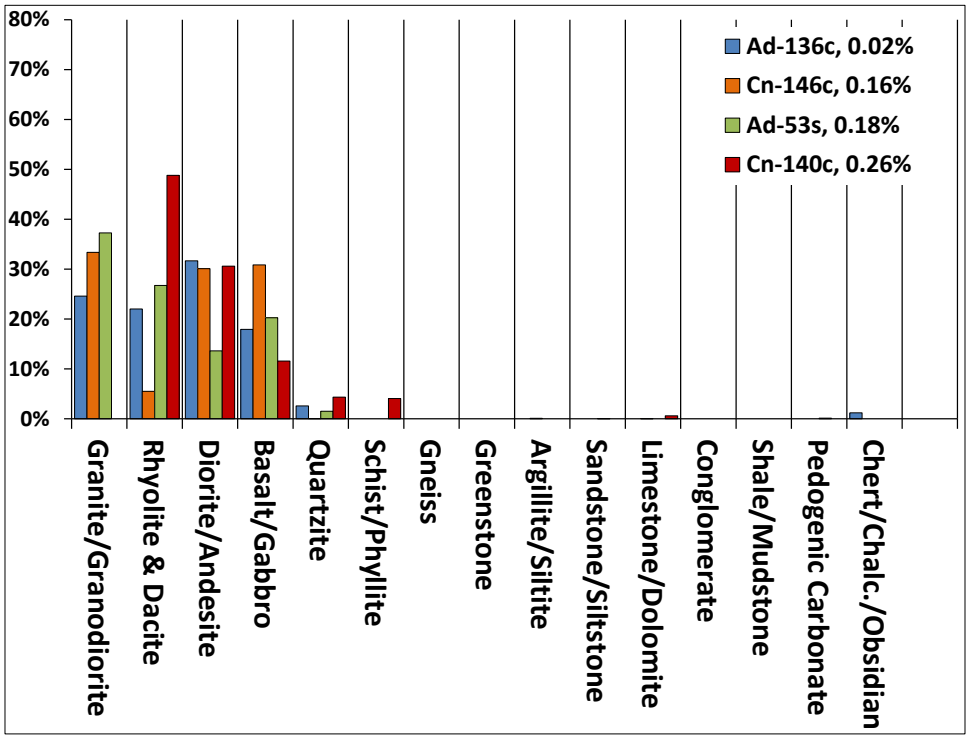

Figure 48. District 3 Boise River Source Lithologic Inventories and AASHTO T 303 Test Values (Upper Right) for Ad-136c, Cn-146c, Ad-53s and Cn-140c

Fine Aggregate Lithologic Inventories Relative to ASR from District 3

No FA was analyzed from Cn-146c and Vy-56c because both sources had only washed stock available for sampling. FA from Ad-136c and Ad-53s contain trace amounts of opal, which probably originated from pedogenic opaline coatings formed on larger clasts that were observed in the field and in the lab

(Figures 52 and 53). Quartz, granitic minerals and granite/granodiorite make up the majority of fines in Boise River and Payette River sources (Ad-136c, Ad-53s, Vy-52c, Bo-61c, Gm-46c, Cn-140c; Figures 53 - 57). Fines from Ad-136c and Ore-16c also contained small amounts of silica-cemented very fine sands (Figures 52 and 58). Amorphous silica, although only present in small amounts, was found in fines from all Snake River Plain sources. Opal was present in fines from Ow-117c, Ore-16c and El-37c in trace amounts (<5 percent), however opal makes up 20 percent of fines from El-116c (Figures 58 - 61). Obsidian makes up less than 5 percent of fines from Ow-117c, while chalcedony and obsidian comprise 5 percent of fines from Ore-8c (Figure 62)and nearly 10 percent of fines from Ore-16c.

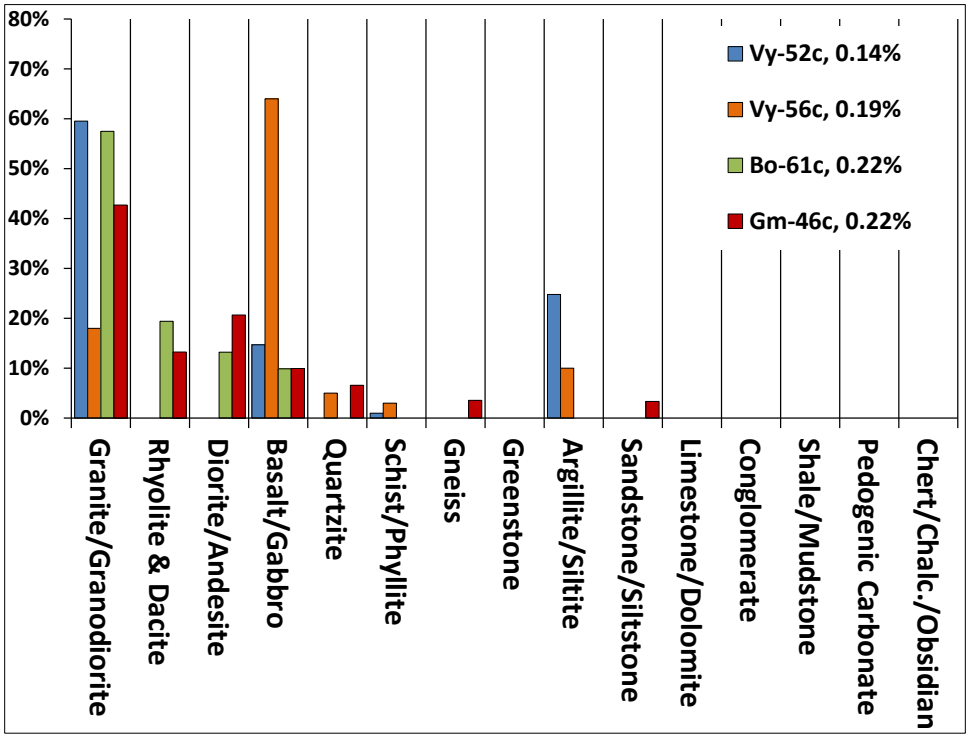

Figure 49. District 3 Payette River Source Lithologic Inventories and AASHTO T 303 Test Values (Upper Right) for Vy-52c, Vy-56c, Bo-61c and Gm-46c

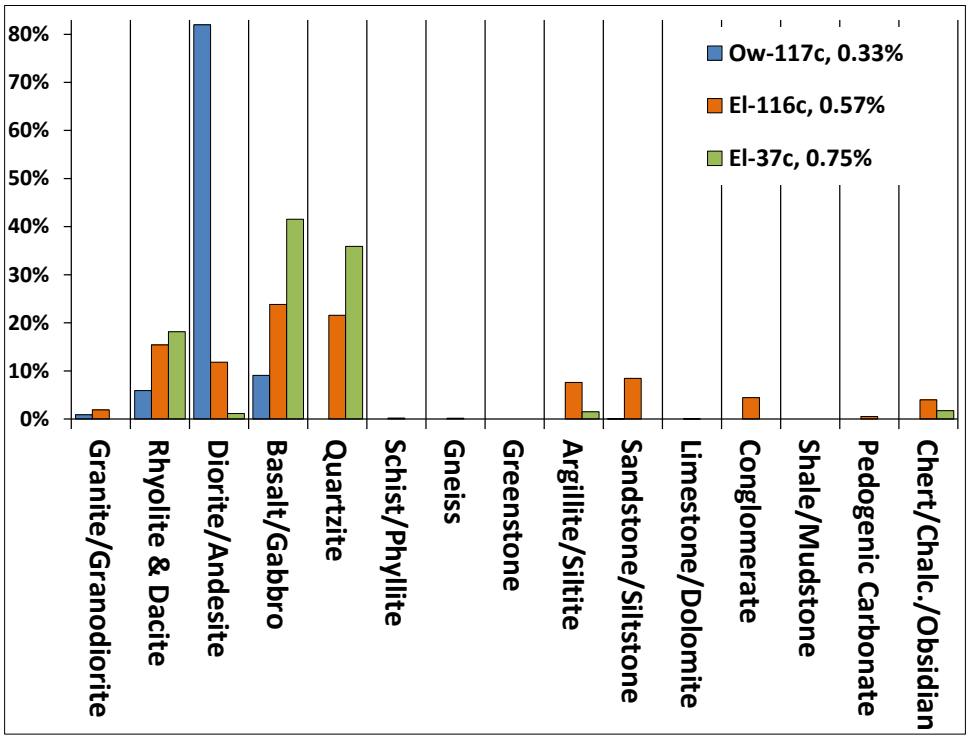

Figure 50. District 3 Snake River Plain Source Lithologic Inventories and AASHTO T 303 Test Values (Upper Right) for Ow-117c, El-116c and El-37c

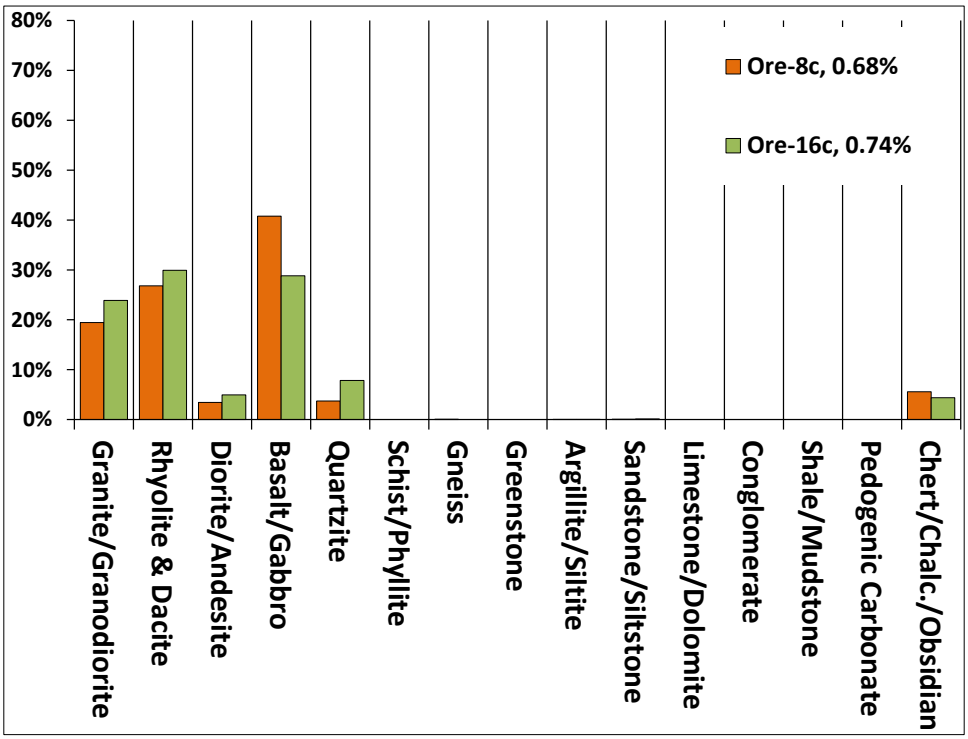

Figure 51. District 3 Ontario, Oregon Source Lithologic Inventories and AASHTO T 303 Test Values (Upper Right) for Ore-8c and Ore-16c

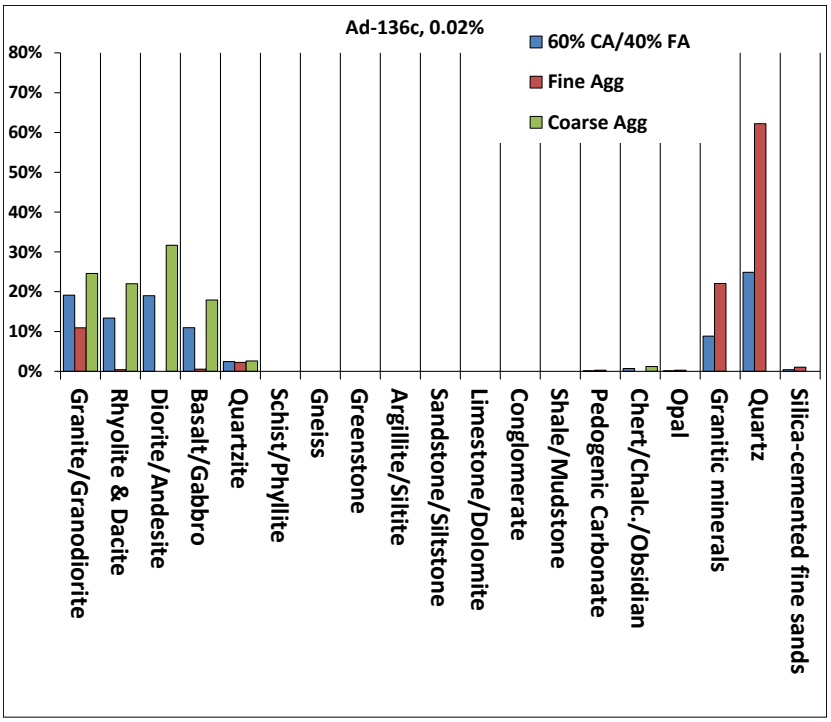

Figure 52. District 3 Ad-136c Lithologic Inventory (CA, FA and 60% CA/40% FA) and AASHTO T 303 Test Value (Upper Center)

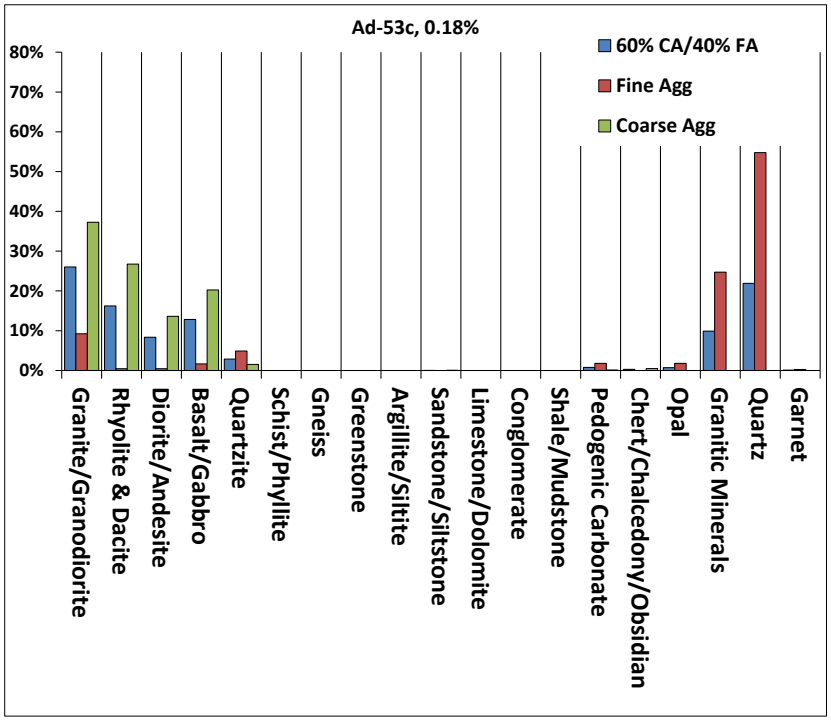

Figure 53. District 3 Ad-53s Lithologic Inventory (CA, FA and 60% CA/40% FA) and AASHTO T 303 Test Value (Upper Center)

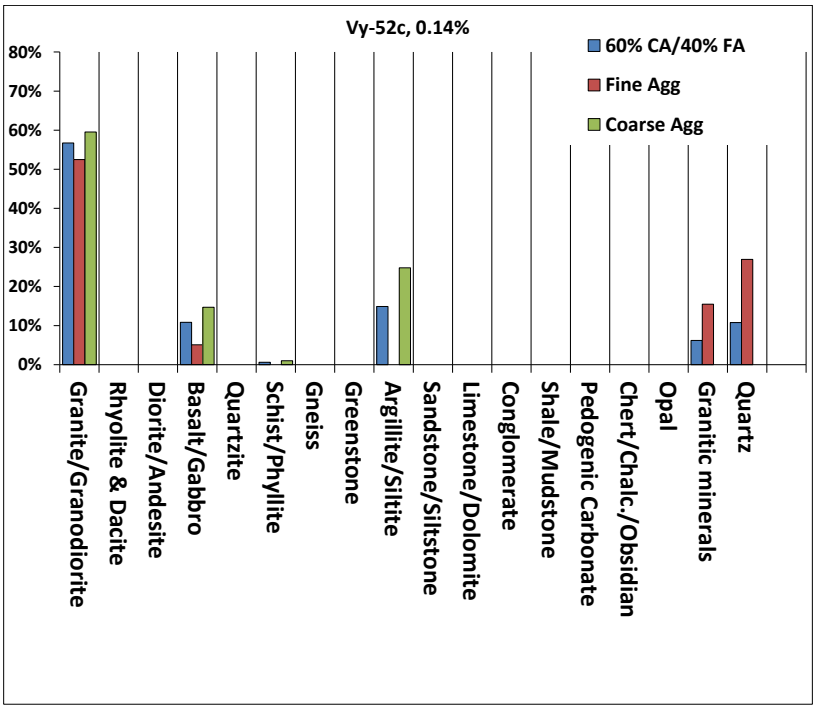

Figure 54. District 3 Vy-52c Lithologic Inventory (CA, FA and 60% CA/40% FA) and AASHTO T 303 Test Value (Upper Center)

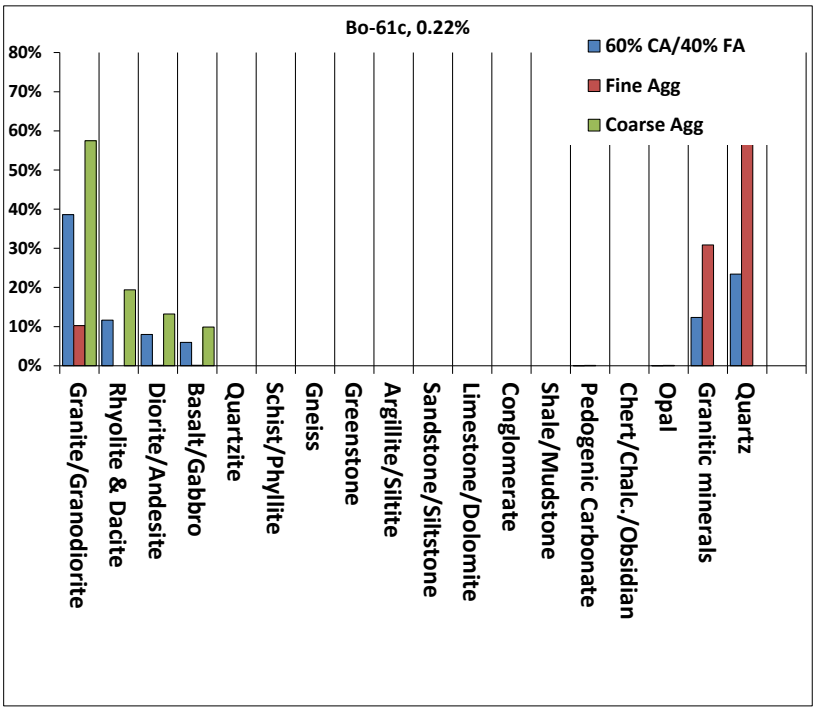

Figure 55. District 3 Bo-61c Lithologic Inventory (CA, FA and 60% CA/40% FA) and AASHTO T 303 Test Value (Upper Center)

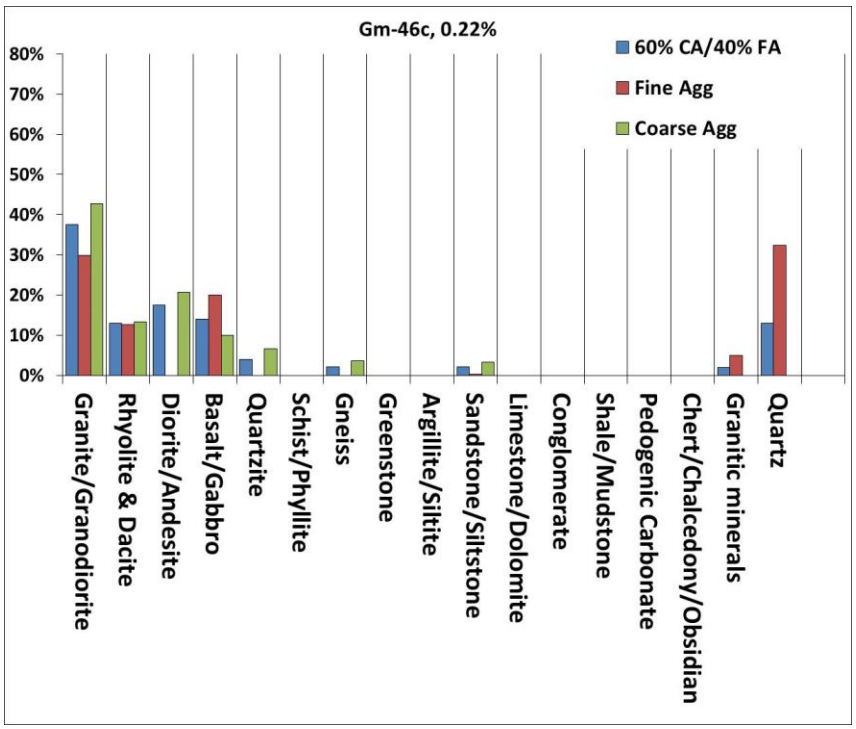

Figure 56. District 3 Gm-46c Lithologic Inventory (CA, FA and 60% CA/40% FA) and AASHTO T 303 Test Value (Upper Center)

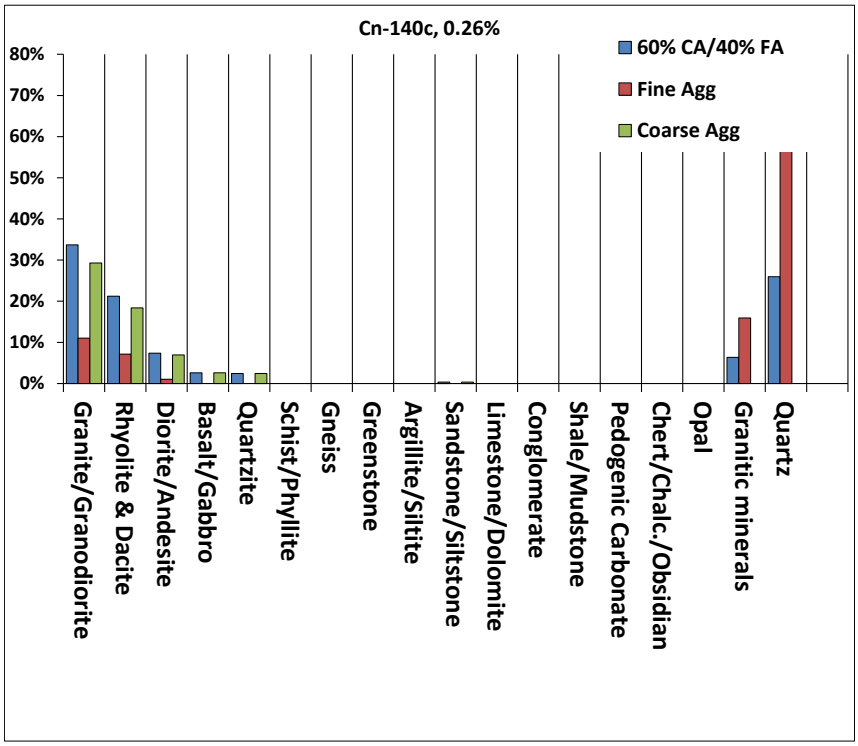

Figure 57. District 3 Cn-140c Lithologic Inventory (CA, FA and 60% CA/40% FA) and AASHTO T 303 Test Value (Upper Center)

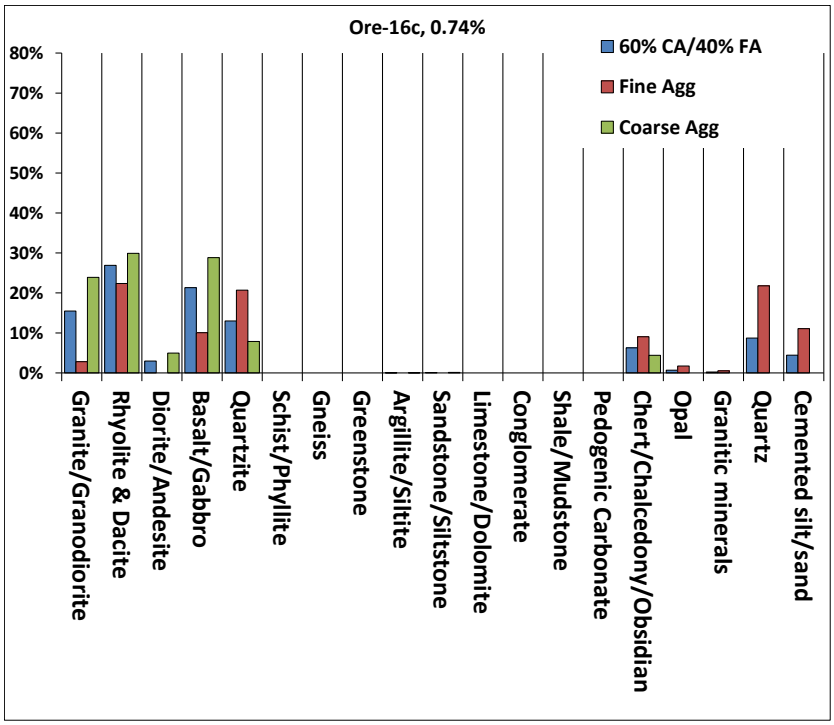

Figure 58. District 3 Ore-16c Lithologic Inventory (CA, FA and 60% CA/40% FA) and AASHTO T 303 Test Value (Upper Center)

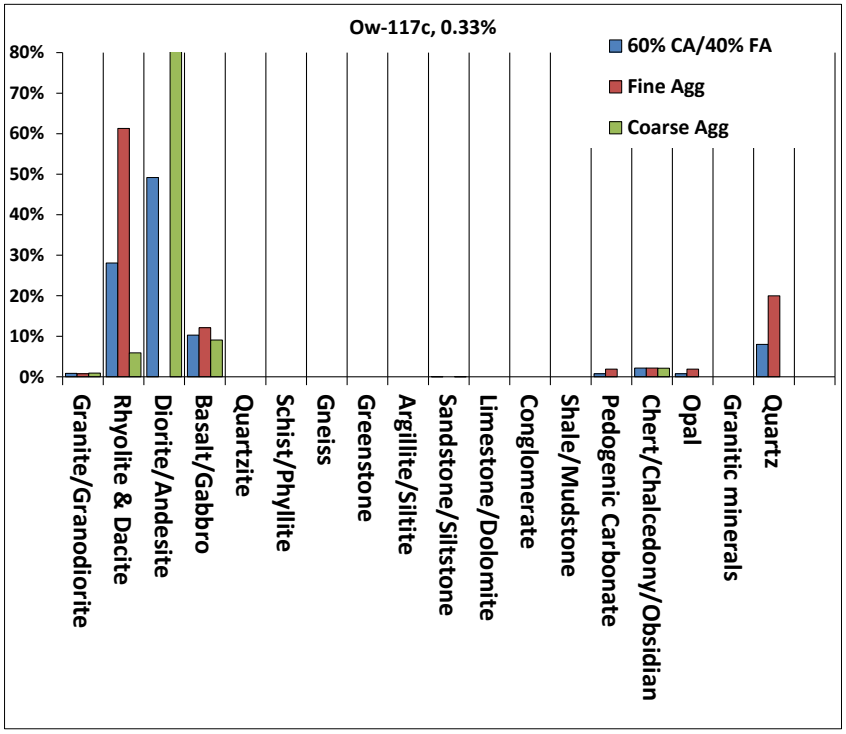

Figure 59. District 3 Ow-117c Lithologic Inventory (CA, FA and 60% CA/40% FA) and AASHTO T 303 Test Value (Upper Center)

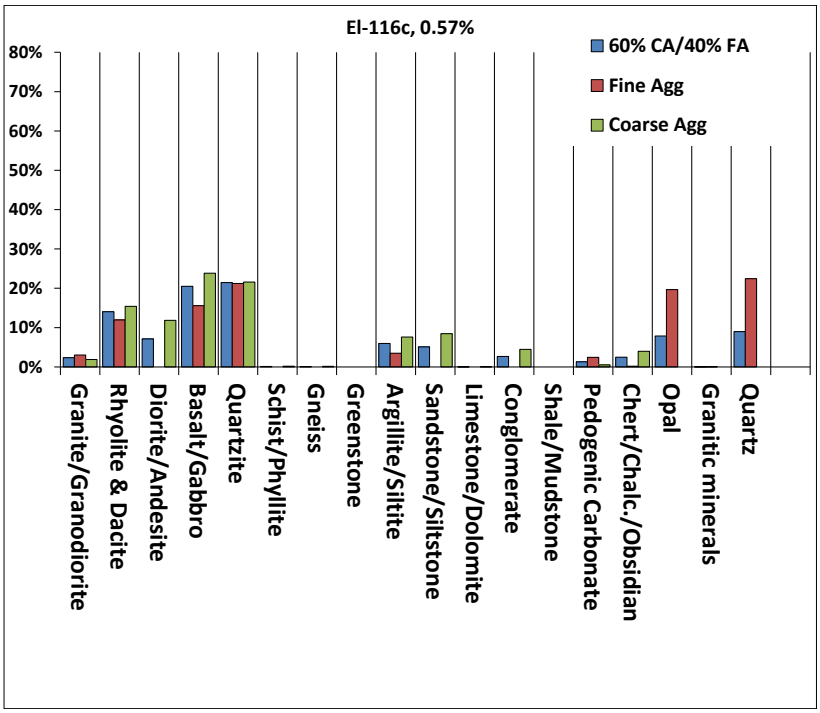

Figure 60. District 3 El-116c Lithologic Inventory (CA, FA and 60% CA/40% FA) and AASHTO T 303 Test Value (Upper Center)

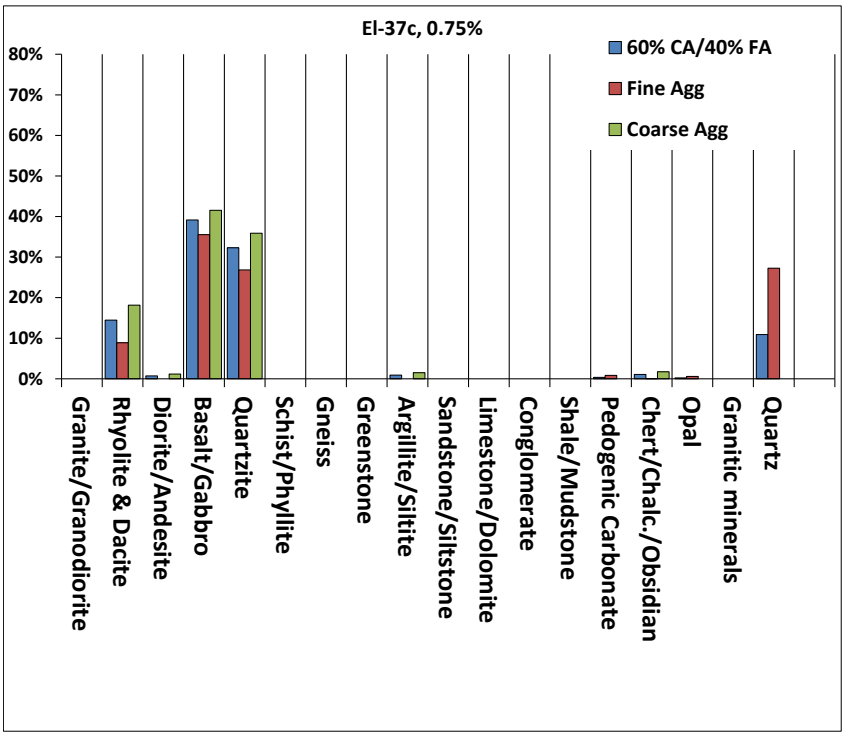

Figure 61. District 3 El-37c Lithologic Inventory (CA, FA and 60% CA/40% FA) and AASHTO T 303 Test Value (Upper Center)

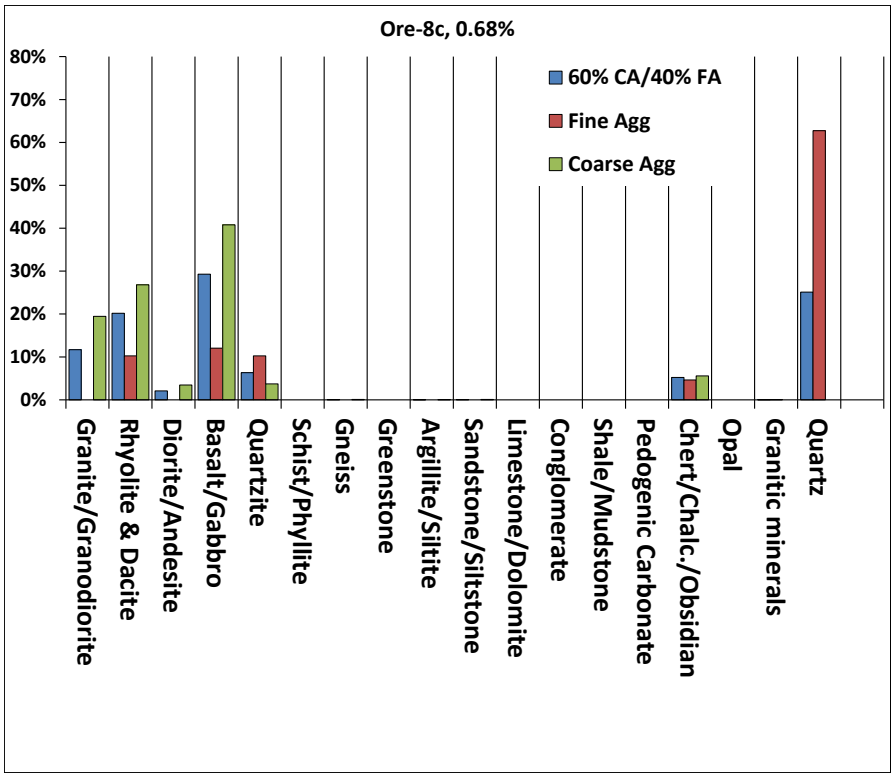

Figure 62. District 3 Ore-8c Lithologic Inventory (CA, FA and 60% CA/40% FA) and AASHTO T 303 Test Value (Upper Center)

District 4 (South-Central Idaho)

Sampled sources from District 4 include: Cs-186c, Ln-80c and Md-45. El-116c supplies aggregate to both Districts 3 and 4; lithologic results for El-116c are included in the preceding section on District 3. AASHTO T 303 values are moderately high in District 4 sources, ranging from 0.47 - 0.57 percent (Table 7; Figure 63).

Table 7. District 4 Source Locations, ASR and Descriptions

ITD Name	Latitude	Longitude	AASHTO T 303 (Percent)	ASTM C 1293 (Percent)	Location Description	Geologic Unit (Cited if Mapped)	Cites
Cs-186c	42.358318	-113.883036	0.47	0.029	South of Burley, ID, North of Oakley, ID	Alluvium of Goose Creek	
Ln-80c	43.160274	-114.315621	0.47	0.025	East of SH-75, North of Shoshone, ID	Alluvium of Big Wood River	31
Md-45c	42.652026	-113.575231	0.54		On Snake River, Southeast of Acequia, ID	Alluvium of Snake River	

Coarse Aggregate Lithologic Inventories Relative to ASR from District 4

All District 4 sampled sources contain 20 - 40 percent rhyolite and dacite, and 10 - 25 percent sandstone/siltstone, with quartzite, diorite and basalt making up the remainder of each source (Figure 63). Amorphous silica (2.5 percent chert and 11 percent obsidian) was found in Cs-186c, and 15 percent obsidian in Md-45c. Siliceous argillite accounts for 10 percent of lithologies identified in

Ln-80c and may originate from the same source as argillite found in the downstream source El-116c, which supplies aggregate to both District 3 and 4.

Fine Aggregate Lithologic Inventories Relative to ASR from District 4

FA from Cs-186c shows very little lithologic variation from its CA counterparts, except for the notable decrease in obsidian from 15 percent in CA to 5 percent in FA (Figure 64). FA from Ln-80c shows significant increases in basalt and quartz, while FA from Md-45c has increased amounts of quartz and opal makes up 1 percent (Figures 65 and 66).

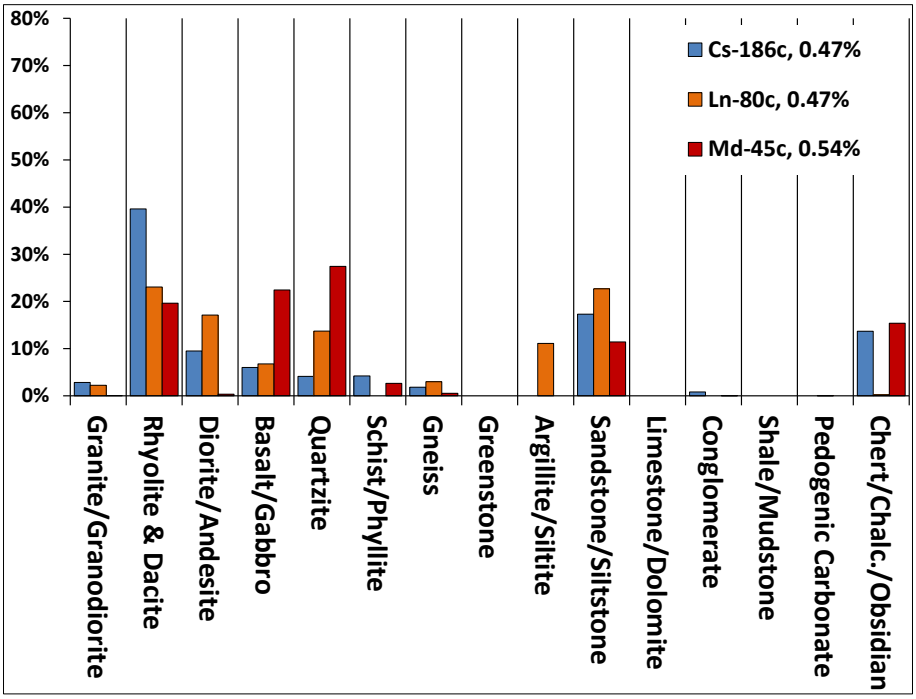

Figure 63. District 4 Lithologic Inventories and AASHTO T 303 Test Values (Upper Right) for Cs-186c, Ln-80c and Md-45c

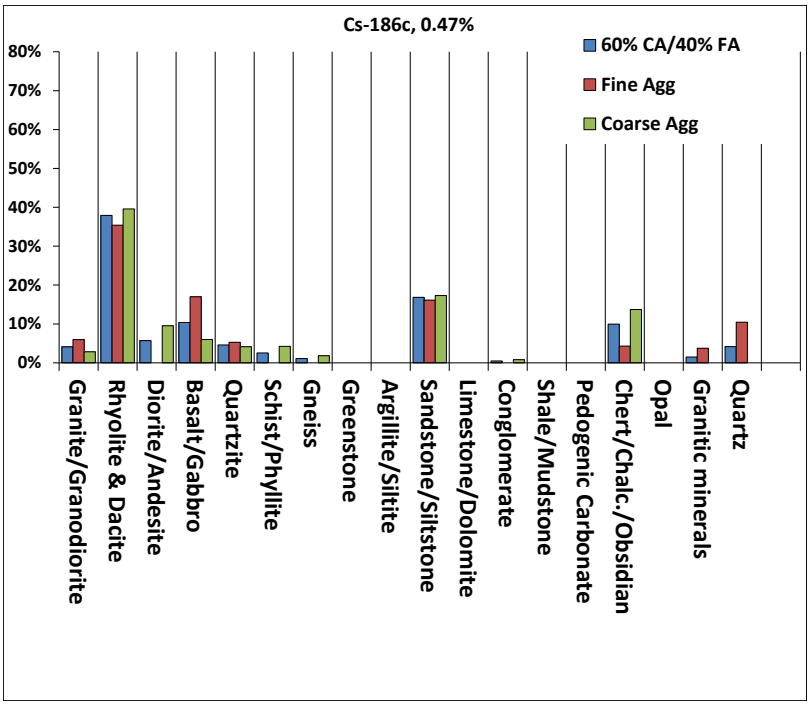

Figure 64. District 4 Cs-186c Lithologic Inventory (CA, FA and 60% CA/40% FA) and AASHTO T 303 Test Value (Upper Center)

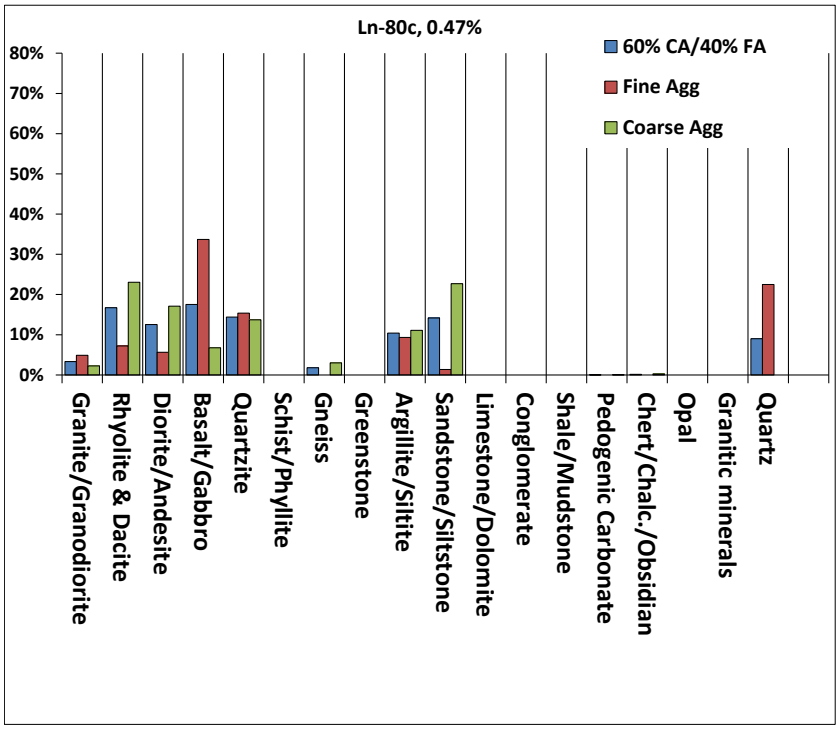

Figure 65. District 4 Ln-80c Lithologic Inventory (CA, FA and 60% CA/40% FA) and AASHTO T 303 Test Value (Upper Center)

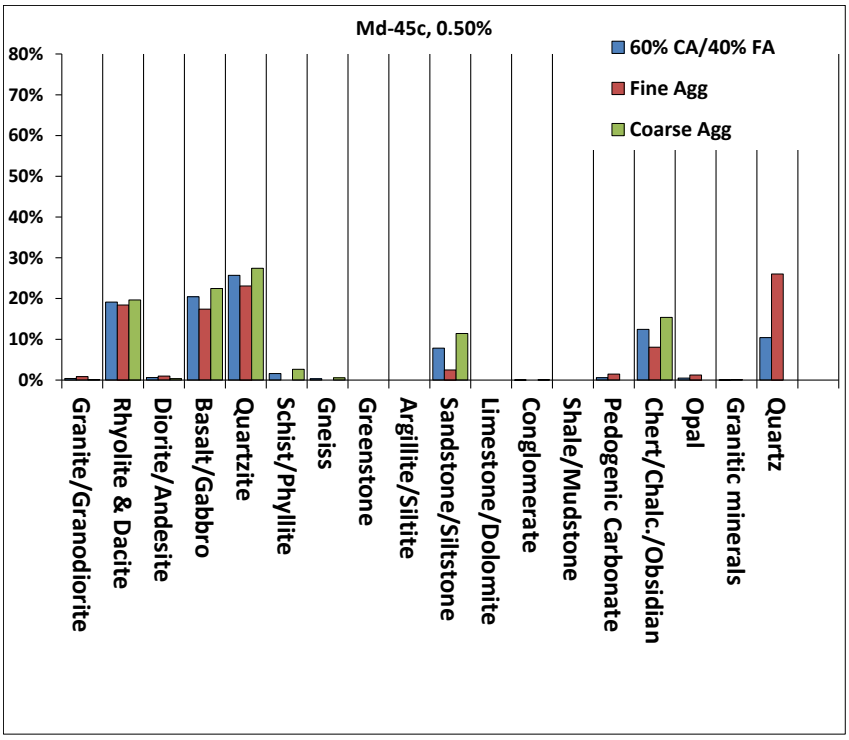

Figure 66. District 4 Md-45c Lithologic Inventory (CA, FA and 60% CA/40% FA) and AASHTO T 303 Test Value (Upper Center)

District 5 (Southeastern Idaho)

Sampled sources from District 5 include: Bl-84c, Bg-111c and Pw-84c. Bl-84c and Bg-111c have low AASHTO T 303 values of 0.16 percent and 0.17 percent, respectively, while the ASR potential at Pw-84c is higher, with an AASHTO T 303 value of 0.33 percent (Table 8).

Table 8. District 5 Source Locations, ASR and Descriptions

ITD Name	Latitude	Longitude	AASHTO T 303 (Percent)	ASTM C 1293 (Percent)	Location Description	Geologic Unit (Cited if Mapped)	Cites
Bg-111c	43.208057	-112.405471	0.17		West of Blackfoot, Idaho	Alluvium of Snake River	
Bl-84c	42.247981	-111.271656	0.16		South of Montpelier, Idaho, and north of Bear Lake	Alluvium of Bear River	
Pw-84c	42.924929	-112.547018	0.33		West of Chubbuck, Idaho	Michaud Gravel, Gravel and Sand Deposits of the Bonneville Flood	36

Coarse Aggregate Lithologic Inventories Relative to ASR from District 5

The source with the lowest ASR in District 5 (Bl-84c) is primarily composed of sedimentary lithologies (40 percent sandstone, 25 percent limestone). This source contains >10 percent chert, an amorphous silica thought to be reactive. Bg-111c and Pw-84c are both approximately 70 percent quartzite.

The remainder of Bg-111c is made up of a combination of volcanic and intrusive lithologies and sedimentary rocks, while the remainder of Pw-84c is comprised of sandstone and limestone (Figure 67).

Fine Aggregate Lithologic Inventories Relative to ASR from District 5

FA from Bl-84c and Bg-111c are predominantly composed of quartz and weathered CA material (Figures 68 and 69). However, both sources show increased amounts of amorphous silica with 20 percent chert in Bl-84 FA and 20 percent obsidian in Bg-111c FA. In contrast, Figure 70 shows that FA from Pw-84c is 80 percent quartzite.

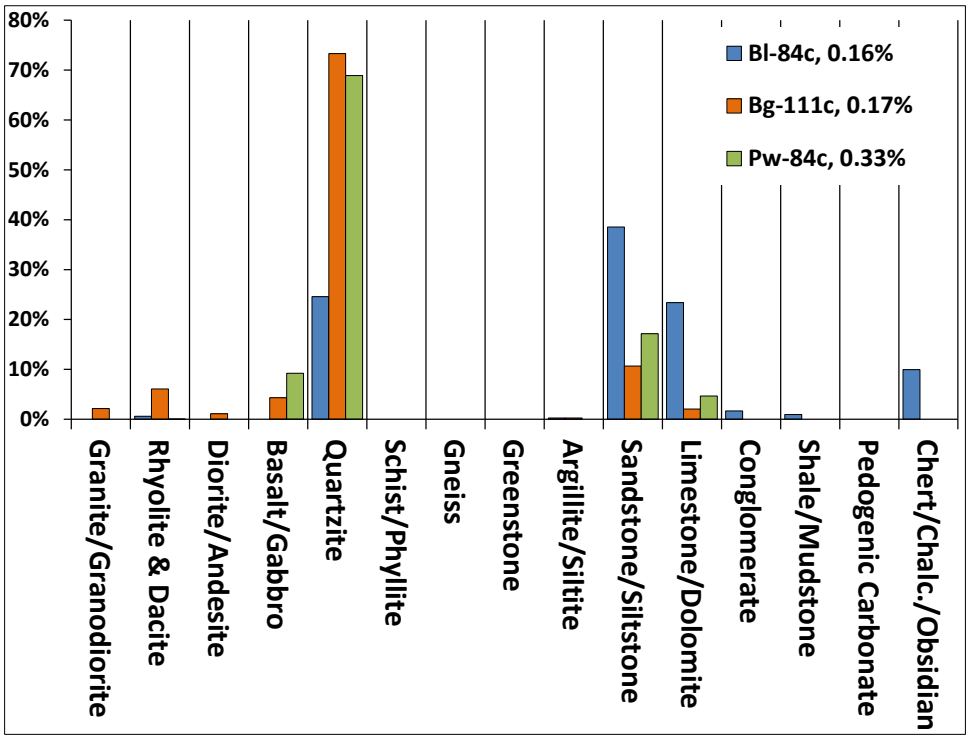

Figure 67. District 5 Lithologic Inventories and AASHTO T 303 Test Values (Upper Right) for Bl-84c, Bg-111c and Pw-84c

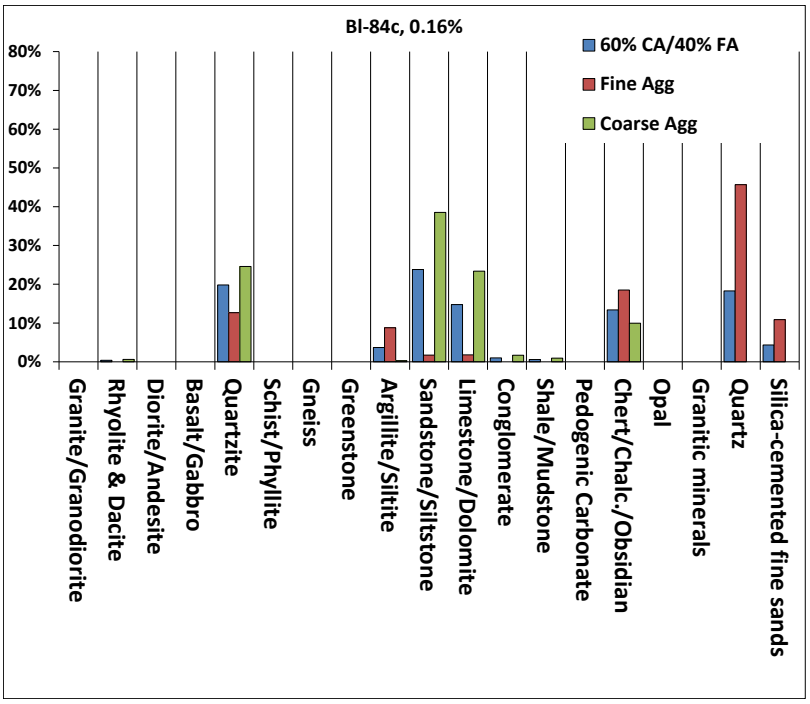

Figure 68. District 5 Bl-84c Lithologic Inventory (CA, FA and 60% CA/40% FA) and AASHTO T 303 Test Value (Upper Center)

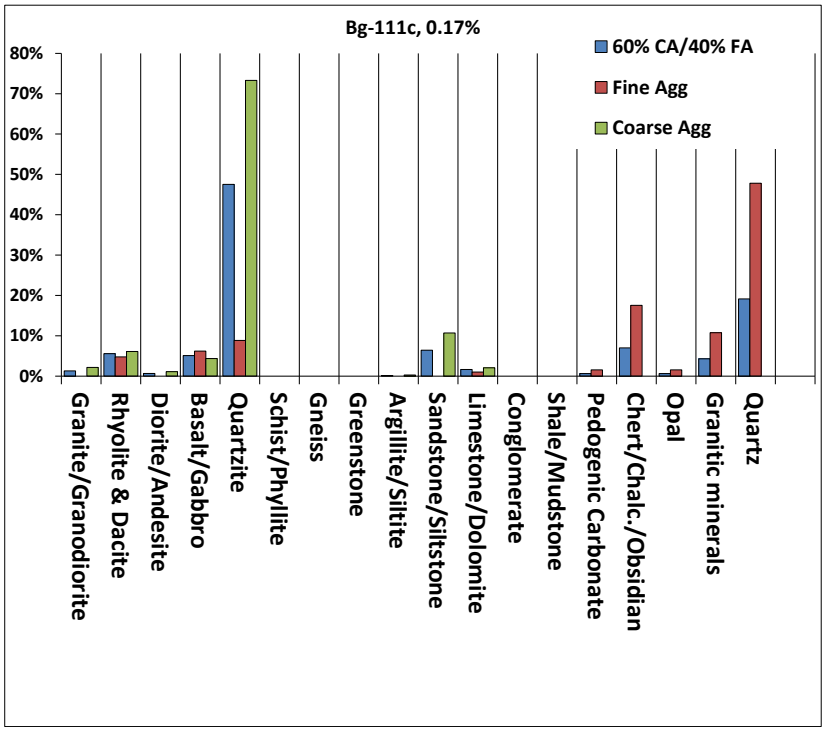

Figure 69. District 5 Bg-111c Lithologic Inventory (CA, FA and 60% CA/40% FA) and AASHTO T 303 Test Value (Upper Center)

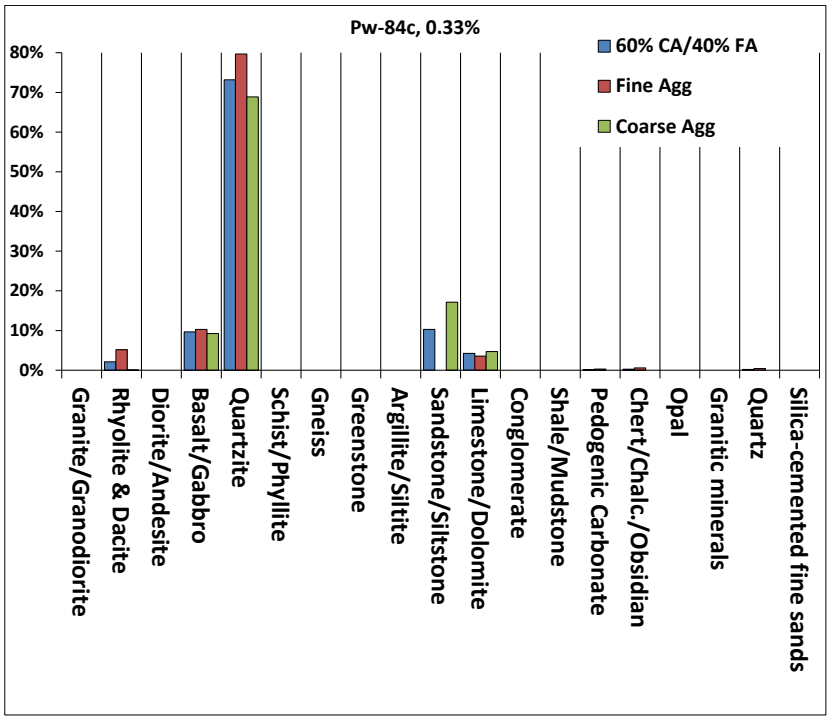

Figure 70. District 5 Pw-84c Lithologic Inventory (CA, FA and 60% CA/40% FA) and AASHTO T 303 Test Value (Upper Center)

District 6 (Eastern and Central Idaho)

Sampled sources from District 6 include: Bn-155c, Cu-73c, Jf-103c, Le-154c, Le-155c, Ma-22c, Ma-68c and Tn-65c (Figures 71 and 72). AASHTO T 303 values for District 6 range from 0.10 to 0.86 percent as shown in Table 9. The source with the lowest measured ASR (0.10 percent) is Tn-65c, located in the Teton Valley of Idaho. Sources with moderate to moderately high AASHTO T 303 values (0.36 – 0.49 percent) are found in fluvial deposits and terrace gravel deposits of the Salmon River (Cu-73c, Le-154c and Le-155c) and in fluvial deposits found in upper reaches of the Snake River (Jf-103c, Ma-68c). Bn-155c, a source in glacial outwash deposits of the upper Snake River plain, has a high AASHTO T 303 value of 0.64 percent. Ma-68c, a source located in alluvium of the Teton River has two AASHTO T 303 tests with vastly different results; the test on FA produced 0.86 percent expansion, while the test using CA from Ma-68c showed an expansion of 0.39 percent.

Coarse Aggregate Lithologic Inventories Relative to ASR from District 6

The source with the lowest ASR in District 6 (Tn-65c) as shown in Figure 71, contains 45 percent granite and 40 percent limestone. Sources Cu-73c, Jf-103c, Ma-22c and Le-154c contain a combination of volcanic rocks and quartzite. Of note, Jf-103c contains 25 percent obsidian. Ma-68c, Le-155c, and Bn-155c contain markedly similar lithologic components (approximately 65 percent quartzite, 10 percent rhyolite and dacite, 10 percent sandstone and <1 percent obsidian); however AASHTO T 303 values are somewhat dissimilar but all sources are reactive (Figure 72).

Table 9. District 6 Source Locations, ASR and Descriptions

ITD Name	Latitude	Longitude	AASHTO T 303 (Percent)	ASTM C 1293 (Percent)	Location Description	Geologic Unit (Cited if Mapped)	Cites
Bn-155c	43.455983	-112.058868	0.64		Near Snake River, South of Idaho Falls, ID	Alluvium of Snake River Glacial Outwash	32
Cu-73c	44.498438	-114.197274	0.36		Near the Salmon River, East of Challis, ID		
Jf-103c	43.670504	-112.098231	0.38		Near Snake River, South of Roberts, ID	Volcanic Lithic Sand	33
Le-154c	45.284319	-113.895239	0.49		On the Salmon River, North of Salmon and South of Carmen, ID	Gravel Terrace Deposits of the Lemhi and Salmon Rivers	34
Le-155c	45.186042	-113.873065	0.48		Northeast of Salmon, ID	Alluvium of Salmon River	
Ma-22c (CA)	43.833352	-111.793792	0.39		Near Teton River, North Side of Rexburg, ID (Within the City Limits)	Alluvium of Teton River	
Ma-22c (FA)	43.833352	-111.793792	0.86		Near Teton River, North Side of Rexburg, ID (Within the City Limits)	Alluvium of Teton River	
Ma-68c	43.765161	-111.828842	0.39		South of Rexburg, ID	Alluvium of the Henry's Fork of the Snake River	
Tn-65c	43.728497	-111.074247	0.10		Near Teton Creek, East of Driggs, ID	Alluvium of Teton River	

Fine Aggregate Lithologic Inventories Relative to ASR from District 6

Tn-65c, Cu-73c and Le-155c show very little compositional changes between FA and CA lithologies (Figures 73 - 75). FA in source Jf-103c is 70 percent obsidian (Figure 76). In source Ma-68c, the composition of FA showed increased pedogenic carbonate (15 percent), obsidian (5 percent) and opal (15 percent; Figure 77). At Bn-155c, obsidian makes up 50 percent and opal 5 percent of FA composition (Figure 78). Figure 79 shows that the FA at Le-154c is 70 percent quartzite. In source Ma-22c, where the FA AASHTO T 303 value (0.86 percent) is significantly higher than the CA AASHTO T 303 value (0.39 percent), obsidian makes up 10 percent and opal accounts for 5 percent of FA (Figure 80).

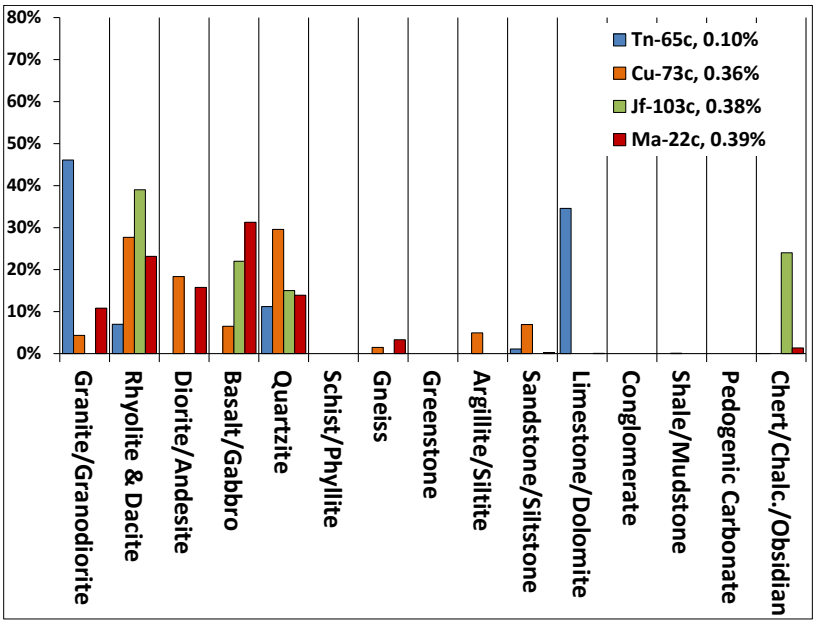

Figure 71. District 6 Lithologic Inventories and AASHTO T 303 Test Values (Upper Right) for Tn-65c, Cu-73c, Jf-103c and Ma-22c

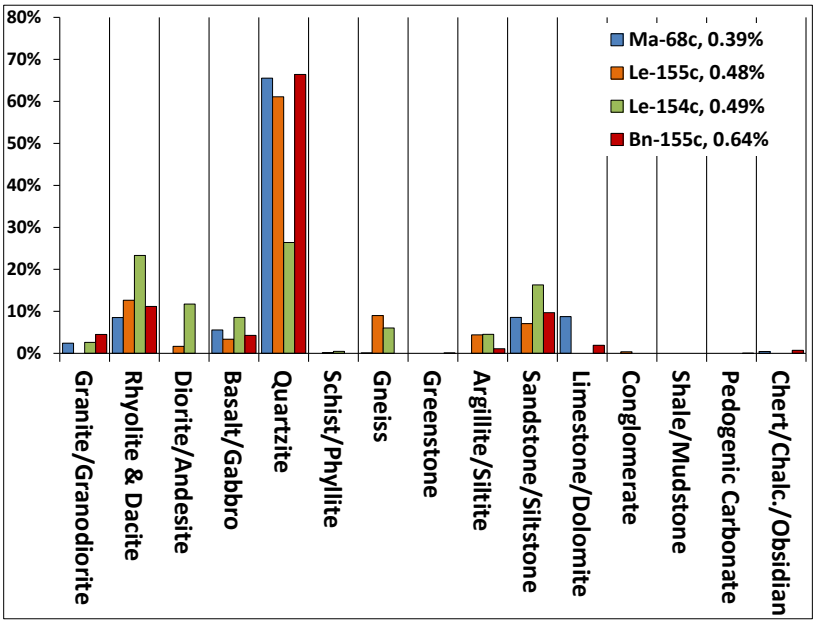

Figure 72. District 6 Lithologic Inventories and AASHTO T 303 Test Values (Upper Right) for Ma-68c, Le-155c, Le-154c and Bn-155c

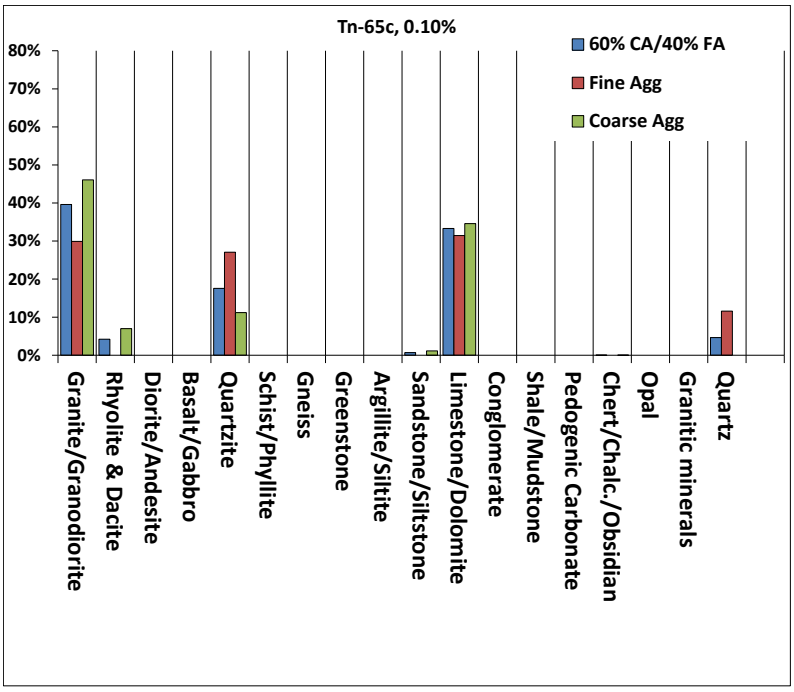

Figure 73. District 6 Tn-65c Lithologic Inventory (CA, FA and 60% CA/40% FA) and AASHTO T 303 Test Value (Upper Center)

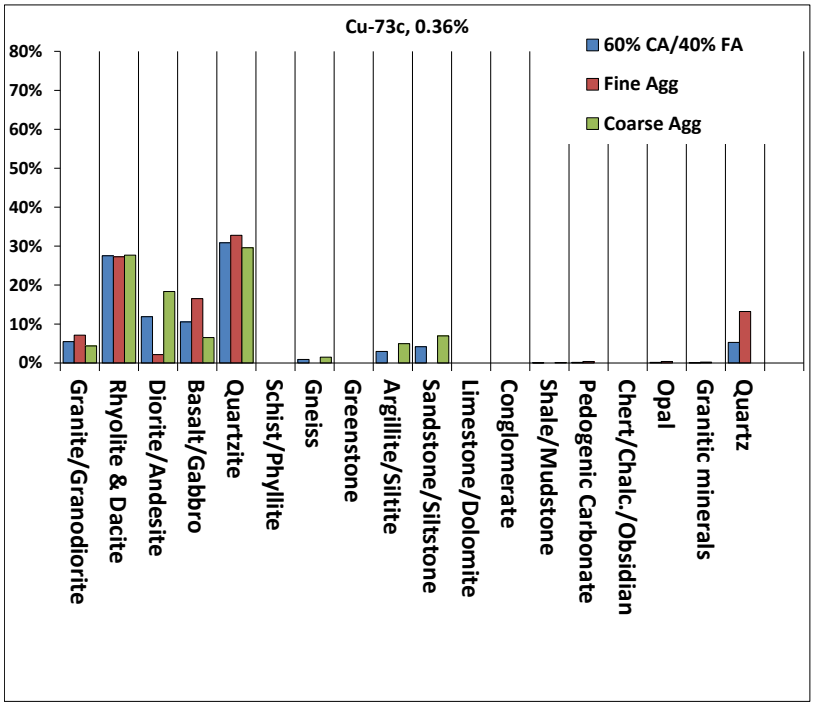

Figure 74. District 6 Cu-73c Lithologic Inventory (CA, FA and 60% CA/40% FA) and AASHTO T 303 Test Value (Upper Center)

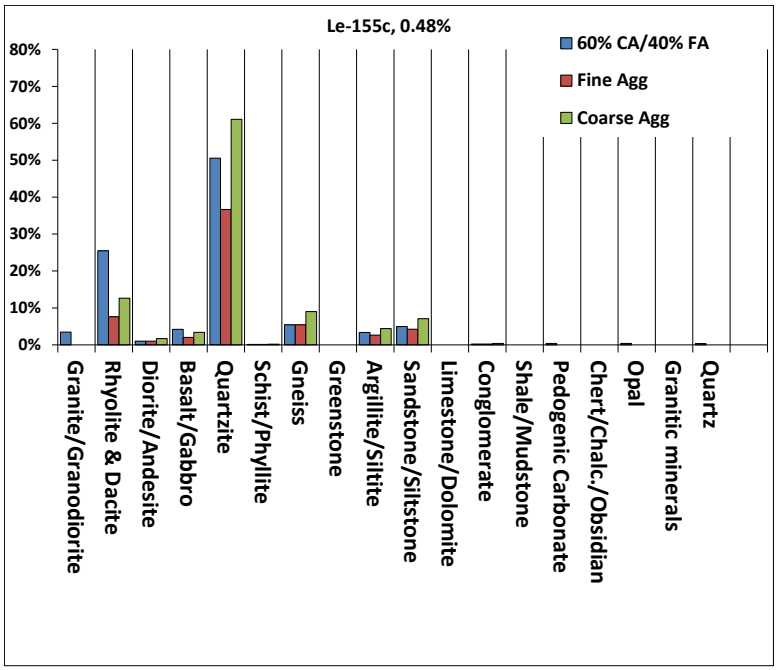

Figure 75. District 6 Le-155c Lithologic Inventory (CA, FA and 60% CA/40% FA) and AASHTO T 303 Test Value (Upper Center)

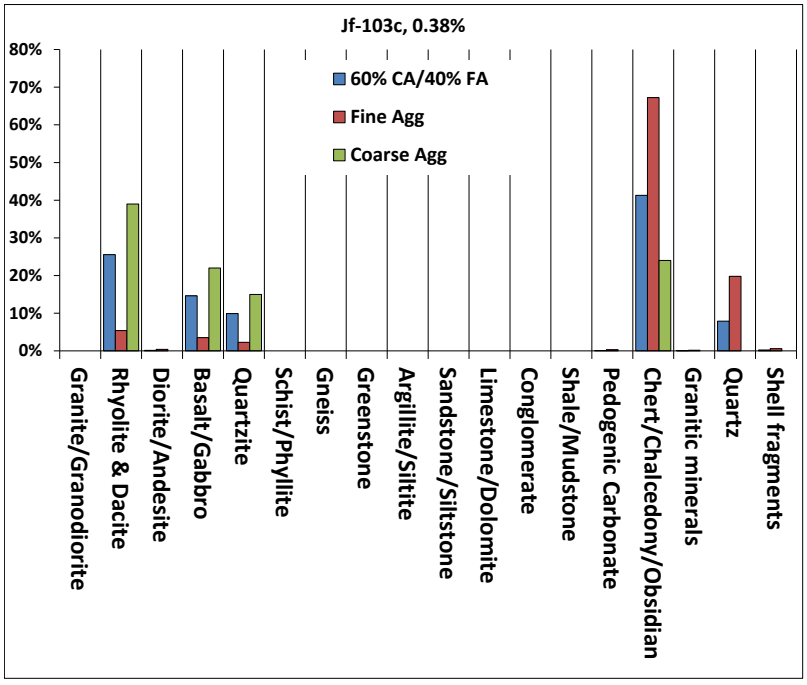

Figure 76. District 6 Jf-103c Lithologic Inventory (CA, FA and 60% CA/40% FA) and AASHTO T 303 Test Value (Upper Center)

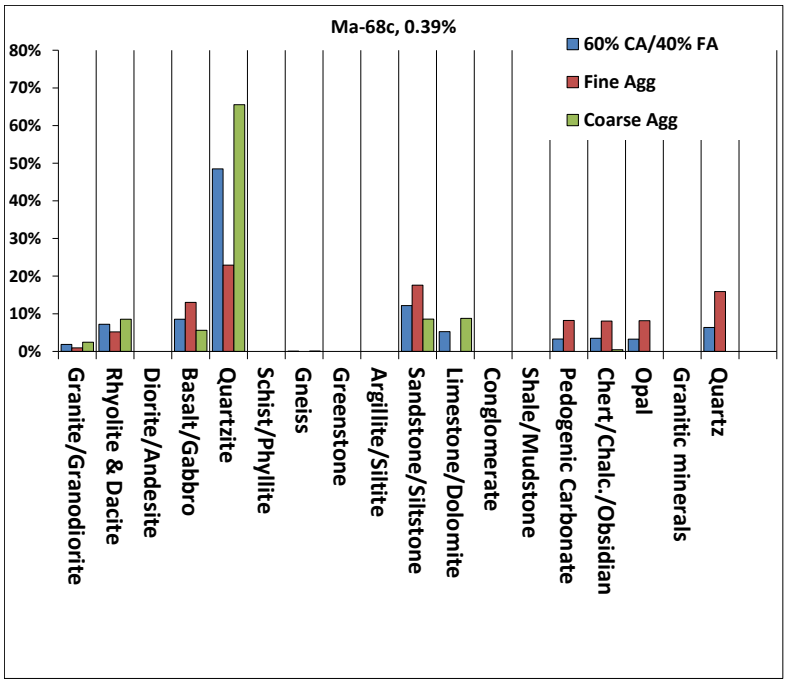

Figure 77. District 6 Ma-68c Lithologic Inventory (CA, FA and 60% CA/40% FA) and AASHTO T 303 Test Value (Upper Center)

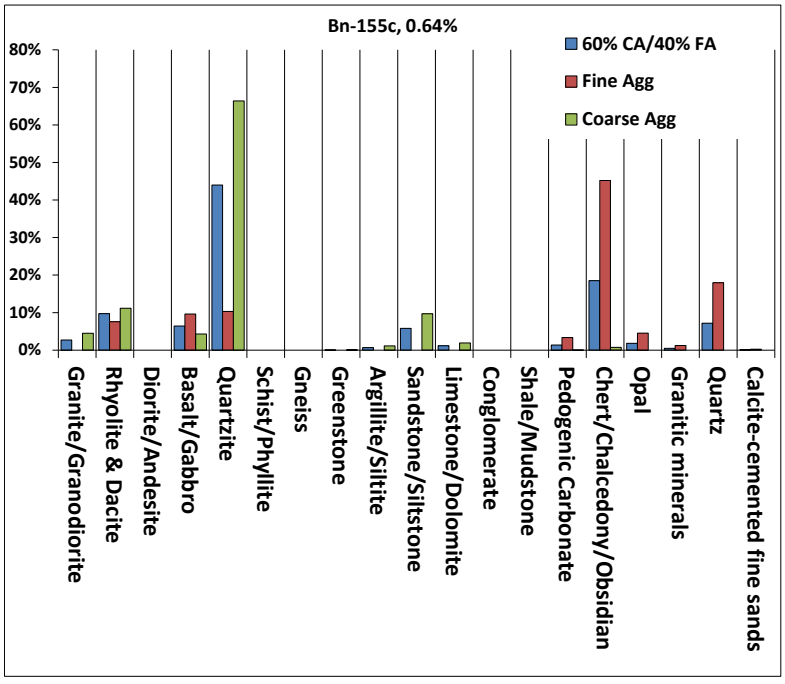

Figure 78. District 6 Bn-155c Lithologic Inventory (CA, FA and 60% CA/40% FA) and AASHTO T 303 Test Value (Upper Center)

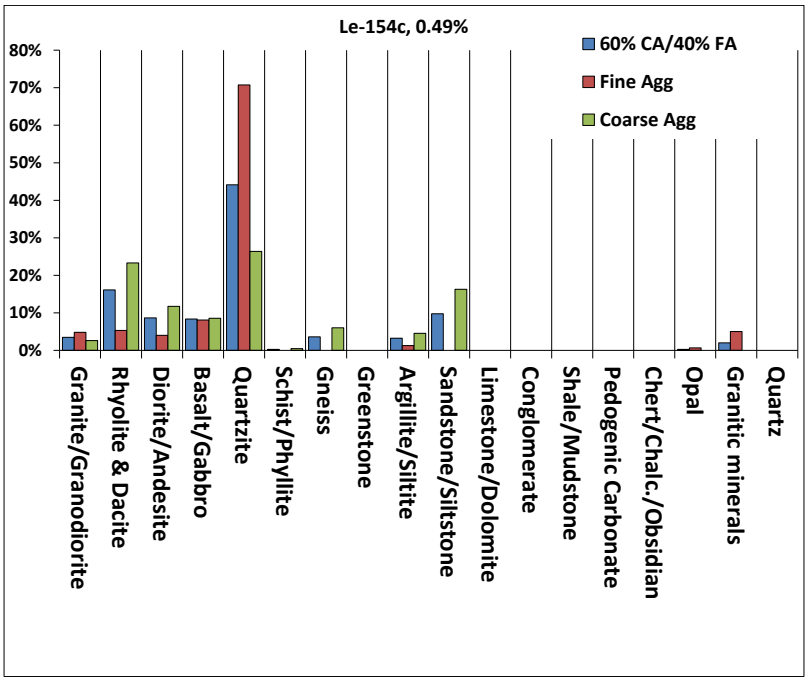

Figure 79. District 6 Le-154c Lithologic Inventory (CA, FA and 60% CA/40% FA) and AASHTO T 303 Test Value (Upper Center)

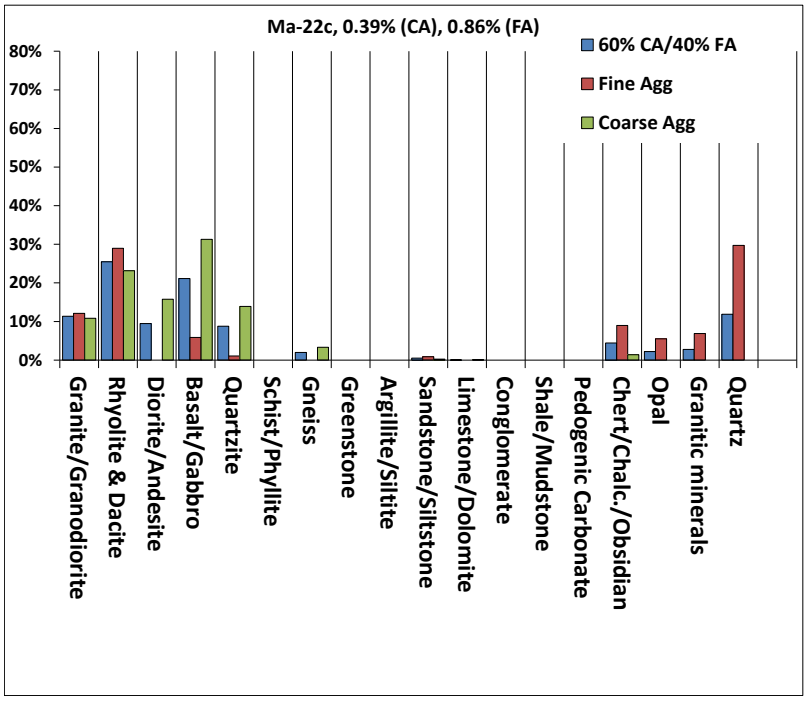

Figure 80. District 6 Ma-22c Lithologic Inventory (CA, FA and 60% CA/40% FA) and AASHTO T 303 Test Value (Upper Center)

Chapter 5
Spatial Correlation of Aggregate Source to Idaho Geology and Drainage Basins

Most of the aggregate sources utilized in Idaho, including most of those sampled for this project, consist of accumulations of fluvial gravels deposited by modern or ancient streams. The sand and gravel present in those streams was derived from rocks and landscapes farther up in the drainage basin, also known as the watershed. Thus, the lithologies in the gravel are a reflection of rocks in their provenance or source terrain upstream of the sampled aggregate pit. Geologic maps document the rock types exposed in an area and also provide a picture of the potential provenance of gravels from a particular source. By utilizing the geologic map as a more comprehensive, but less specific, guide and the lithologic inventories and the ASR test results as more detailed data points, a predictive geologic model can be developed for assessing ASR potential of aggregate over a region.

Watershed basin delineation upstream of each aggregate source allows for correlation between aggregate source lithologic inventories and mapped geologic units.[(1)] Some source watersheds extend beyond the Idaho state borders. In these cases a general description of geologic units exposed outside of Idaho is given, but individual geologic units are not clipped out and shown on the map. Details about aggregate sources and their contributing drainage basins is organized below by ITD District. Some general correlations between source lithologic inventories (percentages are rounded to nearest whole number and generally estimated) and geologic provenance are provided in this chapter with additional discussion in the following chapters.

District 1 (Northern Idaho)

Figures 81 shows the geology and watersheds for District 1 located in northern Idaho. Units are listed in Figure 82. Six sources were sampled. Major rock types and their likely provenance are listed below for each source. Percentages quoted may total less than 100 percent as not all minor rock types are described below.

Br-2c

The drainage basin for Br-2c is the largest source watershed in District 1, covering 22,339 mi^2 with the majority of the watershed located in Montana as shown in Figure 81.

- *Quartzite* (40 - 60 percent of the Br-2c source lithologies) was likely sourced from Belt Supergroup metasedimentary rocks (quartzite, argillite and siltite) of the Upper Missoula Group (Ymiu) and the Ravalli Group (Yra) that are exposed in the northern portion of the watershed in Montana, and more proximally in Idaho.
- *Granodiorite* (approximately 30 percent) probably came from nearby exposures of Challis Volcanic Group granodiorite (Tei) and of the Idaho Batholith granodiorite (Kg).

By-74c and By-80c

Figure 81 shows the watersheds for By-74c and By-80c which cover areas of 3,207 mi^2 and 166 mi^2, respectively. Source lithologic inventories for the 2 sources are almost identical.

- *Quartzite* (60 - 70 percent) likely correlates to Belt Supergroup metasedimentary rocks found in the Lower Missoula Group (Ymil), Prichard Formation (Yp), Piegan Formation (Ypi) and Ravalli Group (Yra), which are all exposed in Northern Idaho and Northern Montana.
- *Argillite* (10 - 15 percent) which also correlates to the Belt Supergroup metasedimentary rocks found in the Lower Missoula Group (Ymil), Prichard Formation (Yp), Piegan Formation (Ypi) and Ravalli Group (Yra) that are exposed in Northern Idaho and Northern Montana.
- *Diorite* (10 - 12 percent) probably corresponds to quartz diorite of the Idaho Batholith (Ktg) exposed in northern Idaho.

Kt-191c

The Kt-191c watershed of 3,783 mi^2 is located entirely within Idaho.

- *Quartzite* (35 percent) of Kt-191c, originates from Belt Supergroup metasedimentary rocks found in the Lower Missoula Group (Ymil), Prichard Formation (Yp), Piegan Formation (Ypi) and Ravalli Group (Yra).
- *Argillite* (5 percent) originates from Belt Supergroup metasedimentary rocks found in the Lower Missoula Group (Ymil), Prichard Formation (Yp), Piegan Formation (Ypi) and Ravalli Group (Yra).
- *Granodiorite* (15 percent) is likely Idaho Batholith (Ktg).
- *Basalt* (25 percent) is from the Columbia River Basalts (Tcr).

Kt-213c

Located entirely in Idaho, the contributing watershed for Kt-213c covers an area of 163 mi^2. However Breckenridge and Othberg mapped the gravel unit that makes up Kt-213c as Missoula flood gravels (Qm) which extends its contributing paleo-watershed into northern Montana.[23]

- *Quartzite* (40 percent) lithologies are likely sourced from Belt Supergroup metasedimentary rocks found in the Lower Missoula Group (Ymil), Prichard Formation (Yp), Piegan Formation (Ypi) and Ravalli Group (Yra).[23]
- *Argillite* (30 percent) is likely sourced from Belt Supergroup metasedimentary rocks found in the Lower Missoula Group (Ymil), Prichard Formation (Yp), Piegan Formation (Ypi) and Ravalli Group (Yra).[23]
- *Weathered Carbonate/Calcareous Siltstone* (approximately 7 percent) is made up of rocks that are from the Piegan Formation (Ypi). This particular lithology is thought to cause “pop-outs” in concrete throughout the Coeur d’Alene area. The pop-outs are typical of freeze-thaw action on concrete containing relatively weak and porous aggregate of sedimentary origin, such as siltstones, sandstones, and limestones.
- *Granodiorite* (10 percent) is likely from the Idaho Batholith (Kog) and Challis Volcanic group.

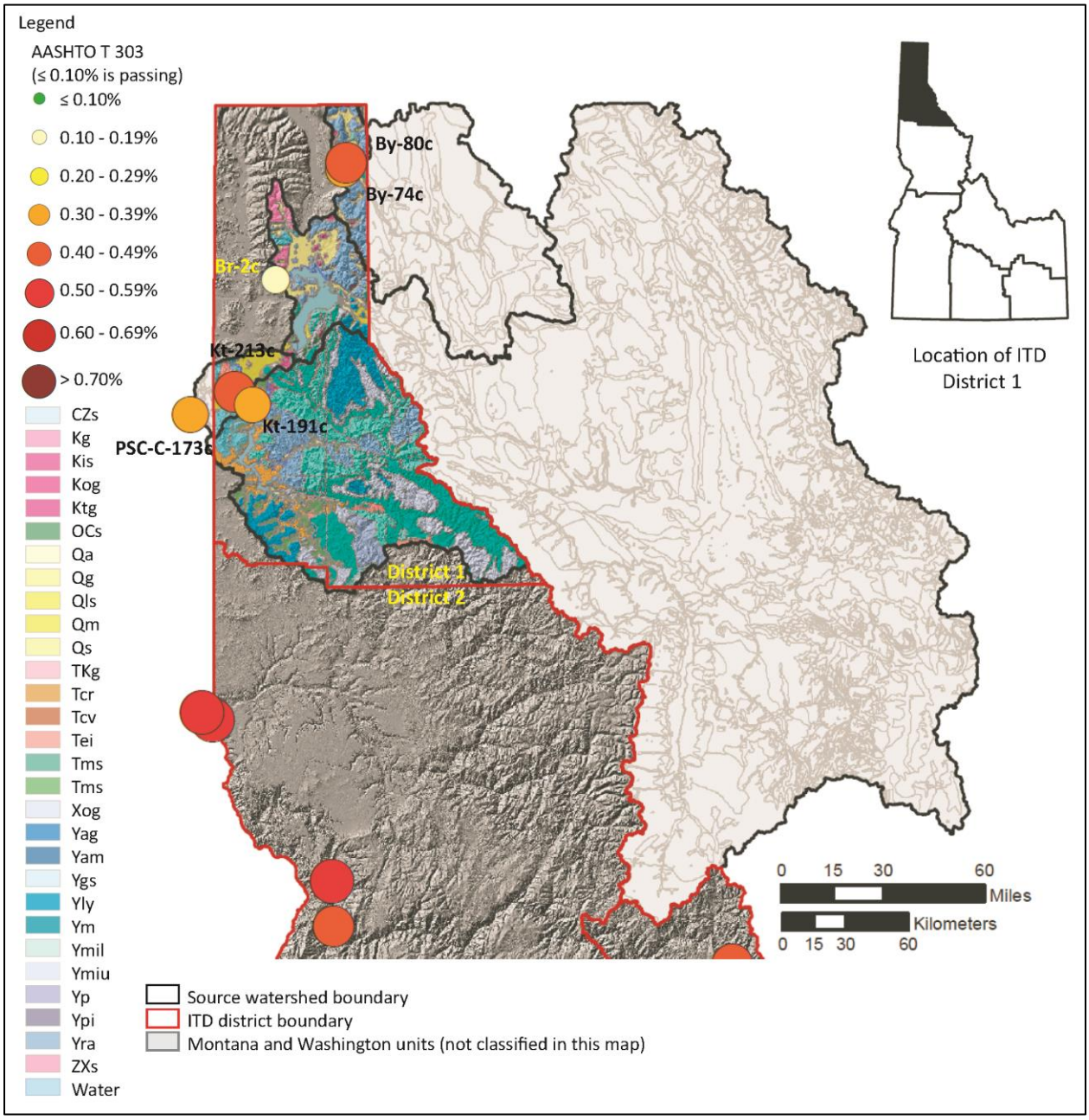

Figure 81. District 1 Source Watersheds and Geologic Units

The legend for this figure is shown in Figure 82

Figure 82. Description of Geologic Units

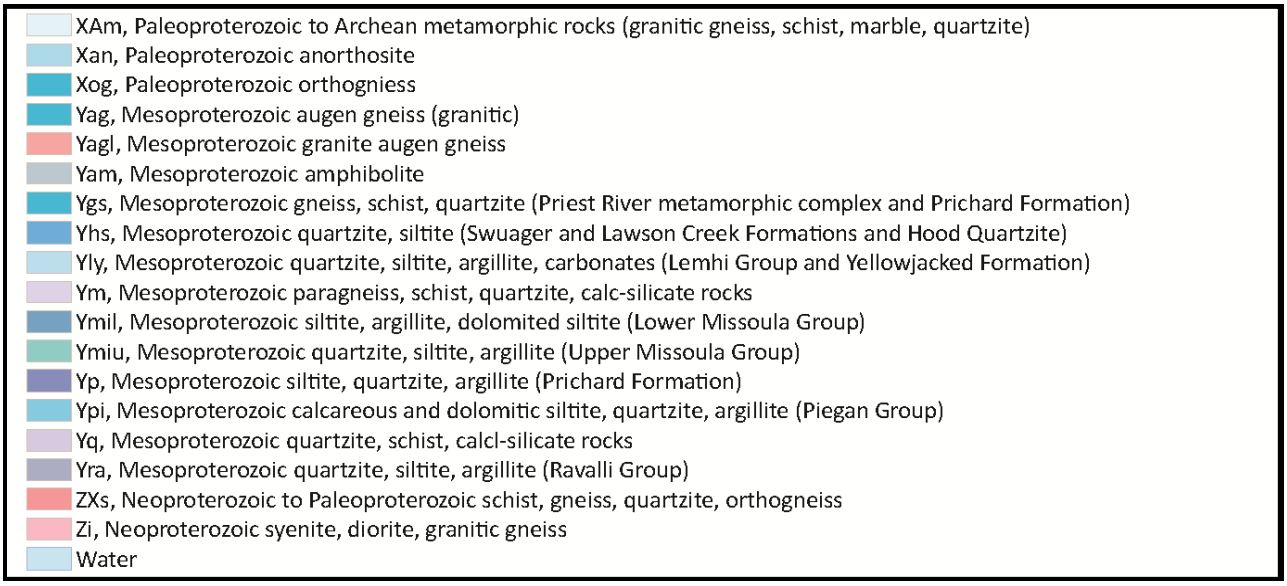

Figure 82 (Cont.) Description of Geologic Units

PSC-173c

The PSC-173c watershed has an area of 4,159 mi^2, and although the source is located west of the Washington border, the bulk of the watershed is in Idaho. Figure 81 shows the location of the source.

- *Quartzite* (approximately 40 percent) likely originates from Belt Supergroup metasedimentary rocks found in the Lower Missoula Group (Ymil), Prichard Formation (Yp), Piegan Formation (Ypi) and Ravalli Group (Yra).
- *Argillite* (approximately 35 percent) likely originate from Belt Supergroup metasedimentary rocks found in the Lower Missoula Group (Ymil), Prichard Formation (Yp), Piegan Formation (Ypi) and Ravalli Group (Yra).
- *Carbonate/Calcareous Siltstone* (15 percent) is a problematic (pop-out causing) siltstone of the Piegan formation (Ypi).
- *Granodiorite* (5 percent) is probably Idaho Batholith (Kog) and Challis Volcanics (Tei).
- *Diorite* (5 percent) is probably are Idaho Batholith (Kog) and Challis Volcanics (Tei).

District 2 (North-Central Idaho)

Figure 83 shows the locations of District 2 contributing watersheds. Since several of the sampled pits are on the Snake River near its confluence with the Clearwater, the watersheds may include nearly the full Snake River basin, which encompasses a large portion of Idaho.

ACW-8c

The contributing watershed for ACW-8c is the largest in this study with an area of 102,630 mi^2. ACW-8c is located on a river terrace and may not represent modern drainage patterns, nevertheless lithologies

of ACW-8c and Np-82c do not vary significantly. The ACW-8c watershed encompasses all of central Idaho, most of southern Idaho and extends into Washington, Oregon, Nevada and Wyoming.

- *Basalt* (approximately 50 percent) is likely from the Columbia River Basalts (Tcr) that outcrop in Idaho, Washington and Oregon, and from the Seven Devils Group (T_Psd) Rhyolite (20 percent) outcrops located throughout the watershed; however, the closest exposures occur in the Seven Devils Group (T_Psd) and to the south of ACW-8c in Oregon, where Miocene-Pliocene aged rhyolites are found.
- *Quartzite* (5 percent) is probably sourced from the Windermere Supergroup (CZs).

Np-82c

Just to the east of ACW-8c and located upstream of the Snake River and Clearwater River confluence, is Np-82c which has the second largest contributing watershed in this study with an area of 93,188 mi^2. This watershed encompasses all of central Idaho, most of southern Idaho and extends into Washington, Oregon, Nevada and Wyoming.

- *Basalt* (35 percent) is likely from the Columbia River Basalts (Tcr) that outcrop into Idaho, Washington and Oregon, and from the Seven Devils Group (T_Psd).
- *Rhyolite* (25 percent) Although rhyolite outcrops throughout the watershed, the closest exposure occurs in the Seven Devils Group (T_Psd) and to the south of ACW-8c in Oregon, where Miocene-Pliocene aged rhyolites are found.
- *Quartzite* (20 percent) is probably sourced from the Windermere Supergroup (CZs).

Id-121c

Located entirely in Idaho the Id-121c watershed has an area of 13,359 mi^2.

- *Quartzite* (>50 percent) Although there are several sources for quartzite within the watershed, the closest quartzite exposures are found in Precambrian metamorphic rocks (Ym), the Lemhi Group (Yl) and Hoodoo Quartzite (Yha).
- *Basalt* (15 percent) probably originates from the Seven Devils Group (T_Psd) and the Challis Volcanic Group (Tcr).
- *Andesite* (12 percent) probably originates from the Seven Devils Group (T_Psd) and the Challis Volcanic Group (Tcr).
- *Rhyolite* (5 percent) probably originates from the Seven Devils Group (T_Psd) and the Challis Volcanic Group (Tcr).

Id-272c

The contributing watershed for Id-272c has an area of 13,097 mi^2 and is located entirely in Idaho. The lithologic inventory of Id-272c indicate that the source is roughly split among 5 prominent lithologies.

- *Granodiorite* (20 percent) likely originates from the Idaho Batholith (Kg).
- *Rhyolite* (15 percent) and *Intermediate Volcanics* (25 percent) are probably from the Challis Volcanic Group (Tcv).
- *Basalt* (15 percent) is likely from nearby Columbia River Basalts (Tcr).

- *Quartzite* (15 percent), may have originated from Precambrian metasedimentary rocks (PzYs) and metasedimentary rocks found in the Windermere Supergroup (CZs).

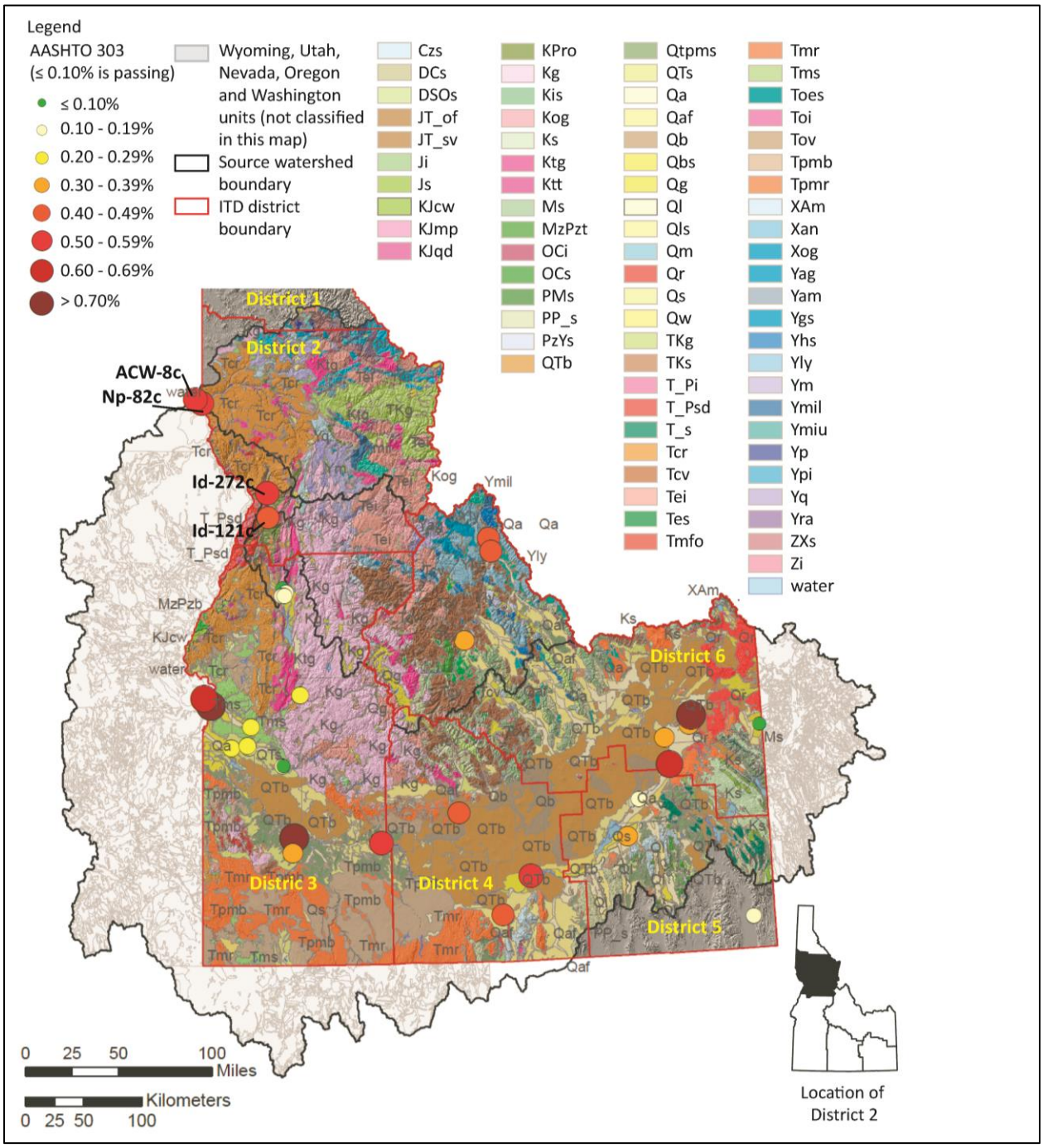

Figure 83. District 2 Source Watersheds and Geologic Units
The legend for this figure is shown in Figure 82

District 3 (Southwestern Idaho)

Located in Southwestern Idaho, District 3 drainage basins are included within the southern Snake River Plain, Payette River and Boise River Basins. These drainage basins and the geology of District 3 are shown in Figure 84.

Ad-136c and Ad-53s

Sources Ad-136c and Ad-53s are located less than a quarter of a mile apart on the same surficial geologic unit, the Gowen Terrace gravel, so only 1 drainage basin was delineated for the 2 sources. The watershed covers an area of 2,713 mi^2.[27]

- *Granodiorite* (25 percent of Ad-136c and 38 percent of Ad-53s) is Idaho Batholith (Kg and Ktg).
- *Rhyolite and Dacite* (20 percent of Ad-136c and 25 percent of Ad-53s) is likely derived from the Challis Volcanics (Tei).
- *Basalt and Andesite* (50 percent of Ad-136c and 30 percent of Ad-53s) could have come from Pleistocene-Pliocene aged intermediate to mafic volcanics (QTb), Pliocene-Miocene aged intermediate to mafic volcanics (Tpmb) and Columbia River Basalts (Tcr) plus Eocene-age dikes related to the Challis Group.

Bo-61c

The contributing watershed for Bo-61c has an area of 1,161 mi^2.

- *Granodiorite* (approximately 60 percent) most likely came from Idaho Batholith (Kg and Ktg) but some of it could be from the Challis intrusive rocks (Tei).
- *Rhyolite/Dacite* (20 percent) are likely Eocene Challis volcanic or subvolcanic rocks (Tcv).
- *Basalt* (10 percent) is probably from the Columbia River Basalt group (Tcr).

Cn-140c and Cn-146c

Cn-140c is located about 8 miles west of Cn-146c, however they are both located in the modern floodplain (Qa) and no confluence occurs between the 2 locations, therefore we delineated one watershed for both sources.[27] The watershed has an area of 3,780 mi^2 . Despite the proximity of the two sources there are differences.

- *Granodiorite* (none in Cn-140c but 30 percent of Cn-146c) probably originated from the Idaho Batholith (Kg and Ktg) and from Challis intrusive rocks (Tei).
- *Rhyolite/Dacite* (5 percent of Cn-146c and 50 percent of Cn-140c) are classified as Miocene rhyolites (Tmr).
- *Andesite* (30 percent of each source) likely from Pliocene-Pleistocene aged volcanic rocks (QTb).
- *Basalt* (30 percnt of Cn-146c and 10 percent of Cn-140c) is likely from Pliocene-Pleistocene aged volcanic rocks (QTb).

Gm-46c

The drainage basin for Gm-46c has an area of 2,752 mi^2 .

- *Grandiorite* (40 percent) is from the Idaho Batholith (Ktg and Kg).
- *Diorite* (20 percent) is from the Eocene Challis Volcanic Group (Tei or Tcv).
- *Rhyolite/Dacite* (15 percent) from Miocene rhyolites (Tmr).
- *Basalt* (10 percent) likely originated from either the Columbia River Basalts (Tcr or possibly the Challis Volcanics Group (Tcv).

El-116c

The El-116c watershed has a large area of 35,648 mi^2 as located in Figure 84.

- *Basalt* (25 percent) is from from the Snake River Plain, the majority of which is Pleistocene-Pliocene-aged basalt (Qtb).
- *Quartzite* (approximately 20 percent) likely comes from a variety of locations.
    - White, massive quartzite found in El-116c may come from Northern Utah where Cambrian-age quartzite is found.
    - Fine to medium-grained, white to peach colored quartzite probably came from Proterozoic Elba quartzite that outcrops near the Idaho-Utah border (CZs).
    - Fine to medium-grained, gray quartzite in El-116c likely comes from the Permian Dollarhide Formation in the Wood River Valley and is consistent with the occurrence of lesser amounts of siliceous argillite, sandstone/siltstone and conglomerate that are likely from the Hailey Member of the Wood River Formation and the Milligen formation in the Wood River Valley (units shown on map).[1,35]
- *Rhyolite/Dacite* (15 percent) could originate from Miocene-aged Snake River Plain volcanics (Tmr and Tmfo), or from the Challis Volcanic Group which outcrops to the north (Tcv).
- *Andesite* (15 percent) is also likely from the Challis Volcanic Group (Tcv).

El-37c

The contributing watershed for El-37c has a large area of 41,589 mi^2.

- *Basalt* (40 percent) occurs very close to the source as Pliocene-Miocene-aged basalts (Tpmb).
- *Rhyolite* (20 percent) also is present very close to the source as Miocene-aged rhyolites (Tmr).
- *Quartzite* (35 percent) resembles the quartzite clasts found in source El-116c, which is about 45 miles upstream of El-37c. Due to similar characteristics we assume that the quartzite likely came from Cambrian-aged outcrops in Northern Utah, the Wood River Valley and Proterozoic outcrops near the Idaho-Utah border (CZs).[1]

Ore-8c

The drainage basin for Ore-8c is the largest source watershed in District 3, with an area of 63,909 mi^2 draining all of the Snake River Plain and parts of Utah, Nevada and Oregon. Ore-8c is located on an older river terrace.

- *Basalt* (greater than 40 percent) is likely from Miocene basalts found in eastern Oregon and southwestern Idaho (Tpmb).
- *Rhyolite* (25 percent) probably comes from Miocene rhyolites found in eastern Oregon and southwestern Idaho (Tpmr; Tmr).
- *Granodiorite* (approximately 20 percent) likely comes from Idaho Batholith (Kg and Ktg) and Challis intrusive rocks (Tei).

Ore-16c

Located 5 miles southeast of Ore-8c, Ore-16c drains an area of 59,142 mi^2. Ore-16c sits in the modern flood plain.

- *Basalt* (30 percent) is likely from Miocene basalts found in eastern Oregon and southwestern Idaho (Tpmb).
- *Rhyolite* (25 percent) probably comes from Miocene rhyolites found in eastern Oregon and southwestern Idaho (Tmr, Tpmr).
- *Granodiorite* (approximately 20 percent) likely comes from Idaho Batholith (Kg and Ktg) and Challis intrusive rocks (Tei).

Ow-117c

The Ow-117c watershed has an area of only 678 mi^2. The basin drains primarily through volcanic units (e.g., rhyolite, andesite and basalt) which are reflected by 100 percent volcanic constituents in the source lithologic inventory. Lithologic units include Pliocene-Miocene basalt (Tpmb) and Miocene Rhyolite (Tmr).

- *Diorite/Andesite (80 percent)*
- *Rhyolite and Basalt (5 percent each)*

Vy-52c

Sources Vy-52c and Vy-56c are only about 0.25 miles apart near the town of McCall, however Vy-52c is located in glacial outwash deposits (Qpoo) and Vy-56c is located in alluvium of the North Fork Payette River (Qal).[30] The watershed for Vy-52c drains an area of 146 mi^2.

- *Granodiorite* (60 percent) is from the Idaho Batholith (Kg, Kog and Ktg).
- *Siltite* (25 percent) is from Paleozoic –Precambrian metasedimentary rocks (PzYs).
- *Basalt* (15 percent) is from Columbia River Basalt Group (Tcr).

Vy-56c

Sources Vy-52c and Vy-56c are only about 0.25 miles apart, however Vy-52c is located in glacial outwash deposits (Qpoo) and Vy-56c is located in alluvium of the North Fork Payette River (Qal).[30] The watershed for Vy-56c has an area of 160 mi^2. Vy-56c is composed of mostly:

- *Basalt* (over 60 percent) is from the Columbia River Basalt Group (Tcr).
- *Granodiorite* (18 percent) is from the Idaho Batholith (Kg, Kog and Ktg).

- *Quartzite/Argillite* (lesser amounts) are from Paleozoic-Precambrian metasedimentary rocks (PzYs).

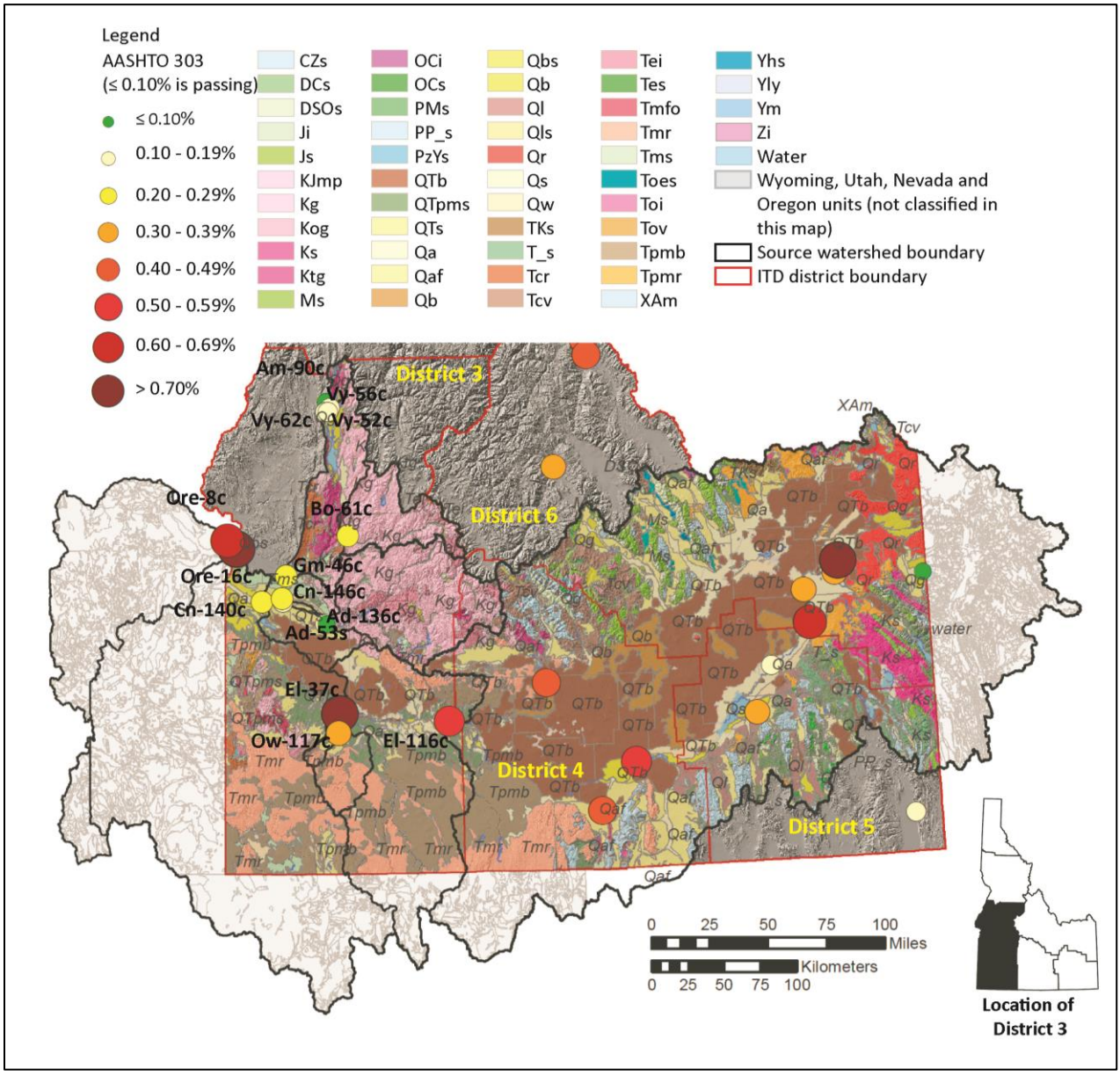

Figure 84. District 3 Source Watersheds and Geologic Units

The legend for this figure is shown in Figure 82

District 4 (South-Central Idaho)

Table 7 and Figure 85 provide the details for the District 4 sources. Counties sampled in District 4 include Cassia, Minidoka, and Lincoln.

Cs-186c (Cassia County)

The watershed for Cs-186c covers an area of 971 mi^2.

- *Rhyolite/Dacite* (40 percent) is likely from Miocene outcrops in Idaho, Nevada and Utah (Tmr and Tmfo).
- *Andesite* (10 percent) is sourced from Miocene outcrops in Idaho, Nevada and Utah (Tmr and Tmfo).
- *Obsidian* (11 percent) is probably derived from Miocene silicic rock outcrops in Idaho, Nevada and Utah (Tmr and Tmfo).
- *Sandstone* (20 percent) is from sedimentary rocks of Permian, Eocene and Miocene age in Utah and Nevada.

Ln-80c

The drainage basin for Ln-80c has an area of 1,604 mi^2. The majority of the source is made up of volcanic rocks.

- *Rhyolite* (22 percent) could have come from Miocene rhyolite (Tmr), Pliocene-Miocene rhyolite and basalt (Tpmr and Tpmb), Pleistocene-Pliocene basalt (Qtb) and Challis Volcanic Group (Tcv).
- *Andesite* (20 percent) could have come from, Pliocene-Miocene rhyolite and basalt (Tpmr and Tpmb), Pleistocene-Pliocene basalt (Qtb) and Challis Volcanic Group (Tcv).
- *Basalt* (5 percent) lithologies could have come from Pliocene-Miocene rhyolite and basalt (Tpmr and Tpmb), Pleistocene-Pliocene basalt (Qtb) and Challis Volcanic Group (Tcv).
- *Sandstone* (25 percent) likely originated from Ordovician-Silurian sedimentary rocks (OCs) and Permian-Pennsylvanian sedimentary rocks (PP_s).

Md-45c

The contributing basin for Md-45c has an area of 25,110 mi^2.

- *Rhyolite to Dacite* (20 percent) may be from Pliocene-Miocene rhyolite and basalt (Tpmr and Tpmb), Miocene rhyolite (Tmr and Tmfo), and the Challis Volcanic Group (Tcv).
- *Basalt* (25 percent) likely is from Pliocene-Miocene rhyolite and basalt (Tpmr and Tpmb), Pleistocene-Pliocene basalt (QTb) and the Challis Volcanic Group (Tcv).
- *Obsidian* (15 percent) likely is derived from Pliocene-Miocene rhyolite and basalt (Tpmr and Tpmb), Miocene rhyolite (Tmr and Tmfo).
- *Quartzite* (28 percent).
    - Gray colored quartzite likely is from the Swauger and Lawson (Yhs) formations that outcrop in the Big Lost River valley.
    - Whitish-peach colored quartzite likely originated from the Windermere Supergroup metasediments (CZs) which outcrop to the south and southeast of the source.

- *Sandstone* (10 percent) outcrops of sedimentary rocks are common in this drainage basin, however because sandstone is more friable than other rocks it would likely not transport long distances. For this reason, we suggest that Mississippian sedimentary rocks (Ms) and Permian-Pennsylvanian sedimentary rocks (PP_s) sedimentary rocks are the provenance for Md-45c sandstone because they are the most proximal to the source.

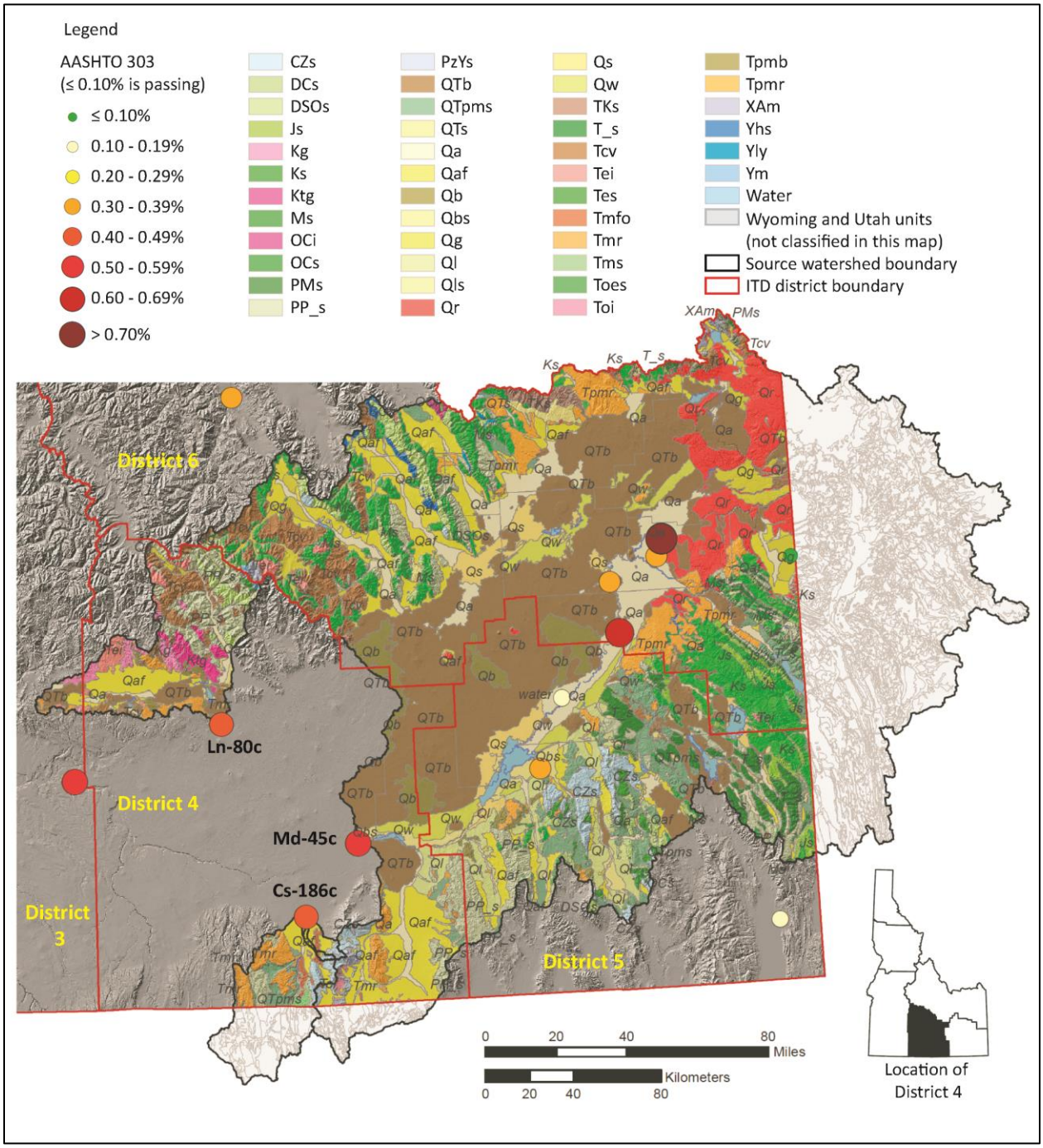

Figure 85. District 4 Source Watersheds and Geologic Units

The legend for this figure is shown in Figure 82

District 5 (Southeastern Idaho)

Table 8 lists the sources in District 5. Figure 86 shows individual source watersheds and geology.

Bg-111c

The watershed for Bg-111c has an area of 18,922 mi^2.

- *Quartzite* (>70 percent) of pink, gray and white color. These quartzites are similar to those found in the upstream source Bn-155c (discussed in the District 6 section), which suggests that they likely have the same provenance. Due to these similarities we suggest that these quartzites are from Ordovician-Cambrian outcrops in Eastern Idaho (OCs).

Bl-84c

The Bl-84c watershed has an area of 2,878 mi^2, and it extends out of Idaho.

- *Quartzite* (20 percent). However, clipped geologic units for the basin do not show any quartzite within the basin. Given the durability of quartzite, the presence of quartzite in the source suggests that these clasts were likely transported in a paleodrainage. Alternatively, these clasts could be very well-cemented sandstone that in hand sample resembles quartzite.
- *Sandstone* (35 percent) are derived from nearby Triassic, Jurassic and Cretaceous aged sediments (T_s, Js and Ms).
- *Limestone/Dolostone* (25 percent) are derived from nearby Triassic, Jurassic and Cretaceous aged sediments (T_s, Js and Ms).
- *Chert* (10 percent) units are very proximal to the source and include Triassic, Jurassic and Cretaceous aged sediments (T_s, Js and Ms).

Pw-84c

The contributing drainage basin for Pw-84c has an area of 1,325 mi^2, however the source location is mapped as Bonneville Flood deposits so near surface lithologies likely were transported from more distant locations.

- *Quartzite* (over 65 percent), many clasts of which are pink, tan and maroon laminated and cross-bedded quartzite that field observation confirms as the same quartzite found in the Gibson Jack area near Pocatello. This quartzite is mapped as Cambrian to Proterozoic Camelback Mountain Quartzite (CZc) and Late Proterozoic Caddy Canyon Quartzite (Zc) and as part of the Windermere Supergroup (CZs).[36]
- *Sedimentary Rocks* (sandstone and limestone/dolostone) make up the remainder of the source, and came from nearby Paleozoic sedimentary rocks (OCs, Ms and DSOs).

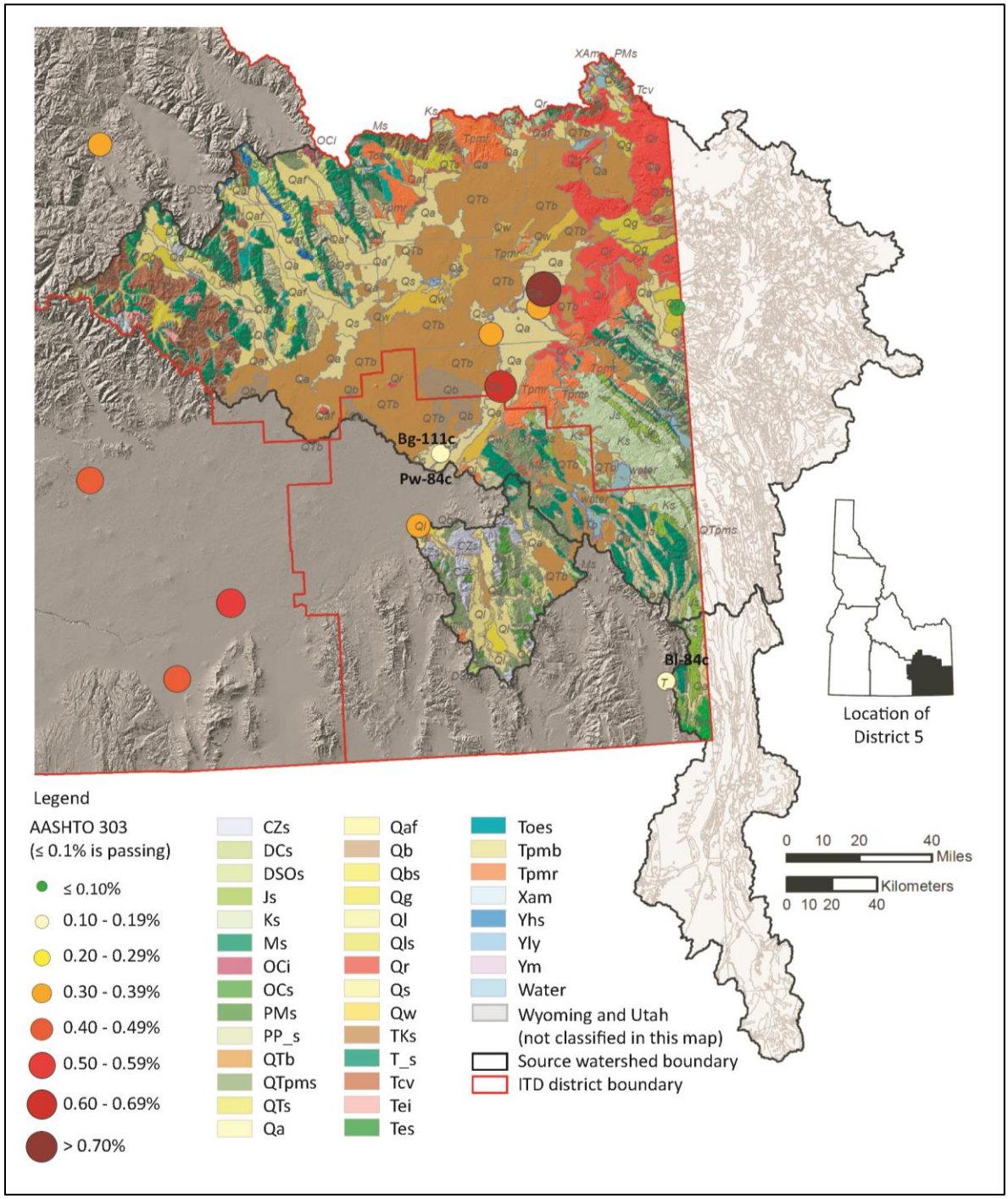

Figure 86. District 5 Source Watersheds and Geologic Units

The legend for this figure is shown in Figure 82

District 6 (Eastern and Central Idaho)

Gravel pits of the District 6 source study are listed in Table 9. Individual source drainage basins and geologic units are shown in figure 87.

Bn-155c

The watershed for Bn-155c has an area of 16,697 mi^2.

- *Volcanic Rocks: Basalt and Rhyolite* (over 15 percent), *Obsidian* (approximately 15 percent) are likely Pliocene rhyolite and basalt (Tpmr and Tpmb) and Pleistocene rhyolite and basalt (Qr and QTb).
- *Quartzite* (45 percent) likely is from nearby Ordovician-Cambrian outcrops (OCs) or possibly more distant Precambrian metamorphic rocks (Xam).

Jf-103c

The Jf-103c watershed covers an area of 25,780 mi^2 however Phillips and Welhan thought that lithologic compositions better matched deposition by the Henry's Fork of the Snake River, rather than the South Fork of the Snake River.[33] This suggests that the paleodrainage was smaller and may resemble the size and drainage patterns of the Ma-68c watershed.

- *Volcanic Lithologies: Rhyolite/Dacite* (25 percent), *Basalt* (12 percent) and *Obsidian* (45 percent) are most likely sourced from Pliocene rhyolite and basalt (Tpmr and Tpmb) and Pleistocene rhyolite and basalt (Qr and QTb)
- *Quartzite* (18 percent) that probably came from Precambrian metamorphic rocks (Xam).

Ma-22c

The drainage basin for Ma-22c has an area of 5,251 mi^2.

- *Volcanic rocks: Rhyolite* (25 percent), *Andesite* (10 percent), *Basalt* (20 percent), and *Obsidian* (5 percent) is from Pliocene rhyolite and basalt (Tpmr and Tpmb) and Pleistocene rhyolite and basalt (Qr and QTb).
- *Granite* (10 percent) likely came from Archean granitic gneiss that outcrops in Idaho (Xam) and Archean granitic gneiss that outcrops in Wyoming.

Ma-68c

The watershed for Ma-68c drains 5,399 mi^2 and is nearly identical in shape and size to the contributing watershed for Ma-22c, suggesting that provenance for many of the lithologies is the same between sources.

- *Quartzite* (over 60 percent) has only limited exposures in the basin, making it is difficult to identify the provenance of this particular quartzite unit..
- *Volcanics, Sandstones, and Limestone* each make up less than 10 percent of the lithologies in Ma-68c.

Tn-65c

Tn-65c represents a small drainage basin in Wyoming that has an area of 42 mi^2.

- *Granite* (40 percent) is Archean-aged (Xam) exposed in the Teton Range that makes up the border between Idaho and Wyoming.
- *Limestone* (35 percent) is from nearby Paleozoic sedimentary rocks (OCs, Ms and DSOs).

Cu-73c

The contributing drainage basin for Cu-73c has an area of 2,031 mi^2.

- *Volcanic Rocks: Rhyolite and Dacite, Andesite and Basalt* (45 percent) came from the Challis Volcanics Group (Tcv), an abundant and common lithology in the basin.
- *Quartzite* (30 percent) is likely from Ordovician-Cambrian metasediments (OCs).

Le-155c

Le-155c is only about 7 miles south of Le-154c and the two sources share much of the same drainage basin. The drainage area for Le-155c is 8,067 mi^2. Le-155c is located on a terrace deposit, so Le-155c lithologies may represent deposition in a paleo-drainage.

- *Rhyolite/Dacite* (10 percent) most likely comes from the Challis Volcanic Group (Tcv).
- *Metamorphic Lithologies: Quartzite* (60 percent), *Argillite/Siltite* (5 percent) and *Gneiss* (10 percent) are probably Precambrian metasediments of the Lemhi Group and Yellowjacket Formations (Yly) and the Swuager and Lawson Creek Formations (Yhs), and Precambrian gneiss (Yag).

Le-154c

The drainage area for Le-154c is 8,239 mi^2 and the source has modern flood plain lithologies.

- *Volcanic Components: Rhyolite/Dacite* (25 percent), *Andesite* (10 percent), *Basalt* (7 percent) are most likely from the Challis Volcanic Group (Tcv).
- *Metamorphic Rocks: Quartzite* (25 percent), *Argillite/Siltite* (5 percent) and *Gneiss* (5 percent) from the Lemhi Group and Yellowjacket Formations (Yly) and the Swauger and Lawson Creek Formations (Yhs), and Precambrian gneiss (Yag).

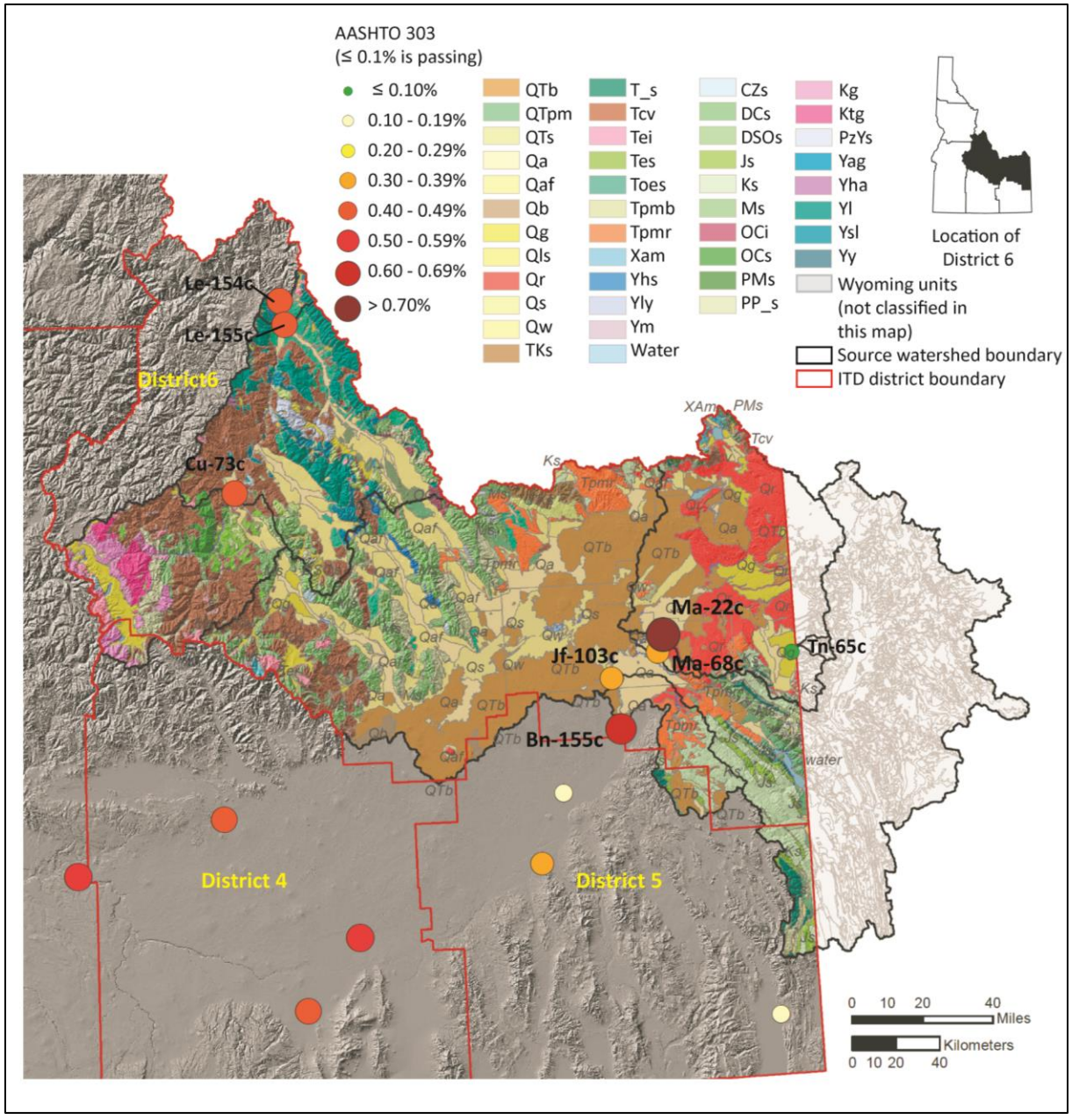

Figure 87. District 6 Source Watersheds and Geologic Units

The legend for this figure is shown in Figure 82

Chapter 6
Discussion

Lithologic inventories of 40 aggregate sources certified to produce concrete for ITD provide useful information regarding potential for ASR in specific rock types and in specific regions of Idaho. These inventories also show several geologic units and rock types in Idaho that likely have a low ASR potential (e.g., granite and granodiorite). Separate analysis of CA versus FA shows more problematic lithologies, such as opaline material, are sometimes found in FA, suggesting that particular care in mining and processing of fines is important. Furthermore, comparison of source lithologic inventories with mapped geologic units and delineated drainage basins indicate that spatially there are areas in Idaho where ASR potential is greater or less than in other areas. The geologic relationships and lithologic inventory results discussed in Chapters 4 and 5 of this report clearly support and explain the prior "experiential" knowledge of operators and ITD staff that gravels from the most youthful terraces of the Boise River are of high quality and have a low potential for ASR. Based on the comparison discussed in Chapter 5 and below, the Payette River watershed is the most similar to the Boise River in its lithologies. Conversely, certain Idaho rock units, including volcanic and sedimentary and meta-sedimentary lithologies, correlate with high potential for ASR, as discussed below. Figure 88 is a simplified geologic map of all of Idaho with the AASHTO T 303 and ASTM C 1293 results for each certified source superimposed. The ITD district watershed geologic maps presented in Chapter 5 were clipped from the detailed version of the state geologic map.[1]

Granitic Rocks

Granite is generally considered a non-reactive lithology and has been used in ASR experiments as a "nonreactive" control aggregate.[37,38] Consistent with the findings of this study, sources containing ≥ 25 percent granitic rocks have AASHTO T 303 values that are less than 0.22 percent (Br-2c, Ad-136c, Vy-52c, Cn-146c, Ad-53s, Bo-61, Gm-46c, Tn-65c). The silica in granite is present as the mineral quartz and is usually medium-grained to coarse-grained, which also makes it more stable and less reactive than very fine-grained or cryptocrystalline quartz (i.e. chalcedony or opal) or volcanic glass. This is an important finding for Idaho aggregate source operators and concrete producers because granitic rocks from the Cretaceous-age Idaho Batholith and felsic intrusive rocks from the Eocene Challis Intrusive Group outcrop in large areas of northern, central and southwestern Idaho.

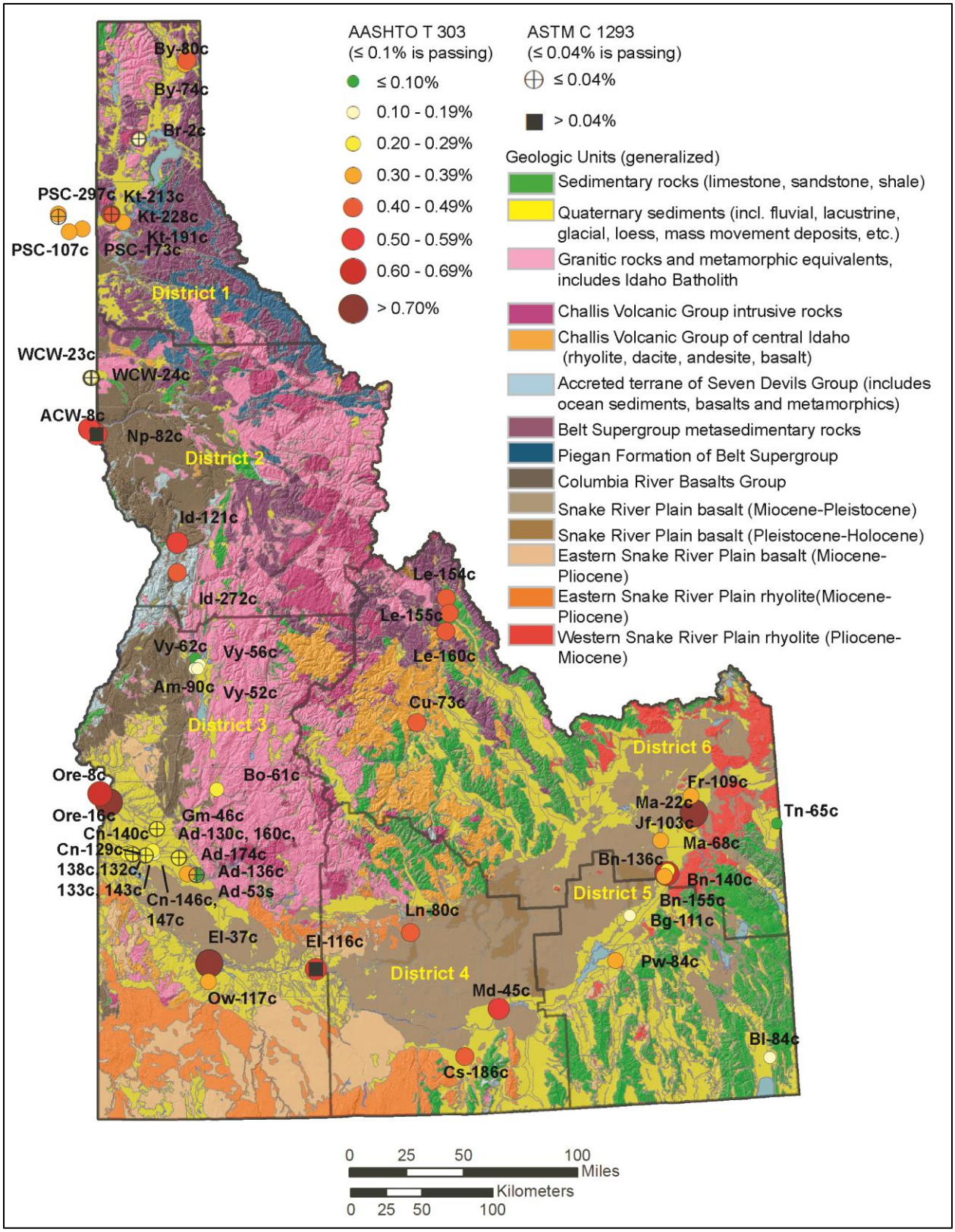

Figure 88. Geologic Map of Idaho with Certified Aggregate Sources and ASR Test Values

Basalt

Lithologic inventories of 7 mixed lithology sources in Idaho with >25 percent basalt have AASHTO T 303 expansion values of 0.39 to 0.74 percent (Kt-191c, ID-121c, Np-80c, ACW-8c, El-37c, Ore-8c, Ore, 16c, Ma-22c). In the literature, basalt has been shown to be generally non-reactive, although basalts with volcanic glass in their matrix may have slightly higher AASHTO T 303 expansion values (>0.10 percent).[39] In Idaho there are 2 basalt sources in west-central Idaho (Vy-62c and Am-90c), 2 basalt sources in eastern Washington (WCW-23c and WCW-24c), and 1 aggregate source (Vy-56c) with 65 percent basalt that have AASHTO T 303 expansion values of 0.12 to 0.25 percent, as listed in Table 5 and Table 6. These basalts are all sourced from the Columbia River Basalts, suggesting that this particular basalt is relatively non-reactive in the ASR process. By definition, basalt has lower silica and alkalis than other volcanic rock types such as rhyolite or dacite. Figures 11, 18, 26 and 27 show the petrographic images of gel pat tested concrete and mortar bars containing Miocene to Pleistocene aged basalts from the Snake River Plain. No cracking or expansion took place in these basalt clasts. In addition, crushed basalt was added in mortar bars containing pedogenic carbonate as shown in Figures 24 and 26. Petrographic analysis showed that these basalts did not show any post AASHTO T 303 cracking or expansion. Our study indicates that basalt, although possibly moderately reactive with 0.10 to 0.20 percent AASHTO T 303 expansion, is likely not a problematic lithology with regards to ASR.

Rhyolite

A study in Japan by Wakizaka concluded that older rhyolite (Miocene or older, corresponding to over 23 Ma) is less reactive than more recently erupted rhyolite (Miocene to Holocene aged, i.e. less than 23 million years old).[40] The Japanese study showed that highly altered (older) rhyolite has undergone almost complete devitrification, while younger rhyolite has not completed the devitrification process, and therefore higher levels of potentially reactive amorphous silica have not yet been removed from the younger rhyolite.[40] In Idaho this was tested by making a mortar bar from Eocene-aged (approximately 45 Ma) Challis Volcanic Group from rhyolite clasts in the Boise River(IGS-5; Figures 29, 30) and a mortar bar from the Miocene-aged (approximately 15 Ma – 5 Ma) rhyolite of the Western Snake River Plain (IGS-6; Figures 31, 32). Although both mortar bars exceeded AASHTO T 303 expansion limits, the Eocene-aged rhyolites experienced 0.45 percent expansion, while the much younger, Miocene-aged rhyolites experienced much higher AASHTO T 303 expansion of 0.70 percent in a 28-day test. Petrographic analysis of the mortar bars indicates that the Miocene-aged rhyolites experienced very intense cracking and even dissolution compared to the Eocene-aged rhyolite which experienced moderate to heavy cracking as shown (Figures 29-33). Geographically, the same relationship appears to hold true. Figure 89 illustrates that higher AASHTO T 303 values spatially correspond with Miocene and younger rhyolites of the Snake River Plain, while lower AASHTO T 303 values spatially correspond with the older, Eocene-aged rhyolite in the Boise River watershed sources. A lesser amount of Eocene rhyolite and related porphyries, such as dacite, are also found in the Payette River drainage.

The relevance of the age difference and increased expansion of the younger rhyolites is probably due to both composition and textures, particularly grain size and and the amount of glass or crystallinity of the

rhyolite matrix. The volcanic glass forms by very rapid cooling as the magma, i.e. liquid rock, escapes the volcanic vent. The rapid cooling prevents the atoms from growing stable mineral crystals and forms a disordered volcanic glass. Over time (probably thousands to millions of years in most cases), the disordered glass converts to the more thermodynamically stable crystalline state (i.e., devitrifies). Miocene to Holocene rhyolites in Idaho contain volcanic glass in variable amounts, even when the whole unit is not mapped as "obsidian." The spherulitic textures (Figure 31), such as seen in the IGS-6 mortar bar of rhyolite from Owyhee County are common and are produced by devitrification of an original glassier matrix. As the original glass is inherently unstable, it will devitrify over time, but because the glass is metastable, it is also more chemically reactive and thus is likely to be more susceptible to ASR. AASHTO T 303 results suggest that increased devitrification over time causes older rhyolites to be less susceptible to ASR.

Gravel clasts or outcrops of volcanic flows containing macroscopic obsidian, spherulites, gas cavities, thunder eggs, vitrophyres, agate, opal, or exhibiting glassy textures in general would almost certainly require mitigation for use in concrete. Such lithologies should be avoided if possible. In general, the Miocene to Holocene-aged (< 23 Ma) rhyolites and related units such as obsidian and other volcanic glass (amorphous silica) outcrop in the Snake River Plain canyons and adjoining volcanic highlands. Older rhyolites and related dacites from the Eocene Challis Volcanic Group which outcrops in central Idaho are also susceptible to ASR but are not as reactive as the Snake River Plain rhyolites.

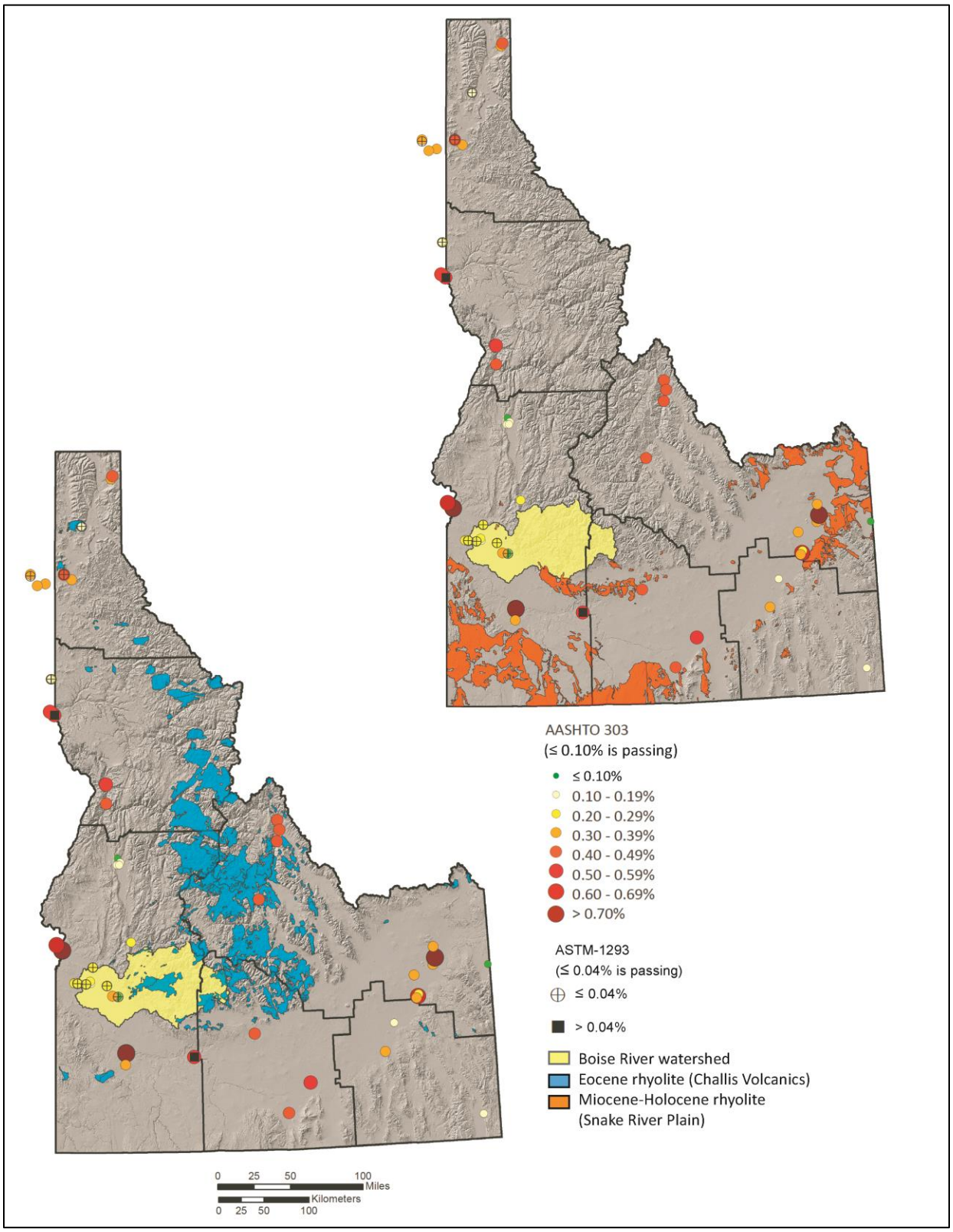

Figure 89. The Upper Map Highlights Younger, Miocene-Holocene Aged Rhyolites in Orange The Lower Map Highlights Older, Eocene Aged Rhyolite in Blue

Quartzite

Berube et al. concluded that quartzite is non-reactive, however West identified high ASR in individual grains of metamorphic strained quartz.[41,42] The results of our study suggest that quartzite is likely problematic but its contribution to ASR varies because Idaho has many different "quartzites" with very distinct characteristics. A number of different properties are used by geologists to describe a quartzite; these commonly include grain size, color, clast rounding and angularity, clast and matrix composition, and degree of lithification or metamorphism. Although lithologic inventories show that quartzite is the majority constituent in 3 sources with low AASHTO T 303 values (Bg-111c, Br-2c, Bl-84c), quartzite also accounts for the majority of clasts in many sources with high AASHTO T 303 values (Bn-115c, By-74c, By-80c, Kt-213c, Le-154c, Le-155c, Ma-68c, Md-45c, PSC-173c, Pw-84c). This implies that quartzite clasts in those sources could be a significant cause of the high AASHTO T 303 results and thus elevated ASR risk. Some of the properties, such as metamorphic grade and composition, are likely to exert more control on ASR than other properties, such as color.

The metamorphic grade of quartzite may have some control on ASR. For example, in District 1 of northern Idaho, quartzite from low grade metamorphic rocks of the Belt Supergroup make up 50 - 70 percent of some sources (Br-2c, By-74c, By-80c) and 30 - 50 percent of other sources (Kt-191c, Kt-272c, PSC-173c).[1] All of these sources exceed AASHTO T 303 limits with expansion values between 0.20 percent and 0.49 percent, however Br-2c and Kt-213c did pass the 1-year ASTM C 1293 test. Perhaps, these low grade metamorphic rocks are more reactive than higher grade metamorphic quartzites seen in inventories for District 5 sources, such as Bg-111c with an AASHTO T 303 value of 0.17 percent expansion or source Pw-84c with 0.33 percent expansion. Clearly, metamorphic grade alone does not seem to explain the variability. However, the lower grade quartzites and related siltites (meta-siltstones) of the Belt Supergroup in northern Idaho and Lemhi and Custer County area are geologically distinct from certain higher grade quartzites found in southeastern Idaho, some of which might produce aggregate that is less susceptible to ASR.

Petrographic analysis of mortar bars containing quartzite suggest that hand sample identification alone may be insufficient to define the most critical parameters, which is why geologists often require petrographic analysis and other microscopic techniques in their work. For example, some hand samples of clasts identified as quartzite in sources in the mid-Snake drainage were identified in thin section as well-lithified sandstones composed of a fine-grained silica cement or matrix in between the larger, detrital quartz grains. These cherty quartzites and impure sandstone were the most affected with cracking or dissolution along grain boundaries and cracking in the matrix during the AASHTO T 303 testing. Clasts of strongly metamorphosed, pure quartzite with sutured boundaries were generally sparse in the limited number of thin section samples examined but appeared less susceptible to ASR than the cherty quartzite during the AASHTO T 303 procedure. Additional sampling and petrographic analysis of the multiple quartzite units in Idaho would undoubtedly assist in identification of those units most at risk of ASR-related expansion, so they could be avoided if possible. However, literature sources suggest that the topic of quartzites and ASR is not simple, and Idaho has many quartzites.

Another issue is that quartzites can be recycled during multiple periods of erosion, and thus their place of origin may be more difficult to discern than other rock types. Quartzite's resistance to mechanical breakdown suggests that clasts could have originated from a location that is no longer part of the modern drainage system (i.e., quartzite clasts may have been transported by a paleodrainage). Because quartzite and well-lithified sandstone are very resistant to mechanical weathering and erosional processes of river and glacial transport, it is not surprising that these lithologies are found in every sampled source with the exception of 3 District 3 sources, Bo-61c, Ow-117c and Vy-52c. As previously mentioned, quartzite is found in some watersheds where no quartzite is mapped at the scale available. For example, roughly 20 percent of Bl-84c was inventoried as quartzite; however no quartzite is mapped within the physical confines of its contributing drainage basin, making it very difficult to correlate mapped geologic units with quartzite clasts found in such aggregate sources. No petrographic work was done on the Bl-84c source, and so a detailed description of that quartzite and that of many other sources is not currently available. Still, it would be valuable to know more precisely why Bl-84c has one of the lowest AASHTO T 303 test results in the state. Presumably the lack of volcanics is one reason, but the quartzite there is apparently not a major problem. What about the multiple quartzites in northern Idaho or in District 6 sources? The widespread distribution of quartzites in Idaho aggregate sources and the indication that certain quartzites, especially those seen in samples from the mid-Snake and Wood River Valley area, may have high potential for ASR necessitates further research. Preparation and petrography on additional mortar bars manufactured with the various quartzites and related rocks around the state would be one way of evaluating which of the quartzites are most at risk for high ASR and related expansion if they are used as concrete aggregate.

Sedimentary Rocks

Only 2 sources in this study contain significant amounts of unmetamorphosed sandstone, siltstone, limestone and dolostone (Bl-84c and Tn-65c). Both sources are located within close proximity of sedimentary sequences. Interestingly, both sources have low AASHTO T 303 values suggesting that limestone and sandstone are non-reactive with respect to ASR. However, only two certified sources with a majority of carbonate and other Paleozoic sedimentary rocks were sampled for this study, and such sedimentary rocks are not abundant in much of Idaho. Thus, there is insufficient data in this study to draw conclusions about the ASR potential of limestone and sandstone in Idaho, though these rock types are not typically considered as prone to ASR. Nor has the potential for alkali-carbonate reactivity (ACR) been studied for these Idaho aggregates, although ACR has been reported elsewhere [(43)].

Amorphous Silica (Obsidian, Chalcedony, Opal and Chert)

ITD has established limits for volcanic glass or obsidian at a maximum of 3 percent.[(2)] If the source lithologic composition exceeds this amount then SCM or other mitigation is required. These mitigation requirements seem reasonable. For example, Jf-103c is a source certified to produce FA, and it contains approximately 70 percent obsidian. The AASHTO T 303 expansion value for this unmitigated source is 0.38 percent. Other sources with high AASHTO T 303 expansion values that contain 1 - 15 percent obsidian include Cs-186c, El-37c, El-116c, Ma-22c, Md-45c, Ore-8c and Ore-16c.

ITD limits chalcedony to 3 percent of source lithologic composition before mitigation is required.[2] Chalcedony was found in trace amounts in El-116c, Ore-8c and Ore-16c. However, field observations at these sources suggest that chalcedony may account for a greater percent of the source compositions. Possibly the chalcedony veins or coatings are fragile or fractured and break up easily into very fine material during processing.

ITD limits opal (amorphous, hydrated silica) to 0.5 percent of the source lithologic composition before mitigation is required.[2] In this study, opal was not found in any CA. However, pedogenically accumulated carbonate ($CaCO_3$) coatings with secondary opal form on clasts in duripan or caliche horizons in older terrace deposits of the Boise River Basin as noted by Othberg.[44] Such coatings were observed on clasts at several sources in older river terrace deposits as shown in Figure 90. These coatings can be chipped away or removed from larger clasts during mining and processing, but the crushed coatings will easily find their way into the FA. Our study showed greater than 0.5 percent opal in the following sources: Ad-53s, Ad-136c, El-116c, Bn-155c, Bo-61c, El-37c, Id-121c, Ma-68c, Md-45c, Ore-16c and Ow-117. Duripan and caliche horizons can be easily recognized in pit high walls and typically form whitish layers within a specific depth. This depth varies from source to source. We recommend that care be taken to remove duripan horizons before mining the pit face for concrete aggregate, or to screen out the fine material, including such coatings and friable, duripan fragments, during processing to remove the opal as well as related pedogenic material.

ITD limits chert to 3 percent of source lithologic composition before mitigation is required.[2] Chert is not common in Idaho but can be found in association with Paleozoic sedimentary rocks of southeastern Idaho. Bl-84c was the only source that we sampled containing significant chert (approximately 10 percent). AASHTO T 303 testing of this particular source indicates a low potential for ASR, even though chert is often considered prone to ASR. The chert at Bl-84c is from a Paleozoic unit and perhaps because of its older age is less reactive. However, more work would need to be done to determine this.

Figure 90. Pedogenically Formed Carbonate Coatings (Mixed with Opaline Material) in Duripan/Caliche Horizons at Ad-53s

Payette River and Boise River Watersheds

Spatially clustered areas where ASR potential is low are found in District 3 near Boise in the Boise River watershed, and near McCall, Garden Valley and Emmett in the Payette River watershed as shown in Figure 84. In these areas, all but one source have AASHTO T 303 values lower than 0.30 percent and several sources have passing AASHTO T 303 values. Several sources from these watersheds that have AASHTO T 303 values in the 0.20 -0.29 percent range have passed the 1-year ASTM C 1293 test, indicating that sources in these basins that failed the AASHTO T 303 test would likely pass the ASTM C 1293 test. Based only on the sampling conducted in this study, this is the only area in the state with abundant certified material sources and regionally consistent “low or moderately low” ASR potential as measured by the tests and by inference from clast provenances of granitic and older (i.e. Eocene-age) felsic to intermediate porphyry terranes plus minor basalt. Thus, the Payette and Boise River watersheds are the most prospective terranes for sources of future aggregate with a low risk of ASR.

Petrographic Analysis and Laboratory Work

As observed in this study, young Idaho rhyolite, which is typically composed of approximately 70 percent silica, consistently showed very high potential for ASR. The most reactive lithologies were the uniformly fine-grained or aphyric rhyolite and spherulitic rhyolite. Mortar bars with these rhyolite clasts show intense visual cracking and in thin section indicate probable dissolution of the bulk rock mass. These fine-grained units are associated with the young (Miocene to recent) volcanism of the Snake River Plain.

Welded tuffs, which are similar in composition and age but differ in texture, experienced equal cracking and expansion during the AASHTO T 303 test and gel pat test. Obsidian and opal which are known to be susceptible to ASR have limited distribution but may be locally significant in southern Idaho as larger percentages of some aggregate (i.e. Jf-103c, Cs-186c, El-37c, El-116c, Ma-22c, Md-45c, Ore-8c, and Ore-16c). These sources are those with a large component of young volcanic rocks, such as are present in the Snake River Plain, Owyhee County and parts of eastern Idaho. Opal or cryptocrystalline silica associated with pedogenic carbonate coatings is locally important but very hard to quantify as it does not form large, visible clasts. It may also be associated with pedogenic clasts and surficial material with durability issues, irrespective of any chemical reactivity. The opal may be released from caliche-related coatings during aggregate processing, and thus it ends up concentrated primarily in the fine aggregate where it is difficult to identify. ITD currently limits aggregate designated for concrete to 0.5 percent opal.

Cherty quartzite or sandstone is perhaps the second most reactive lithology observed in this study in terms of chemical durability. As seen in the I-84 pavement it is a fairly distinctive rock in thin section, but its source location is currently unknown. As seen in thin section, the fine-grained silica cement (chert or chalcedony) and hydrothermal overgrowths on coarse quartz detritus seem to be especially susceptible to dissolution. It is possible that this dissolution partly explains the large volume of silica released during the gel pat tests. It is hypothesized that this clast type, seen in the Mountain Home pavement and pits from the central Snake River Plain, is sourced from the Wood River Valley and similar locales. However, further research is necessary to more adequately determine the provenance and identification of these units. Additional field work and petrography could probably identify the unit and its source terrane.

Other quartzites and sedimentary rocks, including metamorphic quartzite, mudstones, muddy quartzites, and others are considered less susceptible to ASR based on the very limited petrographic data. Samples for petrography were predominantly from southwestern Idaho, but other areas in the state have a wider variety and greater abundance of these rock types. These sedimentary rocks are typically less prone to ASR than volcanics, although the moderately high AASHTO T 303 results in Districts 1, 4, and 6 for sources with significant percentages of quartzite and related rocks, suggest that in Idaho some of these lithologies also have significant risk of ASR. As discussed earlier, the petrography results, limited though they are, suggest that the most metamorphosed quartzites may have less susceptibility to ASR. Further research would be needed to determine specific units and confirm this observation.

Intermediate composition (i.e. andesite to dacite) volcanics and older rhyolite porphyry to dacite porphyry, as well as coarser-grained, granitic intrusive rocks experienced less expansion-related cracking during the mortar bar tests. But significantly, basalt clasts are usually not affected by the ASR testing solutions. Likewise, carbonate clasts are also nonreactive for ASR, though their potential for alkali-aggregate reaction (AAR), including alkali-carbonate reaction (ACR) was not studied.

As noted by Tremblay, the cracked Mountain Home I-84 pavement shows only modest amounts of classic ASR gel and expansive matrix cracking under the microscope.[8] Reed identified significant ASR in his inspection of the surface of the concrete pavement, and more particularly in the examination of select cores extracted from heavily cracked slabs of the Mountain Home I-84 pavement, shortly after the

slabs were removed [4,5]. However, based on the petrography and mortar results summarized here, there could also be another, slightly different chemical mechanism creating a loss of strength in the concrete and aggregate within a relatively short time span. Chemical dissolution of silica from the rhyolites, tuffs and cryptocrystalline matrix sandstones appears to create voids and open fractures which may contribute to a decrease in the actual physical strength of the clasts and thus the concrete. Any open fractures, even tiny ones, would accelerate opening and growth of additional cracks due to freeze thaw and thermal expansion and contraction. Under the wear and applied load of traffic on the pavement, premature cracking could be the result. Additional factors such as freeze thaw of susceptible aggregate (or any existing ASR gel itself) would intensify the result. The silica dissolved from slices of concrete during the gel pat experiment far exceeded any leaching of alkalis or other major constituents. As the pH was quite high, and silica is known to dissolve at very high or very low pH, this may be expected.[45] In addition to a pH control, silica solubility in natural weathering systems increases as the grain size and crystallinity decrease. Experimental studies document that the less ordered phase, amorphous silica, is significantly more soluble than crystalline quartz.[45, 46] Certain types of Idaho aggregate, such as those containing reactive or amorphous silica as opal, obsidian, devitrifying volcanic glass, or secondary chalcedonic quartz overgrowths, may be extremely susceptible to silica leaching under alkaline conditions, and simple dissolution of a silica matrix in a clast could initiate premature failure and cracking of the concrete without actual expansive gel forming. Broekmans provides a recent discussion of the complexities of silica solubility and ASR gel formation.[46] As he notes, field conditions may be much harder to understand than simple laboratory experiments. Additional research, and particularly additional microanalytical studies or aggregate or concrete would be needed to fully illuminate the ASR reactions, exact mechanisms and causative factors at work in Idaho.

Chapter 7
Conclusions and Recommendations

In the past decade, a considerable amount of literature and time has been devoted to the study of ASR and the aggregates and conditions which generate it, as well as to documentation of the effects of ASR on concrete structures and roadways [7]. While various measures have been and are being developed to mitigate ASR before and after concrete placement, mitigation can be costly and is not always totally effective. Fernandes et al. and Broekmans and Pollmann, as well as a number of papers given at the ICAAR 2012 conference, summarize the numerous scientific and engineering advances in ASR recognition and understanding and new technical specifications.[47, 48, 49] However, as noted by Fernandes and others, "distinction of potentially deleterious from innocuous rock types can be problematic."[47] In part this is because the aggregate used in structures and field pavements is so variable in its geology, lithology and geologic history. The basic rock composition has been modified over eons by fluids, heat, and pressure to produce a rock that is truly unique. Those subtleties of texture, structure and composition may require an expert petrographer or geologist to identify the regional context or estimate the effect of microscopic differences on ASR potential. Statewide studies of aggregate and ASR in transportation and construction are few, though Stanton's original work was done in the 1940's and the subject has garnered much international study and work. A systematic study in New Hampshire done in 2002 and 2005 is the most similar to this project.[50, 51] Hudson and Shrimer (2012) reported lithologic inventories of fluvial aggregate from two sources in British Columbia, and other papers presented at ICAAR 2012 looked at ASR potential of specific rock types used in aggregate in different parts of the globe.[52]

This project provided an excellent opportunity to address the problem of ASR starting with a more comprehensive geologic look at aggregate within a specific, large geographic region, Idaho, and to correlate ASR potential (as based on available standard commercial tests) with detailed lithologic studies from sampling of 40 source locations around the state, petrography, and recent statewide geologic mapping available from the Idaho Geological Survey.[1]

Overall, there is a clear correlation of ASR potential of aggregate sources with mapped geology and specific lithologies in Idaho. As discussed in Chapter 6, the aggregate rock types with the greatest potential for developing ASR are young rhyolites, various forms of amorphous silica (opal and volcanic glass), and certain quartzites or siliceous sandstones. Based on a general review of the literature, these rock types are problematic in other parts of the world as well, although the lithologies most important in ASR development vary with the regional geology.[47, 53, 54, 55, 56, 57] A large number of rock types have been found to enable ASR in concrete when moisture and alkalis are present. As the spatial analysis presented in Chapter 5 shows, certain basins, e.g. the Snake River Plain and volcanic highlands, within Idaho contain greater amounts of these problematic lithologies than other areas, such as the Boise River or Payette River drainage. Unfortunately, as a result of Idaho's geology, aggregate lithologies with a high ASR potential are widespread, and as studies have shown, only a few percent of a deleterious material can affect the reactivity of the aggregate. In addition to the conclusions and discussion in Chapters 5 and 6, results of this study are summarized below.

Geology and Alkali Silica Reactivity

The only characteristic which this study examined was ASR. No attempt was made to tabulate or review other important properties such as hardness, durability, etc., which might render some of the units of low ASR potential less favorable for aggregate production and use. Conversely, transportation costs and logistical considerations may require the use of aggregate with known high ASR potential and in those cases, extra care and testing should be taken to insure that the mitigation will be effective.

Lithologic inventories from Idaho aggregate sources and petrographic analysis demonstrate that rock types most susceptible to ASR, and likely to be causing many ASR problems, are the young, Miocene to Holocene rhyolites (i.e. less than 23 million years old) and related units such as obsidian and other volcanic glass (amorphous silica) that outcrop in the Snake River Plain river canyons and adjoining volcanic highlands. Older rhyolites from the Eocene Challis Volcanic Group that occur in central Idaho are also susceptible to ASR but are not as reactive as Snake River Plain rhyolites.

Some southern Idaho “quartzites” in the mid-Snake River Plain region’s highly reactive sources (i.e. El-116c and El-37c) were classified under the microscope as silica-cemented, impure sandstones. Such siliceous sandstones, which displayed quartz overgrowths and fine-grained, cherty silica matrix, were highly reactive in accelerated mortar bar tests. In sources derived primarily from the central Snake River basin, the mixture of rhyolites and welded tuffs with reactive quartzites, has produced aggregate with the highest AASHTO T 303 results (> 0.5 percent expansion) in the state.

Moderately elevated AASHTO T 303 values (0.3-0.4 percent expansion) in northern Idaho sources composed of low grade metamorphic quartzites, and associated argillite and siltite suggests that these lithologies are potentially reactive. This includes Belt Supergroup rocks which are abundant in the Panhandle of Idaho and northeastern Montana. Mortar bars from the northern Idaho sources were not available, and many of the Belt units are nearly impossible to differentiate in outcrop, so petrographic analysis of the Belt metamorphics was not attempted in this initial study. The only thin sections made of north Idaho concrete were of concrete from the Lake Creek Bridge which has had numerous “pop outs.” Silty carbonate rocks, most likely from the Piegan Formation were identified as the cause of the pop outs. However, it is uncertain if the pop out rocks also produce greater risk of ASR.

Petrographic analysis of basalts and granitic rocks indicates that these lithologies are typically non-reactive. Spatial correlations of lower AASHTO T 303 values with lithologic inventories dominated by granite or limestone units suggest that granite and limestone/dolostone are also typically non-reactive for ASR. Some sources with high amounts of basalt (and elevated AASHTO T 303 results) also have significant amounts of rhyolite. It is likely that the rhyolite and other problematic lithologies are the dominating contributors to ASR expansion in those source tests, as noted in Chapter 6.

Opal is well known to have a high ASR expansion potential. Secondary pedogenic (i.e., soil forming) processes often precipitate opaline coatings (SiO_2) within carbonate ($CaCO_3$) horizons (i.e., duripans or caliche).[27,44] Because these duripans take >100,000 years to form, they are dominantly found in older terrace gravels.[44] In southern Idaho, the duripans are abundant within loess, basalt, and gravels, with

visible caliche horizons from 1 foot to as much as 20 feet below the land surface. Thus, aggregate sources in modern floodplains will usually not contain these opaline coatings and thus would not require mitigation for ASR associated with pedogenically-formed opal. Through field visits to aggregate sources, operators were found to be extremely knowledgeable about their sources. Most operators can readily identify these white layers as caliche zones. As the caliche may contribute to ASR and be deleterious to the aggregate quality, it should be avoided as part of concrete aggregate. Screening out of suspect FA, where the crushed opal concentrates, during processing may the easiest way to avoid its high ASR risk.

Spatial Correlations to Geography and Geology

In District 3 in southwestern Idaho, the younger Boise River and Payette River watershed-derived gravels provide aggregate with relatively low AASHTO T 303 test values (<0.30 percent expansion) which is slightly higher than a passing value (≤0.10 percent expansion). However, several of these same sources have passed the one year ASTM C 1293 test. This study indicates that a mix of granite, Eocene rhyolites and intermediate to mafic porphyry, plus some basalt is a typical composition in the Boise and Payette River drainages. However, the extensive urbanization in the Treasure Valley, i.e. the Boise River watershed, has led to many sources of good gravel with passing or relatively low ASR risk being sequestered under subdivisions or otherwise taken out of future transportation or commercial use. Older terraces comprised of these less ASR prone Boise River gravels have undergone greater degrees of pedogenic processes that have precipitated reactive opaline duripan coatings on gravel clasts and also increased weathering of granite clasts.[27,44] Planning for future needs is imperative, as other sources, such as those in the Snake River Plain, contain much higher ASR potential and will require proven ASR mitigation techniques.

Larger, more complex drainages of the Snake River or of paleodrainages within the Snake River Plain contain many more clasts with high ASR potential. It is also more difficult to evaluate such areas without extensive sampling, mapping, and testing. For this reason, mitigation for ASR is especially important in sources located in the Snake River Plain. Smaller drainage basins, as above, can more accurately be evaluated, both from the literature and geologic mapping as well as sampling.

Younger volcanic terrains, including the Owyhee County area and the young rhyolites of the Snake River Plain contain lithologies with very high ASR potential. Older rhyolites from the Challis Volcanic Group are also reactive, but to a lesser extent, and they do not pose as great a threat for ASR as the younger rhyolites.

Further Research

Petrographic analysis of mortar bars made from hand selected lithologies (before and after AASHTO T 303 tests), and gel pat tests provided invaluable information about specific lithologies that were actually experiencing cracking and expansion associated with ASR. Detailed petrography, including microscopic examination, is a valuable and relatively inexpensive tool for correlating rock types and ASR. However, it needs to be combined with a solid geologic database, such as adequate geologic mapping,

to have practical applications for local transportation planning. The petrographic work done in this study was primarily on samples from District 3, in part because the ASR issues were known to be most serious there and in part due to logistics and sample and mortar bar availability. Future research could include petrographic examination of mortar bars, if available or manufactured, and rock types from northern Idaho and/or eastern Idaho.

Many sources that failed the AASHTO T 303 test actually passed the 1-year ASTM C 1293 test, particularly in the Boise and Payette River watersheds of District 3. The ASTM C 1293 test is considered a more reliable test by industry standards and is more representative of actual field conditions. Additional research on Idaho aggregates under longer term testing scenarios would be helpful to better understand the processes and time-dependence of ASR for different aggregate types. For example, the 28-day mortar bar curves showed changes in the behavior of various samples which the shorter 14-day test did not. The 28-day mortar bar tests suggest that some of the medium or less reactive rock types will expand quickly at first under the hotter and stronger alkaline solutions in the AASHTO T 303 test, but the rate quickly slows down. This pattern may occur during the ASTM C 1293 test but the 14-day test appears to be too short to capture this reaction trend. Other rocks, such as the Miocene or younger, fine-grained rhyolites, may continue a rapid rate of expansion, shown by steeper and more linear slopes on the graph, far beyond the 14-day duration of the AASHTO T 303 test. More research and testing is needed to better assess long-term concrete performance, particularly on Idaho aggregate with abundant quartzite or siliceous sandstone which may be less straightforward than the volcanic rocks. It is also notable that this study looked only at ASR test results for unmitigated samples in order to reflect the geologic contribution to ASR rather than the SCM contribution. Assessing the performance or efficacy of different SCMs and mitigation options is another area of research and testing needed for specific Idaho aggregates, although some work has already been done by ITD.

As transportation pavements and structures are built, constructing a simple and accessible digital archive and database of aggregate and project characteristics and practices is highly recommended. Such a database should include for each project: aggregate sources used, concrete product category/type, concrete mix design, ASR test results and other test data, SCM (supplementary cementitious materials) mitigation or other additives used, contractors, construction dates, construction methods and practices implemented, and pavement/structure performance. Documenting the concrete performance and especially any adverse results, such as premature cracking, with the multiple factors would be highly desirable and could lead to future cost-savings and more efficient operational assessments for ITD. Some SCMs may work better on a specific ASR-generating rock type, such as a rhyolite, while other SCMs may work better on quartzites. Researching the pattern, based on petrography, geology and comparisons with other studies in the literature, as well as Idaho specific aggregate could produce a blueprint for future, more effective mitigation. Another factor to evaluate is roadway application of salt and other de-icers, which could be a source of alkalis and promote ASR.

This study looked only at ASR potential of aggregate and did not consider other important properties, such as hardness, durability, and alkali-carbonate reaction. ASR is one variety of AAR (alkali-aggregate reactivity). The other major type is ACR or alkali-carbonate reactivity. That was not studied in this project, but it is a potential issue for aggregate sources in eastern Idaho, and rarely for western Idaho,

areas with significant carbonate (limestone and dolostone) rocks. A future project that is focused more on future supply and operations in those geographic areas should include examination of ACR risk in the relevant aggregate sources.

The GIS analysis proved to be a very useful way to compare the geologic map with a specific property of aggregate, in this case ASR risk. However, additional research on properties such as hardness and durability as well as ACR and ASR might be a useful exploration and planning guide for ITD as it seeks high quality aggregate over the next several decades. GIS-based analysis of watersheds and aggregate source provenance is useful, but additional sampling and data would enhance our understanding of the sources and the relationship of ASR to specific geologic units. Many very large watersheds in Idaho make identifying clast sources difficult with the limited sampling done in this study.

This study identified several drainage basins with low ASR potential. Those areas, particularly the portions not yet urbanized, could be sampled and evaluated more comprehensively for securing future aggregate sources. Regions of the lowest ASR potential, due to their aggregate and underlying geology are in the Boise River watershed, Payette River watershed, certain areas in southeastern Idaho and the hard rock sources of the Columbia River basalt areas in western Idaho (Figure 88). Some of these areas, such as southeastern Idaho, had relatively few certified sources that were sampled in this study. Other areas, such as District 4 have few sources and those have moderate to high ASR potential. However, a more extensive, geologic-based exploration program might find improve the chances of finding aggregate of higher quality.

As discussed earlier, some of the ASR risk and other factors that contribute to lower quality aggregate could be partially alleviated by consistent and improved implementation of ITD standards and practices during mining and processing. A field-based, short course training program for operators (and ITD field personnel) might provide education that would help with this. In particular, providing a geology lesson for operators could assist them to recognize duripans and other pedogenic material. If duripans are present, devising a better system to screen out the fines where any pedogenic opal coatings or soft tuffaceous material accumulates would improve the saleable product and decrease the potential for ASR-related cracking.

References

1. **Lewis, R. S., P. K. Link, L. R. Stanford, and S. P. Long.** *Geologic Map of Idaho*. Moscow, ID: Idaho Geological Survey, Scale 1:750,000, 2012.

2. **Idaho Transportation Department**. *Standard Specifications for Highway Construction.* Boise, ID: Idaho Transportation Department, 2012.

3. **Kosmatka, S. H. and M. L. Wilson**. *Design and Control of Concrete Mixtures: The Guide to Applications, Methods and Materials*. Skokie, IL: Portland Cement Association, 2011.

4. **Reed, W. Rich**. *I84, MP 90 to MP 114 ASR Cracking-Mitigation Study - Geology and Potential for ASR of Aggregate Sources*. Boise, ID: Idaho Engineering & Geology Inc., 2005.

5. **Reed, W. Rich**. *ITD I84 MP 90 - 114 ASR Cracking & Mitigation Study, Summary Report of Cause & Nature of Cracking of Concrete Pavement and Alternative Treatments and Repair*. Boise, ID: Idaho Engineering & Geology Inc., January 12, 2007 and related monitoring reports.

6. **Federal Highway Administration.** *Alkali-Silica Reactivity – Selection, Implementation and Evaluation of Field Application and Demonstration Projects.* Washington, DC: Federal Highwayt Adminstration. http://www.fhwa.dot.gov/pavement/concrete/asrfield.cfm (Accessed November 9, 2011).

7. **Thomas, M. D. A., B. Fournier, and K. J. Folliard.** *Selecting Measures to Prevent Deleterious Alkali-Silica Reaction in Concrete: Rationale for the AASHTO P65 Prescriptive Approach*. Washington DC: Office of Pavement Technology, Federal Highway Administration, 2012.

8. **Tremblay, S.** *Etude de L'efficacite D' adjuvants a Base de Lithium Afin de Controler la Reaction Alcali-Silice dans le Beton Frais et Dans les Structure Existantes Incorporant cet Adjuvant*. Master's Thesis, University Laval, Quebec. 2011.

9. **Thomas, M. D. A., B. Fournier, K. J. Folliard, and Y. A. Resendez.** *Alkali-Silica Reactivity Field Identification Handbook.* Washington, DC: U. S. Department of Transportation, Federal Highway Administration, 2011.

10. **Stanton, T. E.** "Expansion of Concrete through Reaction Between Cement and Aggregate." *Proceedings of the American Society of Civil Engineers*, Vol. 66, No. 10 (1941): 1781-1811.

11. **Fournier, B., M. Berube, K. J. Folliard, and M. Thomas.** *Report on Diagnosis, Prognosis, and Mitigation of Alkali-Silica Reaction (ASR) in Transportation Structures.* Washington DC: Office of Pavement Technology, Federal Highway Administration, 2010.

12. **Thomas, M. D. A., B. Fournier, K. J. Folliard, J. Ideker, and M. Shehata.** "Test Methods for Evaluating Preventive Measure for Controlling Expansion Due to Alkali-Silica Reaction in Concrete." *Cement and Concrete Research,* Vol. 36, No. 10 (2006): 1842-1856.

13. **Guthrie, G. D. and J. W. Carey.** "A Simple Environmentally Friendly and Chemically Specific Method for the Identification and Evaluation of the Alkali-Silica Reaction." *Cement and Concrete Research,* Vol. 27, No. 9 (1997): 1407-1417.

14. **Rivard, P., J. Ollivier, and G. Ballivy.** "Characterization of the ASR Rim Application to the Potsdam Sandstone." *Cement and Concrete Research,* Vol. 32 (2002): 1259-1267.

15. **Ahlstrom, G. M.** *The United States Federal Highway Adminstration's Alkali-Silica Reactivity Development and Deployment Program*. Washington, DC: Office of Pavement Technology, Federal Highway Adminstration, 2012.

16. **Henkel, G., P. J. Modreski, and E. R. Verbeek.** *The Henkel Glossary of Flourescent Minerals.* Tarzana, CA: The Flourescent Mineral Society, 1989.

17. **Hanson, K. F., T. J. Van Dam, K. R. Peterson, and L. L. Sutter.** "Effect of Sample Preparation on Chemical Composition and Morphology of Alkali-Silica Reaction Products." *Transportation Research Record, Journal of the Transportation Research Board,* No. 1834, (2003): 1-7.

18. **Fournier B., and M. A. Berube,** "Recent Applications of a Modified Gel Pat Test to Determine the Potential Alkali-Silica Reactivity of Carbonate Aggregates." *Cement and Concrete Composites,* Vol. 15, No. 1-2 (1993): 49-73.

19. **Gesch, D., G. Evans, J. Mauck, J. Hutchinson, and W. J. Carswell.** "The National Map—Elevation U. S. Geological Survey." *National Map Viewer*, http://viewer.nationalmap.gov/viewer/ (Accessed November 11, 2012).

20. **Lewis, R. S., R. F. Burmester, R. M. Breckenridge, S. E. Box, and M. D. McFadden.** *Geologic Map of the Sandpoint Quadrangle, Bonner County, Idaho*. Moscow, ID: Idaho Geological Survey, Digital Web Map 76 (2006): Scale 1:24,000.

21. **Burmester, R. F., R. M. Breckenridge, M. D. McFadden, and R. S. Lewis**. *Geologic Map of the Moyie Springs Quadrangle, Boundary County, Idaho.* Moscow, ID: Idaho Geological Survey, Digital Web Map 118 (2010): Scale 1:24,000.

22. **Breckenridge, R. M., and K. L. Othberg.** *Surficial Geologic Map of the Coeur d'Alene Quadrangle, Kootenai County, Idaho.* Moscow, ID: Idaho Geological Survey, Surficial Geologic Map 7 (1999): Scale 1:24,000.

23. **Breckenridge, R. M., and K. L. Othberg.** *Surficial Geologic Map of the Rathdrum Quadrangle and Part of the Newman Lake Quadrangle, Kootenai County, Idaho.* Moscow, ID: Idaho Geological Survey, Surficial Geologic Map 6 (1998): Scale 1:24,000.

24. **Schmidt, K. L., J. D. Kauffman, D. E. Stewart, K. L. Othberg, and D. L. Garwood.** *Geologic Map of the Slate Creek Quadrangle, Idaho County, Idaho.* Moscow, ID: Idaho Geological Survey, Digital Web Map 110 (2009): Scale 1:24,000.

25. **Lewis, R. S., K. L. Schimdt, K. L. Othberg, D. E. Stewart, and J. D. Kauffman**. *Geologic Map of the Lucile Quadrangle, Idaho County, Idaho.* Moscow, ID: Idaho Geological Survey, Digital Web Map 126 (2011): Scale 1:24,000.

26. **Othberg, K. L., R. M. Breckenridge, T. C. Walker, and D. W. Weisz**. *Surficial Geologic Map of the Lewiston Orchards South Quadrangle and Part of the Asotin Quadrangle, Nez Perce County, Idaho.* Moscow, ID: Idaho Geological Survey, Digital Web Map 9 (2003): Scale 1:24,000.

27. **Othberg, K. L. and L. R. Stanford.** *Digital Geologic Map of the Boise Valley and Adjoining Area, Western Snake River Plain, Idaho.* Moscow, ID: Idaho Geological Survey, Technical Report T-93-3 (1993): Scale 1:24,000.

28. **Breckenridge, R. M., and K. L. Othberg.** *Geologic Map of the Bellevue Quadrangle, Blaine County, Idaho.* Moscow, ID: Idaho Geological Survey, Digital Web Map 57 (2006): Scale 1:24,000.

29. **Jenks, M. D., Bonnichsen, B. and M. M. Godchaux.** *Geologic Map of the Grand View-Bruneau Area, Owyhee County, Idaho.* Moscow, ID: Idaho Geological Survey, Technical Report T-98-1 (1998): Scale 1:100,000.

30. **Breckenridge, R. M. and K. L. Othberg.** Surficial Geologic Map of the McCall Quadrangle, Valley and Adams Counties, Idaho. Moscow, ID: Idaho Geological Survey, Digital Web Map 44 (2005): Scale 1:24,000.

31. **Kauffman, J. D., K. L. Othberg, J. W. Shervais, and M. F. Cooke.** Geologic Map of the Shoshone Quadrangle, Lincoln County, Idaho. Moscow, ID: Idaho Geological Survey, Digital Web Map 44, (2005): Scale 1:24,000.

32. **Phillips, W. M. and J. A. Welhan**. *Geologic Map of the Idaho Falls South Quadrangle, Bingham and Bonneville Counties, Idaho.* Moscow, ID: Idaho Geological Survey, Digital Web Map 78 (2011): Scale 1:24,000.

33. **Phillips, W. M. and J. A. Welhan**. *Geologic Map of the Lewisville Quadrangle, Jefferson and Bonneville Counties, Idaho.* Moscow, ID: Idaho Geological Survey, Digital Web Map 135 (2011): Scale 1:24,000.

34. **Othberg, K. L., L. R. Stanford, and R. S. Lewis.** *Geologic Map of the East of Salmon Quadrangle.* Moscow, ID: Idaho Geological Survey, Digital Web Map 125 (2011): Scale 1:24,000.

35. **Breckenridge, R.M. and K.L. Othberg.** *Surface Geologic Map of the Wood River Valley Area, Blaine, County, Idaho***.** Idaho Geological Survey, Digital Web Map (2006): Scale 1:50,000.

36. **Link, P. K. and L. R. Stanford.** *Geologic Map Compilation of the Pocatello 30 x 60 Quadrangle, Idaho.* Moscow, ID: Idaho Geological Survey, Technical Report T-99-2 (1999): Scale 1:100,000.

37. **Fatt, N. T., J. K. Raj, and A. A. Ghani**. "Potential for Alkali-Reactivity of Granite Aggregates in the Bukit Lagong Area, Selangor, Peninsular Malaysia." *Sains Malaysiana.* Vol. 42, No. 6 (2013): 773-781.

38. **Prezzi, M., J. M. Paulo, and G. Spito.** "The Alkali-Silica Reaction, Part 1: Use of the Double-Layer Theory to Explain the Behavoir of Reaction-Product Gels." *ACI Materials Journal*. Vol. 94, No. 1 (1997): 10-16.

39. **Korkanc, M. and A. Tugrul**. "Evaluation of Selected Basalts from the Point of Alkali-Silica Reactivity." *Cement and Concrete Research*. Vol. 35, No. 3 (2005): 505-515.

40. **Wakizaki, Y.** "Alkali-Silica Reactivity of Japanese Rocks." *Engineering Geology.* Vol. 56 (2000): 211-221.

41. **Berube, M. A., J. Duchesne, J. F. Dorion, and M. Rivest**. "Laboratory Assessment of Alkali Contribution by Aggregates to Concrete and Application to Concrete Structures Affected by Alkali – Silica Reactivity." *Cement and Concrete Research*. Vol. 32 (2002): 1215-1227.

42. **West, G.** *Alkali-Aggregate Reaction in Concrete Roads and Bridges*. London, England: Geology Division, Public Works Research Institute, Ministry of Construction, 1996.

43. **Thomas, M. D. A., B. Fournier, and K. J. Folliard.** *Report on Determining the Reactivity of Concrete Aggregates and Selecting Appropriate Measure for Preventing Deleterious Expansion in new Concrete Construction.* Washington, DC: Office of Pavement Technology, Federal Highway Administration, 2008.

44. **Othberg, K. L., J. E. O'Conner, and P. A. McDaniel.** *Field Guide to the Quaternary Geology of the Boise Valley and Adjacent Snake River Plain, Idaho.* Moscow, ID: Idaho Geological Survey, Staff Report S-96-1, 1996.

45. **Dove, P. M.** "Kinetic and Thermodynamic Controls on Silica Reactivity in Weathering Environments." *Reviews in Mineralogy and Geochemistry*, Vol. 31, (1995): 235-290.

46. **Broekmans, M. A. T. M.** "Deleterious Reactions of Aggregate with Alkalis in Concrete." *Reviews in Mineralogy and Geochemistry*, Vol. 74, (2012): 279-364.

47. **Fernandes, I., M. A. T. M. Broekmans, P. Nixon, I. Sims, M. Ribeiro, F. Noronha, and B. Wigum.** "Alkali-Silica Reactivity of Some Common Rock Types. A Global Petrographic Atlas." *Quarterly Journal of Engineering Geology and Hydrogeology*, Vol. 46, (2013): 215-220.

48. **Broekmans, M. A. T. M. and H. Pollman.** Applied Mineralogy of Cement and Concrete. *Reviews in Mineralogy and Geochemistry*, Vol. 31, (2012): 364

49. **Gillerman, V. S.** *Summary of ICAAR 2012 with Papers Attached. Memorandum to K. Nottingham,* Boise, ID: Idaho Transportation Department, 2012.

50. **Lane, R. M. and M. F. Fish.** *New Hampshire's Concrete Aggregate and Alkali-Silica Reactivity-Statewide Assessment of Fine and Coarse Concrete Aggregate*. Concord, NH: New Hampshire Department of Transportation, 2002.

51. **Lane, R. M. and M. F. Fish.** *Mitigation of Alkali-Silica Reactivity in New Concrete in New Hampshire – Phase 2 - Minimum Amounts of Admixture(s) Needed to Significanlty Minimize ASR.* Concord, NH: New Hampshire Department of Transportation, 2005.

52. **Hudson, B. and F. Shrimer.** "Geology and Particle Size Effects on Alkali-Aggregate-Reactivity in Western Canada." *International Conference on Alkali-Aggregate Reaction (Concrete)*. SHRI, Paper 021811, 2012.

53. **Nomara, M., A. Komatsubara, A., M. Kuroyanagi, and K. Torii.** "Evaluation of the Residual Expansivity of Cores Due to Alkali-Silica Reaction in Hokuriku District, Japan." *International Conference on Alkali-Aggregate Reaction (Concrete)*. NOMU, Paper 021611, 2012.

54. **Hagelia, P. and I. Fernandes.** "On the AAR Susceptibility of Granitic and Quartzitic Aggregates in View of Petrographic Characteristics and Accelerated Testing." *International Conference on Alkali-Aggregate Reaction (Concrete)*. HAGE, Paper 030811, 2012.

55. **Tiecher, F., P. H. Rolim, N. P. Hasparyk, D. S. Coitinho Dal Molin, M. E. Boscato Gomes, and P. Glieze**. "Reactivity Study of Brazilian Aggregates through Silica Dissolution Analysis." *International Conference on Alkali-Aggregate Reaction (Concrete)*. TIEC, Paper 021811, 2012.

56. **Seidlova, Z., R. Prikryl, Z. Pertold, and S. Sachlova.** "Alkali-Silica Reaction of Volcanic Rocks." *International Conference on Alkali-Aggregate Reaction (Concrete)*. No Paper Number, 2012.

57. **Marfil, S., O. Batie, and P. Maiza.** "Petrography of Potentially Alakli-Reactive Sandstone from Argentina." *International Conference on Alkali-Aggregate Reaction (Concrete)*. MARF, Paper 021311, 2012.

AASHTO, ASTM and ITD Tests

1. **AASHTO T 303**. Standard Method of Test for Accelerated Detection of Potentially Deleterious Expansion of Mortar Bars Due to Alkali-Silica Reaction. Washington, DC: American Association of State Highway and Transportation Officials, 2008.

2. **ASTM C 29M-09**. *"Standard Test Method for Bulk Density ("Unit Weight") and Voids in Aggregate. ASTM Committee on Concrete and Concrete Aggregates*. West Conshohocken, PA: American Society for Testing and Materials, Annual Book of ASTM Standards (04.02): Concrete and Aggregates, 2012.

3. **ASTM C 33M-08.** *Standard Specifications for Concrete Aggregates*. American Society for Testing and Materials, West Conshohocken, PA: Annual Book of ASTM Standards (04.02): Concrete and Aggregates, 2012.

4. **ASTM C 127-12.** *Standard Test Method for Density, Relative Density (Specific Gravity), and Absorption of Coarse Aggregate.* West Conshohocken, PA: American Society for Testing and Materials, Annual Book of ASTM Standards (04.02): Concrete and Aggregates, 2012.

5. **ASTM C 138.** *Standard Test Method for Density (Unit Weight), Yield, and Air Content (Gravimetric) of Concrete.* West Conshohocken, PA: American Society for Testing and Materials, Annual Book of ASTM Standards (04.02): Concrete and Aggregates, 2012.

6. **ASTM C 143**. Standard Test Method for Slump of Hydraulic-Cement Concrete. West Conshohocken, PA: American Society for Testing and Materials, Annual Book of ASTM Standards (04.02): Concrete and Aggregates, 2012.

7. **ASTM C 192.** Standard Practice for Making and Curing Concrete Test Specimens in the Laboratory. West Conshohocken, PA: American Society for Testing and Materials, Annual Book of ASTM Standards (04.02): Concrete and Aggregates, 2012.

8. **ASTM C 231**. Standard Test Method for Air Content of Freshly Mixed Concrete by the Pressure Method. West Conshohocken, PA: American Society for Testing and Materials, Annual Book of ASTM Standards (04.02): Concrete and Aggregates, 2012.

9. **ASTM C 1252-06.** Standard Test Methods for Uncompacted Void Content of Fine Aggregate (as Influenced by Particle Shape, Surface Texture, and Grading). West Conshohocken, PA: American Society for Testing and Materials, Annual Book of ASTM Standards (04.02): Concrete and Aggregates, 2012.

10. **ASTM C 1293.** *Standard Test Method for Determination of Length Change of Concrete Due to Alkali-Silica Reaction.* West Conshohocken, PA: American Society for Testing and Materials, Annual Book of ASTM Standards (04.02): Concrete and Aggregates, 2012.

11. **IR-146-06**. *Idaho Standard Practice for Investigation of Aggregate and Burrow Deposits.* Boise, ID: Idaho Transportation Department, Materials Manual, 2012.

Appendix A
Photos of ¾ Inch Aggregate

District 1 - ¾ in. Aggregate

Figure 91. Br-2c - ¾ Inch Aggregate

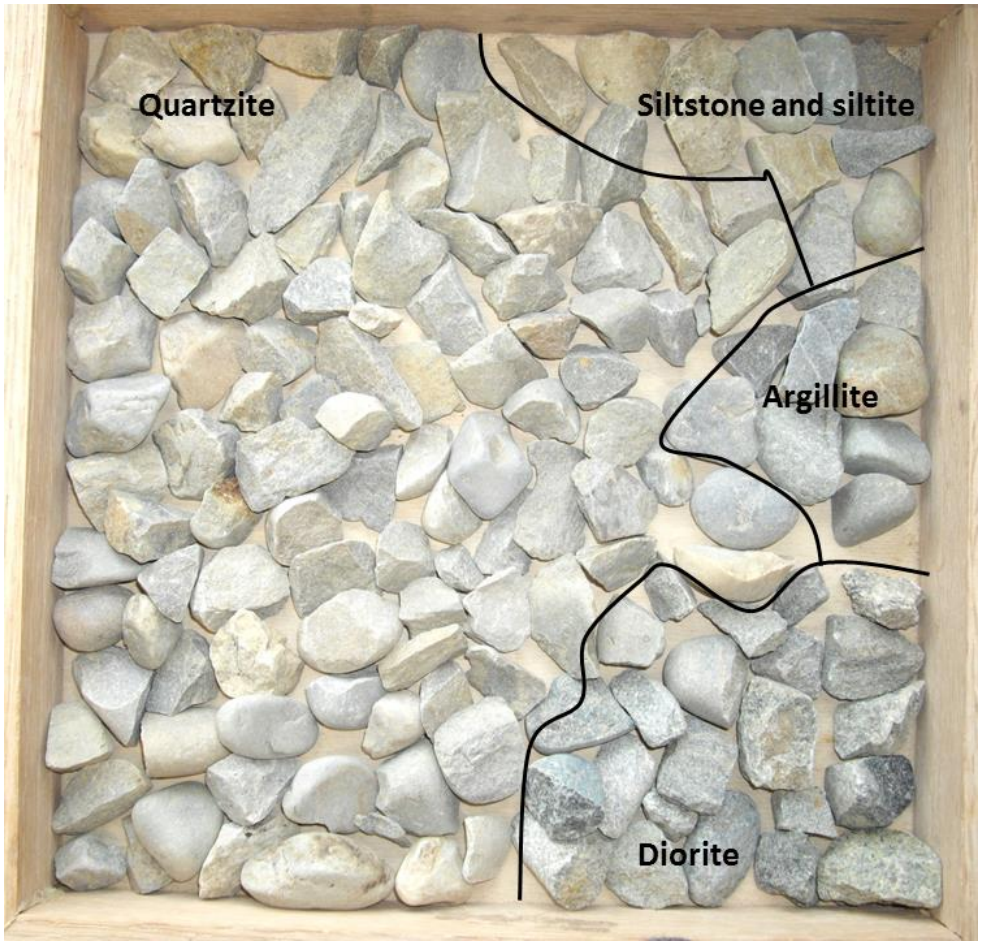

Figure 92. By-74c - 3/4 Inch Aggregate

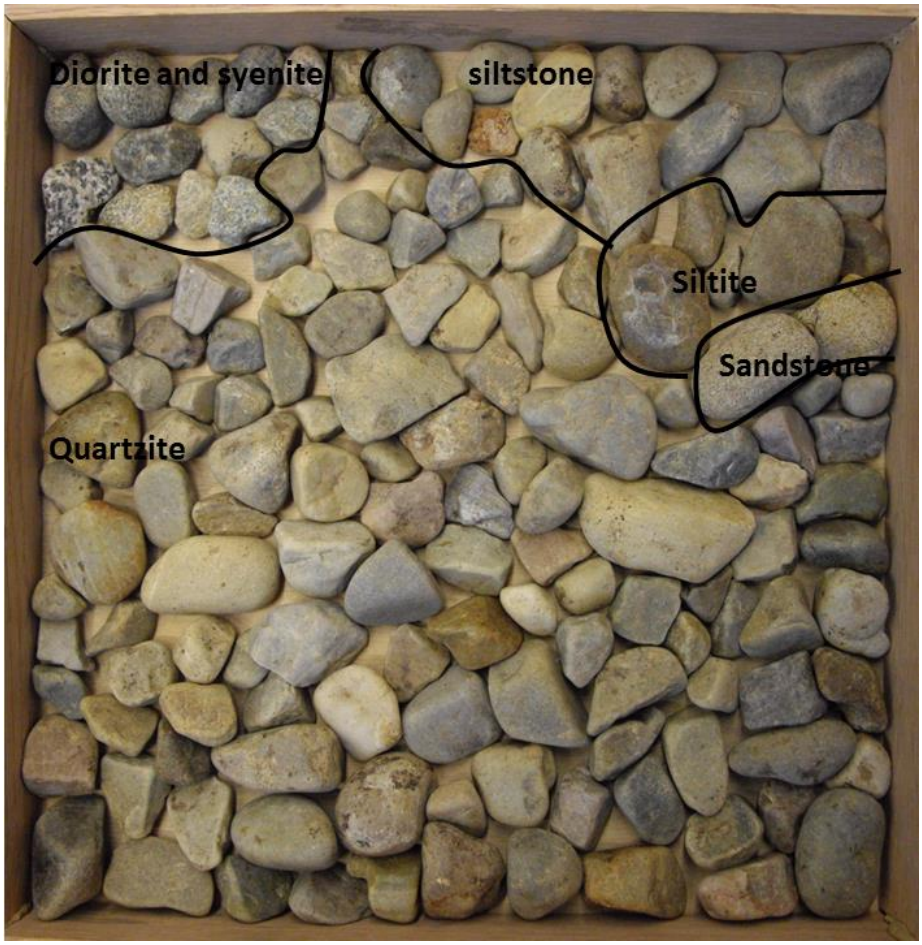

Figure 93. By-80c - ¾ Inch Aggregate

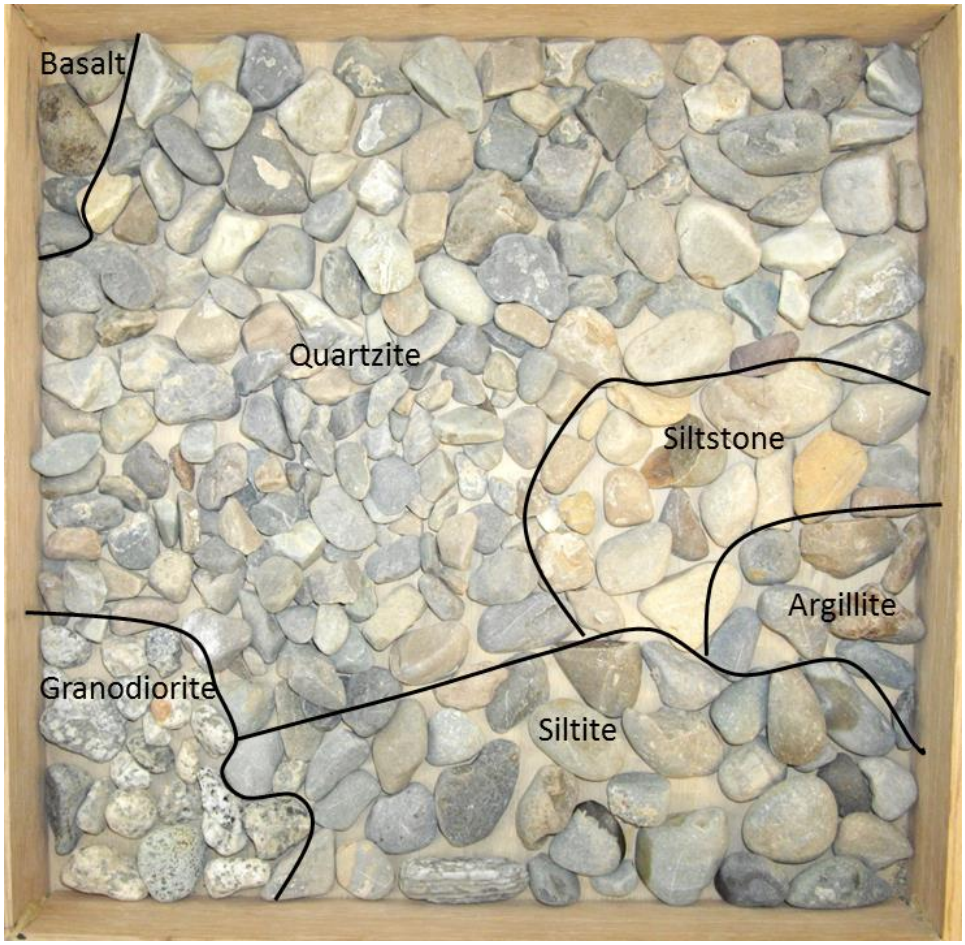

Figure 94. Kt-191c - ¾ Inch Aggregate

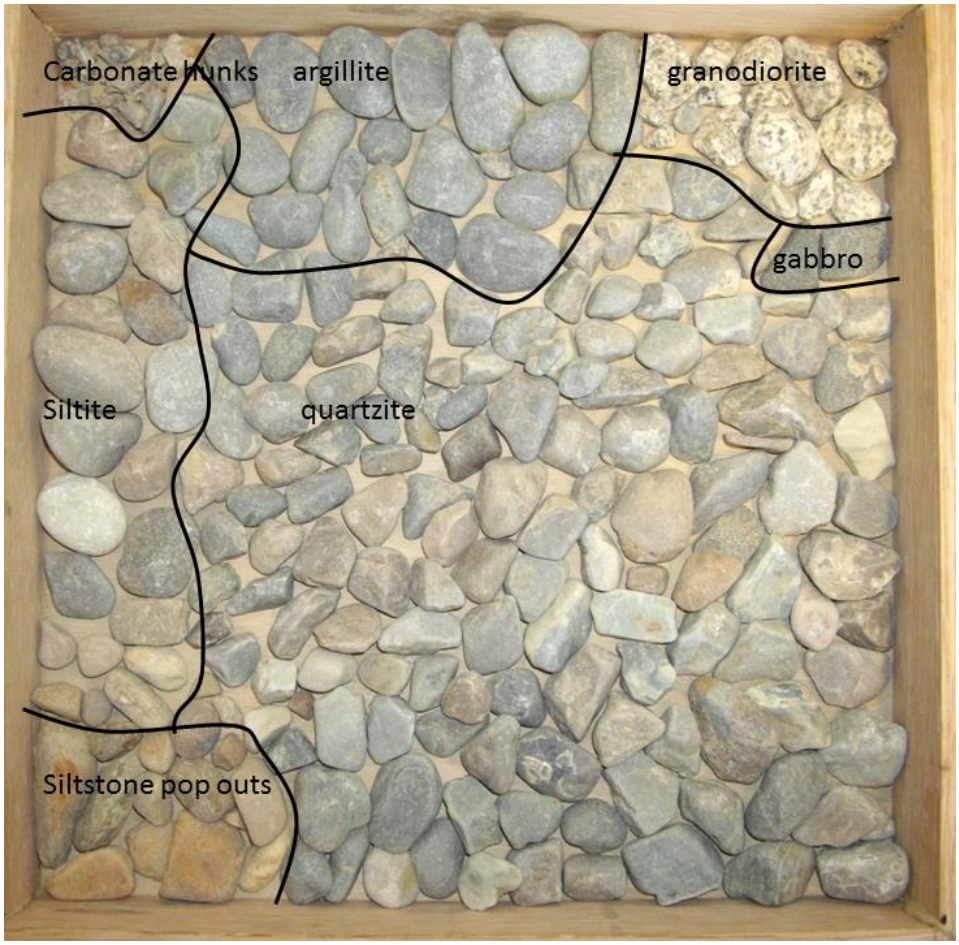

Figure 95. Kt-213c - ¾ Inch Aggregate

Figure 96. PSC-173 - ¾ Inch Aggregate

District 2 - ¾ Inch Aggregate

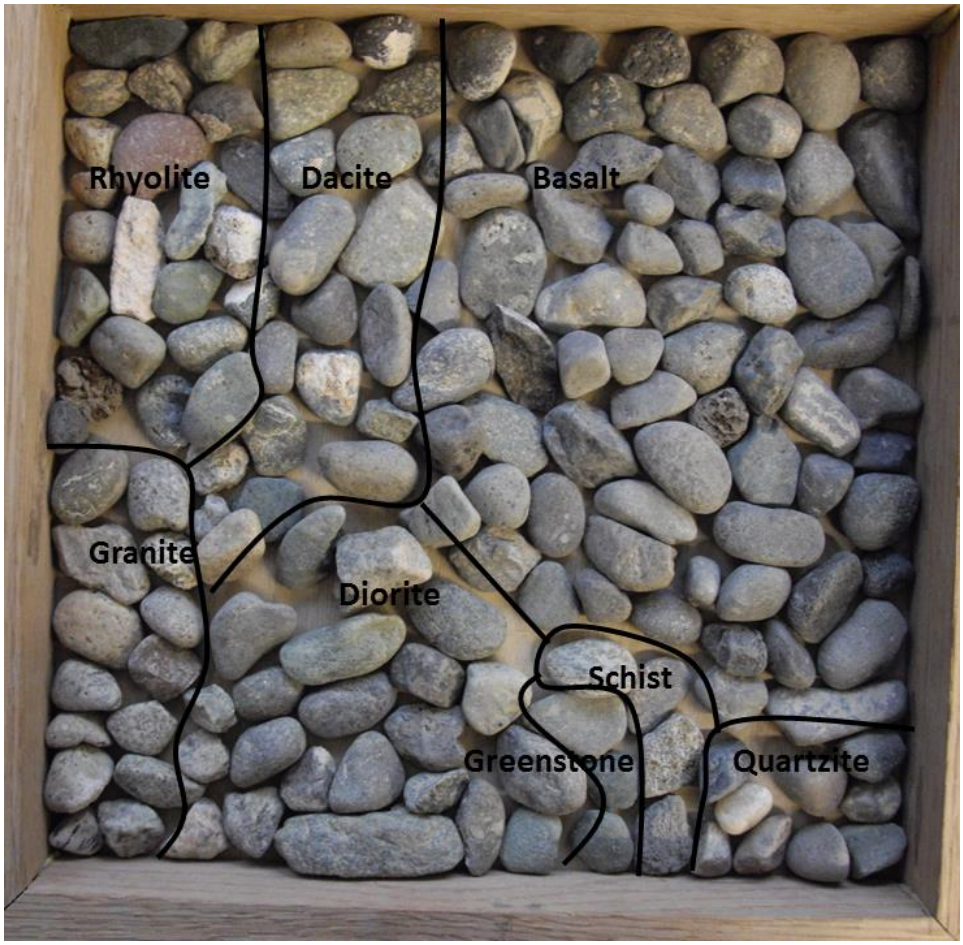

Figure 97. Id-121c - ¾ Inch Aggregate

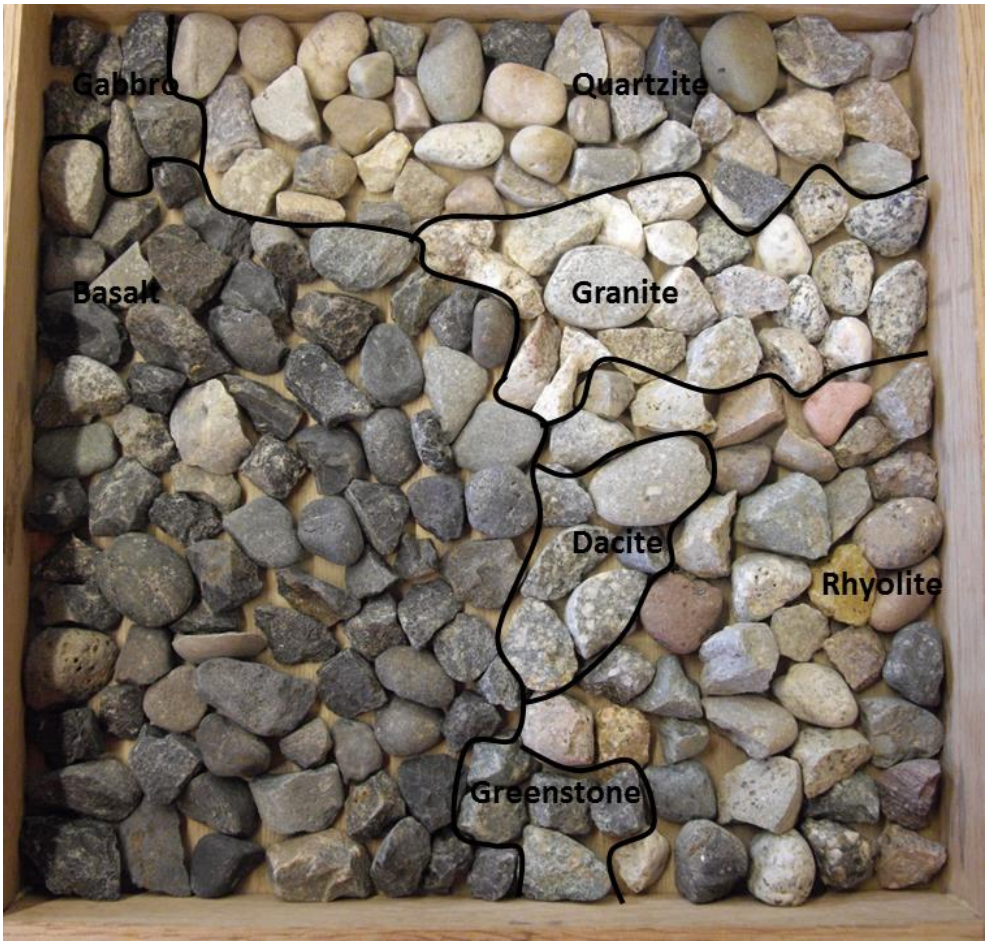

Figure 98. Id-272c - ¾ Inch Aggregate

District 3 - ¾ Inch Aggregate

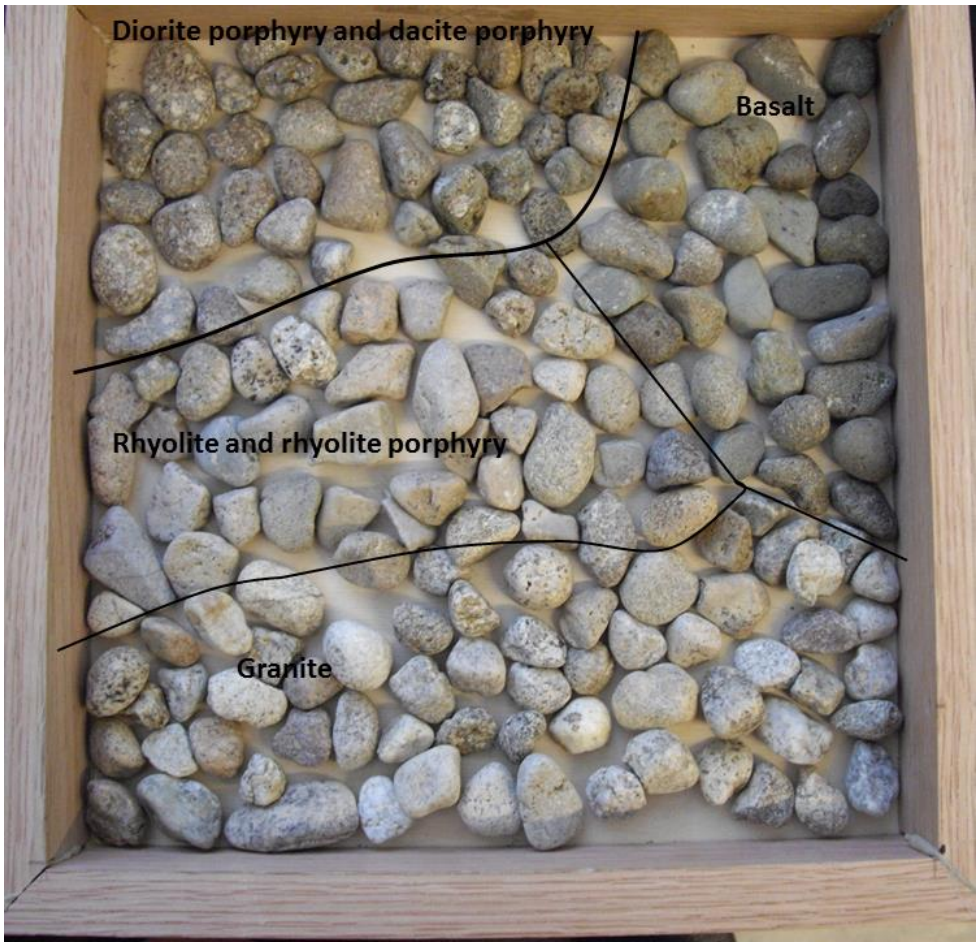

Figure 99. Ad-53s + ½ Inch Pit Run Box 10 Inch Interior

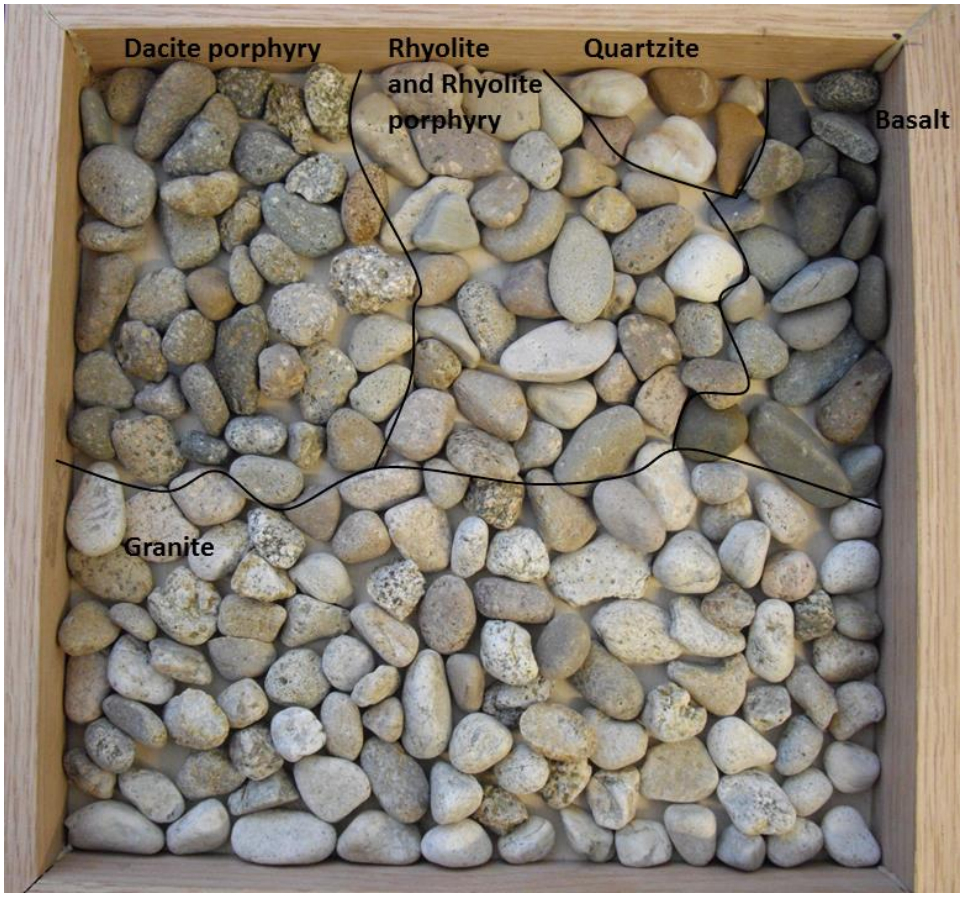

Figure 100. Cn-140c Top ½ Inch Pit Run Tray = 10 Inch Interior

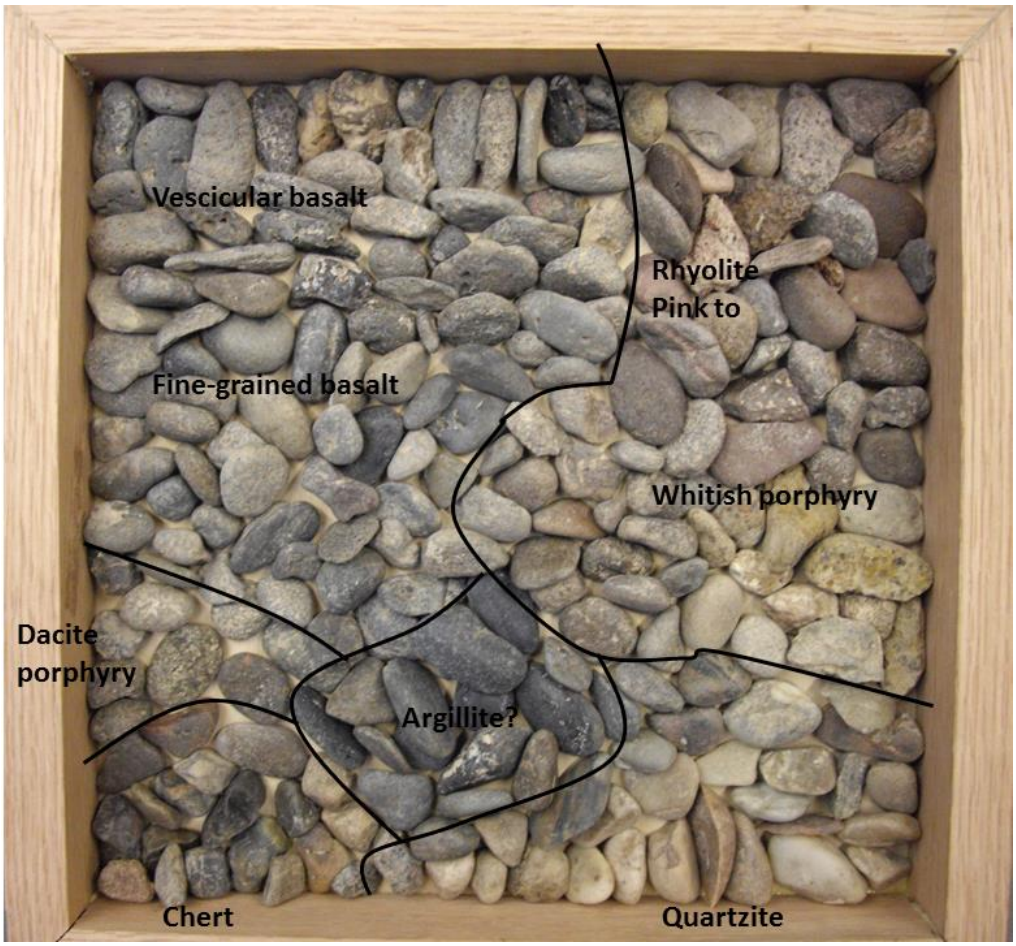

Figure 101. El-37c - ½ Inch Pit Run

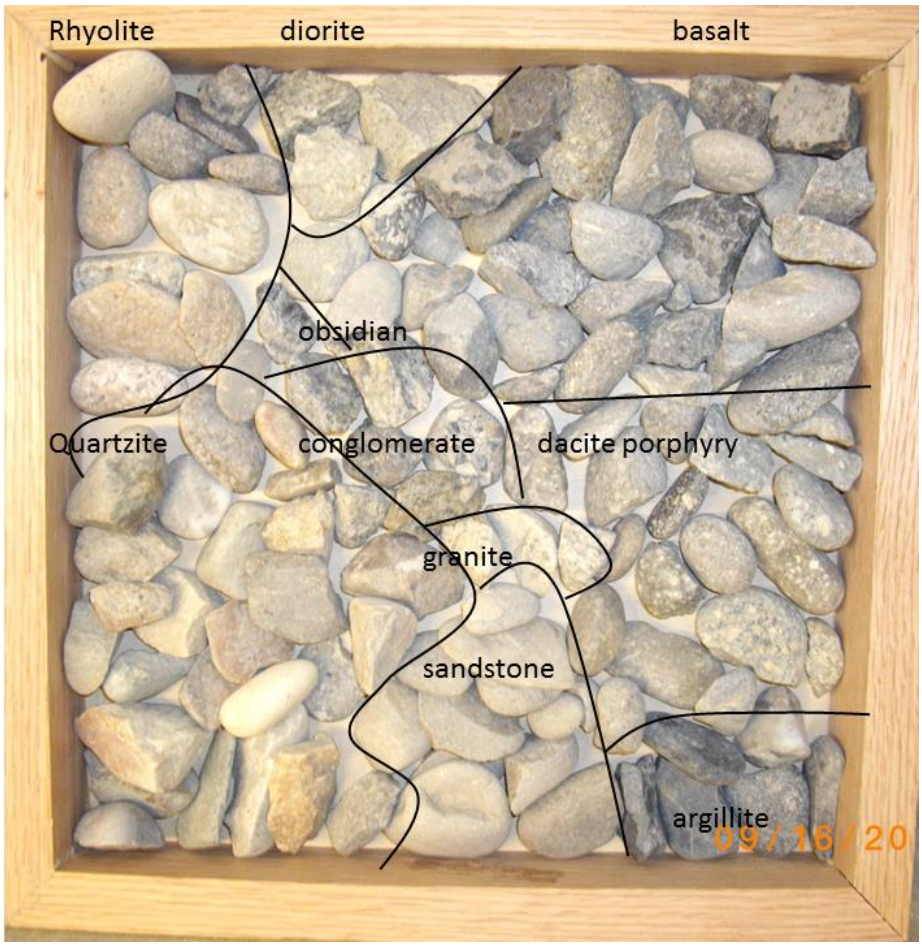

Figure 102. El-116c - 1 Inch Stock

Figure 103. Bo-61c - ¾ Inch Aggregate

Figure 104. Ore-16c - ¾ Inch Aggregate

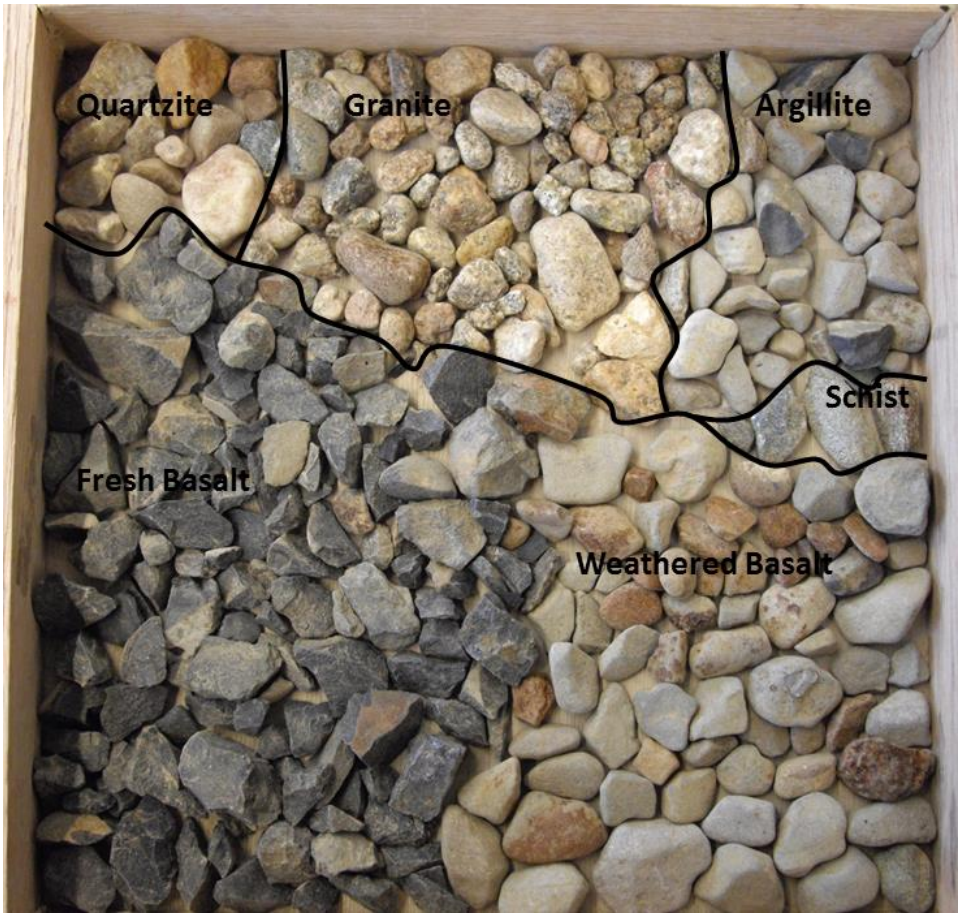

Figure 105. Vy-56c- ¾ Inch Aggregate

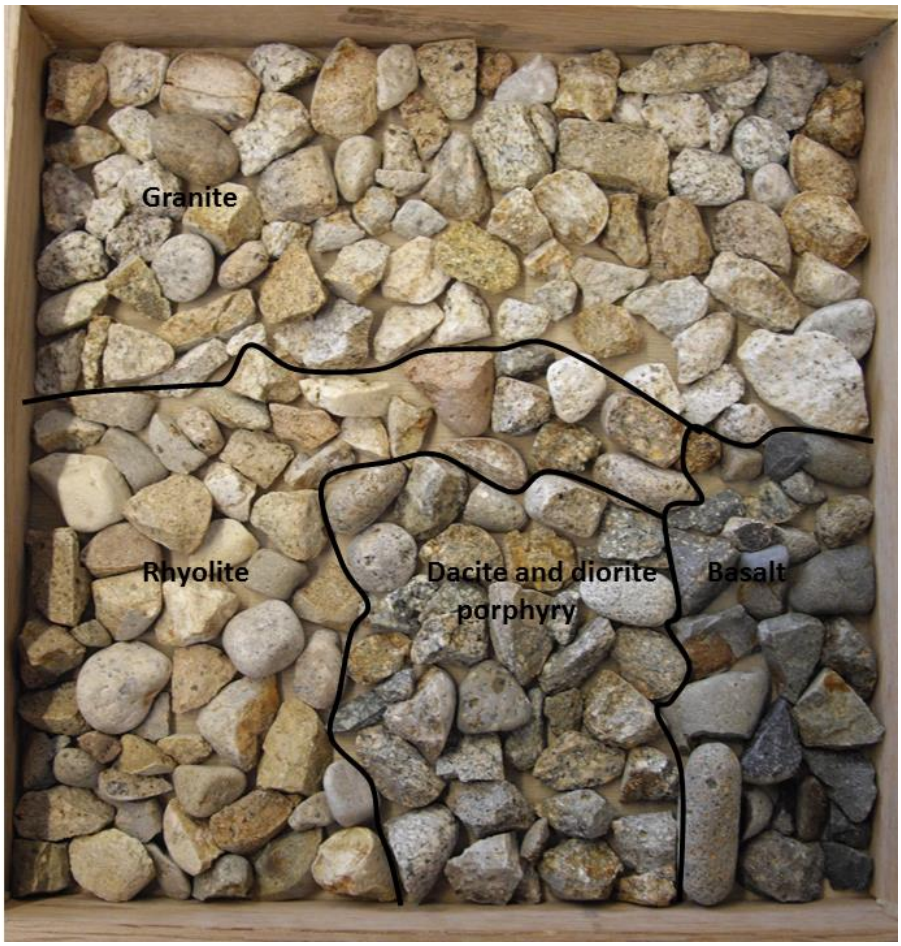

Figure 106. Cn-146c - ¾ Inch Aggregate

District 4 - ¾ Inch Aggregate

Figure 107. Ln-80c - ¾ Inch Aggregate

Figure 108. Cs-186 - ¾ Inch Aggregate

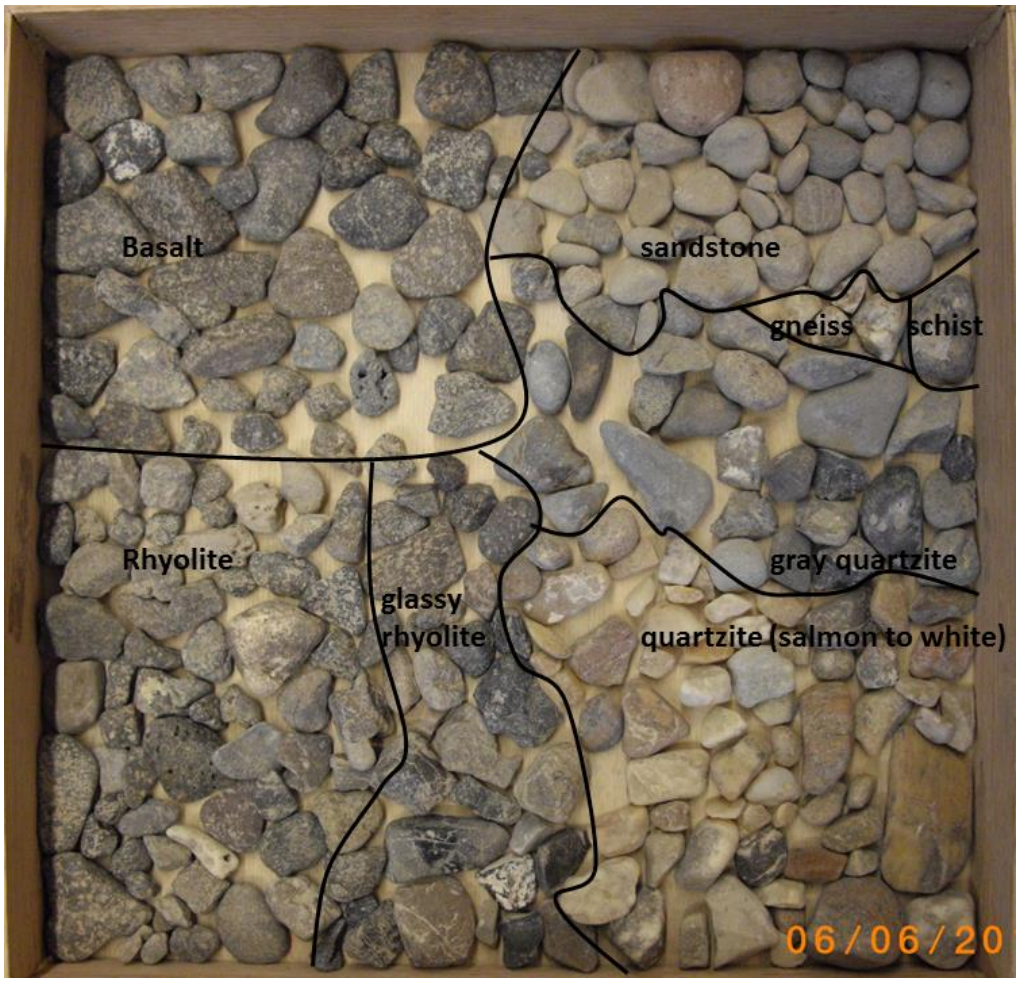

Figure 109. Md-45c - ¾ Inch Aggregate

District 5 - ¾ Inch Aggregate

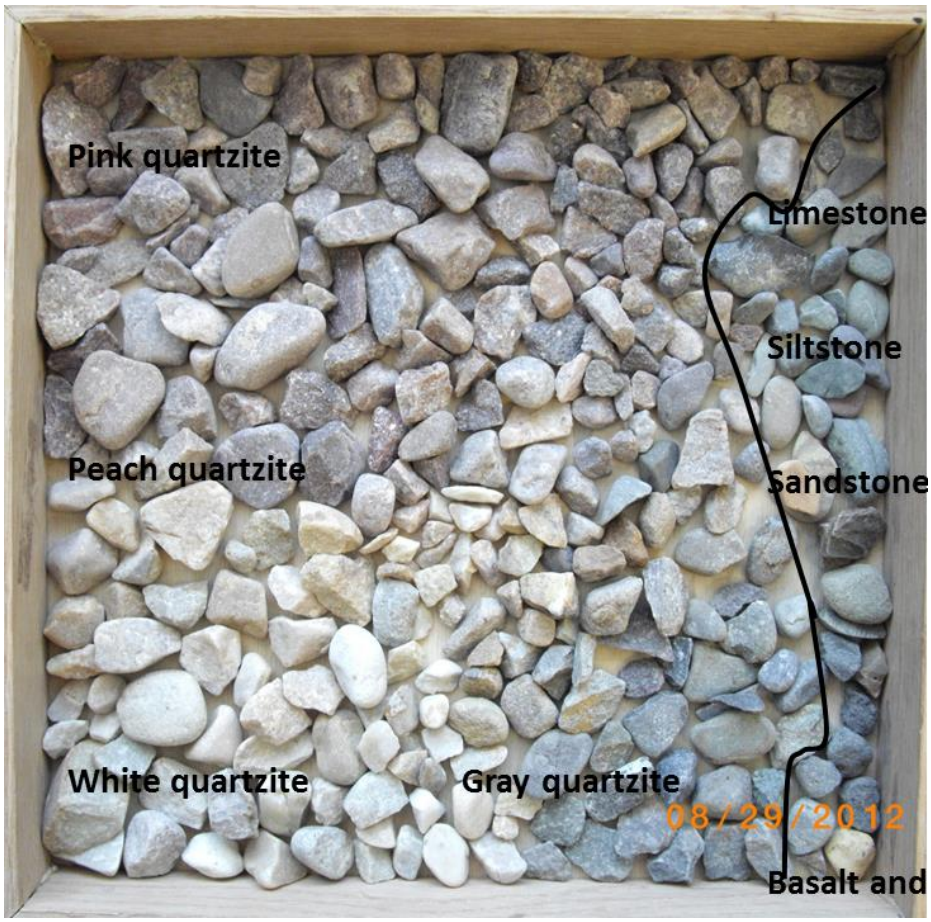

Figure 110. Pw-84c - ¾ Inch Aggregate

Figure 111. Bg-111c - ¾ Inch Aggregate

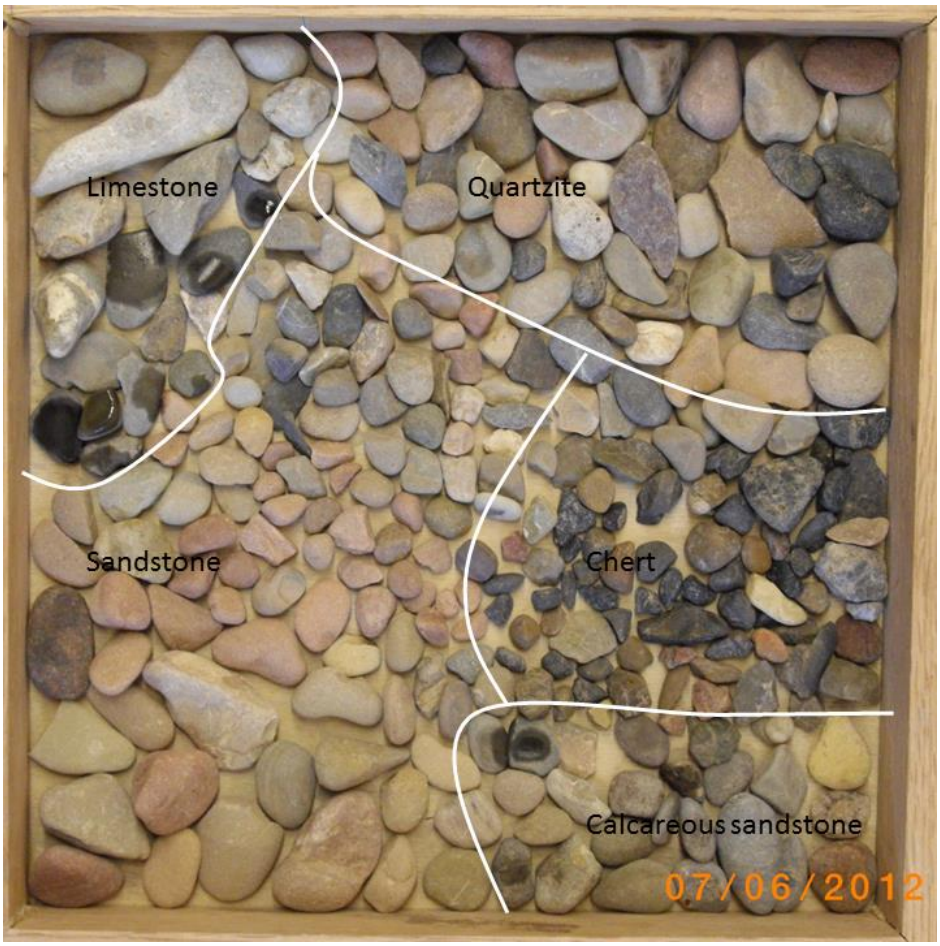

Figure 112. Bl-84c – ¾ Inch Aggregate

District 6 - ¾ Inch Aggregate

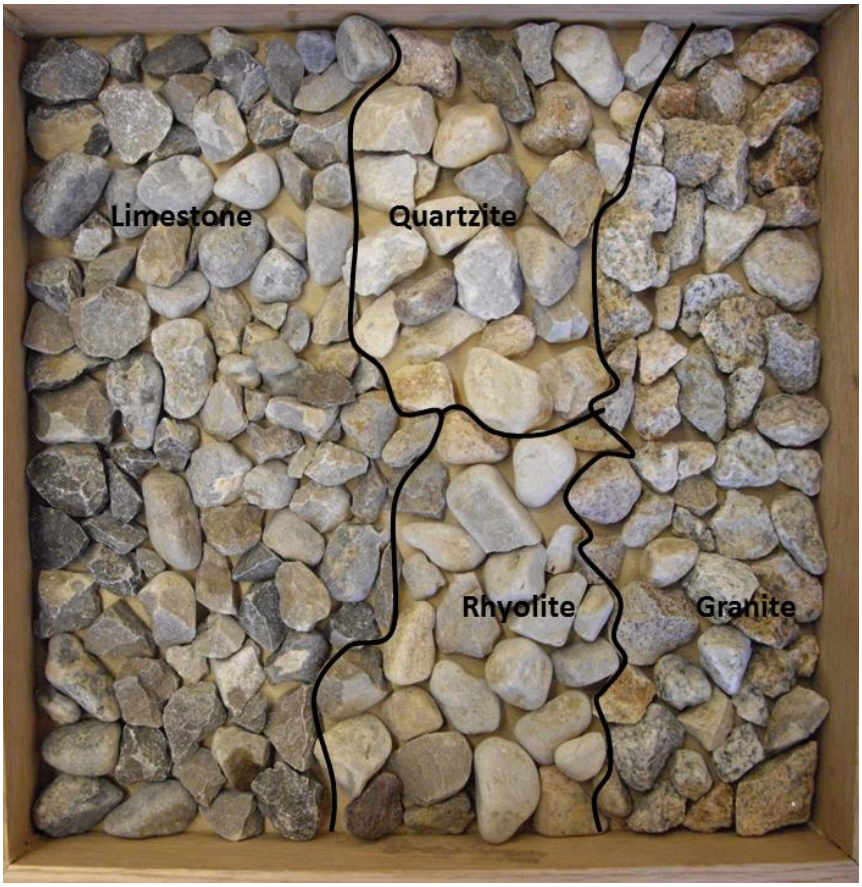

Figure 113. Tn-65c – ¾ Inch Aggregate

Figure 114. Bn-155c - ¾ Inch Aggregate

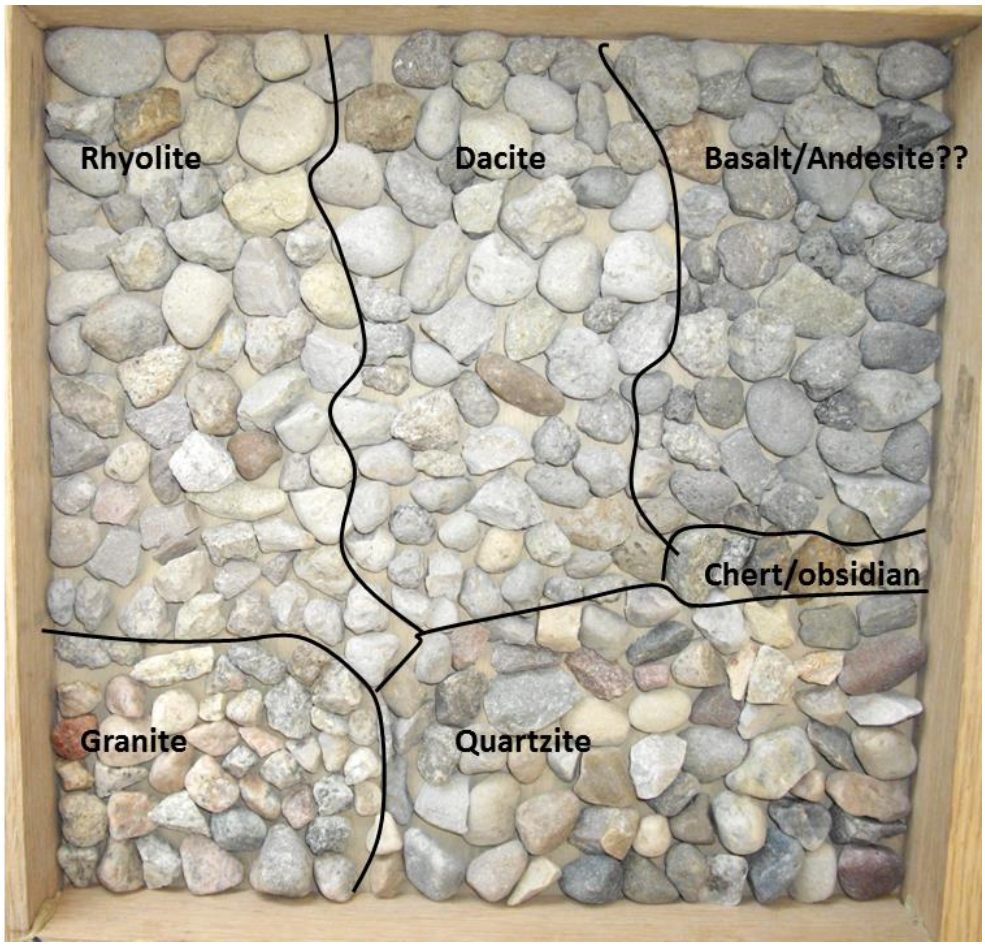

Figure 115. Ma-22c – ¾ Inch Aggregate

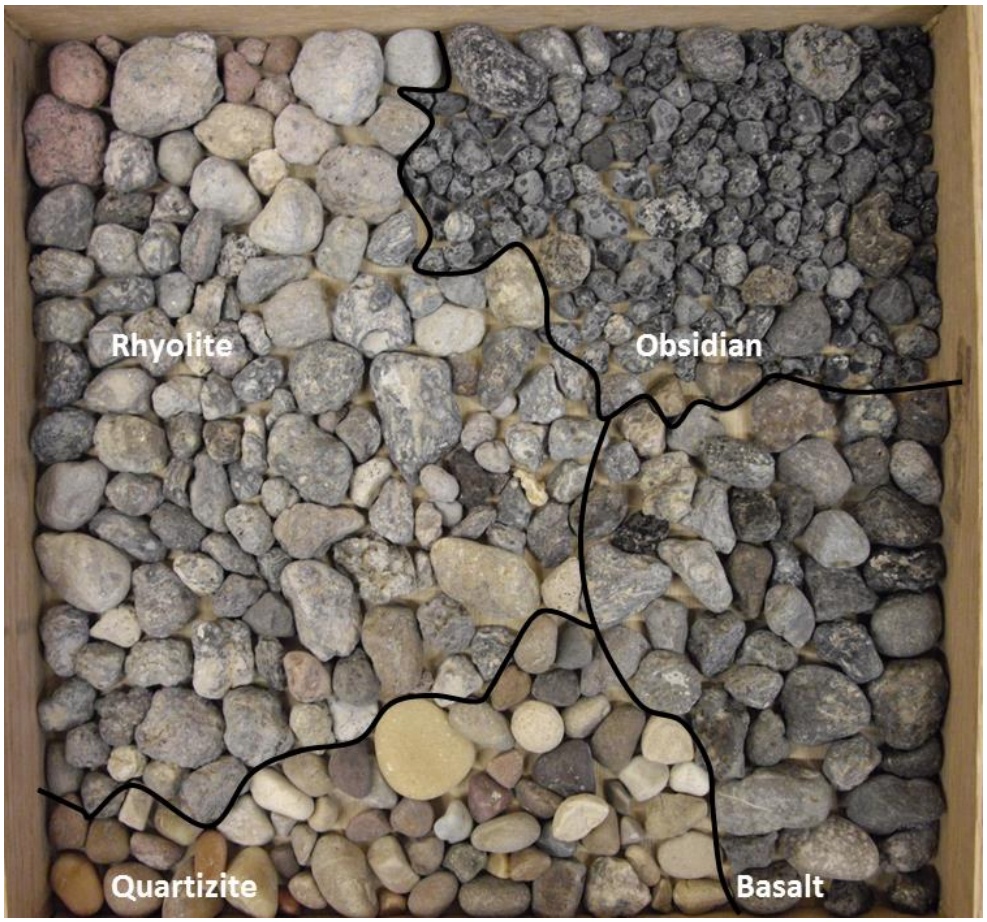

Figure 116. Jf-103c - ½ Inch Screened

Figure 117. Le-154c – ¾ Inch Aggregate

Figure 118. Cu-73c – ¾ Inch Aggregate

Figure 119. Le-155c – ½ Inch Pit
(No ¾ Inch Aggregate, This was Most Comparable)

Appendix B
Basin Delineation Using ArcGIS

Below is a sequential description of the Arc Toolbox tools used in basin delineation.

1. A filled DEM was created from the DEM. The “fill” tool fills sinks in the data and removes imperfections.

2. A flow direction raster was created from the filled DEM. The “flow direction” tool generates a flow direction raster from each cell to its steepest downslope neighbor.

3. A flow accumulation raster was created from the flow direction raster. The “flow accumulation” tool creates a raster of accumulated flow into each cell. The flow accumulation raster shows actual drainages and streams.

4. The stream and river channels were created from the flow accumulation raster. The “reclassify” tool was used to reclassify pixels into two classes (channel = 1 and non-channel = nodata). The channel formation threshold (break value) was set at 1000 and the maximum number of pixels was set as the upper threshold (break value). In the table, under New Values “1” was changed to “nodata“ and “2“ was changed to “1.“

5. A point was placed on the actual drainage at, or near, the sampled source location. The point was then converted to a feature and used to “snap pour point“

6. Lastly, the “watershed“ tool is used on the flow direction raster and the pour point to determine the contributing area above the pour point.

7. Watershed polygons were used to clip geologic layers.[1] To identify provenance, clipped geologic layers per drainage basin were compared with source lithologic inventories.

Appendix C
Lithology Inventory of Coarse Aggregate Data Tables

Table 10. ACW-8c Coarse Aggregate Inventory

	ACW-8c	
Rock Type	**Lithology**	**Percent Composition (Based on total pit weighted average)**
Igneous Intrusives	Granite	0.00
	Granodiorite	0.00
	Diorite	0.04
	Gabbro	0.00
Igneous Volcanics and Sub-volcanics	Rhyolite	0.22
	Dacite Porphyry	0.01
	Andesite	0.00
	Basalt	0.48
Metamorphics	Quartzite	0.06
	Schist	0.00
	Gneiss	0.04
	Siltite	0.00
	Phyllite	0.00
	Argillite	0.04
	Greenstone	0.03
Sedimentary Rocks	Limestone/Dolomite	0.00
	Sandstone	0.04
	Siltstone	0.04
	Conglomerate	0.00
	Shale/Mudstone	0.00
	Pedogenic carbonate	0.00
Amorphous Silica	Chert	0.00
	Chalcedony	0.00
	Obsidian	0.00
		1.00

Table 11. Ad-53s Coarse Aggregate Inventory

	Ad-53c	
Rock Type	**Lithology**	**Percent Composition (Based on total pit weighted average)**
Igneous Intrusives	Granite	0.31
	Granodiorite	0.06
	Diorite	0.03
	Gabbro	0.00
Igneous Volcanics and Sub-volcanics	Rhyolite	0.27
	Dacite Porphyry	0.11
	Andesite	0.00
	Basalt	0.20
Metamorphics	Quartzite	0.02
	Schist	0.00
	Gneiss	0.00
	Siltite	0.00
	Phyllite	0.00
	Argillite	0.00
	Greenstone	0.00
Sedimentary Rocks	Limestone/Dolomite	0.00
	Sandstone	0.00
	Siltstone	0.00
	Conglomerate	0.00
	Shale/Mudstone	0.00
	Pedogenic carbonate	0.00
Amorphous Silica	Chert	0.00
	Chalcedony	0.00
	Obsidian	0.00
		1.00

Table 12. Ad-136c Aggregate Inventory

	Ad-136c	
Rock Type	**Lithology**	**Percent Composition (Based on total pit weighted average)**
Igneous Intrusives	Granite	0.25
	Granodiorite	0.00
	Diorite	0.10
	Gabbro	0.07
Igneous Volcanics and Sub-volcanics	Rhyolite	0.22
	Dacite porphyry	0.07
	Andesite	0.15
	Basalt	0.11
Metamorphics	Quartzite	0.03
	Schist	0.00
	Gneiss	0.00
	Siltite	0.00
	Phyllite	0.00
	Argillite	0.00
	Greenstone	0.00
Sedimentary Rocks	Limestone/Dolomite	0.00
	Sandstone	0.00
	Siltstone	0.00
	Conglomerate	0.00
	Shale/mudstone	0.00
	Pedogenic carbonate	0.00
Amorphous Silica	Chert	0.01
	Chalcedony	0.00
	Obsidian	0.00
		1.00

Table 13. Bg-111c Coarse Aggregate Inventory

	Bg-111c	
Rock Type	**Lithology**	**Percent Composition (Based on total pit weighted average)**
Igneous Intrusives	Granite	0.02
	Granodiorite	0.00
	Diorite	0.01
	Gabbro	0.02
Igneous Volcanics and Sub-volcanics	Rhyolite	0.06
	Dacite Porphyry	0.00
	Andesite	0.00
	Basalt	0.02
Metamorphics	Quartzite	0.73
	Schist	0.00
	Gneiss	0.00
	Siltite	0.00
	Phyllite	0.00
	Argillite	0.00
	Greenstone	0.00
Sedimentary Rocks	Limestone/Dolomite	0.02
	Sandstone	0.11
	Siltstone	0.00
	Conglomerate	0.00
	Shale/Mudstone	0.00
	Pedogenic Carbonate	0.00
Amorphous Silica	Chert	0.00
	Chalcedony	0.00
	Obsidian	0.00
		1.00

Table 14. Bl-84c Coarse Aggregate Inventory

	Bl-84c	
Rock Type	**Lithology**	**Percent Composition (Based on total pit weighted average)**
Igneous Intrusives	Granite	0.00
	Granodiorite	0.00
	Diorite	0.00
	Gabbro	0.00
Igneous Volcanics and Sub-volcanics	Rhyolite	0.01
	Dacite Porphyry	0.00
	Andesite	0.00
	Basalt	0.00
Metamorphics	Quartzite	0.25
	Schist	0.00
	Gneiss	0.00
	Siltite	0.00
	Phyllite	0.00
	Argillite	0.00
	Greenstone	0.00
Sedimentary Rocks	Limestone/Dolomite	0.23
	Sandstone	0.37
	Siltstone	0.01
	Conglomerate	0.02
	Shale/Mudstone	0.01
	Pedogenic Carbonate	0.00
Amorphous Silica	Chert	0.10
	Chalcedony	0.00
	Obsidian	0.00
		1.00

Table 15. Bn-155c Coarse Aggregate Inventory

	Bn-155c	
Rock Type	**Lithology**	**Percent Composition (Based on total pit weighted average)**
Igneous Intrusives	Granite	0.04
	Granodiorite	0.01
	Diorite	0.00
	Gabbro	0.00
Igneous Volcanics and Sub-volcanics	Rhyolite	0.11
	Dacite Porphyry	0.00
	Andesite	0.00
	Basalt	0.04
Metamorphics	Quartzite	0.66
	Schist	0.00
	Gneiss	0.00
	Siltite	0.00
	Phyllite	0.00
	Argillite	0.01
	Greenstone	0.00
Sedimentary Rocks	Limestone/Dolomite	0.02
	Sandstone	0.09
	Siltstone	0.01
	Conglomerate	0.00
	Shale/Mudstone	0.00
	Pedogenic Carbonate	0.00
Amorphous Silica	Chert	0.01
	Chalcedony	0.00
	Obsidian	0.00
		1.00

Table 16. Bo-61c Coarse Aggregate Inventory

	Bo-61c	
Rock Type	Lithology	Percent Composition (Based on total pit weighted average)
Igneous Intrusives	Granite	46.02%
	Granodiorite	11.47%
	Diorite	8.03%
	Gabbro	0.00%
Igneous Volcanics and Sub-volcanics	Rhyolite	19.40%
	Dacite porphyry	4.33%
	Andesite	0.86%
	Basalt	9.89%
Metamorphics	Quartzite	0.00%
	Schist	
	Gneiss	
	Siltite	0.00%
	Phyllite	
	Argillite	
	Greenstone	
Sedimentary Rocks	Limestone/Dolomite	0.00%
	Sandstone	
	Siltstone	
	Conglomerate	
	Shale/mudstone	
	Pedogenic carbonate	
Amorphous Silica	Chert	
	Chalcedony	
	Obsidian	
		100.00%

Table 17. Br-2c Coarse Aggregate Inventory

	Br-2c	
Rock Type	**Lithology**	**Percent Composition (Based on total pit weighted average)**
Igneous Intrusives	Granite	0.06
	Granodiorite	0.22
	Diorite	0.03
	Gabbro	0.00
Igneous Volcanics and Sub-volcanics	Rhyolite	0.00
	Dacite Porphyry	0.00
	Andesite	0.00
	Basalt	0.02
Metamorphics	Quartzite	0.60
	Schist	0.03
	Gneiss	0.00
	Siltite	0.01
	Phyllite	0.00
	Argillite	0.00
	Greenstone	0.00
Sedimentary Rocks	Limestone/Dolomite	0.00
	Sandstone	0.02
	Siltstone	0.00
	Conglomerate	0.00
	Shale/Mudstone	0.01
	Pedogenic Carbonate	0.00
Amorphous Silica	Chert	0.00
	Chalcedony	0.00
	Obsidian	0.00
		1.00

Table 18. By-74c Coarse Aggregate Inventory

	By-74c	
Rock Type	**Lithology**	**Percent Composition (Based on total pit weighted average)**
Igneous Intrusives	Granite	0.00
	Granodiorite	0.01
	Diorite	0.12
	Gabbro	0.00
Igneous Volcanics and Sub-volcanics	Rhyolite	0.00
	Dacite Porphyry	0.00
	Andesite	0.00
	Basalt	0.00
Metamorphics	Quartzite	0.61
	Schist	0.01
	Gneiss	0.00
	Siltite	0.06
	Phyllite	0.00
	Argillite	0.08
	Greenstone	0.00
Sedimentary Rocks	Limestone/Dolomite	0.00
	Sandstone	0.05
	Siltstone	0.05
	Conglomerate	0.00
	Shale/Mudstone	0.00
	Pedogenic Carbonate	0.00
Amorphous Silica	Chert	0.01
	Chalcedony	0.00
	Obsidian	0.00
		1.00

Table 19. By-80c Coarse Aggregate Inventory

	By-80c	
Rock Type	**Lithology**	**Percent Composition (Based on total pit weighted average)**
Igneous Intrusives	Granite	0.00
	Granodiorite	0.00
	Diorite	0.09
	Gabbro	0.00
Igneous Volcanics and Sub-volcanics	Rhyolite	0.00
	Dacite Porphyry	0.00
	Andesite	0.00
	Basalt	0.00
Metamorphics	Quartzite	0.71
	Schist	0.00
	Gneiss	0.00
	Siltite	0.08
	Phyllite	0.00
	Argillite	0.01
	Greenstone	0.00
Sedimentary Rocks	Limestone/Dolomite	0.00
	Sandstone	0.09
	Siltstone	0.01
	Conglomerate	0.00
	Shale/Mudstone	0.00
	Pedogenic Carbonate	0.00
Amorphous Silica	Chert	0.00
	Chalcedony	0.00
	Obsidian	0.00
		1.00

Table 20. Cn-140c Coarse Aggregate Inventory

	Cn-140c	
Rock Type	**Lithology**	**Percent Composition (Based on total pit weighted average)**
Igneous Intrusives	Granite	0.46
	Granodiorite	0.03
	Diorite	0.00
	Gabbro	0.00
Igneous Volcanics and Sub-volcanics	Rhyolite	0.31
	Dacite Porphyry	0.12
	Andesite	0.00
	Basalt	0.04
Metamorphics	Quartzite	0.04
	Schist	0.00
	Gneiss	0.00
	Siltite	0.00
	Phyllite	0.00
	Argillite	0.00
	Greenstone	0.00
Sedimentary Rocks	Limestone/Dolomite	0.00
	Sandstone	0.01
	Siltstone	0.00
	Conglomerate	0.00
	Shale/Mudstone	0.00
	Pedogenic Carbonate	0.00
Amorphous Silica	Chert	0.00
	Chalcedony	0.00
	Obsidian	0.00
		1.00

Table 21. Cn-146c Coarse Aggregate Inventory

	Cn-146c	
Rock Type	**Lithology**	**Percent Composition (Based on total pit weighted average)**
Igneous Intrusives	Granite	0.31
	Granodiorite	0.02
	Diorite	0.14
	Gabbro	0.22
Igneous Volcanics and Sub-volcanics	Rhyolite	0.06
	Dacite Porphyry	0.04
	Andesite	0.13
	Basalt	0.09
Metamorphics	Quartzite	0.00
	Schist	0.00
	Gneiss	0.00
	Siltite	0.00
	Phyllite	0.00
	Argillite	0.00
	Greenstone	0.00
Sedimentary Rocks	Limestone/Dolomite	0.00
	Sandstone	0.00
	Siltstone	0.00
	Conglomerate	0.00
	Shale/Mudstone	0.00
	Pedogenic Carbonate	0.00
Amorphous Silica	Chert	0.00
	Chalcedony	0.00
	Obsidian	0.00
		1.00

Table 22. Cs-186c Coarse Aggregate Inventory

	Cs-186c	
Rock Type	**Lithology**	**Percent Composition (Based on total pit weighted average)**
Igneous Intrusives	Granite	0.03
	Granodiorite	0.00
	Diorite	0.00
	Gabbro	0.00
Igneous Volcanics and Sub-volcanics	Rhyolite	0.40
	Dacite Porphyry	0.01
	Andesite	0.08
	Basalt	0.06
Metamorphics	Quartzite	0.04
	Schist	0.04
	Gneiss	0.02
	Siltite	0.00
	Phyllite	0.00
	Argillite	0.00
	Greenstone	0.00
Sedimentary Rocks	Limestone/Dolomite	0.00
	Sandstone	0.03
	Siltstone	0.14
	Conglomerate	0.01
	Shale/Mudstone	0.00
	Pedogenic Carbonate	0.00
Amorphous Silica	Chert	0.02
	Chalcedony	0.00
	Obsidian	0.11
		1.00

Table 23. Cu-73c Coarse Aggregate Inventory

	Cu-73c	
Rock Type	**Lithology**	**Percent Composition (Based on total pit weighted average)**
Igneous Intrusives	Granite	0.04
	Granodiorite	0.00
	Diorite	0.03
	Gabbro	0.00
Igneous Volcanics and Sub-volcanics	Rhyolite	0.28
	Dacite Porphyry	0.11
	Andesite	0.04
	Basalt	0.07
Metamorphics	Quartzite	0.30
	Schist	0.00
	Gneiss	0.01
	Siltite	0.01
	Phyllite	0.00
	Argillite	0.04
	Greenstone	0.00
Sedimentary Rocks	Limestone/Dolomite	0.00
	Sandstone	0.02
	Siltstone	0.04
	Conglomerate	0.00
	Shale/Mudstone	0.00
	Pedogenic Carbonate	0.00
Amorphous Silica	Chert	0.00
	Chalcedony	0.00
	Obsidian	0.00
		1.00

Table 24. El-37c Coarse Aggregate Inventory

	El-37c	
Rock Type	**Lithology**	**Percent Composition (Based on total pit weighted average)**
Igneous Intrusives	Granite	0.00
	Granodiorite	0.00
	Diorite	0.00
	Gabbro	0.00
Igneous Volcanics and Sub-volcanics	Rhyolite	0.18
	Dacite Porphyry	0.01
	Andesite	0.00
	Basalt	0.42
Metamorphics	Quartzite	0.36
	Schist	0.00
	Gneiss	0.00
	Siltite	0.00
	Phyllite	0.00
	Argillite	0.02
	Greenstone	0.00
Sedimentary Rocks	Limestone/Dolomite	0.00
	Sandstone	0.00
	Siltstone	0.00
	Conglomerate	0.00
	Shale/Mudstone	0.00
	Pedogenic Carbonate	0.00
Amorphous Silica	Chert	0.00
	Chalcedony	0.02
	Obsidian	0.00
		1.00

Table 25. El-116c Coarse Aggregate Inventory

	El-116c	
Rock Type	**Lithology**	**Percent Composition (Based on total pit weighted average)**
Igneous Intrusives	Granite	0.01
	Granodiorite	0.01
	Diorite	0.02
	Gabbro	0.02
Igneous Volcanics and Sub-volcanics	Rhyolite	0.15
	Dacite Porphyry	0.10
	Andesite	0.00
	Basalt	0.22
Metamorphics	Quartzite	0.22
	Schist	0.00
	Gneiss	0.00
	Siltite	0.00
	Phyllite	0.00
	Argillite	0.08
	Greenstone	0.00
Sedimentary Rocks	Limestone/Dolomite	0.00
	Sandstone	0.08
	Siltstone	0.00
	Conglomerate	0.04
	Shale/Mudstone	0.00
	Pedogenic Carbonate	0.01
Amorphous Silica	Chert	0.03
	Chalcedony	0.00
	Obsidian	0.01
		1.00

Table 26. Gm-46c Coarse Aggregate Inventory

	Gm-46c	
Rock Type	**Lithology**	**Percent Composition (Based on total pit weighted average)**
Igneous Intrusives	Granite	0.16
	Granodiorite	0.25
	Diorite	0.01
	Gabbro	0.00
Igneous Volcanics and Sub-volcanics	Rhyolite	0.13
	Dacite Porphyry	0.14
	Andesite	0.05
	Basalt	0.10
Metamorphics	Quartzite	0.06
	Schist	0.00
	Gneiss	0.03
	Siltite	0.03
	Phyllite	0.00
	Argillite	0.00
	Greenstone	0.01
Sedimentary Rocks	Limestone/Dolomite	0.00
	Sandstone	0.00
	Siltstone	0.03
	Conglomerate	0.00
	Shale/Mudstone	0.00
	Pedogenic Carbonate	0.00
Amorphous Silica	Chert	0.00
	Chalcedony	0.00
	Obsidian	0.00
		1.00

Table 27. Id-121c Coarse Aggregate Inventory

	Id-121c	
Rock Type	**Lithology**	**Percent Composition (Based on total pit weighted average)**
Igneous Intrusives	Granite	0.01
	Granodiorite	0.03
	Diorite	0.04
	Gabbro	0.00
Igneous Volcanics and Sub-volcanics	Rhyolite	0.08
	Dacite Porphyry	0.05
	Andesite	0.06
	Basalt	0.55
Metamorphics	Quartzite	0.07
	Schist	0.02
	Gneiss	0.01
	Siltite	0.00
	Phyllite	0.00
	Argillite	0.00
	Greenstone	0.06
Sedimentary Rocks	Limestone/Dolomite	0.00
	Sandstone	0.00
	Siltstone	0.00
	Conglomerate	0.02
	Shale/Mudstone	0.00
	Pedogenic Carbonate	0.01
Amorphous Silica	Chert	0.00
	Chalcedony	0.00
	Obsidian	0.00
		1.00

Table 28. Id-272c Coarse Aggregate Inventory

	Id-272c	
Rock Type	**Lithology**	**Percent Composition (Based on total pit weighted average)**
Igneous Intrusives	Granite	0.02
	Granodiorite	0.18
	Diorite	0.06
	Gabbro	0.00
Igneous Volcanics and Sub-volcanics	Rhyolite	0.16
	Dacite Porphyry	0.17
	Andesite	0.00
	Basalt	0.16
Metamorphics	Quartzite	0.15
	Schist	0.06
	Gneiss	0.00
	Siltite	0.00
	Phyllite	0.00
	Argillite	0.00
	Greenstone	0.01
Sedimentary Rocks	Limestone/Dolomite	0.00
	Sandstone	0.01
	Siltstone	0.00
	Conglomerate	0.00
	Shale/Mudstone	0.00
	Pedogenic Carbonate	0.00
Amorphous Silica	Chert	0.00
	Chalcedony	0.00
	Obsidian	0.00
		1.00

Table 29. Jf-103 Coarse Aggregate Inventory

	Jf-103	
Rock Type	Lithology	Percent Composition (Based on total pit weighted average)
Igneous Intrusives	Granite	0.00
	Granodiorite	0.00
	Diorite	0.00
	Gabbro	0.00
Igneous Volcanics and Sub-volcanics	Rhyolite	0.39
	Dacite porphyry	0.00
	Andesite	0.00
	Basalt	0.22
Metamorphics	Quartzite	0.15
	Schist	0.00
	Gneiss	0.00
	Siltite	0.00
	Phyllite	0.00
	Argillite	0.00
	Greenstone	0.00
Sedimentary Rocks	nestone/Dolom	0.00
	Sandstone	0.00
	Siltstone	0.00
	Conglomerate	0.00
	Shale/mudstone	0.00
	Pedogenic carbona	0.00
Amorphous Silica	Chert	0.00
	Chalcedony	0.00
	Obsidian	0.24
		1.00

Table 30. Kt-191c Coarse Aggregate Inventory

	Kt-191c	
Rock Type	**Lithology**	**Percent Composition (Based on total pit weighted average)**
Igneous Intrusives	Granite	0.00
	Granodiorite	0.15
	Diorite	0.00
	Gabbro	0.00
Igneous Volcanics and Sub-volcanics	Rhyolite	0.00
	Dacite Porphyry	0.00
	Andesite	0.00
	Basalt	0.25
Metamorphics	Quartzite	0.32
	Schist	0.02
	Gneiss	0.00
	Siltite	0.12
	Phyllite	0.00
	Argillite	0.04
	Greenstone	0.00
Sedimentary Rocks	Limestone/Dolomite	0.02
	Sandstone	0.00
	Siltstone	0.05
	Conglomerate	0.02
	Shale/Mudstone	0.00
	Pedogenic Carbonate	0.00
Amorphous Silica	Chert	0.00
	Chalcedony	0.00
	Obsidian	0.00
		1.00

Table 31. Kt-213c Coarse Aggregate Inventory

	Kt-213c	
Rock Type	**Lithology**	**Percent Composition (Based on total pit weighted average)**
Igneous Intrusives	Granite	0.03
	Granodiorite	0.09
	Diorite	0.00
	Gabbro	0.00
Igneous Volcanics and Sub-volcanics	Rhyolite	0.00
	Dacite Porphyry	0.00
	Andesite	0.00
	Basalt	0.01
Metamorphics	Quartzite	0.42
	Schist	0.01
	Gneiss	0.00
	Siltite	0.16
	Phyllite	0.00
	Argillite	0.19
	Greenstone	0.00
Sedimentary Rocks	Limestone/Dolomite	0.00
	Sandstone	0.00
	Calcareous Siltstone (Piegan)	0.08
	Conglomerate	0.00
	Shale/Mudstone	0.00
	Pedogenic Carbonate	0.00
Amorphous Silica	Chert	0.00
	Chalcedony	0.00
	Obsidian	0.00
		1.00

Table 32. Le-154c Coarse Aggregate Inventory

	Le-154c	
Rock Type	**Lithology**	**Percent Composition (Based on total pit weighted average)**
Igneous Intrusives	Granite	0.03
	Granodiorite	0.00
	Diorite	0.00
	Gabbro	0.00
Igneous Volcanics and Sub-volcanics	Rhyolite	0.23
	Dacite Porphyry	0.10
	Andesite	0.01
	Basalt	0.09
Metamorphics	Quartzite	0.26
	Schist	0.00
	Gneiss	0.06
	Siltite	0.02
	Phyllite	0.00
	Argillite	0.02
	Greenstone	0.00
Sedimentary Rocks	Limestone/Dolomite	0.00
	Sandstone	0.06
	Siltstone	0.11
	Conglomerate	0.00
	Shale/Mudstone	0.00
	Pedogenic Carbonate	0.00
Amorphous Silica	Chert	0.00
	Chalcedony	0.00
	Obsidian	0.00
		1.00

Table 33. Le-155c Coarse Aggregate Inventory

	Le-155c	
Rock Type	**Lithology**	**Percent Composition (Based on total pit weighted average)**
Igneous Intrusives	Granite	0.00
	Granodiorite	0.00
	Diorite	0.00
	Gabbro	0.00
Igneous Volcanics and Sub-volcanics	Rhyolite	0.12
	Dacite porphyry	0.00
	Andesite	0.02
	Basalt	0.03
Metamorphics	Quartzite	0.61
	Schist	0.00
	Gneiss	0.09
	Siltite	0.04
	Phyllite	0.00
	Argillite	0.00
	Greenstone	0.00
Sedimentary Rocks	Limestone/Dolomite	0.00
	Sandstone	0.07
	Siltstone	0.00
	Conglomerate	0.00
	Shale/mudstone	0.00
	Pedogenic carbonate	0.00
Amorphous Silica	Chert	0.00
	Chalcedony	0.00
	Obsidian	0.00
		1.00

Table 34. Ln-80c Coarse Aggregate Inventory

	Ln-80c	
Rock Type	**Lithology**	**Percent Composition (Based on total pit weighted average)**
Igneous Intrusives	Granite	0.02
	Granodiorite	0.00
	Diorite	0.00
	Gabbro	0.00
Igneous Volcanics and Sub-volcanics	Rhyolite	0.23
	Dacite Porphyry	0.11
	Andesite	0.06
	Basalt	0.07
Metamorphics	Quartzite	0.14
	Schist	0.00
	Gneiss	0.03
	Siltite	0.05
	Phyllite	0.00
	Argillite	0.06
	Greenstone	0.00
Sedimentary Rocks	Limestone/Dolomite	0.00
	Sandstone	0.21
	Siltstone	0.02
	Conglomerate	0.00
	Shale/Mudstone	0.00
	Pedogenic Carbonate	0.00
Amorphous Silica	Chert	0.00
	Chalcedony	0.00
	Obsidian	0.00
		1.00

Table 35. Ma-22c Coarse Aggregate Inventory

	Ma-22c	
Rock Type	**Lithology**	**Percent Composition (Based on total pit weighted average)**
Igneous Intrusives	Granite	0.08
	Granodiorite	0.03
	Diorite	0.00
	Gabbro	0.00
Igneous Volcanics and Sub-volcanics	Rhyolite	0.23
	Dacite Porphyry	0.14
	Andesite	0.01
	Basalt	0.31
Metamorphics	Quartzite	0.14
	Schist	0.00
	Gneiss	0.03
	Siltite	0.00
	Phyllite	0.00
	Argillite	0.00
	Greenstone	0.00
Sedimentary Rocks	Limestone/Dolomite	0.00
	Sandstone	0.00
	Siltstone	0.00
	Conglomerate	0.00
	Shale/Mudstone	0.00
	Pedogenic Carbonate	0.00
Amorphous Silica	Chert	0.00
	Chalcedony	0.00
	Obsidian	0.01
		1.00

Table 36. Ma-68c Coarse Aggregate Inventory

	Ma-68c	
Rock Type	**Lithology**	**Percent Composition (Based on total pit weighted average)**
Igneous Intrusives	Granite	0.02
	Granodiorite	0.00
	Diorite	0.00
	Gabbro	0.00
Igneous Volcanics and Sub-volcanics	Rhyolite	0.09
	Dacite Porphyry	0.00
	Andesite	0.00
	Basalt	0.06
Metamorphics	Quartzite	0.66
	Schist	0.00
	Gneiss	0.00
	Siltite	0.00
	Phyllite	0.00
	Argillite	0.00
	Greenstone	0.00
Sedimentary Rocks	Limestone/Dolomite	0.09
	Sandstone	0.05
	Siltstone	0.03
	Conglomerate	0.00
	Shale/Mudstone	0.00
	Pedogenic Carbonate	0.00
Amorphous Silica	Chert	0.00
	Chalcedony	0.00
	Obsidian	0.00
		1.00

Table 37. Md-45c Coarse Aggregate Inventory

	Md-45c	
Rock Type	**Lithology**	**Percent Composition (Based on total pit weighted average)**
Igneous Intrusives	Granite	0.00
	Granodiorite	0.00
	Diorite	0.00
	Gabbro	0.00
Igneous Volcanics and Sub-volcanics	Rhyolite	0.20
	Dacite Porphyry	0.00
	Andesite	0.00
	Basalt	0.22
Metamorphics	Quartzite	0.27
	Schist	0.03
	Gneiss	0.01
	Siltite	0.00
	Phyllite	0.00
	Argillite	0.00
	Greenstone	0.00
Sedimentary Rocks	Limestone/Dolomite	0.00
	Sandstone	0.11
	Siltstone	0.00
	Conglomerate	0.00
	Shale/Mudstone	0.00
	Pedogenic Carbonate	0.00
Amorphous Silica	Chert	0.00
	Chalcedony	0.00
	Obsidian	0.15
		1.00

Table 38. Np-82c Coarse Aggregate Inventory

	Np-82c	
Rock Type	**Lithology**	**Percent Composition (Based on total pit weighted average)**
Igneous Intrusives	Granite	0.00
	Granodiorite	0.07
	Diorite	0.02
	Gabbro	0.00
Igneous Volcanics and Sub-volcanics	Rhyolite	0.25
	Dacite Porphyry	0.10
	Andesite	0.00
	Basalt	0.36
Metamorphics	Quartzite	0.19
	Schist	0.00
	Gneiss	0.00
	Siltite	0.00
	Phyllite	0.00
	Argillite	0.00
	Greenstone	0.02
Sedimentary Rocks	Limestone/Dolomite	0.00
	Sandstone	0.00
	Siltstone	0.00
	Conglomerate	0.00
	Shale/Mudstone	0.00
	Pedogenic Carbonate	0.00
Amorphous Silica	Chert	0.00
	Chalcedony	0.00
	Obsidian	0.00
		1.00

Table 39. Ore-8c Coarse Aggregate Inventory

	Ore-8c	
Rock Type	**Lithology**	**Percent Composition (Based on total pit weighted average)**
Igneous Intrusives	Granite	0.00
	Granodiorite	0.19
	Diorite	0.00
	Gabbro	0.00
Igneous Volcanics and Sub-volcanics	Rhyolite	0.27
	Dacite Porphyry	0.03
	Andesite	0.00
	Basalt	0.41
Metamorphics	Quartzite	0.04
	Schist	0.00
	Gneiss	0.00
	Siltite	0.00
	Phyllite	0.00
	Argillite	0.00
	Greenstone	0.00
Sedimentary Rocks	Limestone/Dolomite	0.00
	Sandstone	0.00
	Siltstone	0.00
	Conglomerate	0.00
	Shale/Mudstone	0.00
	Pedogenic Carbonate	0.00
Amorphous Silica	Chert	0.00
	Chalcedony	0.01
	Obsidian	0.05
		1.00

Table 40. Ore-16c Coarse Aggregate Inventory

	Ore-16c	
Rock Type	**Lithology**	**Percent Composition (Based on total pit weighted average)**
Igneous Intrusives	Granite	0.24
	Granodiorite	0.00
	Diorite	0.00
	Gabbro	0.03
Igneous Volcanics and Sub-volcanics	Rhyolite	0.30
	Dacite Porphyry	0.05
	Andesite	0.00
	Basalt	0.26
Metamorphics	Quartzite	0.08
	Schist	0.00
	Gneiss	0.00
	Siltite	0.00
	Phyllite	0.00
	Argillite	0.00
	Greenstone	0.00
Sedimentary Rocks	Limestone/Dolomite	0.00
	Sandstone	0.00
	Siltstone	0.00
	Conglomerate	0.00
	Shale/Mudstone	0.00
	Pedogenic Carbonate	0.00
Amorphous Silica	Chert	0.02
	Chalcedony	0.00
	Obsidian	0.02
		1.00

Table 41. Ow-117c Coarse Aggregate Inventory

	Ow-117c	
Rock Type	**Lithology**	**Percent Composition (Based on total pit weighted average)**
Igneous Intrusives	Granite	0.01
	Granodiorite	0.00
	Diorite	0.00
	Gabbro	0.00
Igneous Volcanics and Sub-volcanics	Rhyolite	0.06
	Dacite Porphyry	0.82
	Andesite	0.00
	Basalt	0.09
Metamorphics	Quartzite	0.00
	Schist	0.00
	Gneiss	0.00
	Siltite	0.00
	Phyllite	0.00
	Argillite	0.00
	Greenstone	0.00
Sedimentary Rocks	Limestone/Dolomite	0.00
	Sandstone	0.00
	Siltstone	0.00
	Conglomerate	0.00
	Shale/Mudstone	0.00
	Pedogenic Carbonate	0.00
Amorphous Silica	Chert	0.00
	Chalcedony	0.00
	Obsidian	0.02
		1.00

Table 42. PSC-173c Coarse Aggregate Inventory

	PSC-173c	
Rock Type	**Lithology**	**Percent Composition (Based on total pit weighted average)**
Igneous Intrusives	Granite	0.02
	Granodiorite	0.04
	Diorite	0.05
	Gabbro	0.01
Igneous Volcanics and Sub-volcanics	Rhyolite	0.00
	Dacite Porphyry	0.01
	Andesite	0.00
	Basalt	0.00
Metamorphics	Quartzite	0.40
	Schist	0.00
	Gneiss	0.01
	Siltite	0.14
	Phyllite	0.00
	Argillite	0.18
	Greenstone	0.01
Sedimentary Rocks	Limestone/Dolomite	0.00
	Sandstone	0.00
	Calcareous Siltstone (Piegan)	0.15
	Conglomerate	0.00
	Shale/Mudstone	0.00
	Pedogenic Carbonate	0.00
Amorphous Silica	Chert	0.00
	Chalcedony	0.00
	Obsidian	0.00
		1.00

Table 43. Pw-84c Coarse Aggregate Inventory

	Pw-84c	
Rock Type	**Lithology**	**Percent Composition (Based on total pit weighted average)**
Igneous Intrusives	Granite	0.00
	Granodiorite	0.00
	Diorite	0.00
	Gabbro	0.00
Igneous Volcanics and Sub-volcanics	Rhyolite	0.00
	Dacite Porphyry	0.00
	Andesite	0.00
	Basalt	0.09
Metamorphics	Quartzite	0.69
	Schist	0.00
	Gneiss	0.00
	Siltite	0.00
	Phyllite	0.00
	Argillite	0.00
	Greenstone	0.00
Sedimentary Rocks	Limestone/Dolomite	0.05
	Sandstone	0.12
	Siltstone	0.05
	Conglomerate	0.00
	Shale/Mudstone	0.00
	Pedogenic Carbonate	0.00
Amorphous Silica	Chert	0.00
	Chalcedony	0.00
	Obsidian	0.00
		1.00

Table 44. Tn-65c Coarse Aggregate Inventory

	Tn-65c	
Rock Type	**Lithology**	**Percent Composition (Based on total pit weighted average)**
Igneous Intrusives	Granite	0.46
	Granodiorite	0.00
	Diorite	0.00
	Gabbro	0.00
Igneous Volcanics and Sub-volcanics	Rhyolite	0.07
	Dacite Porphyry	0.00
	Andesite	0.00
	Basalt	0.00
Metamorphics	Quartzite	0.11
	Schist	0.00
	Gneiss	0.00
	Siltite	0.00
	Phyllite	0.00
	Argillite	0.00
	Greenstone	0.00
Sedimentary Rocks	Limestone/Dolomite	0.35
	Sandstone	0.01
	Siltstone	0.00
	Conglomerate	0.00
	Shale/Mudstone	0.00
	Pedogenic Carbonate	0.00
Amorphous Silica	Chert	0.00
	Chalcedony	0.00
	Obsidian	0.00
		1.00

Table 45. Vy-52c Coarse Aggregate Inventory

	Vy-52c	
Rock Type	**Lithology**	**Percent Composition (Based on total pit weighted average)**
Igneous Intrusives	Granite	0.60
	Granodiorite	0.00
	Diorite	0.00
	Gabbro	0.00
Igneous Volcanics and Sub-volcanics	Rhyolite	0.00
	Dacite Porphyry	0.00
	Andesite	0.00
	Basalt	0.15
Metamorphics	Quartzite	0.00
	Schist	0.01
	Gneiss	0.00
	Siltite	0.00
	Phyllite	0.00
	Argillite	0.00
	Greenstone	0.00
Sedimentary Rocks	Limestone/Dolomite	0.00
	Sandstone	0.25
	Siltstone	0.00
	Conglomerate	0.00
	Shale/Mudstone	0.00
	Pedogenic Carbonate	0.00
Amorphous Silica	Chert	0.00
	Chalcedony	0.00
	Obsidian	0.00
		1.00

Table 46. Vy-56c Coarse Aggregate Inventory

	Vy-56c	
Rock Type	**Lithology**	**Percent Composition (Based on total pit weighted average)**
Igneous Intrusives	Granite	0.18
	Granodiorite	0.00
	Diorite	0.00
	Gabbro	0.00
Igneous Volcanics and Sub-volcanics	Rhyolite	0.00
	Dacite Porphyry	0.00
	Andesite	0.00
	Basalt	0.64
Metamorphics	Quartzite	0.05
	Schist	0.03
	Gneiss	0.00
	Siltite	0.00
	Phyllite	0.00
	Argillite	0.10
	Greenstone	0.00
Sedimentary Rocks	Limestone/Dolomite	0.00
	Sandstone	0.00
	Siltstone	0.00
	Conglomerate	0.00
	Shale/Mudstone	0.00
	Pedogenic Carbonate	0.00
Amorphous Silica	Chert	0.00
	Chalcedony	0.00
	Obsidian	0.00
		1.00

Appendix D
Lithology Inventory of Fine Aggregate Data Tables

Table 47. ACW-8c Fine Aggregate Inventory

ACW-8c	Percent Composition (Based on total fines weighted average)
Granite/Granodiorite	0.00
Diorite/Porphyry	0.03
Rhyolite	0.04
Andesite	0.03
Dacite Porphyry	0.00
Basalt	0.06
Quartzite	0.09
Schist	0.00
Gneiss	0.00
Limestone	0.00
Sandstone	0.00
Argillite	0.00
Chert	0.06
Chalcedony	0.00
Obsidian	0.00
Opal	0.02
Carbonate	0.02
Quartz	0.45
Muscovite	0.04
Plagioclase	0.00
Orthoclase	0.01
Hornblende/Amphibole	0.01
Silica-Cemented Fine-Sand Pedogenic Coats	0.12
Sum	1.00

Table 48. Ad-136c Fine Aggregate Inventory

AD-136c	Percent Composition (Based on total fines weighted average)
Granite/Granodiorite	0.11
Diorite/Porphyry	0.00
Rhyolite	0.00
Andesite	0.00
Dacite Porphyry	0.00
Basalt	0.01
Quartzite	0.02
Schist	0.00
Gneiss	0.00
Limestone	0.00
Sandstone	0.00
Argillite	0.00
Chert	0.00
Chalcedony	0.00
Obsidian	0.00
Opal	0.00
Carbonate	0.00
Quartz	0.62
Mica	0.02
Plagioclase	0.00
Orthoclase	0.19
Hornblende/Amphibole	0.01
Silica-Cemented Fine-Sand Pedogenic Coats	0.01
Sum	1.00

Table 49. Ad-53s Fine Aggregate Inventory

AD-53c	Percent Composition (Based on total fines weighted average)
Granite/Granodiorite	0.09
Diorite/Porphyry	0.00
Rhyolite	0.00
Andesite	0.00
Dacite Porphyry	0.00
Basalt	0.02
Quartzite	0.05
Schist	0.00
Gneiss	0.00
Limestone	0.00
Sandstone	0.00
Argillite	0.00
Chert	0.00
Chalcedony	0.00
Obsidian	0.00
Opal	0.02
Carbonate	0.02
Quartz	0.55
Mica	0.02
Plagioclase	0.11
Orthoclase	0.10
Hornblende/Amphibole	0.02
Silica-Cemented Fine-Sand Pedogenic Coats	0.00
Sum	1.00

Table 50. Bg-111c Fine Aggregate Inventory

Bg-111c	Percent Composition (Based on total fines weighted average)
Granite/Granodiorite	0.00
Diorite/Porphyry	0.00
Rhyolite	0.05
Andesite	0.00
Dacite Porphyry	0.00
Basalt	0.06
Quartzite	0.09
Schist	0.00
Gneiss	0.00
Limestone	0.01
Sandstone	0.00
Argillite	0.00
Chert	0.00
Chalcedony	0.00
Obsidian	0.18
Opal	0.02
Carbonate	0.02
Quartz	0.48
Mica	0.07
Plagioclase	0.02
Orthoclase	0.02
Hornblende/Amphibole	0.00
Silica-Cemented Fine-Sand Pedogenic Coats	0.00
Sum	1.00

Table 51. Bl-84c Fine Aggregate Inventory

Bl-84c	Percent Composition (Based on total fines weighted average)
Granite/Granodiorite	0.00
Diorite/Porphyry	0.00
Rhyolite	0.00
Andesite	0.00
Dacite Porphyry	0.00
Basalt	0.00
Quartzite	0.13
Schist	0.00
Gneiss	0.00
Limestone	0.02
Sandstone	0.02
Argillite	0.09
Chert	0.18
Chalcedony	0.00
Obsidian	0.00
Opal	0.00
Carbonate	0.00
Quartz	0.46
Mica	0.00
Plagioclase	0.00
Orthoclase	0.00
Hornblende/Amphibole	0.00
Silica-Cemented Fine-Sand Pedogenic Coats	0.11
Sum	1.00

Table 52. Bn-155c Fine Aggregate Inventory

Bn-155c	Percent Composition (Based on total fines weighted average)
Granite/Granodiorite	0.00
Diorite/Porphyry	0.00
Rhyolite	0.08
Andesite	0.00
Dacite Porphyry	0.00
Basalt	0.10
Quartzite	0.10
Schist	0.00
Gneiss	0.00
Limestone	0.00
Sandstone	0.00
Argillite	0.00
Chert	0.00
Chalcedony	0.00
Obsidian	0.45
Opal	0.05
Carbonate	0.03
Quartz	0.18
Mica	0.01
Plagioclase	0.00
Orthoclase	0.00
Hornblende/Amphibole	0.00
Silica-Cemented Fine-Sand Pedogenic Coats	0.00
Sum	1.00

Table 53. Bo-61c Fine Aggregate Inventory

Bo-61c	Percent Composition (Based on total fines weighted average)
Granite/Granodiorite	0.10
Diorite/Porphyry	0.00
Rhyolite	0.00
Andesite	0.00
Dacite Porphyry	0.00
Basalt	0.00
Quartzite	0.00
Schist	0.00
Gneiss	0.00
Limestone	0.00
Sandstone	0.00
Argillite	0.00
Chert	0.00
Chalcedony	0.00
Obsidian	0.00
Opal	0.00
Carbonate	0.00
Quartz	0.59
Mica	0.09
Plagioclase	0.22
Orthoclase	0.00
Hornblende/Amphibole	0.00
Silica-Cemented Fine-Sand Pedogenic Coats	0.00
Sum	1.00

Table 54. Br-2c Fine Aggregate Inventory

Br-2c	Percent Composition (Based on total fines weighted average)
Granite/Granodiorite	0.14
Diorite/Porphyry	0.00
Rhyolite	0.00
Andesite	0.00
Dacite Porphyry	0.00
Basalt	0.00
Quartzite	0.19
Schist	0.00
Gneiss	0.00
Limestone	0.00
Sandstone	0.00
Argillite	0.01
Chert	0.00
Chalcedony	0.00
Obsidian	0.00
Opal	0.00
Carbonate	0.00
Quartz	0.49
Mica	0.08
Plagioclase	0.05
Orthoclase	0.04
Hornblende/Amphibole	0.00
Silica-Cemented Fine-Sand Pedogenic Coats	0.00
Sum	1.00

Table 55. By-84c Fine Aggregate Inventory

By-84c	Percent Composition (Based on total fines weighted average)
Granite/Granodiorite	0%
Diorite/Porphyry	2%
Rhyolite	0%
Andesite	0%
Dacite Porphyry	0%
Basalt	0%
Quartzite	52%
Schist	0%
Gneiss	0%
Limestone	0%
Sandstone	3%
Argillite	2%
Chert	0%
Chalcedony	0%
Obsidian	0%
Opal	0%
Carbonate	0%
Quartz	34%
Mica	0%
Plagioclase	0%
Orthoclase	0%
Hornblende/Amphibole	7%
Silica-Cemented Fine-Sand Pedogenic Coats	0%
Sum	1.00

Table 56. By-80c Fine Aggregate Inventory

By-80c	Percent Composition (Based on total fines weighted average)
Granite/Granodiorite	0.02
Diorite/Porphyry	0.04
Rhyolite	0.00
Andesite	0.00
Dacite Porphyry	0.00
Basalt	0.00
Quartzite	0.60
Schist	0.02
Gneiss	0.00
Limestone	0.00
Sandstone	0.00
Argillite	0.02
Chert	0.00
Chalcedony	0.00
Obsidian	0.00
Opal	0.00
Carbonate	0.00
Quartz	0.23
Mica	0.02
Plagioclase	0.01
Orthoclase	0.00
Hornblende/Amphibole	0.04
Silica-Cemented Fine-Sand Pedogenic Coats	0.00
Sum	1.00

Table 57. Cn-140c Fine Aggregate Inventory

Cn-140c	Percent Composition (Based on total fines weighted average)
Granite/Granodiorite	0.11
Diorite/Porphyry	0.01
Rhyolite	0.07
Andesite	0.00
Dacite Porphyry	0.00
Basalt	0.00
Quartzite	0.00
Schist	0.00
Gneiss	0.00
Limestone	0.00
Sandstone	0.00
Argillite	0.00
Chert	0.00
Chalcedony	0.00
Obsidian	0.00
Opal	0.00
Carbonate	0.00
Quartz	0.65
Mica	0.07
Plagioclase	0.05
Orthoclase	0.02
Hornblende/Amphibole	0.02
Silica-Cemented Fine-Sand Pedogenic Coats	0.00
Sum	1.00

Table 58. Cn-146c Fine Aggregate Inventory

Cn-140c	Percent Composition (Based on total fines weighted average)
Granite/Granodiorite	0.06
Diorite/Porphyry	0.00
Rhyolite	0.35
Andesite	0.00
Dacite Porphyry	0.00
Basalt	0.17
Quartzite	0.05
Schist	0.02
Gneiss	0.00
Limestone	0.00
Sandstone	0.16
Argillite	0.00
Chert	0.00
Chalcedony	0.00
Obsidian	0.04
Opal	0.00
Carbonate	0.00
Quartz	0.10
Mica	0.02
Plagioclase	0.01
Orthoclase	0.00
Hornblende/Amphibole	0.01
Silica-Cemented Fine-Sand Pedogenic Coats	0.00
Sum	1.00

Table 59. Cs-186c Fine Aggregate Inventory

Cs-186c	Percent Composition (Based on total fines weighted average)
Granite/Granodiorite	0.06
Diorite/Porphyry	0.00
Rhyolite	0.35
Andesite	0.00
Dacite Porphyry	0.00
Basalt	0.17
Quartzite	0.05
Schist	0.02
Gneiss	0.00
Limestone	0.00
Sandstone	0.16
Argillite	0.00
Chert	0.00
Chalcedony	0.00
Obsidian	0.04
Opal	0.00
Carbonate	0.00
Quartz	0.10
Mica	0.02
Plagioclase	0.01
Orthoclase	0.00
Hornblende/Amphibole	0.01
Silica-Cemented Fine-Sand Pedogenic Coats	0.00
Sum	1.00

Table 60. Cu-73c Fine Aggregate Inventory

Cu-73c	Percent Composition (Based on total fines weighted average)
Granite/Granodiorite	0.07
Diorite/Porphyry	0.00
Rhyolite	0.18
Andesite	0.02
Dacite Porphyry	0.10
Basalt	0.17
Quartzite	0.33
Schist	0.00
Gneiss	0.00
Limestone	0.00
Sandstone	0.00
Argillite	0.00
Chert	0.00
Chalcedony	0.00
Obsidian	0.00
Opal	0.00
Carbonate	0.00
Quartz	0.13
Mica	0.00
Plagioclase	0.00
Orthoclase	0.00
Hornblende/Amphibole	0.00
Silica-Cemented Fine-Sand Pedogenic Coats	0.00
Sum	1.00

Table 61. El-116c Fine Aggregate Inventory

El-116c	Percent Composition (Based on total fines weighted average)
Granite/Granodiorite	0.03
Diorite/Porphyry	0.00
Rhyolite	0.12
Andesite	0.00
Dacite Porphyry	0.00
Basalt	0.16
Quartzite	0.21
Schist	0.00
Gneiss	0.00
Limestone	0.00
Sandstone	0.00
Argillite	0.04
Chert	0.00
Chalcedony	0.00
Obsidian	0.00
Opal	0.20
Carbonate	0.02
Quartz	0.22
Mica	0.00
Plagioclase	0.00
Orthoclase	0.00
Hornblende/Amphibole	0.00
Silica-Cemented Fine-Sand Pedogenic Coats	0.00
Sum	1.00

Table 62. El-37c Fine Aggregate Inventory

El-37c	Percent Composition (Based on total fines weighted average)
Granite/Granodiorite	0.00
Diorite/Porphyry	0.00
Rhyolite	0.09
Andesite	0.00
Dacite Porphyry	0.00
Basalt	0.36
Quartzite	0.27
Schist	0.00
Gneiss	0.00
Limestone	0.00
Sandstone	0.00
Argillite	0.00
Chert	0.00
Chalcedony	0.00
Obsidian	0.00
Opal	0.01
Carbonate	0.01
Quartz	0.27
Mica	0.00
Plagioclase	0.00
Orthoclase	0.00
Hornblende/Amphibole	0.00
Silica-Cemented Fine-Sand Pedogenic Coats	0.00
Sum	1.00

Table 63. Id-121c Fine Aggregate Inventory

Id-121c	Percent Composition (Based on total fines weighted average)
Granite/Granodiorite	0.03
Diorite/Porphyry	0.00
Rhyolite	0.02
Andesite	0.00
Dacite Porphyry	0.00
Basalt	0.20
Quartzite	0.26
Schist	0.00
Gneiss	0.00
Limestone	0.00
Sandstone	0.00
Argillite	0.00
Chert	0.00
Chalcedony	0.00
Obsidian	0.00
Opal	0.04
Carbonate	0.01
Quartz	0.39
Mica	0.06
Plagioclase	0.00
Orthoclase	0.00
Hornblende/Amphibole	0.00
Silica-Cemented Fine-Sand Pedogenic Coats	0.00
Sum	1.00

Table 64. Jf-103c Fine Aggregate Inventory

Jf-103c	Percent Composition (Based on total fines weighted average)
Granite/Granodiorite	0.00
Diorite/Porphyry	0.00
Rhyolite	0.05
Andesite	0.00
Dacite Porphyry	0.00
Basalt	0.04
Quartzite	0.02
Schist	0.00
Gneiss	0.00
Limestone	0.00
Sandstone	0.00
Argillite	0.00
Chert	0.00
Chalcedony	0.00
Obsidian	0.67
Opal	0.00
Carbonate	0.00
Quartz	0.20
Mica	0.00
Plagioclase	0.00
Orthoclase	0.00
Hornblende/Amphibole	0.00
Shell Fragments	0.01
Sum	1.00

Table 65. Kt-213c Fine Aggregate Inventory

Kt-213c	Percent Composition (Based on total fines weighted average)
Granite/Granodiorite	0.09
Diorite/Porphyry	0.00
Rhyolite	0.00
Andesite	0.00
Dacite Porphyry	0.00
Basalt	0.00
Quartzite	0.27
Schist	0.00
Gneiss	0.00
Limestone	0.02
Sandstone	0.05
Argillite	0.19
Chert	0.00
Chalcedony	0.00
Obsidian	0.00
Opal	0.00
Carbonate	0.00
Quartz	0.02
Mica	0.00
Plagioclase	0.00
Orthoclase	0.00
Hornblende/Amphibole	0.00
Mudstone	0.35
Sum	1.00

Table 66. Le-154c Fine Aggregate Inventory

Le-154c	Percent Composition (Based on total fines weighted average)
Granite/Granodiorite	0.05
Diorite/Porphyry	0.00
Rhyolite	0.05
Andesite	0.04
Dacite Porphyry	0.00
Basalt	0.08
Quartzite	0.71
Schist	0.00
Gneiss	0.00
Limestone	0.00
Sandstone	0.00
Argillite	0.01
Chert	0.00
Chalcedony	0.00
Obsidian	0.00
Opal	0.00
Carbonate	0.00
Quartz	0.05
Mica	0.01
Plagioclase	0.00
Orthoclase	0.00
Hornblende/Amphibole	0.00
Silica-Cemented Fine-Sand Pedogenic Coats	0.00
Sum	1.00

Table 67. Le-155c Fine Aggregate Inventory

Le-155c	Percent Composition (Based on total fines weighted average)
Granite/Granodiorite	0.09
Diorite/Porphyry	0.00
Rhyolite	0.26
Andesite	0.00
Dacite Porphyry	0.19
Basalt	0.05
Quartzite	0.35
Schist	0.00
Gneiss	0.00
Limestone	0.00
Sandstone	0.02
Argillite	0.02
Chert	0.00
Chalcedony	0.00
Obsidian	0.00
Opal	0.01
Carbonate	0.01
Quartz	0.01
Mica	0.00
Plagioclase	0.00
Orthoclase	0.00
Hornblende/Amphibole	0.00
Silica-Cemented Fine-Sand Pedogenic Coats	0.00
Sum	1.00

Table 68. Ln-80c Fine Aggregate Inventory

Ln-80c	Percent Composition (Based on total fines weighted average)
Granite/Granodiorite	0.05
Diorite/Porphyry	0.00
Rhyolite	0.06
Andesite	0.06
Dacite Porphyry	0.01
Basalt	0.34
Quartzite	0.15
Schist	0.00
Gneiss	0.00
Limestone	0.00
Sandstone	0.01
Argillite	0.09
Chert	0.00
Chalcedony	0.00
Obsidian	0.00
Opal	0.00
Carbonate	0.00
Quartz	0.22
Mica	0.00
Plagioclase	0.00
Orthoclase	0.00
Hornblende/Amphibole	0.00
Silica-Cemented Fine-Sand Pedogenic Coats	0.00
Sum	1.00

Table 69. Ma-22c Fine Aggregate Inventory

Ma-22c	Percent Composition (Based on total fines weighted average)
Granite/Granodiorite	0.12
Diorite/Porphyry	0.00
Rhyolite	0.24
Andesite	0.00
Dacite Porphyry	0.05
Basalt	0.06
Quartzite	0.01
Schist	0.00
Gneiss	0.00
Limestone	0.00
Sandstone	0.01
Argillite	0.00
Chert	0.00
Chalcedony	0.00
Obsidian	0.09
Opal	0.06
Carbonate	0.00
Quartz	0.30
Mica	0.03
Plagioclase	0.02
Orthoclase	0.02
Hornblende/Amphibole	0.00
Silica-Cemented Fine-Sand Pedogenic Coats	0.00
Sum	1.00

Table 70. Ma-68c Fine Aggregate Inventory

Ma-68c	Percent Composition (Based on total fines weighted average)
Granite/Granodiorite	0.01
Diorite/Porphyry	0.00
Rhyolite	0.05
Andesite	0.00
Dacite Porphyry	0.00
Basalt	0.13
Quartzite	0.23
Schist	0.00
Gneiss	0.00
Limestone	0.00
Sandstone	0.18
Argillite	0.00
Chert	0.00
Chalcedony	0.00
Obsidian	0.08
Opal	0.08
Carbonate	0.08
Quartz	0.16
Mica	0.00
Plagioclase	0.00
Orthoclase	0.00
Hornblende/Amphibole	0.00
Silica-Cemented Fine-Sand Pedogenic Coats	0.00
Sum	1.00

Table 71. Md-45c Fine Aggregate Inventory

Md-45c	Percent Composition (Based on total fines weighted average)
Granite/Granodiorite	0.01
Diorite/Porphyry	0.00
Rhyolite	0.18
Andesite	0.01
Dacite Porphyry	0.01
Basalt	0.17
Quartzite	0.23
Schist	0.00
Gneiss	0.00
Limestone	0.00
Sandstone	0.02
Argillite	0.00
Chert	0.00
Chalcedony	0.00
Obsidian	0.08
Opal	0.01
Carbonate	0.01
Quartz	0.26
Mica	0.00
Plagioclase	0.00
Orthoclase	0.00
Hornblende/Amphibole	0.00
Silica-Cemented Fine-Sand Pedogenic Coats	0.00
Sum	1.00

Table 72. Np-82c Fine Aggregate Inventory

Np-82c	Percent Composition (Based on total fines weighted average)
Granite/Granodiorite	0.01
Diorite/Porphyry	0.00
Rhyolite	0.01
Andesite	0.14
Dacite Porphyry	0.00
Basalt	0.20
Quartzite	0.23
Schist	0.00
Gneiss	0.00
Limestone	0.00
Sandstone	0.00
Argillite	0.00
Chert	0.00
Chalcedony	0.00
Obsidian	0.01
Opal	0.00
Carbonate	0.00
Quartz	0.40
Mica	0.00
Plagioclase	0.00
Orthoclase	0.00
Hornblende/Amphibole	0.00
Silica-Cemented Fine-Sand Pedogenic Coats	0.00
Sum	1.00

Table 73. Ore-16c Fine Aggregate Inventory

Ore-16c	Percent Composition (Based on total fines weighted average)
Granite/Granodiorite	0.03
Diorite/Porphyry	0.00
Rhyolite	0.22
Andesite	0.00
Dacite Porphyry	0.00
Basalt	0.10
Quartzite	0.21
Schist	0.00
Gneiss	0.00
Limestone	0.00
Sandstone	0.00
Argillite	0.00
Chert	0.00
Chalcedony	0.01
Obsidian	0.08
Opal	0.02
Carbonate	0.00
Quartz	0.22
Mica	0.01
Plagioclase	0.00
Orthoclase	0.00
Hornblende/Amphibole	0.00
Hunks of Silt and Sand	0.11
Sum	1.00

Table 74. Ore-8c Fine Aggregate Inventory

Ore-8c	Percent Composition (Based on total fines weighted average)
Granite/Granodiorite	0.01
Diorite/Porphyry	0.00
Rhyolite	0.01
Andesite	0.14
Dacite Porphyry	0.00
Basalt	0.20
Quartzite	0.23
Schist	0.00
Gneiss	0.00
Limestone	0.00
Sandstone	0.00
Argillite	0.00
Chert	0.00
Chalcedony	0.00
Obsidian	0.01
Opal	0.00
Carbonate	0.00
Quartz	0.40
Mica	0.00
Plagioclase	0.00
Orthoclase	0.00
Hornblende/Amphibole	0.00
Silica-Cemented Fine-Sand Pedogenic Coats	0.00
Sum	1.00

Table 75. Ow-117c Fine Aggregate Inventory

Ow-117c	Percent Composition (Based on total fines weighted average)
Granite/Granodiorite	0.01
Diorite/Porphyry	0.00
Rhyolite	0.13
Andesite	0.00
Dacite Porphyry	0.49
Basalt	0.12
Quartzite	0.00
Schist	0.00
Gneiss	0.00
Limestone	0.00
Sandstone	0.00
Argillite	0.00
Chert	0.00
Chalcedony	0.00
Obsidian	0.02
Opal	0.02
Carbonate	0.02
Quartz	0.20
Mica	0.00
Plagioclase	0.00
Orthoclase	0.00
Hornblende/Amphibole	0.00
Silica-Cemented Fine-Sand Pedogenic Coats	0.00
Sum	1.00

Table 76. PSC-173c Fine Aggregate Inventory

PSC-173c	Percent Composition (Based on total fines weighted average)
Granite/Granodiorite	0.11
Diorite/Porphyry	0.00
Rhyolite	0.00
Andesite	0.00
Dacite Porphyry	0.00
Basalt	0.00
Quartzite	0.39
Schist	0.00
Gneiss	0.00
Limestone	0.00
Sandstone	0.00
Argillite	0.44
Chert	0.00
Chalcedony	0.00
Obsidian	0.00
Opal	0.00
Carbonate	0.00
Quartz	0.03
Mica	0.01
Plagioclase	0.00
Orthoclase	0.00
Hornblende/Amphibole	0.00
Silstone with Carbonate Cement	0.02
Sum	1.00

Table 77. Pw-84c Fine Aggregate Inventory

Pw-84c	Percent Composition (Based on total fines weighted average)
Granite/Granodiorite	0.00
Diorite/Porphyry	0.00
Rhyolite	0.05
Andesite	0.00
Dacite Porphyry	0.00
Basalt	0.10
Quartzite	0.80
Schist	0.00
Gneiss	0.00
Limestone	0.04
Sandstone	0.00
Argillite	0.00
Chert	0.00
Chalcedony	0.00
Obsidian	0.01
Opal	0.00
Carbonate	0.00
Quartz	0.00
Mica	0.00
Plagioclase	0.00
Orthoclase	0.00
Hornblende/Amphibole	0.00
Silstone with Carbonate Cement	0.00
Sum	1.00

Table 78. Tn-65c Fine Aggregate Inventory

Tn-65c	Percent Composition (Based on total fines weighted average)
Granite/Granodiorite	0.30
Diorite/Porphyry	0.00
Rhyolite	0.00
Andesite	0.00
Dacite Porphyry	0.00
Basalt	0.00
Quartzite	0.27
Schist	0.00
Gneiss	0.00
Limestone	0.31
Sandstone	0.00
Argillite	0.00
Chert	0.00
Chalcedony	0.00
Obsidian	0.00
Opal	0.00
Carbonate	0.00
Quartz	0.12
Mica	0.00
Plagioclase	0.00
Orthoclase	0.00
Hornblende/Amphibole	0.00
Silstone with Carbonate Cement	0.00
Sum	1.00

Table 79. Vy-52c Fine Aggregate Inventory

Vy-52c	Percent Composition (Based on total fines weighted average)
Granite/Granodiorite	0.52
Diorite/Porphyry	0.00
Rhyolite	0.00
Andesite	0.00
Dacite Porphyry	0.00
Basalt	0.05
Quartzite	0.00
Schist	0.00
Gneiss	0.00
Limestone	0.00
Sandstone	0.00
Argillite	0.00
Chert	0.00
Chalcedony	0.00
Obsidian	0.00
Opal	0.00
Carbonate	0.00
Quartz	0.27
Mica	0.08
Plagioclase	0.00
Orthoclase	0.00
Hornblende/Amphibole	0.08
Silstone with Carbonate Cement	0.00
Sum	1.00